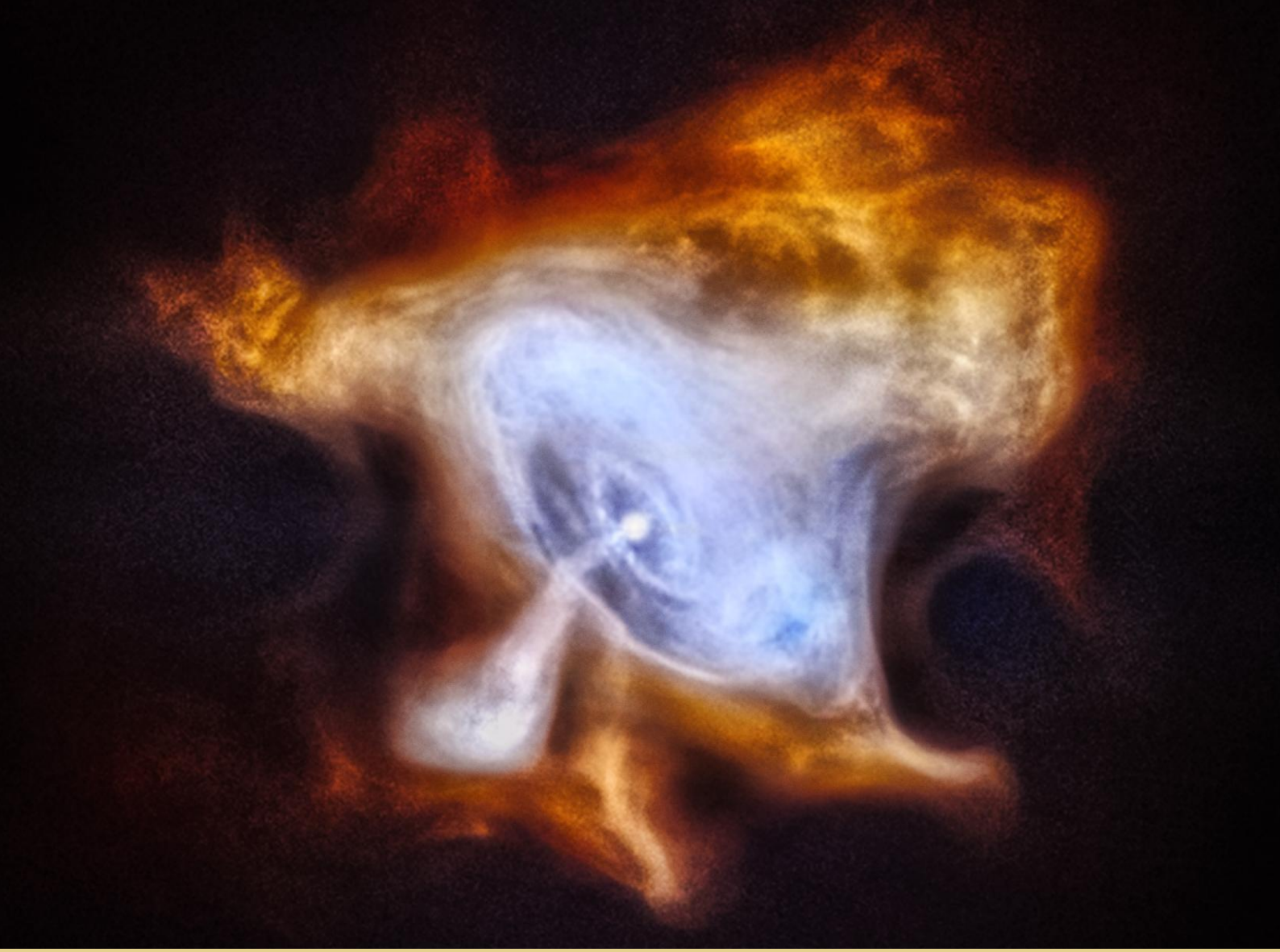

Renan Câmara Pereira

Chiral Transition and Deconfinement in Hybrid Stars

Dissertation presented to the Physics Department at
University of Coimbra to obtain the Master's degree in Physics

July 2016

· U C ·

Universidade de Coimbra

University of Coimbra

Master Thesis

Chiral Transition and Deconfinement in Hybrid Stars

Author:
Renan C. Pereira

Supervisors:
Dr. Pedro Costa
Dr. Constança Providência

A thesis submitted in fulfillment of the requirements for the Master's Degree in Physics

in the

Centre for Physics of the University of Coimbra
Physics Department

August 2, 2016

"*People think dreams aren't real just because they aren't made of matter, of particles. Dreams are real. But they are made of viewpoints, of images, of memories and puns and lost hopes.*"

- Neil Gaiman, *The Sandman*

Abstract

In this work, we make a two-model approach to the description of the equation of state of compact stars with two independent models: one which describes the hadronic phase while another describes the quark phase. In the quark phase we have considered the usual Nambu−Jona-Lasinio (**NJL**) model alongside vector-isoscalar and vector-isovector terms.

The importance of reproducing the same baryonic mass of the nucleon in the vacuum for both phases is discussed. A phenomenological Bag constant is introduced to make the transition between the hadronic and quark models coincide with the chiral symmetry restoration of the quark model. The hadronic phase is described by a relativistic mean field model (NL3$\omega\rho$) while the quark phase is described by the **NJL** in its two and three flavour versions, allowing to take into account the role of *strangeness* in compact stars.

Subsequently, a modified Polyakov−Nambu−Jona-Lasinio (**mPNJL**), in $SU_f(3)$, is used to describe the quark phase, allowing the study of colour deconfinement in compact stars and relating the phenomenological bag constant to gluonic degrees of freedom through the Polyakov loop field.

It is shown that fixing the vacuum quark constituent mass with a value that is one third of the vacuum nucleon mass allows the appearance of a pure quark core in the center of a neutron star while a strong enough vector coupling will result in stars with masses above $2M_\odot$ and low *strangeness* content. However, using the **mPNJL** model, the onset of *strangeness* occurs at lower densities, which gives rise to stars with larger fractions of *strange* quarks.

Resumo

Neste trabalho, equações de estado que descrevem estrelas compactas são construídas usando dois modelos independentes: um modelo que descreve a fase hadrónica e outro que descreve a fase de quarks. Na fase de quarks consideramos o modelo Nambu−Jona-Lasinio (**NJL**) usual possibilitando a existência de termos vectoriais-isoescalares e vectoriais-isovectoriais.

A importância de reproduzir a mesma massa bariónica do nucleão no vácuo, em ambas as fases, é discutida. Uma constante fenomenológica do Bag é introduzida de modo a fazer a transição entre o modelo hadrónico e modelo de quarks coincidir com a restauração da simetria quiral do modelo de quarks. A fase hadrónica é descrita por um modelo relativista de campo médio (NL3$\omega\rho$) enquanto a fase de quarks é descrita pelo modelo **NJL** nas suas versões de dois e três sabores, permitindo o estudo da *estranheza* em estrelas compactas.

Posteriormente, uma versão modificada do modelo de Polyakov−Nambu−Jona-Lasinio (**mPNJL**), em $SU_f(3)$, é usada para descrever a fase de quarks, permitindo a possibilidade de estudar o desconfinamento na cor em estrelas compactas e relacionar a constante fenomenológica do Bag com graus de liberdade gluónicos através do campo de Polyakov.

É mostrado que fixar a massa constituinte do quark a um valor que corresponde a um terço da massa do nucleão no vácuo, permite a existência de estrelas de neutrões estáveis com um centro composto apenas por matéria de quarks. Uma constante de acoplamento vectorial suficientemente forte irá resultar em estrelas com massas acima de $2M_{\odot}$ e baixa fracção de *estranheza*. Contudo, usando o modelo **mPNJL**, a *estranheza* aparece a densidades mais baixas, o que dá origem a estrelas com uma maior fracção de quarks *estranhos*.

Agradecimentos

Em primeiro lugar, gostaria de agradecer aos meus orientadores, Dr. Pedro Costa e Profª. Dra. Constança Providência. Ao Doutor Pedro Costa, pelas incontáveis horas passadas em discussões e resolução de problemas, sem as quais, este trabalho nunca teria sido concretizado. À Professora Doutora Constança Providência, por me ter proposto este projecto, estando sempre disponível a ajudar com qualquer dúvida que surgisse. Sem a vossa ajuda e dedicação este trabalho não seria possível.

Gostaria de fazer um enorme agradecimento à minha família, ao meu pai por me ter mostrado a incrível magia dos (preciosos) ímanes, à minha mãe por estar sempre disposta a ajudar naquilo que eu precisasse e à minha irmã, por sempre acreditar em mim. O vosso amor incondicional fez de mim aquilo que sou hoje.

Um agradecimento especial à minha melhor amiga e amada Maria Guerra, por todos os momentos bons e menos bons que partilhamos. Obrigado por me fazeres sorrir mesmo quando achava que tal era impossível.

Ao André Ferreira, o meu amigo mais antigo, um enorme obrigado. A tua amizade, sinceridade e apoio ao longo de todos estes anos nunca serão esquecidos. Queria deixar também um agradecimento ao Bernardo Marques, Bruno Conceição e Eduardo Preto, pelo vosso enorme apoio ao longo dos anos.

Finalmente, agradeço também a todos os meus amigos e colegas de curso, tanto aos que estão perto como aos que, de momento, estão longe. Ter-vos ao meu lado ao longo desta jornada tornou o caminho até à meta muito mais interessante e enriquecedor.

Dedicado aos meus avós.

Contents

List of Figures

List of Tables

List of Abbreviations

BCS	**B**ardeen–**C**ooper-**S**chrieffer
EoS	**E**quation **o**f **S**tate
HA	**H**artree **A**pproximation
MFA	**M**ean **F**ield **A**pproximation
NJL	**N**ambu–**J**ona-**L**asinio
PNJL	**P**olyakov–**N**ambu–**J**ona-**L**asinio
QCD	**Q**uantum **C**hromo**d**ynamics
QED	**Q**uantum **E**lectro**d**ynamics
QFT	**Q**uantum **F**ield **T**heory
QHD	**Q**uantum **H**adro**d**ynamics
RMF	**R**elativistic **M**ean **F**ield
SLAC	**S**tanford **L**inear **Ac**celerator
TOV	**T**olman–**O**ppenheimer–**V**olkoff
VEV	**V**acuum **E**xpectation **V**alue

Units and Conventions

Throughout this work we will use Planck units:

$$c = \hbar = k_B = 1,$$

where c is the speed of light, $\hbar$ is the reduced Planck constant and k_B is the Boltzmann constant. In this system:

$$[lenght] = [time] = [energy]^{-1} = [mass]^{-1} = [temperature]^{-1}.$$

We can use the following conversion factor:

$$\hbar c = 197.326 \text{ MeV fm}.$$

The signature of the metric tensor $g_{\mu\nu}$ is defined as $(+,-,-,-)$. In Minkowski space the metric tensor is:

$$(\eta_{\mu\nu}) = \begin{pmatrix} 1 & 0 & 0 & 0 \\ 0 & -1 & 0 & 0 \\ 0 & 0 & -1 & 0 \\ 0 & 0 & 0 & -1 \end{pmatrix}.$$

The components of the four-vectors $k_\mu = (k_0, -\boldsymbol{k})$ and $k^\mu = (k^0, \boldsymbol{k})$ are such that:

$$kk = k_\mu k^\mu = k_0 k^0 - \boldsymbol{k} \cdot \boldsymbol{k}.$$

The derivatives in respect to covariant coordinates (x_μ) and contravariant coordinates (x^μ) are:

$$\partial^\mu \equiv \frac{\partial}{\partial x_\mu} = (\partial_t, -\boldsymbol{\nabla}),$$
$$\partial_\mu \equiv \frac{\partial}{\partial x^\mu} = (\partial_t, \boldsymbol{\nabla}).$$

The $N \times N$ unit matrix will be represented by $\mathbb{1}_{N\times N}$.

Chapter 1

Introduction

1.1 Motivations

There are four known fundamental forces of nature: the gravitational force, the electromagnetic force and the weak and strong nuclear forces.

Gravity, was the first fundamental force to receive a mathematical model by Isaac Newton which was later improved by Albert Einstein, with the theory of general relativity. With the advent of quantum field theory, classical electromagnetism gave origin to quantum electrodynamics (**QED**) that was later unified with the weak force to form the electroweak theory.

The strong force, due to its unprecedented properties like scaling, asymptotic freedom and confinement, was the last fundamental force to be mathematically formulated in the theory of quantum chromodynamics (**QCD**). In this theory, all hadrons are composed of quarks, more fundamental particles which carry colour charge, a new quantum number. However, all observed hadrons are colorless, which means some colour confinement mechanism must exist in **QCD**, although no analytic proof exists in that direction. This makes the strong force one of the few physical theories where we know the fundamental degrees of freedom, but are unable to calculate its low energy behaviour due to the strong coupling[1].

The **QCD** phase diagram is currently a widely studied topic in both experimental and theoretical physics. In Figure 1.1, some of the possible phases of hadronic matter are shown. As density (temperature) increases, the baryons start to overlap, the distance between quarks becomes very short, and distinct baryons gradually cease to exist. This means that hadronic matter goes through a transition to a new state of matter, the quark-gluon plasma. Chiral symmetry, an important symmetry of **QCD**, which is spontaneously broken in the vacuum, is expected to be restored at high densities and temperatures, meaning another transition. Is there some connection between the two phenomena? Are deconfinement and

[1] At low momentum transfers **QCD** is non-perturbative.

chiral symmetry restoration in some way connected? Does one transition induce the other? These are open questions, some of which are addressed in this work.

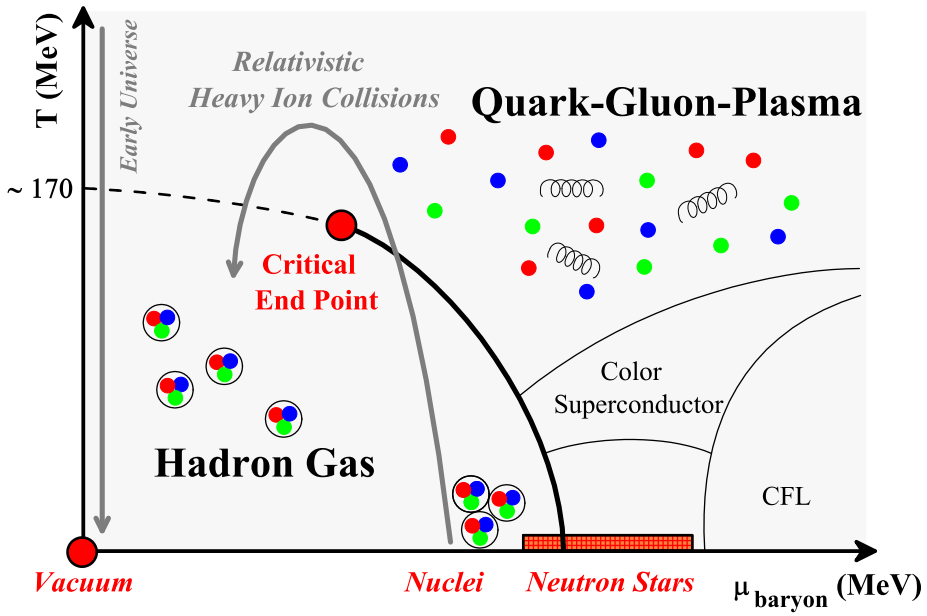

FIGURE 1.1: **QCD** phase diagram.

An interesting regime to study hadronic matter is the one present inside very compact stars. After all, compact stars are natural laboratories to investigate the properties of strongly interacting matter at high densities and small temperatures. Due to their very large central densities, several times larger than normal saturation density, it is possible that the deconfinement phase transition and the restoration of chiral symmetry can occur.

To study the behaviour of matter under extreme conditions such as in the interior of neutron stars, it is necessary to take into account that, at low densities the relevant degrees of freedom are hadrons while at high densities quark degrees of freedom are required. Thus, in the present work, a two phase model is used: the hadronic sector is described within the relativistic mean field model (**RMF**) and the quark sector is described by the Nambu−Jona-Lasinio (**NJL**) model in its $SU_f(2)$ and $SU_f(3)$ versions. Later, a modified version of the Polyakov−Nambu−Jona-Lasinio model[2], which describes the confinement-deconfinement transition will be used to describe the quark sector of the equation of state (**EoS**), giving us the ability to infer about the colour deconfinement inside compact stars.

Thus, in the first part of the present work (when the **NJL** is used to describe the quark sector) deconfinement means the change of degrees of freedom and the corresponding

[2]In these models the Polyakov loop effective field is not a dynamical degree of freedom due to the lack of dynamical term in the Lagrangian and the gluon dynamics is reduced to a chiral-point coupling between quarks, together with a simple static background field representing the Polyakov loop [1].

Lagrangian. In the second part, after the introduction of the **PNJL** model, deconfinement means the transition described by an order parameter like the Polyakov loop[3].

In fact, in the usual **PNJL**-type models at $T = 0$, the quark sector decouples from the gauge one, and the **PNJL** model is reduced to the **NJL** model [3]. However, to study colour deconfinement in compact stars, we will use improved models where explicit chemical potential dependencies in the Polyakov loop potential were added [4, 5]. The mean-field contribution of the Polyakov loop potential at $T = 0$ could be viewed as a μ-dependent modification of the Bag function which considers possible changes in the pressure of the gluon sector that are related to a partial melting of the gluon condensate at finite chemical potential [4].

Any **EoS** that tries to describe compact stars is subject to observational constraints. The two solar mass pulsars PSR J0348+0432 ($M = 2.01 \pm 0.04\ M_\odot$) [6] and PSR J1614-2230 (with the recently updated mass $1.928 \pm 0.017\ M_\odot$ [7, 8]) set a strong constraint on the high density **EoS** of hadronic matter, in particular, on the possible existence of exotic matter inside neutron stars, including hyperons, a kaon condensate or quark matter.

In [9] it was shown that within the $SU_f(3)$ **NJL** model a pure quark phase would not occur inside a neutron star, although quarks could exist as part of a non-homogenous quark-hadronic phase in the center of the star. Hadronic matter was described within a relativistic mean field model. Similar results are obtained when a Brueckner Hartree-Fock approach is applied to describe the hadronic phase, and even if a superconducting quark phase is considered for the quark phase [10]. At finite temperature it was possible to obtain pure quark matter in the star center for a particular hadronic **RMF** interaction, a non-linear Walecka model for the hadron matter and the MIT Bag model and **NJL** model for the quark matter [11]. A stable cold quark phase has been obtained within $SU_f(3)$ **NJL** model if it is assumed that the deconfinement occurs at the same chemical potential as the chiral phase transition[4] [12] . However, as in previous cases, no two solar mass hybrid stars are predicted. In [13] the fixing condition of the Bag constant was relaxed and the density of deconfinement, which is chosen beforehand, determines the constant. Stars with over two solar masses and a quark core in a color super-conducting phase are obtained if a vector interaction is added to the **NJL** Lagrangian density. However, in [14] the consequences of quark nucleation were studied and it is shown that not all two solar mass hybrid star configurations are populated after nucleation. In all the studies indicated, the **NJL** couplings are fitted to the meson vacuum properties, and in most cases the same interaction is used [15, 16]. In the present study, we will fix the model parameters imposing that the vacuum quark mass is ~ 313 MeV, corresponding to a 939 MeV nucleon mass. The vacuum values for the meson masses became slightly modified when compared with the usual parametrizations but, as we will show, this is an important condition when an

[3]The Polyakov loop is the order parameter for the deconfinement phase transition only in the limit where quark masses are infinitely heavy. However, in the presence of light quarks the rapid change of the Polyakov Loop is still an indication for the deconfinement [2].

[4]Which was achieved by the introduction of an effective Bag constant which guarantees that the chiral symmetry restoration coincides with the transition from the hadronic to the quark matter.

hybrid star is built from two independent **EoS**, one for the hadronic phase and another for the quark phase: both models should reproduce the same baryonic mass in the vacuum.

The role of the vector interaction (which excites vector and pseudovector mesons) in the properties of compact stars has been extensively studied by using the $SU_f(3)$ **NJL** model (see for example [4, 12–14, 17–23]). However, in spite of its importance, the value of the vector coupling, G_V, has not yet been definitively settled: its value in the vacuum can be determined by fitting the vector meson spectrum [24] but it is not evident that the value of G_V in the medium has to be the same as in the vacuum [25]. In fact, there is still no constraint for the choice of G_V in dense quark matter and its effects might be related to in-medium modifications [25].

Nevertheless, it is already well know that when G_V is positive the vector interaction can provide a repulsive interaction between quarks. This aspect is very important because it stiffens the **NJL** equation of state which is essential to describe high-mass hybrid stars (models with a larger G_V give larger maximum star masses [18]).

Concerning the effect of the vector interaction on **QCD** phase diagram, in the **NJL** model, namely on the chiral first-order transition, it has been shown that when G_V is positive (negative) it contributes to weaken (strengthen) the first-order transition due to repulsive (attractive) nature of the interaction [25]. Indeed, a repulsive interaction shrinks the first-order transition region, which forces the critical end point to occur at smaller temperatures, and as G_V increases the first-order transition occurs at higher baryonic chemical potentials. We will follow most of the literature and take G_V as a free parameter.

1.2 Quantum chromodynamics

The early attempts to construct field theories of the strong nuclear force were made in the 1950s [26]. Following Yukawa, the first attempts used nucleon fields (proton and neutron) which interact through a pion exchange. With the rapid discovery of different particles it became clear that the nucleons and pion were not special. All hadrons, *strange* baryons and mesons seemed to be equally fundamental.

In 1963 the quark model was introduced by Murray Gell-Mann and George Zweig to explain this increasingly complex list of stable hadrons and hadronic resonances. It was known that isospin was a very good symmetry of the strong interactions and that a $U(1)$ quantum number, a charge called *strangeness*, was conserved by them. These two symmetries were then combined into a larger symmetry group, flavour-$SU(3)$ ($SU_f(3)$), which was found to be conserved in a good approximation, but not exactly, by the strong interactions. The quark model describes mesons as bound states of a quark and an antiquark. Baryons are described as composed of three quarks, and antibaryons of three antiquarks. Since mesons have integer spin, while baryons have half-integer spin, it was further supposed that quarks have spin $1/2$. Three flavours of quarks (*up*, *down*, and *strange*) were necessary to explain

the spectrum of hadrons then known (today we know there are three more quarks, *charm*, *bottom*, and *top*).

In 1968, James Bjorken discovered what is known as scaling, a phenomenon in the deep inelastic scattering of light on hadrons: experimentally observed hadrons, when probed at high energies, behave as collections of point-like constituents.

Richard Feynman employed the concept of scaling in the parton model, to explain the quark composition of hadrons at high energies.

The predictions of the Bjorken scaling and the parton model were confirmed in experiments at **SLAC** (Stanford Linear Accelerator), in which quarks were "seen" for the first time.

However, no quantum field theory at the time explained scaling. To explain the experiments performed at **SLAC**, David Gross and Frank Wilczek conceived a plan to prove that local field theory could not explain scaling. First, they proved that the vanishing of the effective coupling at short distances (asymptotic freedom), was necessary to explain scaling. In **QED** the effective charge grows larger at short distances; for the strong interaction, the effective coupling is contrary to **QED**, decreases at short distances. Second, they would prove that no local field theory was asymptotically free. However, they discovered that the theory of Chen-Ning Yang and Robert Mills was asymptotically free. **QCD**, Yang-Mills with quarks, is consistent with all the properties of the strong interactions.

It is based on the gauge group $SU_c(3)$, the special unitary group in three (complex) dimensions, whose elements are the set of unitary 3×3 matrices with determinant one [27]. Since there are nine linearly independent unitary complex matrices, one of which has determinant -1, there are a total of eight independent directions in this matrix space, corresponding to eight different generators, indicating that they are in the adjoint representation[5] of $SU_c(3)$. The **QCD** Lagrangian is:

$$\mathscr{L} = \overline{\psi}^i \left[(i\gamma^\mu)(D_\mu)_{ij} - m_{ij} \right] \psi^j - \frac{1}{4} \mathcal{F}^a_{\mu\nu} \mathcal{F}^{a\mu\nu}, \tag{1.1}$$

where ψ^i is a quark field with colour index $i = 1, .., N_c$, indicating that they are in the fundamental representation[6] of $SU_c(3)$. $\mathcal{F}^a_{\mu\nu}$ is the gluon field strength tensor for a gluon with colour index a:

$$\mathcal{F}^a_{\mu\nu} = \partial_\mu \mathcal{A}^a_\nu - \partial_\nu \mathcal{A}^a_\mu + g_s f_{abc} \mathcal{A}^b_\mu \mathcal{A}^c_\nu, \tag{1.2}$$

with $\mathcal{A}^a_\mu$ the gluon field with colour index a, g_s the strong coupling constant[7] and f_{abc} are the totally antisymmetric structure constants of $SU_c(3)$, defined by:

$$\left[\lambda^a, \lambda^b \right] = 2i f^{abc} \lambda^c, \tag{1.3}$$

[5] The dimension of the adjoint representation is equal to the number of generators.
[6] The dimension of the fundamental representation is the degree of the group, $N = 3$ for $SU_c(3)$.
[7] Related to α_s through $g_s^2 = 4\pi\alpha_s$.

here λ^a are the hermitian and traceless Gell-Mann matrices of $SU_c(3)$. Finally, D_μ is the covariant derivative in **QCD**:

$$(D_\mu)_{ij} = \delta_{ij}\partial_\mu - ig_s\frac{\lambda^a_{ij}}{2}\mathcal{A}^a_\mu, \tag{1.4}$$

m_{ij} is a colour-independent phenomenological mass matrix in flavour space, that can be brought to diagonal form through flavour-mixing transformations, so that:

$$\overline{\psi}^i m_{ij}\psi^j = \hat{m}_f\overline{\psi}^i\psi^i. \tag{1.5}$$

The $\hat{m}_f$ can be estimated through current algebra relations, after all, they are not observables of **QCD** because of the confinement properties of the theory. These are called the quark current masses (see Table 1.1), generated by the Higgs mechanism.

Quark name	Symbol	Mass [28]
up	u	$2.3^{+0.7}_{-0.5}$MeV
down	d	$4.8^{+0.5}_{-0.3}$MeV
strange	s	95 ± 5MeV
charm	c	1.275 ± 0.025GeV
bottom	b	4.18 ± 0.03GeV
top	t	173.21 ± 0.51GeV

TABLE 1.1: The u,d and s quark masses are estimates from a mass-independent subtraction scheme such as $\overline{MS}$ at a scale $\mu \approx 2$GeV. The c and b quark masses are the "running" masses in the $\overline{MS}$ scheme. The t mass is taken from direct measurements.

QCD is also invariant under CPT (charge conjugation, parity transformation and time reversal) transformations however, from the point of view of gauge invariance, the **QCD** Lagrangian could also involve a term of the type:

$$\mathscr{L}_\theta = \frac{g_s^2 N_f}{64\pi^2}\epsilon^{\mu\nu\lambda\sigma}\mathcal{F}^a_{\mu\nu}\mathcal{F}^a_{\lambda\sigma}, \tag{1.6}$$

with N_f being the number of flavours and $\epsilon^{\mu\nu\lambda\sigma}$ denotes the totally antisymmetric Levi-Civita tensor. This term is called θ-term and implies an explicit P and CP violation of the strong interactions. However, the present empirical information indicates that this term is small [29].

To understand the effect of the running coupling constant we introduce the β function from the renormalization group, $\beta(\alpha)$, which encodes the dependence of a coupling parameter α, on the energy scale μ, of a given physical process described by a quantum field theory. It is defined as:

$$\beta(\alpha) = \frac{d\alpha(Q^2)}{d\ln\alpha(Q^2)} = -\left(\beta_0\alpha^2 + \beta_1\alpha^3 + \beta_2\alpha^4 + ...\right). \tag{1.7}$$

To calculate the propagator loop correction in **QCD**, we do not only have to consider quark loops, but also gluon loops (see Figure 1.2). The quark loop will give rise to a positive

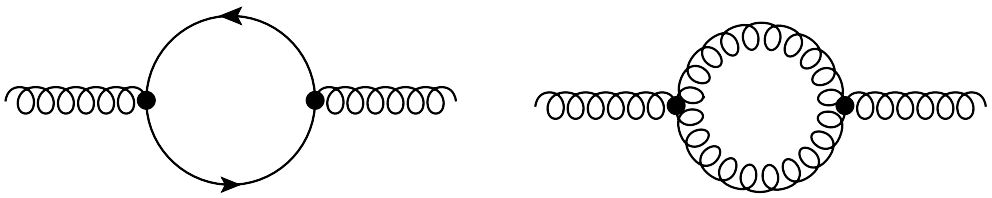

FIGURE 1.2: Feynman diagram for the quark loop on the left and for the gluon loop on the right.

contribution to the beta function (screening) while the gluon loop contribution will be negative (antiscreening). The formula for the one-loop running coupling constant in **QCD** is:

$$\alpha_s\left(Q^2\right) = \frac{\alpha_s\left(\mu^2\right)}{1+\beta_0\alpha_s\left(\mu^2\right)\ln\left(Q^2/\mu^2\right)} \quad \text{with} \quad \beta_0 = \frac{11N_c - 2N_f}{12\pi}. \tag{1.8}$$

For the standard model the β function (to one loop) is:

$$\beta = -7/4\pi < 0. \tag{1.9}$$

This means that the coupling constant decreases with increasing Q^2 after all, once $\beta_0 > 0$, when $Q^2 \longrightarrow \infty$, $\alpha_s \longrightarrow 0$. This causes the quarks inside hadrons to behave more or less as free particles, when probed at large energies. On the other hand, at increasing distance the coupling becomes so strong that it is impossible to isolate a quark from a hadron (it becomes energetically more favourable to create a quark-antiquark pair). This mechanism is called confinement. Confinement is verified in *lattice* **QCD** calculations [30] but has not yet been mathematically proven from first principles [31]. All continuous symmetries of **QCD** are summarized in Table 1.2.

Symmetry	Transformation	Current	Realization
$SU_V(N_f)$	$\psi \to e^{-i\Gamma^i\Theta^i/2}\psi$	$j^i_\mu = \overline{\psi}\gamma_\mu\Gamma^i\psi$	approximate isospin, Eightfold Way
$SU_A(N_f)$	$\psi \to e^{-i\Gamma^i\Theta^i\gamma_5/2}\psi$	$j^i_\mu = \overline{\psi}\gamma_\mu\gamma_5\Gamma^i\psi$	spontaneously broken Nambu-Goldstone mode
$U_V(1)$	$\psi \to e^{-i\alpha}\psi$	$j_\mu = \overline{\psi}\gamma_\mu\psi$	conserved baryon number conservation
$U_A(1)$	$\psi \to e^{-i\alpha\gamma_5}\psi$	$j_\mu = \overline{\psi}\gamma_\mu\gamma_5\psi$	$U_A(1)$ puzzle instanton induced effects
$SU_c(3)$	$\psi \to e^{-i\lambda^i\Theta^i/2}\psi$	$j^i_\mu = \overline{\psi}\gamma_\mu\lambda^i\psi$	conserved hidden through confinement

TABLE 1.2: **QCD** continuous symmetries and respective conserved currents and realization. Here, Γ^i are N_f^2 operators that form the $SU\left(N_f\right)$ algebra and λ^i are the Gell-Man matrices of $SU_c(3)$.

Intermediate-energy hadronic physics which runs over the MeV − GeV energy range, should be well described by the dynamics of the lowest mass quarks u, d and s. Considering these

three flavours of quarks, the quark field can be written as:

$$\psi^T = (\psi_u \;\; \psi_d \;\; \psi_s)\,, \tag{1.10}$$

and a diagonal mass matrix $\hat{m} = diag\,(m_u, m_d, m_s)$. For massless quarks, the Lagrangian density (1.1) is invariant under the transformation

$$\psi \to \psi' = U\psi, \tag{1.11}$$

where U is a global transformation that belongs to the group:

$$U_V(3) \otimes U_A(3) = SU_V(3) \otimes SU_A(3) \otimes U_V(1) \otimes U_A(1). \tag{1.12}$$

The transformations under $U_V(1)$ and $SU_V(3)$ (which include the γ^μ matrix but not the γ_5 matrix) are related to baryon number conservation and isospin conservation, respectively. While the first is always conserved in nature, the second is only approximately conserved due to different quark masses (Eightfold Way). This symmetry is almost respected in the two flavour case ($m_u \approx m_d$) but it is more severely broken in the three flavour case. One can see this explicitly, by projecting the mass matrix on the eight λ^a matrices of $SU_f(3)$ plus the identity matrx λ^0, to obtain:

$$\hat{m}_f = \frac{m_u + m_d + m_s}{\sqrt{6}}\lambda_0 + \frac{m_u - m_d}{2}\lambda_3 + \frac{(m_u + m_d)/2 - m_s}{\sqrt{3}}\lambda_8. \tag{1.13}$$

Transformations under $SU_A(3)$ and $U_A(1)$ (which include the γ^5 matrix) are the so-called chiral or axial symmetries. Axial transformations change the parity of a given state. Thus, a Wigner-Weyl[8] realization of $SU_A(3)$ symmetry would require that each isospin multiplet be accompanied by degenerate multiplet with opposite parity. However, such multiplet is not observed in nature, which means that $SU_A(3)$ should not be directly realized by **QCD**. This symmetry is realized in the Nambu-Goldstone[9] mode via chiral symmetry breaking, giving origin to the pion octet. Likewise, a Wigner-Weyl realization of $U_A(1)$ would imply a parity partner to all hadrons which again, is not verified in nature. Thus, another Goldstone boson, a pseudoscalar meson with zero isospin is expected, with roughly the same mass as the pions. Nevertheless, no boson is observed, giving origin to the $U_A(1)$ puzzle: what happened to the Goldstone boson? The problem was solved by Gerard 't Hooft [32, 33], who showed that due to instanton induced effects, the $U_A(1)$ symmetry should not result in physical manifestations.

One can introduce the right and left projection operators P_R and P_L:

$$P_{R,L} = \frac{1 \pm \gamma_5}{2}, \tag{1.14}$$

[8]Wigner-Weyl realization of a symmetry: invariance of the Lagrangian density under a symmetry group should lead to a degeneracy of the energy eigenstates corresponding to irreducible representations of the group.

[9]Nambu-Goldstone realization of a symmetry: non invariance of the vacuum under the symmetry operation. In this case the Goldstone theorem implies the existence of massless spinless particles.

having the following properties:

$$P_R + P_L = \mathbb{1}, \tag{1.15}$$

$$(P_{R,L})^N = P_{R,L} \quad \text{with} \quad N \geq 1, \tag{1.16}$$

$$P_{R,L}P_{L,R} = 0. \tag{1.17}$$

Projecting the quark fields ψ and $\overline{\psi}$, one obtains the so-called right- and left-handed fields,

$$\psi_R = P_R\psi = \frac{1+\gamma_5}{2}\psi, \tag{1.18}$$

$$\psi_L = P_L\psi = \frac{1-\gamma_5}{2}\psi, \tag{1.19}$$

for massless quarks the Lagrangian density becomes invariant under a global transformation U, that belongs to the group:

$$U_R(3) \otimes U_L(3) = SU_R(3) \otimes SU_L(3) \otimes U_R(1) \otimes U_L(1), \tag{1.20}$$

which is just another decomposition of the group in (1.12). However, the quark mass term (1.5), mixes right- and left-handed fields:

$$\hat{m}_f\overline{\psi}\psi = \hat{m}_f\left(\overline{\psi}_R\psi_L + \overline{\psi}_L\psi_R\right), \tag{1.21}$$

breaking explicitly the chiral symmetry of the theory. The existence of different quark masses will give rise to the physical pseudoscalar meson spectra i.e., will give mass to the Goldstone bosons (pion octet).

1.3 Effective models

Due to asymptotic freedom, at high momentum transfers **QCD** is a perturbative theory. However, at low momentum transfers, perturbation theory is not plausible. In this regime, the options are limited: one can use *lattice* **QCD** and endure the high computing power demand[10]; non-perturbative solutions of the Dyson-Schwinger equations; or use an effective field theory of **QCD**. In the present work, the latter strategy is used.

Effective theories try to isolate the relevant physics of some processes within a physical phenomenon, by creating mathematically tractable models that serve to accentuate its features. In the case of field theories, a very powerful tool in the construction of these effective models are the symmetries (and their possible breaking) of the original theory. However, symmetry is not sufficient to determine the form of the effective interactions. They are further dictated by phenomenology and simplicity.

Throughout history, several "fundamental" theories were later discovered to be effective theories. **QED** and even the standard model of particle physics, are effective field theories

[10]For finite chemical potential *lattice* **QCD** is not even defined, due to the famous sign problem [34].

because they break down at the mass of the W boson and the gravity energy scale, respectively. Thus, the use of effective theories, i.e., theories that work within a certain energy scale, is completely justified.

An effective chiral theory of **QCD** should highlight all of its chiral properties: (approximate) chiral symmetry at the Lagrangian level and some mechanism for its spontaneous break[11]; invariance under $SU_R(N_f) \otimes SU_L(N_f)$ and an asymmetrical vacuum, reducing the symmetry to $SU(N_f)$ and the existence of $N_f^2 - 1$ Goldstone bosons.

1.4 Discussion layout

The structure of this Thesis is as follows:

In Chapter 2, the objective is to introduce mathematical and physical techniques used throughout the work, setting-up the foundation.

In Chapter 3, a small review of the Nambu–Jona-Lasinio model is made and a quark (**EoS**) is derived for two and three flavours of quarks and several vector interactions.

In Chapter 4, the formation and composition of neutron stars are mentioned. It is given a very brief review of quantum hadrodynamics (**QHD**) and the calculation of the hadronic **EoS** within $(\sigma - \omega)$ model with self-interactions and isospin force. The Gibbs construction and phenomenological Bag constant are introduced within the hybrid approach to neutron stars. A brief introduction to general relativity and the Tolman-Oppenheimer-Volkoff equations (**TOV**) is given.

In Chapter 5, results are presented and discussed.

In Chapter 6, the $Z(3)$ symmetry of discrete **QCD** and its relation to colour deconfinement is laid out. The Polyakov−Nambu–Jona-Lasinio model is introduced, as well as a modified **PNJL** version with an explicit dependence on the chemical potential. Calculation of the **EoS** for this modified model is made and results are presented.

Finally, in Chapter 7, conclusions are drawn and further work is proposed.

[11] Dynamical spontaneous symmetry breaking in the case of the **NJL** model.

Chapter 2

Thermal Field Theory

2.1 Quantum field theory

Quantum field theory (**QFT**) occupies a central role in the description of the laws of nature [35]. It has the ability of describing the creation and annihilation of particles and an incredible predictive power when compared to empirical results, making **QFT** an essential tool in modern physics [36].

Within this formalism, the classical action can be quantized through the canonical quantization process, in which the degrees of freedom of the system, fields $\phi_a(x)$ and respective conjugate momenta $\Pi^a(x)$ are promoted to operators that act on Hilbert spaces and must obey (anti)commutation relations. Since the degrees of freedom are functions of space-time, we are dealing with infinite degrees of freedom [36]. Fields whose quanta are integer spin particles must obey the following (equal time) commutation relations

$$[\phi_a(t,\boldsymbol{x}),\phi_b(t,\boldsymbol{y})] = \left[\Pi^a(t,\boldsymbol{x}),\Pi^b(t,\boldsymbol{y})\right] = 0, \tag{2.1}$$

$$\left[\phi_a(t,\boldsymbol{x}),\Pi^b(t,\boldsymbol{y})\right] = i\delta^{(3)}(\boldsymbol{x}-\boldsymbol{y})\delta^b_a. \tag{2.2}$$

Fields whose quanta are half-integer spin particles, must obey anticommutation relations:

$$\{\phi_a(t,\boldsymbol{x}),\phi_b(t,\boldsymbol{y})\} = \left\{\Pi^a(t,\boldsymbol{x}),\Pi^b(t,\boldsymbol{y})\right\} = 0, \tag{2.3}$$

$$\left\{\phi_a(t,\boldsymbol{x}),\Pi^b(t,\boldsymbol{y})\right\} = \delta^{(3)}(\boldsymbol{x}-\boldsymbol{y})\delta^b_a. \tag{2.4}$$

A more elegant approach to field quantization, is the path integral formalism, which was first introduced by Richard Feynman for quantum mechanics [37]. In this formalism, the amplitude between an initial and a final state in the Heisenberg picture is given by the weighted sum of all possible paths connecting the two points,

$$\langle x_f|\, e^{-i(t_f-t_i)\hat{\mathcal{H}}}\,|x_i\rangle = \mathcal{N}\int \mathcal{D}x\; e^{i\mathcal{S}[x]}, \tag{2.5}$$

where the functional integration is made over all degrees of freedom. $\hat{\mathcal{H}}$ is the Hamiltonian of the system, $\mathcal{N}$ is an irrelevant normalization constant and $\mathcal{S}$ is the classical action, defined as:

$$\mathcal{S}[x] = \int_{t_i}^{t_f} dt\, \mathscr{L}(x(t), \dot{x}(t)). \tag{2.6}$$

Here, $\mathscr{L}(x(t), \dot{x}(t))$ is the Lagrangian density of the system.

When generalizing the formalism to fields the transition amplitude is given by:

$$\langle \phi |\, e^{-it_f \hat{\mathcal{H}}}\, | \phi \rangle = \mathcal{N} \int_{\phi(0,\boldsymbol{x})}^{\phi(t_f,\boldsymbol{x})} \mathcal{D}\phi\; e^{i\mathcal{S}[\phi]}, \tag{2.7}$$

where the action is:

$$\mathcal{S}[\phi] = \int_0^{t_f} dt \int d^3x\; \mathscr{L}\left(\phi, \partial_\mu \phi\right). \tag{2.8}$$

We are interested in the vacuum to vacuum transition amplitude in the presence of an external source, $J(x)$, known as the generating functional $\mathcal{Z}[J]$, which generates time ordered correlation functions, or Green's functions of the theory [38]:

$$\mathcal{Z}[J] = \mathcal{N} \int \mathcal{D}\phi\; e^{i\mathcal{S}[\phi] + i\int d^4x\; J(x)\phi(x)}. \tag{2.9}$$

The irrelevant constant $\mathcal{N}$ is infinite due to the infinite degrees of freedom of the system and is chosen to be such that, $\mathcal{Z}[0] = 1$.

The generating functional, being a functional of the source $J(x)$, should be invariant under an infinitesimal change of the field ϕ (supposing that the integration measure is invariant likewise[1])

$$\frac{\delta \mathcal{Z}[J]}{\delta \phi(x)} = 0, \tag{2.10}$$

which implies that,

$$\frac{\delta \mathcal{S}[\phi]}{\delta \phi(x)} = -J(x). \tag{2.11}$$

Consider the functional defined by the phase of the generating functional $\mathcal{Z}[J]$:

$$\mathcal{W}[J] = -i \ln \mathcal{Z}[J], \tag{2.12}$$

which is known as the generating functional of the fully connected Green's functions (connected Feynman's graphs). The n-point connected correlation functions of the theory can be obtained by calculating functional derivatives of the above functional ($\mathcal{T}$ is the time

[1] The non-invariance of the integration measure plays a large role in the study of anomalies.

ordering operator):

$$\left.\frac{\delta^n \mathcal{W}[J]}{\delta J(x_1)...\delta J(x_n)}\right|_{J=0} = \frac{(-i)^n}{\mathcal{Z}[J]} \left.\frac{\delta^n \mathcal{Z}[J]}{\delta J(x_1)...\delta J(x_n)}\right|_{J=0} = \langle 0| \mathcal{T}\left[\phi(x_1)...\phi(x_n)\right] |0\rangle . \quad (2.13)$$

Setting $n = 1$ in (2.13), gives the definition of the 1-point correlation function.When $J(x)$ is non zero, the expectation value of the field operator in the vacuum can be interpreted as a functional of the source:

$$\frac{\delta \mathcal{W}[J]}{\delta J(x)} = \frac{-i}{\mathcal{Z}[J]} \frac{\delta \mathcal{Z}[J]}{\delta J(x)} = \langle 0| \phi(x) |0\rangle_J = \phi_c(x). \quad (2.14)$$

The expectation value of the field in the vacuum is called the classical field, $\phi_c(x)$. When the source vanishes, due to Poincaré invariance and uniqueness of the vacuum state in the Hilbert space, the classical field must be a constant [38] (zero if there are no spontaneous symmetry breaking and non-zero if any symmetry was spontaneously broken).

$$J(x) \to 0 \Rightarrow \phi_c(x) \to \phi_c. \quad (2.15)$$

The "conjugate" relation between the source and the classical field in Equation (2.14), suggests the definition of another functional, independent from the source, through a Legendre transformation. This functional is called the effective action:

$$\Gamma[\phi_c] = \mathcal{W}[J] - \int d^4x \; J(x)\phi_c(x). \quad (2.16)$$

This functional generates the one particle irreducible (1PI) Green's functions, i.e., the ones that correspond to Feynman diagrams which cannot be disconnected when an internal line is removed. In **QFT**, being able to calculate all the 1PI's means solving the theory.

2.1.1 The background field method and mean field approximation

The background field method [39] is a useful method to calculate the effective action by Taylor expanding the field around its classical value. One starts by splitting the field into a classical background field $\phi_c(x)$ and a field $\eta(x)$ containing quantum fluctuations:

$$\phi(x) = \phi_c(x) + \eta(x). \quad (2.17)$$

The phase of the generating functional, can be written as:

$$\begin{aligned} \mathcal{W}[J] = & \int d^4x \left[\mathscr{L}[\phi_c] + J(x)\phi_c(x)\right] \\ & + \int d^4x \eta(x) \left[\left.\frac{\delta \mathscr{L}[\phi]}{\delta \phi(x)}\right|_{\phi=\phi_c} + J(x)\right] \\ & + \int d^4x d^4y \; \eta(x)\eta(y) \frac{1}{2} \left.\frac{\delta \mathscr{L}[\phi]}{\delta \phi(x)\delta \phi(y)}\right|_{\phi=\phi_c} + \mathcal{O}\left(\eta^3\right). \end{aligned} \quad (2.18)$$

The first term is independent from the quantum fluctuations $\eta(x)$ and the second term in the expansion is zero due to Equation (2.11). Substituting this expansion in (2.12), yields the following generating functional (to second order in $\eta(x)$):

$$\mathcal{Z}[J] \simeq \mathcal{N}\, e^{i\mathcal{S}[\phi_c]+i\int d^4x J(x)\phi_c(x)} \int \mathcal{D}\eta\, e^{\frac{i}{2}\int d^4x d^4y\, \eta(x)\eta(y)\, \frac{\delta\mathscr{L}[\phi]}{\delta\phi(x)\delta\phi(y)}\Big|_{\phi=\phi_c}}. \tag{2.19}$$

The path integral over the η field has a gaussian form and can be computed explicitly:

$$\int \mathcal{D}\eta\, e^{\frac{i}{2}\int d^4x d^4y\, \eta(x)\eta(y)\, \frac{\delta\mathscr{L}[\phi]}{\delta\phi(x)\delta\phi(y)}\Big|_{\phi=\phi_c}} \simeq \det{}^{\mp\frac{1}{2}} \left[\frac{\delta\mathcal{S}[\phi]}{\delta\phi^2}\Big|_{\phi=\phi_c}\right]. \tag{2.20}$$

The negative or positive power of the determinant, depends on whether the fields are bosonic or fermionic. Substituting this expression in Equation (2.19) yields:

$$\mathcal{Z}[J] \simeq \mathcal{N}\, e^{i\mathcal{S}[\phi_c]+i\int d^4x J(x)\phi_c(x)}\, \det{}^{\mp\frac{1}{2}} \left[\frac{\delta\mathcal{S}[\phi]}{\delta\phi^2}\Big|_{\phi=\phi_c}\right]. \tag{2.21}$$

Plugging this expression in Equation (2.12), gives the effective action to second order in η:

$$\Gamma[\phi_c] \simeq \mathcal{S}[\phi_c] \pm \frac{i}{2} \ln\det \left[\frac{\delta\mathcal{S}[\phi]}{\delta\phi^2}\Big|_{\phi=\phi_c}\right]. \tag{2.22}$$

Where the positive sign is for bosonic fields and the negative sign is for fermionic fields. This equation represents the one-loop approximation of the effective action [40]. The first term is simply the classical action and the second term incorporates the first quantum corrections of the theory (loop effects). The Hartree (**HA**) or mean field approximation (**MFA**), consists on neglecting the second term and setting the effective action to be:

$$\Gamma[\phi_c]_{\text{MFA}} = \mathcal{S}[\phi_c]. \tag{2.23}$$

2.2 Finite temperature and density

Conventional **QFT** is formulated at zero temperature and density, and even though its theoretical predictions are in agreement with empirical results in reality, natural phenomena do not occur at these regimes. Temperature and density can be included within the **QFT** formalism to explain condensed matter and nuclear matter in laboratory conditions and it allows the study of several phenomena, like the early Universe, inflation, neutron stars, the electroweak transition, **QCD** phase diagram, etc.

The grand canonical ensemble describes a system in contact with a heat reservoir, allowing the exchange of energy and particles with it. The temperature, volume and chemical potentials are fixed. In the grand canonical ensemble the partition function is given by:

$$\mathcal{Z}(\beta) = \text{tr}\left[e^{-\beta(\hat{\mathcal{H}}-\mu_i\hat{N}_i)}\right], \tag{2.24}$$

where $\mathcal{H}$ is the system Hamiltonian and $\hat{N}_i$ is a set of conserved number operators (baryonic number, electric charge...). The average value of an observable $\hat{\mathcal{O}}$ is:

$$\langle\hat{\mathcal{O}}\rangle = \frac{\mathrm{tr}\left[e^{-\beta\left(\hat{\mathcal{H}}-\mu_i\hat{N}_i\right)}\hat{\mathcal{O}}\right]}{\mathrm{tr}\left[e^{-\beta\left(\hat{\mathcal{H}}-\mu_i\hat{N}_i\right)}\right]} = \mathcal{Z}(\beta)^{-1}\,\mathrm{tr}\left[e^{-\beta\left(\hat{\mathcal{H}}-\mu_i\hat{N}_i\right)}\hat{\mathcal{O}}\right]. \tag{2.25}$$

The grand canonical potential (up to an irrelevant constant) is defined as

$$\Omega = -\frac{1}{\beta V}\ln\left[\mathcal{Z}(\beta)\right] = -\frac{T}{V}\ln\left[\mathcal{Z}(\beta)\right]. \tag{2.26}$$

All thermodynamic quantities of interest like the pressure (P), particle density (ρ_i), entropy density (S), and energy density (ϵ), can be calculated from the grand canonical potential, using the following relations [41–43]:

$$P = \frac{\partial}{\partial V}\left(T\ln\mathcal{Z}\right) = -\frac{\partial}{\partial V}\left(V\Omega\right), \tag{2.27}$$

$$\rho_i = \frac{1}{V}\frac{\partial}{\partial\mu_i}\left(T\ln\mathcal{Z}\right) = -\frac{\partial\Omega}{\partial\mu_i}, \tag{2.28}$$

$$S = \frac{1}{V}\frac{\partial}{\partial T}\left(T\ln\mathcal{Z}\right) = -\frac{\partial\Omega}{\partial T}, \tag{2.29}$$

$$\epsilon = -P + TS + \mu_i\rho_i. \tag{2.30}$$

2.2.1 The Matsubara formalism

We are now able to find the path integral representation of the partition function. Using a complete basis of the coordinate operator, for zero chemical potential[2], the partition function can be written as:

$$\mathcal{Z}(\beta) = \mathrm{tr}\left[e^{-\beta\hat{\mathcal{H}}}\right] = \int dx\,\langle x|\,e^{-\beta\hat{\mathcal{H}}}\,|x\rangle\,. \tag{2.31}$$

Comparing Equations (2.5) and (2.31), one recognizes that there is a great similarity between the two [44]. The time interval $[t_i, t_f]$ in the transition amplitude seems to take the role of β in the partition function. The Matsubara formalism, consists of making a transformation of the type $t \to -i\tau$ and identifying the interval $[t_i, t_f]$ with the interval $[0, \beta]$. This transformation (see Figure 2.1), which rotates the integration in the complex plane by 90º, is called a Wick rotation [44].

[2] Whenever there is a conserved charge $\mathcal{N}$, one must modify the system Hamiltonian by adding a chemical potential μ: $\hat{\mathcal{H}} \to \hat{\mathcal{H}} - \mu\hat{\mathcal{N}}$. The chemical acts like a Lagrange multiplier.

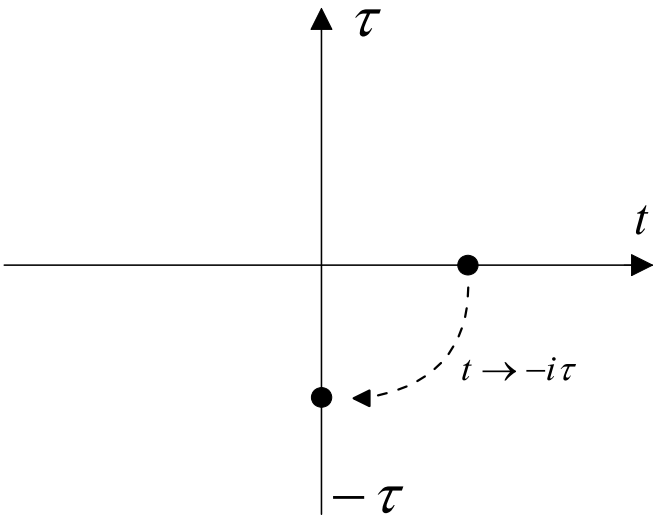

FIGURE 2.1: Wick rotation.

Using the Matsubara formalism, one can write the partition function of a field $\phi(-i\tau, \boldsymbol{x})$ as:

$$\mathcal{Z}(\beta) = \mathcal{N} \int_{\phi(0,\boldsymbol{x})}^{\phi(\beta,\boldsymbol{x})} \mathcal{D}\phi \, e^{\mathcal{S}_E[\phi]}, \tag{2.32}$$

$$S_E[\phi] = \int_0^\beta d\tau \int_V d^3x \, \mathscr{L}(\phi, i\partial_\tau \phi, \boldsymbol{\nabla}\phi). \tag{2.33}$$

After the Wick rotation, the norm between four-vectors is given by the Euclidean norm. Therefore, we denote the classical action by $\mathcal{S}_E$. In some sense, this procedure consists of a backwards analytically continuation of the action in Minkowski to an action in Euclidean space. In this process one needs to be careful to not cross any poles.

In **QFT**, the 2-point correlation function yields the propagator or Green function of the theory. At finite temperature one can define the 2-point thermal Green function as (using Equation (2.25)):

$$\langle \phi(\tau_1, \boldsymbol{x}) \, \phi(\tau_2, \boldsymbol{y}) \rangle = G_\beta(\tau_1, \boldsymbol{x}, \tau_2, \boldsymbol{y}) = \mathcal{Z}^{-1} \operatorname{tr}\left[e^{-\beta\hat{\mathcal{H}}} \mathcal{T}\left[\phi(\tau_1, \boldsymbol{x}) \phi(\tau_2, \boldsymbol{y})\right] \right], \tag{2.34}$$

where $\mathcal{T}$ is the time ordering operator, that acts as:

$$\mathcal{T}\left[\phi(\tau_1, \boldsymbol{x}) \phi(\tau_2, \boldsymbol{y})\right] = \begin{cases} \phi(\tau_1, \boldsymbol{x}) \phi(\tau_2, \boldsymbol{y}), & \text{if } \tau_1 > \tau_2 \\ \pm \phi(\tau_1, \boldsymbol{x}) \phi(\tau_2, \boldsymbol{y}), & \text{if } \tau_1 < \tau_2 \end{cases}, \tag{2.35}$$

where the negative sign arises from the anticommutation relations for fermionic fields in Equation (2.3).

We are interested in knowing what happens to the 2-point thermal Green function after a period β in imaginary time. Thus for two different instants and positions, with $0 < \tau < \beta$,

the thermal propagator is [45]:

$$\begin{aligned} G_\beta(\tau,\boldsymbol{x},0,\boldsymbol{y}) &= \mathcal{Z}^{-1}\,\mathrm{tr}\left[e^{-\beta\hat{\mathcal{H}}}\mathcal{T}\left[\phi(\tau,\boldsymbol{x})\phi(0,\boldsymbol{y})\right]\right] = \\ &= \mathcal{Z}^{-1}\,\mathrm{tr}\left[e^{-\beta\hat{\mathcal{H}}}\phi(\tau,\boldsymbol{x})\phi(0,\boldsymbol{y})\right] = \\ &= \mathcal{Z}^{-1}\,\mathrm{tr}\left[\underbrace{e^{-\beta\hat{\mathcal{H}}}e^{\beta\hat{\mathcal{H}}}}_{=\mathbb{1}}\phi(0,\boldsymbol{y})e^{-\beta\hat{\mathcal{H}}}\phi(\tau,\boldsymbol{x})\right]. \end{aligned} \tag{2.36}$$

Where we have used the cyclic properties of the trace operation and added a unit matrix written as $\mathbb{1} = e^{-\beta\hat{\mathcal{H}}}e^{\beta\hat{\mathcal{H}}}$. We can use [38]:

$$\hat{\mathcal{O}}_H(t) = e^{it\hat{\mathcal{H}}}\hat{\mathcal{O}}(t=0)e^{-it\hat{\mathcal{H}}}, \tag{2.37}$$

which relates an operator in the Heisenberg picture $\hat{\mathcal{O}}_H(t)$, with an operator in the Schrödinger picture $\hat{\mathcal{O}}(t=0)$, and write:

$$\begin{aligned} G_\beta(\tau,\boldsymbol{x},0,\boldsymbol{y}) &= \mathcal{Z}^{-1}\,\mathrm{tr}\left[e^{-\beta\hat{\mathcal{H}}}\underbrace{e^{\beta\hat{\mathcal{H}}}\phi(0,\boldsymbol{y})e^{-\beta\hat{\mathcal{H}}}}_{=\phi(\beta,\boldsymbol{y})}\phi(\tau,\boldsymbol{x})\right] \\ &= \mathcal{Z}^{-1}\,\mathrm{tr}\left[e^{-\beta\hat{\mathcal{H}}}\phi(\beta,\boldsymbol{y})\phi(\tau,\boldsymbol{x})\right]. \end{aligned} \tag{2.38}$$

Writing back the time ordering operator, the thermal propagator yields:

$$\begin{aligned} G_\beta(\tau,\boldsymbol{x},0,\boldsymbol{y}) &= \mathcal{Z}^{-1}\,\mathrm{tr}\left[e^{-\beta\hat{\mathcal{H}}}\phi(\beta,\boldsymbol{y})\phi(\tau,\boldsymbol{x})\right] = \\ &= \pm\mathcal{Z}^{-1}\,\mathrm{tr}\left[e^{-\beta\hat{\mathcal{H}}}\mathcal{T}\left[\phi(\tau,\boldsymbol{x})\phi(\beta,\boldsymbol{y})\right]\right] = \\ &= \pm G_\beta(\tau,\boldsymbol{x},\beta,\boldsymbol{y}). \end{aligned} \tag{2.39}$$

Where, once again, the negative sign represents a fermionic field and the positive sign a bosonic field. From this we can conclude that the 2-point thermal Green function is a periodic function for bosons and an antiperiodic function for fermions.

Due to the (anti)periodicity of the thermal propagators, the fields are only allowed to take discrete frequencies. In order to find these frequencies, we Fourier transform the thermal propagator:

$$G_\beta(\tau) = \frac{1}{\beta}\sum_n e^{-i\omega_n\tau}G_\beta(\omega_n), \tag{2.40}$$

$$G_\beta(\omega_n) = \frac{1}{2}\int_{-\beta}^{\beta} d\tau e^{i\omega_n\tau}G_\beta(\tau). \tag{2.41}$$

From the latter, the following result can be extracted:

$$G_\beta(\omega_n) = \frac{1}{2}\left[1\pm(-1)^n\right]\int_0^\beta d\tau e^{i\omega_n\tau}G_\beta(\tau). \tag{2.42}$$

Again, the negative sign is for fermions and the positive sign is for bosons. The thermal propagator $G_\beta(\omega_n)$, is non-zero for the following discrete frequencies:

$$\omega_n = \begin{cases} 2n\pi T, & \text{for bosons} \\ (2n+1)\pi T, & \text{for fermions} \end{cases} \qquad n = 0, 1, 2, ... \tag{2.43}$$

These frequencies are known as Matsubara frequencies and are the allowed frequencies for bosonic and fermionic fields at finite temperature and density. At finite temperature and density, all definitions of the Feynman diagrams, 1PI, connected... are the same as in conventional **QFT**; the only differences are the (anti)periodic relations that the fields must obey. This leads to energy being discrete and the problem becomes analogous to quantum mechanical states inside a box of length β in the τ direction, where the topology of space-time is a tube, $\mathbb{R}^3 \otimes \mathbb{S}^1$ [44].

2.3 Grand canonical potential for fermions in a mean field potential

With the tools developed in previous sections, we are now ready to calculate the partition function for a fermionic field in a mean field potential. Throughout the present work, the mean field approximation will be employed to the systems. Within this approximation, we can always write the Lagrangian density of a fermionic system in the following form [46],

$$\begin{aligned} \mathscr{L}_{\text{MFA}} &= \overline{\psi}\left[i\gamma^\mu\left(\partial_\mu + iV_0\delta^0_\mu\right) - (\hat{m}+S)\right]\psi + U\left(V_0, S\right) = \\ &= \overline{\psi}\left(i\not{\mathcal{D}} - \hat{M}\right)\psi + U, \end{aligned} \tag{2.44}$$

where $\mathcal{D}_\mu = \partial_\mu + iV_0\delta^0_\mu$, can be interpreted as a covariant derivative and $\hat{M} = \hat{m} + S$ as an effective mass. The constants V_0 and S, are the vacuum expectation values (**VEV**) of some set of auxiliary fields $V_\mu(x)$ and $S(x)$, i.e., $\langle 0|\, V_0(x)\, |0\rangle = V_0$ and $\langle 0|\, S(x)\, |0\rangle = S$. In the **MFA**, the system is in equilibrium thus, dynamic currents disappear i.e. $\langle 0|\, V_i(x)\, |0\rangle = 0$. The mean field potential $U\left(V_0, S\right)$ is independent from the fermion field and from space-time but may depend on the expectation value of the auxiliary fields. The fermion field $\psi(x)$, as well as the auxiliary fields and effective mass, may have several indices like flavour (f) or colour (c). This possible set of indices is omitted to leave the notation tidier and will be denoted by $I = \{f, c, ...\}$.

Following Noether's theorem (Appendix A.1), an invariance of the Lagrangian under a global symmetry leads to a conserved current. In this case the conserved current is,

$$j^\mu = \overline{\psi}\gamma^\mu\psi, \tag{2.45}$$

the zero component of this current is the conserved charge,

$$j^0 = \overline{\psi}\gamma^0\psi. \tag{2.46}$$

The existence of a conserved charge allows the addition of a chemical potential $\hat{\mu}$, to the Hamiltonian of the system. This chemical potential is a diagonal matrix in the space of the I indices. The partition function in the imaginary time formalism is given by

$$\begin{aligned}\mathcal{Z}(\beta) &= \mathcal{N}\int \mathcal{D}\overline{\psi}\,(\tau,\boldsymbol{x})\,\mathcal{D}\psi\,(\tau,\boldsymbol{x})\;\; e^{\mathcal{S}_E[\overline{\psi},\psi]} = \\ &= \mathcal{N}\int \mathcal{D}\overline{\psi}\mathcal{D}\psi\;\exp\left[\int_0^\beta d\tau\int_V d^3x\;\left(\mathscr{L}+\hat{\mu}\overline{\psi}\gamma^0\psi\right)\right],\end{aligned} \tag{2.47}$$

here the functional integration is made over $\overline{\psi}$ and ψ, which are considered as independent fields. Substituting $\mathscr{L}$ yields:

$$\begin{aligned}\mathcal{Z}(\beta) &= \mathcal{N}\int \mathcal{D}\overline{\psi}\mathcal{D}\psi\;\exp\left[\int_0^\beta d\tau\int_V d^3x\;\left(\overline{\psi}\left(i\not{\partial}-\hat{M}\right)\psi+U+\hat{\mu}\overline{\psi}\gamma^0\psi\right)\right] = \\ &= \mathcal{N}\int \mathcal{D}\overline{\psi}\mathcal{D}\psi\;\exp\left[\int_0^\beta d\tau\int_V d^3x\;\left(\overline{\psi}D\psi+U\right)\right],\end{aligned} \tag{2.48}$$

where the operator D is:

$$\begin{aligned}D &= i\not{\partial}-\hat{M}+\hat{\mu}\gamma^0 = i\gamma^\mu\left(\partial_\mu+iV_0\delta^0_\mu\right)-\hat{M}+\hat{\mu}\gamma^0 = \\ &= i\gamma^\mu\partial_\mu-\hat{M}+\underbrace{(\hat{\mu}-V_0)}_{=\tilde{\mu}}\gamma^0 = i\gamma^\mu\partial_\mu-\hat{M}+\tilde{\mu}\gamma^0.\end{aligned} \tag{2.49}$$

The effective chemical potential $\tilde{\mu}$ is defined as:

$$\tilde{\mu} = \hat{\mu}-V_0. \tag{2.50}$$

As seen in Equations (2.39) and (2.43), fermion fields must obey antiperiodic boundary conditions. This condition must be respected when the fermionic field is expressed in momentum space:

$$\begin{aligned}\psi(\tau,\boldsymbol{x}) = \langle\tau,\boldsymbol{x}|\psi\rangle &= \sum_{n,\boldsymbol{p}=-\infty}^{+\infty}\langle\tau,\boldsymbol{x}|\omega_n,\boldsymbol{p}\rangle\,\langle\omega_n,\boldsymbol{p}|\psi\rangle = \\ &= \frac{1}{\sqrt{\beta V}}\sum_{n,\boldsymbol{p}=-\infty}^{+\infty}e^{i(\boldsymbol{p}\cdot\boldsymbol{x}+\omega_n\tau)}\hat{\psi}_n(\boldsymbol{p}),\end{aligned} \tag{2.51}$$

where $\omega_n = (2n+1)\,\pi/\beta$ are the only allowed frequencies for fermionic fields. The action in the $(\tau,\boldsymbol{x})$-space is:

$$\mathcal{S}_E[\overline{\psi},\psi] = \int_0^\beta d\tau\int_V d^3x\;\left[\overline{\psi}(\tau,\boldsymbol{x})D\psi(\tau,\boldsymbol{x})+U\right]. \tag{2.52}$$

Fourier transforming the fermionic fields using (2.51), gives a discrete version of the action in the $(\omega_n, \boldsymbol{p})$-space (the sum's bounds are omitted for simplicity):

$$\mathcal{S}_E[\overline{\psi},\psi] = \int_0^\beta d\tau \int_V d^3x \left[U + \frac{1}{\beta V} \sum_{m,\boldsymbol{q}} e^{-i(\boldsymbol{q}\cdot\boldsymbol{x}+\omega_m\tau)} \hat{\overline{\psi}}_m(\boldsymbol{q}) D \sum_{n,\boldsymbol{p}} e^{i(\boldsymbol{p}\cdot\boldsymbol{x}+\omega_n\tau)} \hat{\psi}_n(\boldsymbol{p}) \right]. \quad (2.53)$$

The action of the operator D in the discrete fermion field $\hat{\psi}_n(\boldsymbol{p})$ is:

$$\begin{aligned} D \sum_{n,\boldsymbol{p}} e^{i(\boldsymbol{p}\cdot\boldsymbol{x}+\omega_n\tau)} \hat{\psi}_n(\boldsymbol{p}) = \\ &= \sum_{n,\boldsymbol{p}} e^{i(\boldsymbol{p}\cdot\boldsymbol{x}+\omega_n\tau)} \left[-\gamma^\mu \partial_\mu \left(\boldsymbol{p}\cdot\boldsymbol{x} + \omega_n\tau \right) - \hat{M} + \tilde{\mu}\gamma^0 \right] \hat{\psi}_n(\boldsymbol{p}) = \\ &= \sum_{n,\boldsymbol{p}} e^{i(\boldsymbol{p}\cdot\boldsymbol{x}+\omega_n\tau)} \left[-\left(\gamma^0 i \frac{\partial}{\partial\tau} \omega_n\tau + \gamma^i p^j \frac{\partial}{\partial x^i} x_j \right) - \hat{M} + \tilde{\mu}\gamma^0 \right] \hat{\psi}_n(\boldsymbol{p}) = \\ &= \sum_{n,\boldsymbol{p}} e^{i(\boldsymbol{p}\cdot\boldsymbol{x}+\omega_n\tau)} \left[-\left(i\gamma^0\omega_n + \gamma^i p_i \right) - \hat{M} + \tilde{\mu}\gamma^0 \right] \hat{\psi}_n(\boldsymbol{p}) = \\ &= \sum_{n,\boldsymbol{p}} e^{i(\boldsymbol{p}\cdot\boldsymbol{x}+\omega_n\tau)} \hat{D} \hat{\psi}_n(\boldsymbol{p}). \end{aligned} \quad (2.54)$$

The operator $\hat{D}$ is defined as:

$$\hat{D} = -i\omega_n\gamma^0 - \gamma^j p_j - \hat{M} + \tilde{\mu}\gamma^0. \quad (2.55)$$

Inserting this results in the discrete action (Equation (2.53)), and making the integral over the mean field potential (independent from space-time) yields:

$$\mathcal{S}_E[\overline{\psi},\psi] = \beta V U + \frac{1}{\beta V} \sum_{\boldsymbol{q},\boldsymbol{p}} \sum_{m,n} \hat{\overline{\psi}}_m(\boldsymbol{q}) \hat{D} \hat{\psi}_n(\boldsymbol{p}) \int_0^\beta d\tau \int_V d^3x e^{i\boldsymbol{x}\cdot(\boldsymbol{p}-\boldsymbol{q})} e^{i\tau(\omega_n-\omega_m)}. \quad (2.56)$$

Using the relations:

$$\int_0^\beta d\tau e^{i\tau(\omega_n-\omega_m)} = \beta\delta\left(\omega_n - \omega_m\right), \quad (2.57)$$

$$\int_V d^3x e^{i\boldsymbol{x}\cdot(\boldsymbol{p}-\boldsymbol{q})} = V\delta^{(3)}\left(\boldsymbol{p}-\boldsymbol{q}\right), \quad (2.58)$$

we can write the discrete action as:

$$\mathcal{S}_E[\overline{\psi},\psi] = \beta V U + \sum_{n,\boldsymbol{p}} \hat{\overline{\psi}}_n(\boldsymbol{p}) \hat{D} \hat{\psi}_n(\boldsymbol{p}). \quad (2.59)$$

The functional integral measure $\mathcal{D}\overline{\psi}\mathcal{D}\psi$, can be altered by the Fourier transformation of the fermion fields. We assume that this possible change does not affect the dynamics of the system and can be absorbed within a new normalization constant, $\mathcal{N}'$. With this

consideration, the partition function is given by:

$$\begin{aligned}\mathcal{Z}(\beta) &= \mathcal{N}' e^{\beta V U} \int \mathcal{D}\hat{\overline{\psi}}\left(\omega_n, \boldsymbol{p}\right) \mathcal{D}\hat{\psi}\left(\omega_n, \boldsymbol{p}\right) \exp\left[\sum_{n,\boldsymbol{p}} \hat{\overline{\psi}}_n(\boldsymbol{p}) \hat{D} \hat{\psi}_n(\boldsymbol{p})\right] = \\ &= \mathcal{N}' e^{\beta V U} \prod_{n,\boldsymbol{p}} \int d\hat{\overline{\psi}}_n d\hat{\psi}_n \; e^{\hat{\overline{\psi}}_n(\boldsymbol{p}) \hat{D} \hat{\psi}_n(\boldsymbol{p})}. \end{aligned} \tag{2.60}$$

Recalling the integral formula for N Grassman variables $\xi_1, \xi_2 ... \xi_N$:

$$\int d\xi_1^\dagger d\xi_1 ... d\xi_N^\dagger d\xi_N \; e^{\xi^\dagger D \xi} = \det D, \tag{2.61}$$

we are able to do the integral in Equation (2.60):

$$\mathcal{Z}(\beta) = \mathcal{N}' e^{\beta V U} \det_{n,\boldsymbol{p},d,I} \hat{D}. \tag{2.62}$$

The determinant present in this equation must be evaluated over all indices (Dirac, momentum, frequency and, if it exists, the set of indices I). This determinant is commonly called the fermionic determinant.

Inserting the calculated partition function in Equation (2.26), gives the grand canonical potential in the **MFA**:

$$\begin{aligned}\Omega_{\text{MFA}} &= \frac{1}{\beta V} \ln\left[\mathcal{N}' e^{\beta V U} \det_{n,\boldsymbol{p},d,I} \hat{D}\right] = \\ &= -U - \frac{T}{V} \ln \det_{n,\boldsymbol{p},d,I} \hat{D}, \end{aligned} \tag{2.63}$$

where the constant $-\ln \mathcal{N}'$ was ignored. After all, we are interested in the derivatives of the grand canonical potential.

We use the identity $\ln\det A = \operatorname{tr}\ln A$, in all indices except in the Dirac index:

$$\Omega_{\text{MFA}} = -U - \frac{T}{V} \operatorname*{tr}_{n,\boldsymbol{p},I} \left(\ln \det_{d} \hat{D}\right), \tag{2.64}$$

To calculate explicitly the determinant over the Dirac index, we use the representation for the gamma matrices presented in Appendix B.1 to write the operator $\hat{D}$:

$$\hat{D} = -i\omega_n \gamma^0 - \gamma^j p_j - \hat{M} + \tilde{\mu}\gamma^0 = \begin{pmatrix} -i\omega_n - \hat{M} + \tilde{\mu} & -\boldsymbol{\sigma}\cdot\boldsymbol{p} \\ \boldsymbol{\sigma}\cdot\boldsymbol{p} & i\omega_n - \hat{M} - \tilde{\mu} \end{pmatrix}. \tag{2.65}$$

Calculating the determinant of the above matrix and substituting it in Equation (2.64) yields:

$$\Omega_{\text{MFA}} = -U - \frac{T}{V} \operatorname*{tr}_{n,\boldsymbol{p},I} \left[\ln\left(E^2 + (\omega_n + i\tilde{\mu})^2\right)^2\right]. \tag{2.66}$$

Where $E = \sqrt{p^2 + \hat{M}^2}$. Since the sum is made over positive and negative values of the frequencies, the substitution $\omega_n \to -\omega_n$ does not change the sum over frequencies:

$$\begin{aligned}\Omega_{\text{MFA}} &= -U - 2\frac{T}{V}\operatorname*{tr}_{n,\boldsymbol{p},I}\left[\ln\left(E^2 + (\omega_n + i\tilde{\mu})^2\right)\right] = \\ &= -U - \frac{T}{V}\operatorname*{tr}_{n,\boldsymbol{p},I}\left[\ln\left(E^2 + (\omega_n + i\tilde{\mu})^2\right) + \ln\left(E^2 + (-\omega_n + i\tilde{\mu})^2\right)\right]. \end{aligned} \tag{2.67}$$

After some algebra, we can isolate the dependence on the frequencies, in order to make the summation simpler:

$$\Omega_{\text{MFA}} = -U - \frac{T}{V}\operatorname*{tr}_{I}\sum_{\boldsymbol{p}=-\infty}^{+\infty}\sum_{n=-\infty}^{+\infty}\left[\ln\left(\omega_n^2 + (E + \tilde{\mu})^2\right) + \ln\left(\omega_n^2 + (E - \tilde{\mu})^2\right)\right]. \tag{2.68}$$

Remembering that $\omega_n = (2n+1)\pi T$, the Matsubara summation can be calculated using several methods to yield the following result (ignoring a possible constant [42, 47]):

$$\sum_{n=-\infty}^{+\infty}\ln\left(\omega_n^2 + (E \pm \tilde{\mu})^2\right) = \beta(E \pm \tilde{\mu}) + 2\ln\left(1 + e^{-\beta(E\pm\tilde{\mu})}\right). \tag{2.69}$$

Taking the continuum limit, we can write the sum over momentum as an integral:

$$\frac{1}{V}\sum_{\boldsymbol{p}=-\infty}^{+\infty} \to \int \frac{d^3p}{(2\pi)^3}. \tag{2.70}$$

Substituting Equations (2.69) and (2.70), the grand canonical potential (2.68) yields:

$$\Omega_{\text{MFA}} - \Omega_0 = -U\left(V_0, S\right) - 2T\operatorname*{tr}_{I}\int\frac{d^3p}{(2\pi)^3}\left[\beta E + \ln\left(1 + e^{-\beta(E+\tilde{\mu})}\right) + \ln\left(1 + e^{-\beta(E-\tilde{\mu})}\right)\right]. \tag{2.71}$$

Here Ω_0 is a constant, usually chosen in such a way that the pressure and energy density vanish in the vacuum. The trace operation over the indices I must be done if the field as any additional index otherwise, it simply yields 1. The factor of 2 represents the spin degeneracy of the 1/2 spin particles (fermions). There is a contribution from the vacuum energy βE, and a term for particles (positive chemical potential) and another for antiparticles (negative chemical potential). These characteristics appeared naturally using this formalism while, for conventional statistical physics, they must be added.

We can relate the grand canonical potential of a field theory (2.26), with the theory's effective action (2.16) in the imaginary time formalism. Their definitions suggests that one can write the grand canonical potential of a theory with a set of fields ϕ as

$$\Omega[\phi] \propto \Gamma[\phi]. \tag{2.72}$$

In the mean field approximation, Equation (2.23) allows the substitution:

$$\begin{aligned}\Omega[\phi]|_{\phi=\phi_c} &\propto \mathcal{S}[\phi]|_{\phi=\phi_c}\,,\\ \Omega[\phi]_{\mathrm{MFA}} &\propto \mathcal{S}[\phi_c].\end{aligned} \tag{2.73}$$

Remembering that when the sources vanishes, the action must be stationary in relation to the fields (2.11) and the **VEV** of the classical field $\phi_c(x)$ is a constant ϕ_c (2.15):

$$\left.\frac{\delta\mathcal{S}[\phi]}{\delta\phi(x)}\right|_{\phi=\phi_c} = 0 \Rightarrow \frac{\partial\mathcal{S}(\phi_c)}{\partial\phi_c} = 0, \tag{2.74}$$

using Equation (2.73), the stationarity of the classical action implies:

$$\frac{\partial\Omega(\phi_c)_{\mathrm{MFA}}}{\partial\phi_c} = 0. \tag{2.75}$$

This relation states that, in the **MFA**, the grand canonical potential must be stationary in relation to any **VEV** of any field ϕ_c, present in the theory. This is usually called thermodynamic consistency relation. From this relation one can obtain the **VEV** of the fields present in the theory (usually through self-consistent equations) and obtain the grand canonical potential as a function of the temperature and chemical potential. If one plugs $\Omega\left(T,\mu\right)$ in the relations (2.27), (2.28), (2.29) and (2.30), all thermodynamics of the system is obtained.

2.4 Fermion gas

Let us apply the techniques developed in the previous section, to calculate the grand canonical potential of a fermion gas, i.e., free fermions of mass m (mean field potential is null). Considering $V_0 = S = 0$ and $U\left(V_0, S\right) = 0$ in expression (2.44), the Lagrangian for free fermion field ψ_j is (the index j just identifies the field):

$$\mathscr{L}_j = \overline{\psi}_j\left(i\partial\!\!\!/ - \hat{m}_j\right)\psi_j. \tag{2.76}$$

The respective grand canonical potential is simply given by Equation (2.71):

$$\Omega_j = \Omega_{0j} - 2T\operatorname*{tr}_I\int\frac{d^3p}{(2\pi)^3}\left[\beta E_j + \ln\left(1+e^{-\beta(E_j+\mu_j)}\right) + \ln\left(1+e^{-\beta(E_j-\mu_j)}\right)\right], \tag{2.77}$$

here Ω_{0j} is zero-point energy contribution and $E_j = \sqrt{p^2+m_j^2}$. The trace over the possible additional indices I is simply given by a degeneracy factor N_I, because both the energy and chemical potential, are diagonal matrices in the I space. Using Equations (2.27), (2.28), (2.29) and (2.30) one may calculate the pressure,

$$P_j = 2TN_I\int\frac{d^3p}{(2\pi)^3}\left[\beta E_j + \ln\left(1+e^{-(E_j+\mu_j)/T}\right) + \ln\left(1+e^{-(E_j-\mu_j)/T}\right)\right] - \Omega_{0j}, \tag{2.78}$$

density,

$$\rho_j = 2N_I \int \frac{d^3p}{(2\pi)^3} \left(n_j - \overline{n}_j\right), \tag{2.79}$$

entropy,

$$S_j = 2N_I \int \frac{d^3p}{(2\pi)^3} \left[\ln\left(1 + e^{-(E_j+\mu_j)/T}\right) + \frac{E_j+\mu_j}{T}\overline{n}_j \right. \\ \left. + \ln\left(1 + e^{-(E_j-\mu_j)/T}\right) + \frac{E_j-\mu_j}{T} n_j \right]. \tag{2.80}$$

and energy density,

$$\epsilon_j = \Omega_{0j} - 2N_I \int \frac{d^3p}{(2\pi)^3} E_j \left(1 - n_j - \overline{n}_j\right), \tag{2.81}$$

Above, n_j and $\overline{n}_j$ are the particle and anti-particle occupation numbers:

$$n_j = \frac{1}{e^{(E_j-\mu_j)/T} + 1}, \tag{2.82}$$

$$\overline{n}_j = \frac{1}{e^{(E_j+\mu_j)/T} + 1}. \tag{2.83}$$

2.4.1 $T = 0$ Limit

In the limit $T = 0$ a Fermi gas is said to be completely degenerate. In this regime, one defines the Fermi energy as the value of the chemical potential at $T = 0$ (see Appendix D.1.1) and the Fermi momentum λ_{F_j} as:

$$\lambda_{F_j} = \sqrt{\mu_j^2 - m_j^2}. \tag{2.84}$$

Using the relations in Appendix D.1.1, we may write in this limit, the pressure, density and energy density as:

$$P_j = \frac{N_I}{\pi^2}\left[\int_{\lambda_{F_j}}^{+\infty} dp\, p^2 E_j + \mu_j \frac{\lambda_{F_j}^3}{3}\right] - \Omega_{0j}, \tag{2.85}$$

$$\rho_j = \frac{N_I}{\pi^2}\frac{\lambda_{F_j}^3}{3}, \tag{2.86}$$

$$\epsilon_j = \Omega_{0j} - \frac{N_I}{\pi^2}\int_{\lambda_{F_j}}^{+\infty} dp p^2 E_j. \tag{2.87}$$

The entropy is automatically zero due to the the third law of thermodynamics.

2.4.2 Pressure for massless fermions

One can define the value of the grand canonical potential in the vacuum as a constant, given by:

$$\Omega_{0j} = 2N_I \int \frac{d^3p}{(2\pi)^3} E_j, \tag{2.88}$$

and subtract it from the pressure because the grand canonical potential is unique up to a constant. Omitting this contribution, for massless particles, the energy is simply $E = |p|$ and the pressure is given by:

$$P_j = 2TN_I \int \frac{d^3p}{(2\pi)^3} \left[\ln\left(1 + e^{-(p+\mu_j)/T}\right) + \ln\left(1 + e^{-(p-\mu_j)/T}\right) \right]. \tag{2.89}$$

Making the integration over the solid angle ($d^3p = 4\pi p^2 dp$) and making an integration by parts, yields the result:

$$P_j = \frac{T^4 N_I}{3\pi^2} \left[\int_0^{+\infty} dx\; x^3 \frac{e^{\mu_j/T}}{e^x + e^{\mu_j/T}} + \int_0^{+\infty} dx\; x^3 \frac{e^{-\mu_j/T}}{e^x + e^{-\mu_j/T}} \right]. \tag{2.90}$$

One can write the above integrals as polylogarithms[3] (see Appendix B.3):

$$\int_0^{+\infty} dx\; x^3 \frac{e^{\mu_j/T}}{e^x + e^{\mu_j/T}} = -\Gamma(4)\, \mathrm{Li}_4\left(-e^{\mu_j/T}\right), \tag{2.91}$$

$$\int_0^{+\infty} dx\; x^3 \frac{e^{-\mu_j/T}}{e^x + e^{-\mu_j/T}} = -\Gamma(4)\, \mathrm{Li}_4\left(-e^{-\mu_j/T}\right). \tag{2.92}$$

Where $\Gamma(z)$ is the gamma function. Substituting in (2.90) gives:

$$P_j = \frac{2T^4 N_I}{\pi^2} \left[-\mathrm{Li}_4\left(-e^{\mu_j/T}\right) - \mathrm{Li}_4\left(-e^{-\mu_j/T}\right) \right]. \tag{2.93}$$

One can Taylor expand the polylogarithm around μ_j and obtain the pressure for gas of massless fermions:

$$P_j \simeq \frac{T^4 N_I}{\pi^2} \left[\frac{7\pi^4}{180} + \frac{\pi^2 \mu_j^2}{6T^2} + \frac{\mu_j^4}{12T^4} \right]. \tag{2.94}$$

2.5 Boson gas

Consider the most simple bosonic field, a free, real, scalar field φ with mass m. The field may have other internal degrees of freedom, like colour for example. The Lagrangian

[3] The polylogarithm arises in the closed form of the integrals of the Fermi-Dirac and Bose-Einstein distributions.

density for such a field can be written as:

$$\mathscr{L} = \frac{1}{2}\partial_\mu\varphi\partial^\mu\varphi - \frac{1}{2}m^2\varphi^2. \tag{2.95}$$

The partition function, in the imaginary time formalism, is given by:

$$\begin{aligned}\mathcal{Z}(\beta) &= \mathcal{N}\int \mathcal{D}\varphi\,(\tau,\boldsymbol{x})\;\, e^{\mathcal{S}_E[\varphi]} = \\ &= \mathcal{N}\int \mathcal{D}\varphi\,(\tau,\boldsymbol{x}) \exp\left[\int_0^\beta d\tau \int_V d^3x\;\mathscr{L}\right],\end{aligned} \tag{2.96}$$

here the functional integration is made over φ. Substituting $\mathscr{L}$ yields:

$$\mathcal{Z}(\beta) = \mathcal{N}\int \mathcal{D}\varphi\,(\tau,\boldsymbol{x}) \exp\left[\frac{1}{2}\int_0^\beta d\tau \int_V d^3x\;\left(\partial_\mu\varphi\partial^\mu\varphi - m^2\varphi^2\right)\right]. \tag{2.97}$$

The dynamical term $\partial_\mu\varphi\partial^\mu\varphi$, can be written as:

$$\partial_\mu\varphi\partial^\mu\varphi = \partial_\mu\left(\varphi\partial^\mu\varphi\right) - \varphi\partial_\mu\partial^\mu\varphi. \tag{2.98}$$

Substituting (2.98) in the partition function, the first term, being a total derivative, vanishes due to the boundary conditions of the functional integration. We are left with:

$$\begin{aligned}\mathcal{Z}(\beta) &= \mathcal{N}\int \mathcal{D}\varphi\,(\tau,\boldsymbol{x}) \exp\left[-\frac{1}{2}\int_0^\beta d\tau \int_V d^3x\;\varphi\left(\partial_\mu\partial^\mu + m^2\right)\varphi\right] = \\ &= \mathcal{N}\int \mathcal{D}\varphi\,(\tau,\boldsymbol{x}) \exp\left[-\frac{1}{2}\int_0^\beta d\tau \int_V d^3x\;\varphi D\varphi\right],\end{aligned} \tag{2.99}$$

where the operator D is:

$$D = \partial_\mu\partial^\mu + m^2. \tag{2.100}$$

As seen in Equations (2.39) and (2.43), boson fields must obey periodic boundary conditions. This condition must be respected when the bosonic field is expressed in momentum space:

$$\begin{aligned}\varphi(\tau,\boldsymbol{x}) = \langle\tau,\boldsymbol{x}|\varphi\rangle &= \sum_{n,\boldsymbol{p}=-\infty}^{+\infty} \langle\tau,\boldsymbol{x}|\omega_n,\boldsymbol{p}\rangle\,\langle\omega_n,\boldsymbol{p}|\varphi\rangle = \\ &= \frac{1}{\sqrt{\beta V}}\sum_{n,\boldsymbol{p}=-\infty}^{+\infty} e^{i(\boldsymbol{p}\cdot\boldsymbol{x}+\omega_n\tau)}\hat{\varphi}_n(\boldsymbol{p}),\end{aligned} \tag{2.101}$$

where $\omega_n = 2n\pi/\beta$ are the only allowed frequencies for bosonic fields (Matsubara frequencies). The action in the $(\tau,\boldsymbol{x})$-space is:

$$\mathcal{S}_E[\varphi] = -\frac{1}{2}\int_0^\beta d\tau \int_V d^3x\;\varphi(\tau,\boldsymbol{x})D\varphi(\tau,\boldsymbol{x}). \tag{2.102}$$

Fourier transforming the bosonic fields using (2.101), gives a discrete version of the action in the $(\omega_n, \boldsymbol{p})$-space (the sum's bounds are omitted for simplicity):

$$\mathcal{S}_E[\varphi] = -\frac{1}{2}\frac{1}{\beta V}\int_0^\beta d\tau \int_V d^3x \sum_{m,\boldsymbol{q}} e^{i(\boldsymbol{q}\cdot\boldsymbol{x}+\omega_m\tau)}\hat{\varphi}_m(\boldsymbol{q}) D \sum_{n,\boldsymbol{p}} e^{i(\boldsymbol{p}\cdot\boldsymbol{x}+\omega_n\tau)}\hat{\varphi}_n(\boldsymbol{p}). \tag{2.103}$$

The action of the operator D in the discrete boson field is:

$$\begin{aligned} D\sum_{n,\boldsymbol{p}} e^{i(\boldsymbol{p}\cdot\boldsymbol{x}+\omega_n\tau)}\hat{\varphi}_n(\boldsymbol{p}) = & \\ &= \sum_{n,\boldsymbol{p}} \left(\partial_\mu\partial^\mu e^{i(\boldsymbol{p}\cdot\boldsymbol{x}+\omega_n\tau)} + m^2 e^{i(\boldsymbol{p}\cdot\boldsymbol{x}+\omega_n\tau)}\right)\hat{\varphi}_n(\boldsymbol{p}) = \\ &= \sum_{n,\boldsymbol{p}} \left[\left(-\frac{\partial^2}{\partial\tau^2} - \nabla^2\right) e^{i(\boldsymbol{p}\cdot\boldsymbol{x}+\omega_n\tau)} + m^2 e^{i(\boldsymbol{p}\cdot\boldsymbol{x}+\omega_n\tau)}\right]\hat{\varphi}_n(\boldsymbol{p}) = \\ &= \sum_{n,\boldsymbol{p}} e^{i(\boldsymbol{p}\cdot\boldsymbol{x}+\omega_n\tau)}\left(\omega_n^2 + p^2 + m^2\right)\hat{\varphi}_n(\boldsymbol{p}) = \\ &= \sum_{n,\boldsymbol{p}} e^{i(\boldsymbol{p}\cdot\boldsymbol{x}+\omega_n\tau)}\hat{D}\hat{\varphi}_n(\boldsymbol{p}). \end{aligned} \tag{2.104}$$

The operator $\hat{D}$ is defined as:

$$\begin{aligned} \hat{D} &= \omega_n^2 + p^2 + m^2 = \\ &= \omega_n^2 + E^2. \end{aligned} \tag{2.105}$$

Inserting this results in the discrete action, yields:

$$\mathcal{S}_E[\varphi] = -\frac{1}{2}\frac{1}{\beta V}\sum_{\boldsymbol{q},\boldsymbol{p}}\sum_{m,n}\hat{\varphi}_m(\boldsymbol{q})\hat{D}\hat{\varphi}_n(\boldsymbol{p})\int_0^\beta d\tau\int_V d^3x e^{i\boldsymbol{x}\cdot(\boldsymbol{p}+\boldsymbol{q})}e^{i\tau(\omega_n+\omega_m)}. \tag{2.106}$$

Using the relations:

$$\int_0^\beta d\tau e^{i\tau(\omega_n+\omega_m)} = \beta\delta\left(\omega_n+\omega_m\right), \tag{2.107}$$

$$\int_V d^3x e^{i\boldsymbol{x}\cdot(\boldsymbol{p}+\boldsymbol{q})} = V\delta^{(3)}\left(\boldsymbol{p}+\boldsymbol{q}\right), \tag{2.108}$$

we can write the discrete action as:

$$\mathcal{S}_E[\varphi] = -\frac{1}{2}\sum_{n,\boldsymbol{p}}\hat{\varphi}_{-n}(-\boldsymbol{p})\hat{D}\hat{\varphi}_n(\boldsymbol{p}). \tag{2.109}$$

We assume that any possible change in the integration measure $\mathcal{D}\varphi$ can be absorbed in a new constant $\mathcal{N}'$. We can write the discrete boson field $\hat{\varphi}_{-n}(-\boldsymbol{p})$ as $\hat{\varphi}_n^*(\boldsymbol{p})$. The partition

function is given by:

$$\begin{aligned}\mathcal{Z}(\beta) &= \mathcal{N}' \int \mathcal{D}\hat{\varphi}\,(\omega_n, \boldsymbol{p})\ \exp\left[-\frac{1}{2}\sum_{n,\boldsymbol{p}} \hat{\varphi}_n^*(\boldsymbol{p})\hat{D}\hat{\varphi}_n(\boldsymbol{p})\right] = \\ &= \mathcal{N}' \prod_{n,\boldsymbol{p}} \int d\hat{\varphi}_n\ e^{-\frac{1}{2}\hat{\varphi}_n^*(\boldsymbol{p})\hat{D}\hat{\varphi}_n(\boldsymbol{p})}.\end{aligned} \tag{2.110}$$

Recalling that field is real, we can use the result for Riemann integrals with a constant matrix D:

$$\int dx_1 ... dx_n\ e^{-x_i D_{ij} x_j} \propto \det{}^{-\frac{1}{2}} D. \tag{2.111}$$

The integration can be performed to give:

$$\mathcal{Z}(\beta) = \mathcal{N}' \det_{n,\boldsymbol{p},I}{}^{-\frac{1}{2}} \hat{D}. \tag{2.112}$$

The determinant present in this equation must be evaluated over momentum, frequency and some other set of indices I, that the field might have.

Inserting the calculated partition function in Equation (2.26), gives the grand canonical potential:

$$\begin{aligned}\Omega &= \frac{1}{\beta V} \ln\left[\mathcal{N}' \det_{n,\boldsymbol{p},I}{}^{-\frac{1}{2}} \hat{D}\right] = \\ &= \frac{T}{V} \ln \det_{n,\boldsymbol{p},I}{}^{-\frac{1}{2}} \hat{D}.\end{aligned} \tag{2.113}$$

Just like for fermionic fields, the constant $-\ln \mathcal{N}'$ was ignored. Using the identity $\ln\det A = \operatorname{tr}\ln A$:

$$\Omega = -\frac{1}{2}\frac{T}{V} \operatorname*{tr}_{n,\boldsymbol{p},I} \ln \hat{D} = -\frac{1}{2}\frac{T}{V} \operatorname*{tr}_{I} \sum_{\boldsymbol{p}=-\infty}^{+\infty} \sum_{n=-\infty}^{+\infty} \ln\left(\omega_n^2 + E^2\right), \tag{2.114}$$

The trace over other indices I, is simply given by a degeneracy factor N_I, which represent other possible degrees of freedom.

Remembering that $\omega_n = 2n\pi T$ for bosons, the Matsubara summation can be calculated using several methods to yield the following result (ignoring a possible constant [42, 47]):

$$\sum_{n=-\infty}^{+\infty} \ln\left(\omega_n^2 + E^2\right) = \beta E + 2\ln\left(1 - e^{-\beta E}\right). \tag{2.115}$$

Taking the continuum limit given in (2.70), and inserting the Matsubara summation in Equation (2.114), yields the grand canonical potential:

$$\Omega - \Omega_0 = -T\ N_I \int \frac{d^3p}{(2\pi)^3} \left[\frac{\beta E}{2} + \ln\left(1 - e^{-\beta E}\right)\right]. \tag{2.116}$$

The pressure is (using Equation (2.27)):

$$P = T\ N_I \int \frac{d^3p}{(2\pi)^3} \left[\frac{\beta E}{2} + \ln\left(1 - e^{-\beta E}\right) \right] - \Omega_0. \tag{2.117}$$

2.5.1 Pressure for massless bosons

The grand canonical potential in the vacuum can be defined as:

$$\Omega_0 = \ N_I \int \frac{d^3p}{(2\pi)^3} \frac{E}{2}, \tag{2.118}$$

With this contribution, considering massless particles, the energy is simply $E = |p|$ and the pressure becomes:

$$P = T\ N_I \int \frac{d^3p}{(2\pi)^3} \ln\left(1 - e^{-\beta p}\right). \tag{2.119}$$

Making the integration over the solid angle and making an integration by parts, yields the result:

$$P = \frac{T^4 N_I}{6\pi^2} \int_0^{+\infty} dx\ \frac{x^3}{e^x - 1}. \tag{2.120}$$

Just like for fermions, one can write the above integral as a polylogarithm (see Appendix B.3):

$$\int_0^{+\infty} dx\ \frac{x^3}{e^x - 1} = \Gamma(4)\,\mathrm{Li}_4\,(1) = \frac{\pi^4}{90}. \tag{2.121}$$

Substituting (2.121) in (2.120), yields the pressure for massless free bosons:

$$P = N_I \frac{\pi^2 T^4}{90}. \tag{2.122}$$

Chapter 3

Nambu–Jona-Lasinio Model

3.1 General aspects

The Nambu–Jona-Lasinio model (**NJL**) was originally introduced in 1961 by Yoichiro Nambu and Giovanni Jona-Lasinio [48], before the assertion of **QCD** as the theory of strong interactions. In its debut, the **NJL** model was presented as theory of nucleons that interact through a local effective two-body interaction in analogy with the Bardeen-Cooper-Schrieffer theory (**BCS**). The central idea was that the mass gap in the Dirac spectrum of the nucleon can be generated analogously to the energy gap of a superconductor in **BCS** theory. The original **NJL** model can be written as:

$$\mathscr{L} = \overline{\psi}\left(i\partial\!\!\!/ - m\right)\psi + G\sum_{a=1}^{3}\left[\left(\overline{\psi}\psi\right)^2 + \left(\overline{\psi}i\gamma_5\tau^a\psi\right)^2\right], \tag{3.1}$$

where ψ is the isospin doublet representing the nucleon field, m is the nucleon bare mass, τ^a are the three Pauli matrices acting in isospin space, and G a coupling constant, strong enough to spontaneously break chiral symmetry.

After the development of **QCD**, the **NJL** model was abandoned due to its non-renormalizability and non-fundamental nature. It was later re-interpreted as a theory whose degrees of freedom are quarks, i.e., an effective theory of **QCD**, after all its symmetries are the same as the symmetries of **QCD**. Within this approach, mesons can be interpreted as quark-antiquark excitations of the vacuum and baryons are bound states of quarks (solitons or quark-diquarks structures). This model does not contain colour confinement or gluons, which implies that the theory cannot be applied to high energies. We emphasize the review works on this model [15, 49–51].

3.1.1 General NJL model

The general Lagrangian density of the **NJL** model for N_f flavours of quarks interacting through a local scalar and pseudoscalar, four point interaction, that respects the symmetries

of **QCD** is given by:

$$\mathscr{L}^{\mathrm{NJL}} = \overline{\psi}\left(i\partial\!\!\!/ - \hat{m}\right)\psi + G_S \sum_{a=0}^{N_f^2-1}\left[\left(\overline{\psi}\Gamma^a\psi\right)^2 + \left(\overline{\psi}i\gamma_5\Gamma^a\psi\right)^2\right]. \tag{3.2}$$

Here ψ is a N_f-component vector in flavour space, where each component is a Dirac spinor, $\hat{m} = diag\left(m_1, ..., m_{N_f}\right)$ is the quark current mass matrix, diagonal in flavour space. The operators Γ^a, are N_f^2 matrix operators that act on flavour space with index $a = 0, 1, ..., N_f^2 - 1$, forming a $U(N_f)$ algebra. The matrix Γ^0, is defined to be proportional to the unit matrix: $\Gamma^0 = \sqrt{2/N_f}\mathbb{1}_{N_f\times N_f}$. For two flavours of quarks ($N_f = 2$), these Γ^a matrices are the three Pauli matrices τ^a of the $SU(2)$ group, plus the identity matrix $\tau^0 = \mathbb{1}_{2\times2}$. For $N_f = 3$, they are the eight Gell-Mann matrices λ^a of the $SU(3)$ group, plus the identity $\lambda^0 = \sqrt{2/3}\mathbb{1}_{3\times3}$ (see Appendix B.2).

The coupling constant G_S has dimensions of E^{-2} and contains gluonic degrees of freedom that substitutes complicated processes involving the exchange of gluons between quarks (see Figure 3.1). The sign of G_S is chosen to give an attraction in the $\sigma, \pi, \rho, ...$quark-antiquark

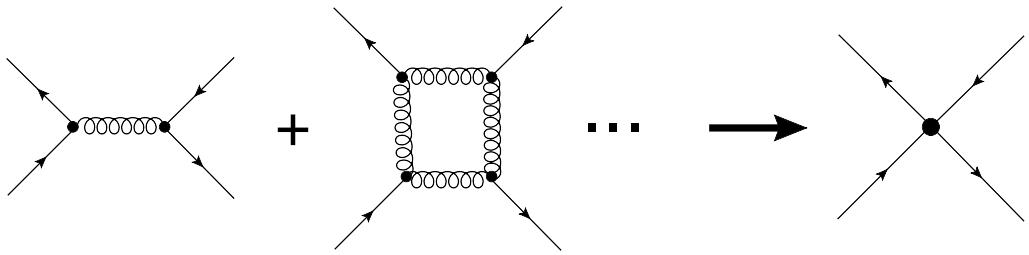

FIGURE 3.1: Four point local interaction that substitutes complicated quark interactions mediated by gluons.

channels. This interaction is strong enough to spontaneously break chiral symmetry in the vacuum by generating a quark-antiquark condensation in the vacuum (and, consequently, a constituent quark mass).

3.1.2 Regularization scheme and parametrization

The local nature of the interaction in the **NJL** model leads to a non-renormalizable theory, which has ultraviolet divergences. Thus, a regularization scheme has to be introduced to deal with the non-convergent integrals in the theory. This has to do with the lack of knowledge of how the low energy effective model (**NJL**) was derived from **QCD**. Various origins can be attributed to this feature: finite instanton size, non-locality of the theory, or asymptotic freedom [40, 51].

There are several possible regularization schemes: non-local regularization; regularization of the real part of the fermion determinant, like Pauli-Villars regularization; and 3-momentum cut-off (to more details on regularization schemes see [40]).

In the present work the later regularization, 3-momentum cut-off is chosen. In this process, the quark field is expanded in a limited momentum basis,

$$\psi(\tau, \boldsymbol{x}) = \frac{1}{\sqrt{V}} \sum_{|\boldsymbol{q}|<\Lambda} \langle \boldsymbol{x}|\boldsymbol{q}\rangle \, \psi(\tau, \boldsymbol{q}), \tag{3.3}$$

where the states are limited to $|\boldsymbol{q}| < \Lambda$ (where Λ is the model's cut-off). This corresponds to a Hilbert space truncation. This regularization breaks the Lorentz covariance of the model and makes impossible to bind quarks into solitons.

This type of regularization, may be seen as a crude implementation of asymptotic freedom after all, the suppressing of the interactions at large momentum, simulates the running coupling constant of **QCD**.

The parameters of the **NJL** model need to be fixed to the current quarks masses and meson properties in the vacuum, like their masses and decay constants, as we will see with more detail in Section 5.

3.1.3 Further quark interactions

The **NJL** model given by the Lagrangian (3.2), has a $U_A(1)$ symmetry which is broken in **QCD**. The lack of the respective Goldstone boson in the meson spectra (due to its breaking) is known as the $U_A(1)$ puzzle (as stated in Section 1.2). Within its resolution [32, 33] 't Hooft suggested that a term of the type

$$\mathscr{L}^{det} = G_D \left(\det_f \left[\overline{\psi} (1+\gamma_5) \psi \right] + \det_f \left[\overline{\psi} (1-\gamma_5) \psi \right] \right), \tag{3.4}$$

can be added to a phenomenological Lagrangian density in order to explicitly break the $U_A(1)$ symmetry, while maintaining the other symmetries:

$$SU_V(N_f) \otimes SU_A(N_f) \otimes U_V(1). \tag{3.5}$$

The determinant in Equation (3.4), is taken over flavour space and corresponds to a maximally flavour mixing $2N_f$ point interaction, involving an incoming and an outgoing quark of each flavour. It is defined as [49]:

$$\det_f \overline{\psi} \mathcal{O} \psi \equiv \sum_{i_1,\ldots,i_{N_f}} \varepsilon_{i_1 \ldots i_{N_f}} \prod_{A=1}^{N_f} \overline{\psi}_A \mathcal{O} \psi_{i_A}. \tag{3.6}$$

This term is not only important to correctly reproduce the symmetries of **QCD**, but is important to get the correct mass splitting of the η and η' mesons in $SU_f(3)$ [51, 52].

It is possible to include other type of quark interactions in the **NJL** model as long as they do not violate the symmetries of **QCD** like chiral symmetry, $SU_c(3)$ and CPT symmetry

(see Table 1.2). Consider the following vector interaction:

$$\mathscr{L}^{vec} = G_{vec} \sum_{a=0}^{N_f^2-1} \left[(\overline{\psi}\gamma^\mu \Gamma^a \psi)^2 + (\overline{\psi}\gamma^\mu \gamma_5 \Gamma^a \psi)^2 \right]. \tag{3.7}$$

This interaction can be decomposed in two parts: a pure vector and pseudovector interaction (or simply vector-isoscalar), with a coupling constant G_ω and a vector-isovector and pseudovector-isovector interaction (or simply vector-isovector), with a coupling constant G_ρ:

$$\mathscr{L}^{vec} = G_\omega \left[(\overline{\psi}\gamma^\mu \Gamma^0 \psi)^2 - (\overline{\psi}\gamma^\mu \gamma_5 \Gamma^0 \psi)^2 \right] + G_\rho \sum_{a=1}^{N_f^2-1} \left[(\overline{\psi}\gamma^\mu \Gamma^a \psi)^2 + (\overline{\psi}\gamma^\mu \gamma_5 \Gamma^a \psi)^2 \right]. \tag{3.8}$$

Due to the quantum numbers of the quark bilinear operators [40] , the first interactions is related to the ω meson, while the second is related to the ρ meson. The **NJL** model has no constrains on the type of vector interaction. Thus, in the present work we will consider 3 types of vector interactions:

$$\begin{aligned} \text{NJL(V+P+VI+PI)}: \ \mathscr{L}_I^{vec} = & G_\omega \left[(\overline{\psi}\gamma^\mu \Gamma^0 \psi)^2 + (\overline{\psi}\gamma^\mu \gamma_5 \Gamma^0 \psi)^2 \right] \\ & + G_\rho \sum_{a=1}^{N_f^2-1} \left[(\overline{\psi}\gamma^\mu \Gamma^a \psi)^2 + (\overline{\psi}\gamma^\mu \gamma_5 \Gamma^a \psi)^2 \right], \end{aligned} \tag{3.9}$$

$$\text{NJL(V+P)}: \ \mathscr{L}_{II}^{vec} = G_\omega \left[(\overline{\psi}\gamma^\mu \Gamma^0 \psi)^2 + (\overline{\psi}\gamma^\mu \gamma_5 \Gamma^0 \psi)^2 \right], \tag{3.10}$$

$$\text{NJL(VI+PI)}: \ \mathscr{L}_{III}^{vec} = G_\rho \sum_{a=1}^{N_f^2-1} \left[(\overline{\psi}\gamma^\mu \Gamma^a \psi)^2 + (\overline{\psi}\gamma^\mu \gamma_5 \Gamma^a \psi)^2 \right]. \tag{3.11}$$

These vector interactions form an invariant chiral set, i.e, they preserve the chiral symmetry of the **NJL** model [40].

We will do all the derivations with the vector interaction given by $\mathscr{L}_I^{vec}$ considering $G_\rho \neq G_\omega$. In the end, we will present the result for each model above, by considering:

- $G_\omega = G_\rho = G_V$ for NJL(V+P+VI+PI);
- $G_\omega = G_V$ and $G_\rho = 0$ for NJL(V+P);
- $G_\rho = G_V$ and $G_\omega = 0$ for NJL(VI+PI);

Where $G_\omega = G_\rho \equiv G_V$. We assume that the ω and ρ mesons are degenerate in the vacuum. The value of vector coupling G_V can be fixed by fitting the meson properties in the vacuum [53]. However, we will take the ratio G_V/G_S as a free parameter once, as pointed out in [25], there is still no constraint for the choice of G_{vec} at finite density even if there are attempts in that direction [54]. Having no definitive knowledge on even its sign, G_{vec}

can be seen as induced in dense quark matter and might be related to an in-medium modification [25]. When G_{vec} is positive (negative) the nature of the vector interaction is repulsive (attractive).

3.1.4 The chemical potential

The **NJL** Lagrangian presented in Equation (3.2), has a conserved charge, given by Equation (2.46). Once we are interested in the investigations of the thermodynamic of these models, due to the presence of the conserved charge, a chemical potential (with colour and flavour indices) can be added to the model (exactly the same case as the Lagrangian presented in Section 2.3). The full **NJL** model studied within this work, with the contribution from the chemical potential, is given by the following expression:

$$\mathscr{L}^{\mathrm{NJL}} = \overline{\psi}\left(i\partial\!\!\!/ - \hat{m} + \hat{\mu}\gamma^0\right)\psi + G_S\sum_{a=0}^{N_f^2-1}\left[\left(\overline{\psi}\Gamma^a\psi\right)^2 + \left(\overline{\psi}i\gamma_5\Gamma^a\psi\right)^2\right] + \mathscr{L}^{det} - \mathscr{L}^{vec}. \tag{3.12}$$

In the following sections we consider the two and three flavour versions of this Lagrangian density.

The chemical potential of a given particle can always be expressed in terms of the chemical potentials associated with conserved quantities, i.e., we can always relate the chemical potential of the quark of flavour i with the baryonic chemical potential (μ_B), electric charge chemical potential (μ_Q), *strangeness* chemical potential (μ_S)... In general the chemical potential of a particle i with baryon charge b_i, electric charge q_i and *strangeness* s_i, can be written as:

$$\mu_i = b_i\mu_B + q_i\mu_Q + s_i\mu_S. \tag{3.13}$$

For the three lightest quarks we have:

	b_i	q_i	s_i
u	$1/3$	$2/3$	0
d	$1/3$	$-1/3$	0
s	$1/3$	$-1/3$	-1

TABLE 3.1: Baryonic, electric and *strangeness* charges of the lightest quarks.

3.1.5 Chiral transition

One of the most important characteristics of the **NJL** model is the spontaneous breaking of the chiral symmetry of the Lagrangian. However, at finite temperature and density, chiral symmetry can be restored [55]. Thus, when analysing the **NJL** model at these conditions,

two phases can be detected, one where the chiral symmetry is broken and another where chiral symmetry is restored (as the temperature and density increase).

However, **NJL** does not uniquely specify an order of the phase transition, it is strongly dependent on the choice of parameters as well as the approximations that are made [51].

Usually, an order parameter is used to distinguish between two distinct phases, in the case of the chiral symmetry of the **NJL** model, this order parameter is the quark condensate: when the quark condensate approaches zero, the chiral symmetry is restored. A phase transition can be classified as follows:

- A first-order phase transition, which is characterized by a discontinuity on the first derivative of the free energy in respect to some thermodynamic variable;
- A second-order phase transitions, which is characterized by a discontinuity on the second derivative of the free energy in respect to some thermodynamic variable, while the first derivative remain continuous;
- A *crossover* between two phases, in which the system changes from one type of behaviour to another continuously. Its change is not associated with any discontinuity in the free energy, or it's derivatives. It is typically smooth taking place in a region, not being possible to identify precisely the phase transition point. In these cases, is necessary to point out the definition of *crossover* used.

In the present work, at $T = 0$, the chiral symmetry restoration point (μ_B^{crit}) is defined in the following way: if the phase transition is of first-order, we search for the μ_B at which there is a discontinuity in the quark condensate (the order parameter). If the transition is a *crossover*, we search for the zeros of the second derivative of the light quark condensates,

$$\frac{\partial^2 \langle \overline{\psi}_i \psi_i \rangle}{\partial {\mu_B}^2} = 0. \tag{3.14}$$

In the cases where there are different chemical potentials for each quark flavour (different phase transitions for each flavour), the chemical potential of the phase transition is defined as the average of the chemical potential of the transition for the light quarks:

$$\mu_B^{\text{crit}} = \frac{\mu_{B(u)}^{\text{crit}} + \mu_{B(d)}^{\text{crit}}}{2}. \tag{3.15}$$

At the densities that the chiral symmetry defined above happens, there is not enough energy in the system for *strangeness* to appear [49]. Having said that, it is possible to define a chiral symmetry restoration point for the *strange* quark however, this happens at densities much higher than those found inside neutron stars whereby, we have chosen in the present work, to define the chiral symmetry restoration point using only the light quarks.

3.2 The two flavour case

The study of the thermodynamics of a system where the degrees of freedom of interest are the lighter quarks, *up* and *down*, can be done in the **NJL** model trough a two flavour analysis of the Lagrangian density presented in Equation (3.12). For equal masses and chemical potentials, the isospin symmetry is completely conserved. However, introducing different chemical potentials, one can study the effect of isospin asymmetry in quark matter (the isospin symmetry will be broken anyway when one imposes $\beta-$equilibrium). The Lagrangian density for two flavours can be written as:

$$\mathscr{L}^{\mathrm{NJL}} = \overline{\psi}\left(i\partial\!\!\!/ - \hat{m} + \hat{\mu}\gamma^0\right)\psi + G_S\sum_{a=0}^{3}\left[\left(\overline{\psi}\tau^a\psi\right)^2 + \left(\overline{\psi}i\gamma_5\tau^a\psi\right)^2\right] + \mathscr{L}^{det} - \mathscr{L}^{vec}. \quad (3.16)$$

ψ is a two component vector in flavour space (where each component is a Dirac spinor), $\hat{m} = diag\,(m_u, m_d)$ is the quark current mass matrix, $\hat{\mu} = diag\,(\mu_u, \mu_d)$ is the quark chemical potential matrix (both matrices are in flavour space), $\tau^0 = \mathbb{1}_{2\times2}$ is the identity matrix and τ^i are the three Pauli matrices of $SU_f(2)$.

In this case, the 't Hooft determinant (3.4) is a 4 point interaction just like the scalars and vector interactions. Using the definition (3.6), the t'Hooft determinant for two flavours can be calculated using (where $\mathcal{O} = 1 \pm \gamma_5$):

$$\det_f \overline{\psi}\mathcal{O}\psi \equiv \sum_{i,j}\varepsilon_{ij}\left(\overline{\psi}_u\mathcal{O}\psi_i\right)\left(\overline{\psi}_d\mathcal{O}\psi_j\right). \quad (3.17)$$

In fact, for two flavours of quarks, one can use the 't Hooft determinant to write the Lagrangian in (3.16) as the original Lagrangian proposed by Nambu and Jona-Lasinio (3.1). Separating the zero component of the τ^a matrices, $\tau^0 = \mathbb{1}_{2\times2}$ and using the result presented in Appendix C.2, one may write,

$$\begin{aligned}\mathscr{L}^{\mathrm{NJL}} = {} & \overline{\psi}\left(i\partial\!\!\!/ - \hat{m} + \hat{\mu}\gamma^0\right)\psi - \mathscr{L}^{vec} \\ & + G_S\left\{\left(\overline{\psi}\tau^0\psi\right)^2 + \left(\overline{\psi}i\gamma_5\tau^0\psi\right)^2 + \sum_{a=1}^{3}\left[\left(\overline{\psi}\tau^a\psi\right)^2 + \left(\overline{\psi}i\gamma_5\tau^a\psi\right)^2\right]\right\} \\ & + \frac{G_D}{2}\left\{\left(\overline{\psi}\tau^0\psi\right)^2 - \left(\overline{\psi}i\gamma_5\tau^0\psi\right)^2 - \sum_{a=1}^{3}\left[\left(\overline{\psi}\tau^a\psi\right)^2 - \left(\overline{\psi}i\gamma_5\tau^a\psi\right)^2\right]\right\}. \quad (3.18)\end{aligned}$$

Reorganizing, we have

$$\begin{aligned}\mathscr{L}^{\mathrm{NJL}} = {} & \overline{\psi}\left(i\partial\!\!\!/ - \hat{m} + \hat{\mu}\gamma^0\right)\psi + \left(G_S + \frac{G_D}{2}\right)\left[\left(\overline{\psi}\tau^0\psi\right)^2 + \sum_{a=1}^{3}\left(\overline{\psi}i\gamma_5\tau^a\psi\right)^2\right] \\ & + \left(G_S - \frac{G_D}{2}\right)\left[\sum_{a=1}^{3}\left(\overline{\psi}\tau^a\psi\right)^2 + \left(\overline{\psi}i\gamma_5\tau^0\psi\right)^2\right] - \mathscr{L}^{vec}.\end{aligned} \quad (3.19)$$

The G_D coupling constant, for $N_f = 2$, is not fixed to any meson property therefore, we may parametrize G_S and G_D in terms of a new coupling constant, G and a mixing parameter α [49]. We write:

$$G_S = (1-\alpha)\, G, \tag{3.20}$$

$$G_D = 2\alpha G. \tag{3.21}$$

When $\alpha = 1/2$

$$\left(G_S + \frac{G_D}{2}\right) = G \quad \wedge \quad \left(G_S - \frac{G_D}{2}\right) = 0, \tag{3.22}$$

the third term in the right hand side cancels and we recover the original Lagrangian (3.1), which is invariant under $U_A(1)$ transformations. The parameter α may vary allowing the study of the original **NJL** model or cases where there is flavour mixing (and explicit $U_A(1)$ symmetry break) [49].

As stated previously, one can study several types of vector interactions. We will study the following vector interactions:

$$\begin{aligned}\text{NJL(V+P+VI+PI)}: \ \mathscr{L}_I^{vec} = & G_\omega \left[(\overline{\psi}\gamma^\mu\tau^0\psi)^2 + (\overline{\psi}\gamma^\mu\gamma_5\tau^0\psi)^2\right] \\ & + G_\rho \sum_{a=1}^{3} \left[(\overline{\psi}\gamma^\mu\tau^a\psi)^2 + (\overline{\psi}\gamma^\mu\gamma_5\tau^a\psi)^2\right],\end{aligned} \tag{3.23}$$

$$\text{NJL(V+P)}: \ \mathscr{L}_{II}^{vec} = G_\omega \left[(\overline{\psi}\gamma^\mu\tau^0\psi)^2 + (\overline{\psi}\gamma^\mu\gamma_5\tau^0\psi)^2\right], \tag{3.24}$$

$$\text{NJL(VI+PI)}: \ \mathscr{L}_{III}^{vec} = G_\rho \sum_{a=1}^{3} \left[(\overline{\psi}\gamma^\mu\tau^a\psi)^2 + (\overline{\psi}\gamma^\mu\gamma_5\tau^a\psi)^2\right]. \tag{3.25}$$

The **EoS** can be obtained through the Matsubara formalism presented in Section 2.2.1. In order to do so, we are going to use the **MFA** to write the **NJL** Lagrangian in the form presented in Equation (2.44) and calculate the respective grand canonical potential.

3.2.1 NJL in the MFA (two flavours)

The **MFA** of the model may be obtained by linearising the original Lagrangian density (action). In order to do it, we need to transform any quark interaction involving more than two quarks, into a two point interaction. One way to accomplish this is to bosonize the action i.e., introduce auxiliary bosonic fields in the Lagrangian which interact with the fermions, and then, treat those auxiliary fields in the **MFA**. This way, a four point-interactions for example, is transformed into to two-point interaction. One of those techniques is called Hubbard-Stratonovich transformation. Let ϕ be a auxiliary bosonic

field, ψ a fermionic field and λ a coupling constant:

$$\exp\left[\int d^4x\ \lambda\left(\overline{\psi}\psi\right)^2\right] \propto \int \mathcal{D}\phi \exp\left[\int d^4x\ \left(2\lambda\overline{\psi}\phi\psi - \lambda\phi^2\right)\right]. \tag{3.26}$$

This transformation consists in substituting the four point interaction in the generating functional (partition function) by the relation given in Equation (3.26). If one treats the auxiliary field ϕ, in the **MFA**, the functional integration over this field vanish and we obtain a fermion field interacting with the mean field $\langle 0|\phi|0\rangle$, linearising the Lagrangian density.

An equivalent approach to Lagrangian linearisation is to write the product between two operators as (derived in Appendix C.1):

$$\hat{\mathcal{O}}_1\hat{\mathcal{O}}_2 \approx \langle\hat{\mathcal{O}}_1\rangle\,\hat{\mathcal{O}}_2 + \hat{\mathcal{O}}_1\,\langle\hat{\mathcal{O}}_2\rangle - \langle\hat{\mathcal{O}}_1\rangle\,\langle\hat{\mathcal{O}}_2\rangle\,. \tag{3.27}$$

Using this equation we may write:

$$\left(\overline{\psi}\tau^a\psi\right)^2 \approx 2\left(\overline{\psi}\tau^a\psi\right)\langle\overline{\psi}\tau^a\psi\rangle - \langle\overline{\psi}\tau^a\psi\rangle^2, \tag{3.28}$$

$$\left(\overline{\psi}i\gamma_5\tau^a\psi\right)^2 \approx 2\left(\overline{\psi}i\gamma_5\tau^a\psi\right)\langle\overline{\psi}i\gamma_5\tau^a\psi\rangle - \langle\overline{\psi}i\gamma_5\tau^a\psi\rangle^2, \tag{3.29}$$

$$\left(\overline{\psi}\gamma^\mu\tau^a\psi\right)^2 \approx 2\left(\overline{\psi}\gamma^\mu\tau^a\psi\right)\langle\overline{\psi}\gamma^\mu\tau^a\psi\rangle - \langle\overline{\psi}\gamma^\mu\tau^a\psi\rangle^2, \tag{3.30}$$

$$\left(\overline{\psi}\gamma^\mu\gamma_5\tau^a\psi\right)^2 \approx 2\left(\overline{\psi}\gamma^\mu\gamma_5\tau^a\psi\right)\langle\overline{\psi}\gamma^\mu\gamma_5\tau^a\psi\rangle - \langle\overline{\psi}\gamma^\mu\gamma_5\tau^a\psi\rangle^2. \tag{3.31}$$

The presence of any field costs energy to the system. Only fields whose **VEV** is non-zero at a given density should exist.

A non-zero barionic density requires the presence of quark condensates that couple to the various densities like scalar, vector, isovector... However, the fundamental state (vacuum) has well-defined charge, spin and parity. Quark bilinear operators which are not diagonal in flavour space produce condensates that change these properties. For example, the condensates $\langle\overline{\psi}\tau^1\psi\rangle$ and $\langle\overline{\psi}\tau^2\psi\rangle$ can be written as a combination of ladder operators, which couple to charged mesons. This means that their **VEV** must be zero. See [49, 56] for a detailed discussion.

We could allow for a non-vanishing expectation value of condensates with pionic quantum numbers to describe a possible pion condensation [49], however we assume the energies are not high enough for this condensation to happen. Due to the fact that we are dealing with quark matter in equilibrium, any currents disappear. Thereby, the only non-vanishing

quark condensates are:

$$\langle\overline{\psi}\tau^0\psi\rangle = \sigma^0, \tag{3.32}$$
$$\langle\overline{\psi}\tau^3\psi\rangle = \sigma^3, \tag{3.33}$$
$$\langle\overline{\psi}\gamma^0\tau^0\psi\rangle = \omega^0, \tag{3.34}$$
$$\langle\overline{\psi}\gamma^0\tau^3\psi\rangle = \rho^3. \tag{3.35}$$

Explicitly, one may write (using the Pauli matrices presented in Appendix B.2):

$$\langle\overline{\psi}\tau^0\psi\rangle = \langle\overline{\psi}_u\psi_u\rangle + \langle\overline{\psi}_d\psi_d\rangle = \sigma_u + \sigma_d, \tag{3.36}$$
$$\langle\overline{\psi}\tau^3\psi\rangle = \langle\overline{\psi}_u\psi_u\rangle - \langle\overline{\psi}_d\psi_d\rangle = \sigma_u - \sigma_d, \tag{3.37}$$
$$\langle\overline{\psi}\gamma^0\tau^0\psi\rangle = \langle\psi_u^\dagger\psi_u\rangle + \langle\psi_d^\dagger\psi_d\rangle = \rho_u + \rho_d, \tag{3.38}$$
$$\langle\overline{\psi}\gamma^0\tau^3\psi\rangle = \langle\psi_u^\dagger\psi_u\rangle - \langle\psi_d^\dagger\psi_d\rangle = \rho_u - \rho_d. \tag{3.39}$$

Taking into account only the non-vanishing condensates and using Equation (C.1), the 't Hooft determinant for two flavours (3.17) in this approximation is (Appendix C.3.1):

$$\begin{aligned}\mathscr{L}^{det} &\approx 2G_D\left[\left(\overline{\psi}_u\psi_u\right)\langle\overline{\psi}_d\psi_d\rangle + \langle\overline{\psi}_u\psi_u\rangle\left(\overline{\psi}_d\psi_d\right) - \langle\overline{\psi}_u\psi_u\rangle\langle\overline{\psi}_d\psi_d\rangle\right] = \\ &= 2G_D\overline{\psi}\Delta\psi - 2G_D\sigma_u\sigma_d,\end{aligned} \tag{3.40}$$

Here, Δ is a matrix in flavour space:

$$\Delta = \begin{pmatrix}\langle\overline{\psi}_d\psi_d\rangle & 0\\ 0 & \langle\overline{\psi}_u\psi_u\rangle\end{pmatrix} = \begin{pmatrix}\sigma_d & 0\\ 0 & \sigma_u\end{pmatrix}. \tag{3.41}$$

Finally, the **NJL** Lagrangian in the **MFA**, for two flavours of quarks, with the 't Hooft determinant and a vector interaction ($\mathscr{L}_I^{vec}$) is:

$$\begin{aligned}\mathscr{L}_{\text{MFA}} = &\overline{\psi}\left(i\partial\!\!\!/ - \hat{m} + \hat{\mu}\gamma^0\right)\psi \\ &+ 2G_S\left(\overline{\psi}\tau^0\psi\right)(\sigma_u + \sigma_d) - G_S\left(\sigma_u + \sigma_d\right)^2 \\ &+ 2G_S\left(\overline{\psi}\tau^3\psi\right)(\sigma_u - \sigma_d) - G_S\left(\sigma_u - \sigma_d\right)^2 \\ &+ 2G_D\overline{\psi}\Delta\psi - 2G_D\sigma_u\sigma_d \\ &- 2G_\omega\left(\overline{\psi}\gamma^0\tau^0\psi\right)(\rho_u + \rho_d) + G_\omega\left(\rho_u + \rho_d\right)^2 \\ &- 2G_\rho\left(\overline{\psi}\gamma^0\tau^3\psi\right)(\rho_u - \rho_d) + G_\rho\left(\rho_u - \rho_d\right)^2.\end{aligned} \tag{3.42}$$

Writing this expression in the form given by expression (2.44) yields:

$$\mathscr{L}_{\text{MFA}} = \overline{\psi}\left[i\gamma^\mu\left(\partial_\mu + iV_0\delta_\mu^0\right) - (\hat{m} + S)\right]\psi + U, \tag{3.43}$$

where:

$$V_0 = 2G_\omega \tau^0 (\rho_u + \rho_d) + 2G_\rho \tau^3 (\rho_u - \rho_d), \tag{3.44}$$

$$S = -2G_S \tau^0 (\sigma_u + \sigma_d) - 2G_S \tau^3 (\sigma_u - \sigma_d) - 2G_D \Delta, \tag{3.45}$$

$$U = -2G_S \left(\sigma_u^2 + \sigma_d^2\right) - 2G_D \sigma_u \sigma_d + G_\omega (\rho_u + \rho_d)^2 + G_\rho (\rho_u - \rho_d)^2. \tag{3.46}$$

The effective mass $\hat{M}$ and chemical potential $\hat{\mu}$ for this model are:

$$\hat{M} = \hat{m} - 2G_S \tau^0 (\sigma_u + \sigma_d) - 2G_S \tau^3 (\sigma_u - \sigma_d) - 2G_D \Delta, \tag{3.47}$$

$$\tilde{\mu} = \hat{\mu} - 2G_\omega \tau^0 (\rho_u + \rho_d) - 2G_\rho \tau^3 (\rho_u - \rho_d). \tag{3.48}$$

Following Section 2.3, it is possible to obtain the grand canonical potential for this Lagrangian. One must just remember that in this case, the fermion field ψ is a quark field, which means that the set of extra indices I, contains colour and flavour indices i.e, $I = \{f, c\}$. The grand canonical potential is then given by Equation (2.71), with the proper substitutions:

$$\begin{aligned}\Omega_{\text{MFA}} - \Omega_0 = {} & 2G_S \left(\sigma_u^2 + \sigma_d^2\right) + 2G_D \sigma_u \sigma_d - G_\omega (\rho_u + \rho_d)^2 - G_\rho (\rho_u - \rho_d)^2 \\ & - 2T \operatorname*{tr}_{f,c} \int \frac{d^3p}{(2\pi)^3} \left[\beta E + \ln\left(1 + e^{-\beta(E+\tilde{\mu})}\right) + \ln\left(1 + e^{-\beta(E-\tilde{\mu})}\right)\right].\end{aligned} \tag{3.49}$$

The irrelevant constant Ω_0 is defined such that the pressure and energy density vanish in the vacuum i.e., $\Omega_0 = \Omega_{\text{MFA}}(T = 0, \mu = 0)$. We are just left with the trace operation under colour and flavour indices. The trace over colour is trivial and is simply given by N_c (number of colours) after all, neither the effective mass or chemical potential have internal structure in colour space. That is not the case for flavour indices. In flavour space, the effective mass is:

$$\begin{aligned}\hat{M} &= \hat{m} - 2G_S \tau^0 (\sigma_u + \sigma_d) - 2G_S \tau^3 (\sigma_u - \sigma_d) - 2G_D \Delta = \\ &= \begin{pmatrix} m_u & 0 \\ 0 & m_d \end{pmatrix} - 2G_S (\sigma_u + \sigma_d) \begin{pmatrix} 1 & 0 \\ 0 & 1 \end{pmatrix} - 2G_S (\sigma_u - \sigma_d) \begin{pmatrix} 1 & 0 \\ 0 & -1 \end{pmatrix} - 2G_D \begin{pmatrix} \sigma_d & 0 \\ 0 & \sigma_u \end{pmatrix} = \\ &= \begin{pmatrix} M_u & 0 \\ 0 & M_d \end{pmatrix}.\end{aligned} \tag{3.50}$$

Where we have defined the effective mass for each flavour of quark:

$$M_u = m_u - 4G_S \sigma_u - 2G_D \sigma_d, \tag{3.51}$$

$$M_d = m_d - 4G_S \sigma_u - 2G_D \sigma_u. \tag{3.52}$$

The effective chemical potential $\tilde{\mu}$ is:

$$\begin{aligned}\tilde{\mu} &= \hat{\mu} - 2G_\omega\tau^0\left(\rho_u+\rho_d\right) - 2G_\rho\tau^3\left(\rho_u-\rho_d\right) = \\ &= \begin{pmatrix}\mu_u & 0\\ 0 & \mu_d\end{pmatrix} - 2G_\omega\left(\rho_u+\rho_d\right)\begin{pmatrix}1 & 0\\ 0 & 1\end{pmatrix} - 2G_\rho\left(\rho_u-\rho_d\right)\begin{pmatrix}1 & 0\\ 0 & -1\end{pmatrix} = \\ &= \begin{pmatrix}\tilde{\mu}_u & 0\\ 0 & \tilde{\mu}_d\end{pmatrix}, \end{aligned} \tag{3.53}$$

here we define the effective chemical potential for each flavour of quark:

$$\tilde{\mu}_u = \mu_u - 2G_\omega\left(\rho_u+\rho_d\right) - 2G_\rho\left(\rho_u-\rho_d\right), \tag{3.54}$$

$$\tilde{\mu}_d = \mu_d - 2G_\omega\left(\rho_u+\rho_d\right) + 2G_\rho\left(\rho_u-\rho_d\right). \tag{3.55}$$

The power of a diagonal matrix is equal to the power of its diagonal entries. Using this fact, the trace of the energy term is:

$$\begin{aligned}\operatorname*{tr}_f \beta E &= \beta \operatorname*{tr}_f \sqrt{p^2+\hat{M}^2} = \beta \operatorname*{tr}_f \left[p^2\mathbb{1}_{2\times2} + \begin{pmatrix}M_u & 0\\ 0 & M_d\end{pmatrix}^2\right]^{1/2} = \\ &= \beta \operatorname*{tr}_f \begin{pmatrix}E_u & 0\\ 0 & E_d\end{pmatrix} = \beta\left(E_u+E_d\right). \end{aligned} \tag{3.56}$$

The trace of the other two terms, involving the logarithmic function can be calculated in a similar way (using the identity $\ln\det A = \operatorname{tr}\ln A$):

$$\begin{aligned}\operatorname*{tr}_f \ln\left(1+e^{-(E\pm\tilde{\mu})/T}\right) &= \ln\det_f\left(1+e^{-(E\pm\tilde{\mu})/T}\right) = \ln\det_f\left(1+\sum_{n=0}^{\infty}\frac{(-\beta)^n(E\pm\tilde{\mu})^n}{n!}\right) = \\ &= \ln\det\left[\mathbb{1}_{2\times2} + \sum_{n=0}^{\infty}\frac{(-\beta)^n}{n!}\begin{pmatrix}E_u\pm\tilde{\mu}_u & 0\\ 0 & E_d\pm\tilde{\mu}_d\end{pmatrix}^n\right], \end{aligned} \tag{3.57}$$

again, the matrix is diagonal:

$$\begin{aligned}\operatorname*{tr}_f \ln\left(1+e^{-(E\pm\tilde{\mu})/T}\right) &= \ln\det\begin{pmatrix}1+\sum\limits_{n=0}^{\infty}\frac{(-\beta)^n}{n!}(E_u\pm\tilde{\mu}_u)^n & 0\\ 0 & 1+\sum\limits_{n=0}^{\infty}\frac{(-\beta)^n}{n!}(E_d\pm\tilde{\mu}_d)^n\end{pmatrix} = \\ &= \ln\det\begin{pmatrix}1+e^{-(E_u\pm\tilde{\mu}_u)/T} & 0\\ 0 & 1+e^{-(E_d\pm\tilde{\mu}_d)/T}\end{pmatrix} = \\ &= \ln\left(1+e^{-(E_u\pm\tilde{\mu}_u)/T}\right) + \ln\left(1+e^{-(E_d\pm\tilde{\mu}_d)/T}\right). \end{aligned} \tag{3.58}$$

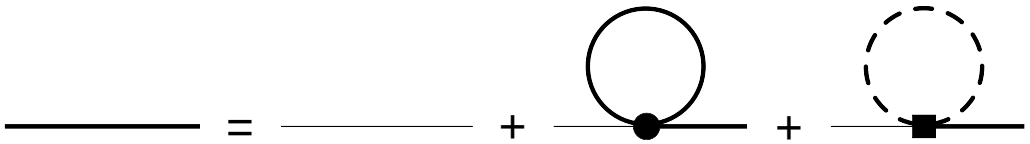

FIGURE 3.2: Diagrammatic representation of the effective mass for flavour i. The dot vertex represents the G_S coupling while the square vertex the G_D coupling. There is a contribution from the condensate of flavour i (full line loop) and from the other condensate, of flavour j (dashed loop).

Finally, the grand canonical potential of the theory is (the sum is to be made over flavours of quarks):

$$\Omega_{\text{MFA}} - \Omega_0 = 2G_S\left(\sigma_u^2 + \sigma_d^2\right) + 2G_D\sigma_u\sigma_d - G_\omega\left(\rho_u + \rho_d\right)^2 - G_\rho\left(\rho_u - \rho_d\right)^2 - 2T\, N_c \sum_{f=u,d}\int \frac{d^3p}{(2\pi)^3}\left[\beta E_f + \ln\left(1 + e^{-\beta\left(E_f+\tilde{\mu}_f\right)}\right) + \ln\left(1 + e^{-\beta\left(E_f-\tilde{\mu}_f\right)}\right)\right]. \tag{3.59}$$

Following Section 2.3, the values of condensates σ_u and σ_d are determined by minimizing the grand canonical potential:

$$\frac{\partial\Omega_{\text{MFA}}}{\partial\sigma_u} = \frac{\partial\Omega_{\text{MFA}}}{\partial\sigma_d} = 0. \tag{3.60}$$

Using these relations (Appendix C.4.1), yields the so-called *gap* equations of the theory (see Figure 3.2):

$$M_i = m_i - 4G_S\sigma_i - 2G_D\sigma_j, \;\; i \neq j \in \{u, d\}, \tag{3.61}$$

here the quark condensate for each flavour is given by:

$$\sigma_i = \langle\overline{\psi}_i\psi_i\rangle = -2N_c\int\frac{d^3p}{(2\pi)^3}\frac{M_i}{E_i}\left(1 - n_i - \overline{n}_i\right). \tag{3.62}$$

Where n_i and $\overline{n}_i$ are the quark and anti-quark occupation numbers given by Equations (2.82) and (2.83). Once again, using the relations given in Equations (2.27), (2.28), (2.29) and (2.30), we can calculate the $i-$quark density,

$$\rho_i = 2N_c\int\frac{d^3p}{(2\pi)^3}\left(n_i - \overline{n}_i\right), \tag{3.63}$$

the pressure,

$$P_{\text{MFA}} = -\Omega_0 - 2G_S\left(\sigma_u^2 + \sigma_d^2\right) - 2G_D\sigma_u\sigma_d + G_\omega\left(\rho_u + \rho_d\right)^2 + G_\rho\left(\rho_u - \rho_d\right)^2 + 2N_c\sum_{f=u,d}\int\frac{d^3p}{(2\pi)^3}\left[E_f + T\ln\left(1 + e^{-(E_f+\tilde{\mu}_f)/T}\right) + T\ln\left(1 + e^{-(E_f-\tilde{\mu}_f)/T}\right)\right], \tag{3.64}$$

entropy,

$$S_{\rm MFA} = 2N_c \sum_{f=u,d} \int \frac{d^3p}{(2\pi)^3} \left[\ln\left(1 + e^{-(E_f+\tilde{\mu}_f)/T}\right) + \frac{E_f + \tilde{\mu}_f}{T}\overline{n}_f \right. \\ \left. + \ln\left(1 + e^{-(E_f-\tilde{\mu}_f)/T}\right) + \frac{E_f - \tilde{\mu}_f}{T} n_f \right], \quad (3.65)$$

and energy density,

$$\epsilon_{\rm MFA} = \Omega_0 + 2G_S\left(\sigma_u^2 + \sigma_d^2\right) + 2G_D\sigma_u\sigma_d - G_\omega\left(\rho_u + \rho_d\right)^2 - G_\rho\left(\rho_u - \rho_d\right)^2 \\ - 2N_c \sum_{f=u,d} \int \frac{d^3p}{(2\pi)^3} \left[E_f\left(1 - n_f - \overline{n}_f\right) + n_f\left(\tilde{\mu}_f - \mu_f\right) + \overline{n}_f\left(\mu_f - \tilde{\mu}_f\right)\right]. \quad (3.66)$$

3.2.2 T=0 Limit (two flavours)

Following Section 2.4.1 and Appendix D.1.1, in the $T = 0$ limit, the Fermi momentum of the quark of flavour f is:

$$\lambda_{F_f} = \sqrt{\tilde{\mu}_f^2 - M_f^2}. \quad (3.67)$$

Every thermodynamic quantity of interest follows (using Appendix D.1.1):

$$P_{\rm MFA} = -\Omega_0 - 2G_S\left(\sigma_u^2 + \sigma_d^2\right) - 2G_D\sigma_u\sigma_d + G_\omega\left(\rho_u + \rho_d\right)^2 + G_\rho\left(\rho_u - \rho_d\right)^2 \\ + \frac{N_c}{\pi^2} \sum_{f=u,d} \int_{\lambda_{F_f}}^{\Lambda} dp p^2 E_f + \frac{N_c}{\pi^2} \sum_{f=u,d} \tilde{\mu}_f \frac{\lambda_{F_f}^3}{3}, \quad (3.68)$$

quark density of flavour f,

$$\rho_f = \frac{N_c}{\pi^2}\frac{\lambda_{F_f}^3}{3}. \quad (3.69)$$

and energy density,

$$\epsilon_{\rm MFA} = \Omega_0 + 2G_S\left(\sigma_u^2 + \sigma_d^2\right) + 2G_D\sigma_u\sigma_d - G_\omega\left(\rho_u + \rho_d\right)^2 - G_\rho\left(\rho_u - \rho_d\right)^2 \\ - \frac{N_c}{\pi^2} \sum_{f=u,d} \int_{\lambda_{F_f}}^{\Lambda} dp p^2 E_f + \frac{N_c}{\pi^2} \sum_{f=u,d} \left(\mu_f - \tilde{\mu}_f\right) \frac{\lambda_{F_f}^3}{3}. \quad (3.70)$$

The quark condensate in this limit is:

$$\sigma_i = -\frac{N_c}{\pi^2} \int_{\lambda_{F_i}}^{\Lambda} dp p^2 \frac{M_i}{E_i}. \quad (3.71)$$

The irrelevant constant Ω_0 is defined as:

$$\Omega_0 = -2G_S\left(\sigma_{u0}^2 + \sigma_{d0}^2\right) - 2G_D\sigma_{u0}\sigma_{d0} + \frac{N_c}{\pi^2} \sum_{f=u,d} \int_0^{\Lambda} dp p^2 E_{f0}, \quad (3.72)$$

where σ_{f0} and E_{f0} are the quark condensate and energy in the vacuum,

$$\sigma_{i0} = -\frac{N_c}{\pi^2}\int_0^\Lambda dpp^2\frac{M_{i0}}{E_{i0}}, \tag{3.73}$$

$$E_{i0} = \sqrt{p^2 + M_{i0}}. \tag{3.74}$$

3.3 The three flavour case

Although in the current conditions of the Universe, matter does not have *strange*, *charm*, *beauty* or *truth* content, at the right conditions (sufficient energies), the formation of hadrons with these quantum numbers may become favourable. Thus, the addition of *strangeness* is necessary to describe the structure of compact stars. In fact, it is expected that in the interior of a neutron star *strangeness* will be present either in the form of hyperons, a kaon condensate or a core of deconfined quark matter [56]. To examine this possibility we use the three flavour version of the **NJL** model:

$$\mathscr{L}^{\rm NJL} = \overline{\psi}\left(i\partial\!\!\!/ - \hat{m} + \hat{\mu}\gamma^0\right)\psi + G_S\sum_{a=0}^{8}\left[\left(\overline{\psi}\lambda^a\psi\right)^2 + \left(\overline{\psi}i\gamma_5\lambda^a\psi\right)^2\right] - \mathscr{L}^{det} - \mathscr{L}^{vec}. \tag{3.75}$$

Here, ψ is three component vector in flavour space, $\hat{m} = diag\,(m_u, m_d, m_s)$ is the quark current mass matrix, $\hat{\mu} = diag\,(\mu_u, \mu_d, \mu_s)$ is the quark chemical potential matrix and is λ^a are matrices of the $U_f(3)$ group, where $\lambda^0 = \sqrt{2/3}\mathbb{1}_{3\times3}$, and λ^i, are the eight Gell-Mann matrices of $SU_f(3)$. In this version of the **NJL** model the sign of the 't Hooft determinant is negative to be consistent with the literature.

For $N_f = 3$, the 't Hooft determinant (3.4) is a six quark interaction. Using the definition (3.6), this term is given by:

$$\det_f \overline{\psi}\mathcal{O}\psi \equiv \sum_{i,j,k}\varepsilon_{ijk}\left(\overline{\psi}_u\mathcal{O}\psi_i\right)\left(\overline{\psi}_d\mathcal{O}\psi_j\right)\left(\overline{\psi}_s\mathcal{O}\psi_k\right). \tag{3.76}$$

The vector interactions for three flavours of quarks are explicitly given by:

$$\begin{aligned}\text{NJL(V+P+VI+PI)}: \ \mathscr{L}_I^{vec} =& G_\omega\left[(\overline{\psi}\gamma^\mu\lambda^0\psi)^2 + (\overline{\psi}\gamma^\mu\gamma_5\lambda^0\psi)^2\right] \\ &+ G_\rho\sum_{a=1}^{8}\left[(\overline{\psi}\gamma^\mu\lambda^a\psi)^2 + (\overline{\psi}\gamma^\mu\gamma_5\lambda^a\psi)^2\right],\end{aligned} \tag{3.77}$$

$$\text{NJL(V+P)}: \ \mathscr{L}_{II}^{vec} = G_\omega\left[(\overline{\psi}\gamma^\mu\lambda^0\psi)^2 + (\overline{\psi}\gamma^\mu\gamma_5\lambda^0\psi)^2\right], \tag{3.78}$$

$$\text{NJL(VI+PI)}: \ \mathscr{L}_{III}^{vec} = G_\rho\sum_{a=1}^{8}\left[(\overline{\psi}\gamma^\mu\lambda^a\psi)^2 + (\overline{\psi}\gamma^\mu\gamma_5\lambda^a\psi)^2\right]. \tag{3.79}$$

The **EoS** can be obtained through the Matsubara formalism presented in Section 2.2.1.

3.3.1 NJL in the MFA (three flavours)

Just like for two flavours, we now apply the **MFA** to the three flavour version of the **NJL** model. Once again, to linearise the Lagrangian density we use the product between two operators given in Equation (C.1). However, as stated previously, the 't Hooft determinant is a six quark interaction. To linearise that section of the Lagrangian we will use the product between three operators in the **MFA** (derived in Appendix C.1):

$$\hat{\mathcal{O}}_1\hat{\mathcal{O}}_2\hat{\mathcal{O}}_3 \approx \hat{\mathcal{O}}_1 \langle\hat{\mathcal{O}}_2\rangle \langle\hat{\mathcal{O}}_3\rangle + \langle\hat{\mathcal{O}}_1\rangle \hat{\mathcal{O}}_2 \langle\hat{\mathcal{O}}_3\rangle + \langle\hat{\mathcal{O}}_1\rangle \langle\hat{\mathcal{O}}_2\rangle \hat{\mathcal{O}}_3 - 2\langle\hat{\mathcal{O}}_1\rangle \langle\hat{\mathcal{O}}_2\rangle \langle\hat{\mathcal{O}}_3\rangle . \tag{3.80}$$

The linearised bilinear operators are:

$$\left(\overline{\psi}\lambda^a\psi\right)^2 \approx 2\left(\overline{\psi}\lambda^a\psi\right)\langle\overline{\psi}\lambda^a\psi\rangle - \langle\overline{\psi}\lambda^a\psi\rangle^2 , \tag{3.81}$$

$$\left(\overline{\psi}i\gamma_5\lambda^a\psi\right)^2 \approx 2\left(\overline{\psi}i\gamma_5\lambda^a\psi\right)\langle\overline{\psi}i\gamma_5\lambda^a\psi\rangle - \langle\overline{\psi}i\gamma_5\lambda^a\psi\rangle^2 , \tag{3.82}$$

$$\left(\overline{\psi}\gamma^\mu\lambda^a\psi\right)^2 \approx 2\left(\overline{\psi}\gamma^\mu\lambda^a\psi\right)\langle\overline{\psi}\gamma^\mu\lambda^a\psi\rangle - \langle\overline{\psi}\gamma^\mu\lambda^a\psi\rangle^2 , \tag{3.83}$$

$$\left(\overline{\psi}\gamma^\mu\gamma_5\lambda^a\psi\right)^2 \approx 2\left(\overline{\psi}\gamma^\mu\gamma_5\lambda^a\psi\right)\langle\overline{\psi}\gamma^\mu\gamma_5\lambda^a\psi\rangle - \langle\overline{\psi}\gamma^\mu\gamma_5\lambda^a\psi\rangle^2 . \tag{3.84}$$

The only non-vanishing quark condensates are:

$$\langle\overline{\psi}\lambda^0\psi\rangle = \sigma^0, \tag{3.85}$$

$$\langle\overline{\psi}\lambda^3\psi\rangle = \sigma^3, \tag{3.86}$$

$$\langle\overline{\psi}\lambda^8\psi\rangle = \sigma^8, \tag{3.87}$$

$$\langle\overline{\psi}\gamma^0\lambda^0\psi\rangle = \omega^0, \tag{3.88}$$

$$\langle\overline{\psi}\gamma^0\lambda^3\psi\rangle = \rho^3 \tag{3.89}$$

$$\langle\overline{\psi}\gamma^0\lambda^8\psi\rangle = \rho^8. \tag{3.90}$$

Explicitly (using the Gell-Mann matrices presented in Appendix B.2):

$$\langle\overline{\psi}\lambda^0\psi\rangle = \sqrt{\frac{2}{3}}\left(\langle\overline{\psi}_u\psi_u\rangle + \langle\overline{\psi}_d\psi_d\rangle + \langle\overline{\psi}_s\psi_s\rangle\right) = \sqrt{\frac{2}{3}}\left(\sigma_u + \sigma_d + \sigma_s\right), \tag{3.91}$$

$$\langle\overline{\psi}\lambda^3\psi\rangle = \langle\overline{\psi}_u\psi_u\rangle - \langle\overline{\psi}_d\psi_d\rangle = \sigma_u - \sigma_d, \tag{3.92}$$

$$\langle\overline{\psi}\lambda^8\psi\rangle = \frac{1}{\sqrt{3}}\left(\langle\overline{\psi}_u\psi_u\rangle + \langle\overline{\psi}_d\psi_d\rangle - 2\langle\overline{\psi}_s\psi_s\rangle\right) = \frac{1}{\sqrt{3}}\left(\sigma_u + \sigma_d - 2\sigma_s\right), \tag{3.93}$$

$$\langle\overline{\psi}\gamma^0\lambda^0\psi\rangle = \sqrt{\frac{2}{3}}\left(\langle\psi_u^\dagger\psi_u\rangle + \langle\psi_d^\dagger\psi_d\rangle + \langle\psi_s^\dagger\psi_s\rangle\right) = \sqrt{\frac{2}{3}}\left(\rho_u + \rho_d + \rho_s\right), \tag{3.94}$$

$$\langle\overline{\psi}\gamma^0\lambda^3\psi\rangle = \langle\psi_u^\dagger\psi_u\rangle - \langle\psi_d^\dagger\psi_d\rangle = \rho_u - \rho_d, \tag{3.95}$$

$$\langle\overline{\psi}\gamma^0\lambda^8\psi\rangle = \frac{1}{\sqrt{3}}\left(\langle\psi_u^\dagger\psi_u\rangle + \langle\psi_d^\dagger\psi_d\rangle - 2\langle\psi_d^\dagger\psi_d\rangle\right) = \frac{1}{\sqrt{3}}\left(\rho_u + \rho_d - 2\rho_s\right). \tag{3.96}$$

The 't Hooft determinant can be written as (see Appendix C.3.2):

$$\begin{aligned}\mathscr{L}^{det} \approx -2G_D \Big[&\left(\overline{\psi}_u\psi_u\right) \langle\overline{\psi}_d\psi_d\rangle \langle\overline{\psi}_s\psi_s\rangle + \langle\overline{\psi}_u\psi_u\rangle \left(\overline{\psi}_d\psi_d\right) \langle\overline{\psi}_s\psi_s\rangle \\ &- \langle\overline{\psi}_u\psi_u\rangle \langle\overline{\psi}_d\psi_d\rangle \left(\overline{\psi}_s\psi_s\right) - 2\langle\overline{\psi}_u\psi_u\rangle \langle\overline{\psi}_d\psi_d\rangle \langle\overline{\psi}_s\psi_s\rangle \Big] = \\ = -2G_D\overline{\psi}\Delta\psi &+ 4G_D\sigma_u\sigma_d\sigma_s, \end{aligned} \tag{3.97}$$

Here, Δ is a matrix in flavour space:

$$\Delta = \begin{pmatrix} \langle\overline{\psi}_d\psi_d\rangle \langle\overline{\psi}_s\psi_s\rangle & 0 & 0 \\ 0 & \langle\overline{\psi}_u\psi_u\rangle \langle\overline{\psi}_s\psi_s\rangle & 0 \\ 0 & 0 & \langle\overline{\psi}_u\psi_u\rangle \langle\overline{\psi}_d\psi_d\rangle \end{pmatrix} = \begin{pmatrix} \sigma_d\sigma_s & 0 & 0 \\ 0 & \sigma_u\sigma_s & 0 \\ 0 & 0 & \sigma_u\sigma_d \end{pmatrix}. \tag{3.98}$$

Finally, the **NJL** Lagrangian in the **MFA**, for three flavours of quarks, with the 't Hooft determinant and a vector interaction ($\mathscr{L}_I^{vec}$) is:

$$\begin{aligned}\mathscr{L}_{\text{MFA}} = &\overline{\psi}\left(i\partial\!\!\!/ - \hat{m} + \hat{\mu}\gamma^0\right)\psi \\ &+ 2G_S\left(\overline{\psi}\lambda^0\psi\right)\sqrt{\frac{2}{3}}\left(\sigma_u+\sigma_d+\sigma_s\right) - \frac{2}{3}G_S\left(\sigma_u+\sigma_d+\sigma_s\right)^2 \\ &+ 2G_S\left(\overline{\psi}\lambda^3\psi\right)\left(\sigma_u-\sigma_d\right) - G_S\left(\sigma_u-\sigma_d\right)^2 \\ &+ 2G_S\left(\overline{\psi}\lambda^8\psi\right)\frac{1}{\sqrt{3}}\left(\sigma_u+\sigma_d-2\sigma_s\right) - \frac{1}{3}G_S\left(\sigma_u+\sigma_d-2\sigma_s\right)^2 \\ &- 2G_D\overline{\psi}\Delta\psi + 4G_D\sigma_u\sigma_d\sigma_s \\ &- 2G_\omega\left(\overline{\psi}\gamma^0\lambda^0\psi\right)\sqrt{\frac{2}{3}}\left(\rho_u+\rho_d+\rho_s\right) + \frac{2}{3}G_\omega\left(\rho_u+\rho_d+\rho_s\right)^2 \\ &- 2G_\rho\left(\overline{\psi}\gamma^0\lambda^3\psi\right)\left(\rho_u-\rho_d\right) + G_\rho\left(\rho_u-\rho_d\right)^2 \\ &- 2G_\rho\left(\overline{\psi}\gamma^0\lambda^8\psi\right)\frac{1}{\sqrt{3}}\left(\rho_u+\rho_d-2\rho_s\right) + \frac{1}{3}G_\rho\left(\rho_u+\rho_d-2\rho_s\right)^2. \end{aligned} \tag{3.99}$$

Once again, writing this expression in the form given by expression (2.44) yields:

$$\mathscr{L}_{\text{MFA}} = \overline{\psi}\left[i\gamma^\mu\left(\partial_\mu + iV_0\delta^0_\mu\right) - \left(\hat{m}+S\right)\right]\psi + U, \tag{3.100}$$

where the auxiliary fields V_0 and S are given by:

$$V_0 = \sqrt{\frac{8}{3}}G_\omega\lambda^0\left(\rho_u+\rho_d+\rho_s\right) + 2G_\rho\lambda^3\left(\rho_u-\rho_d\right) + \frac{2}{\sqrt{3}}G_\rho\lambda^8\left(\rho_u+\rho_d-2\rho_s\right), \tag{3.101}$$

$$S = -\sqrt{\frac{8}{3}}G_S\lambda^0\left(\sigma_u+\sigma_d+\sigma_s\right) - 2G_S\lambda^3\left(\sigma_u-\sigma_d\right) - \frac{2}{\sqrt{3}}G_S\lambda^8\left(\sigma_u+\sigma_d-2\sigma_s\right) + 2G_D\Delta. \tag{3.102}$$

The mean field potential U is:

$$U = -2G_S\left(\sigma_u^2+\sigma_d^2+\sigma_s^2\right)+4G_D\sigma_u\sigma_d\sigma_s + \frac{2}{3}G_\omega\left(\rho_u+\rho_d+\rho_s\right)^2+G_\rho\left(\rho_u-\rho_d\right)^2+\frac{1}{3}G_\rho\left(\rho_u+\rho_d-2\rho_s\right)^2. \tag{3.103}$$

The effective mass M and chemical potential $\hat{\mu}$ for this model are:

$$\hat{M} = \hat{m}-\sqrt{\frac{8}{3}}G_S\lambda^0\left(\sigma_u+\sigma_d+\sigma_s\right)-2G_S\lambda^3\left(\sigma_u-\sigma_d\right) - \frac{2}{\sqrt{3}}G_S\lambda^8\left(\sigma_u+\sigma_d-2\sigma_s\right)+2G_D\Delta, \tag{3.104}$$

$$\tilde{\mu} = \hat{\mu}-\sqrt{\frac{8}{3}}G_\omega\lambda^0\left(\rho_u+\rho_d+\rho_s\right)-2G_\rho\lambda^3\left(\rho_u-\rho_d\right) - \frac{2}{\sqrt{3}}G_\rho\lambda^8\left(\rho_u+\rho_d-2\rho_s\right). \tag{3.105}$$

The grand canonical potential can be obtained in exactly the same way as in the previous section. The fermion field has colour and flavour indices i.e, $I=\{f,c\}$. We get:

$$\Omega_{\mathrm{MFA}}-\Omega_0 = 2G_S\left(\sigma_u^2+\sigma_d^2+\sigma_s^2\right)-4G_D\sigma_u\sigma_d\sigma_s - \frac{2}{3}G_\omega\left(\rho_u+\rho_d+\rho_s\right)^2-G_\rho\left(\rho_u-\rho_d\right)^2-\frac{1}{3}G_\rho\left(\rho_u+\rho_d-2\rho_s\right)^2 - 2T\operatorname*{tr}_{f,c}\int\frac{d^3p}{(2\pi)^3}\left[\beta E+\ln\left(1+e^{-\beta(E+\tilde{\mu})}\right)+\ln\left(1+e^{-\beta(E-\tilde{\mu})}\right)\right]. \tag{3.106}$$

The effective mass in flavour space is:

$$\begin{aligned}\hat{M} &= \hat{m}-\sqrt{\frac{8}{3}}G_S\lambda^0\left(\sigma_u+\sigma_d+\sigma_s\right)-2G_S\lambda^3\left(\sigma_u-\sigma_d\right)-\frac{2}{\sqrt{3}}G_S\lambda^8\left(\sigma_u+\sigma_d-2\sigma_s\right)+2G_D\Delta = \\ &= \begin{pmatrix}m_u&0&0\\0&m_d&0\\0&0&m_s\end{pmatrix}-\frac{4}{3}G_S\left(\sigma_u+\sigma_d+\sigma_s\right)\begin{pmatrix}1&0&0\\0&1&0\\0&0&1\end{pmatrix}-2G_S\left(\sigma_u-\sigma_d\right)\begin{pmatrix}1&0&0\\0&-1&0\\0&0&0\end{pmatrix} \\ &\quad -\frac{2}{3}G_S\left(\sigma_u+\sigma_d-2\sigma_s\right)\begin{pmatrix}1&0&0\\0&1&0\\0&0&-2\end{pmatrix}+2G_D\begin{pmatrix}\sigma_d\sigma_s&0&0\\0&\sigma_u\sigma_s&0\\0&0&\sigma_u\sigma_d\end{pmatrix}= \\ &= \begin{pmatrix}M_u&0&0\\0&M_d&0\\0&0&M_s\end{pmatrix},\end{aligned} \tag{3.107}$$

where the effective mass for each flavour is:

$$M_u = m_u-4G_S\sigma_u+2G_D\sigma_d\sigma_s, \tag{3.108}$$

$$M_d = m_d-4G_S\sigma_d+2G_D\sigma_u\sigma_s, \tag{3.109}$$

$$M_s = m_s-4G_S\sigma_s+2G_D\sigma_u\sigma_d. \tag{3.110}$$

The effective chemical potential $\tilde{\mu}$:

$$\begin{aligned}\tilde{\mu} &= \hat{\mu} - \sqrt{\frac{8}{3}} G_\omega \lambda^0 (\rho_u + \rho_d + \rho_s) - 2G_\rho \lambda^3 (\rho_u - \rho_d) - \frac{2}{\sqrt{3}} G_\rho \lambda^8 (\rho_u + \rho_d - 2\rho_s) = \\ &= \begin{pmatrix} \mu_u & 0 & 0 \\ 0 & \mu_d & 0 \\ 0 & 0 & \mu_s \end{pmatrix} - \frac{4}{3} G_\omega (\rho_u + \rho_d + \rho_s) \begin{pmatrix} 1 & 0 & 0 \\ 0 & 1 & 0 \\ 0 & 0 & 1 \end{pmatrix} - 2G_\rho (\rho_u - \rho_d) \begin{pmatrix} 1 & 0 & 0 \\ 0 & -1 & 0 \\ 0 & 0 & 0 \end{pmatrix} \\ &\quad - \frac{2}{3} G_\rho (\rho_u + \rho_d - 2\rho_s) \begin{pmatrix} 1 & 0 & 0 \\ 0 & 1 & 0 \\ 0 & 0 & -2 \end{pmatrix} = \\ &= \begin{pmatrix} \tilde{\mu}_u & 0 & 0 \\ 0 & \tilde{\mu}_d & 0 \\ 0 & 0 & \tilde{\mu}_s \end{pmatrix}, \end{aligned} \tag{3.111}$$

where:

$$\tilde{\mu}_u = \mu_u - \frac{4}{3} (G_\omega + 2G_\rho) \rho_u - \frac{4}{3} (G_\omega - G_\rho) \rho_d - \frac{4}{3} (G_\omega - G_\rho) \rho_s, \tag{3.112}$$

$$\tilde{\mu}_d = \mu_d - \frac{4}{3} (G_\omega + 2G_\rho) \rho_d - \frac{4}{3} (G_\omega - G_\rho) \rho_s - \frac{4}{3} (G_\omega - G_\rho) \rho_u, \tag{3.113}$$

$$\tilde{\mu}_s = \mu_s - \frac{4}{3} (G_\omega + 2G_\rho) \rho_s - \frac{4}{3} (G_\omega - G_\rho) \rho_u - \frac{4}{3} (G_\omega - G_\rho) \rho_d. \tag{3.114}$$

As before, the trace over the colour indices simply yields a N_c factor. Due to the diagonal nature of the effective mass and effective potential matrices in flavour space (as shown in the previous section), the trace over flavour yields a sum over flavour:

$$\begin{aligned}\Omega_{\text{MFA}} - \Omega_0 = {} & 2G_S \left(\sigma_u^2 + \sigma_d^2 + \sigma_s^2\right) - 4G_D \sigma_u \sigma_d \sigma_s \\ & - \frac{2}{3} G_\omega (\rho_u + \rho_d + \rho_s)^2 - G_\rho (\rho_u - \rho_d)^2 - \frac{1}{3} G_\rho (\rho_u + \rho_d - 2\rho_s)^2 \\ & - 2T N_c \sum_{f=u,d,s} \int \frac{d^3p}{(2\pi)^3} \left[\beta E_f + \ln\left(1 + e^{-\beta\left(E_f + \tilde{\mu}_f\right)}\right) + \ln\left(1 + e^{-\beta\left(E_f - \tilde{\mu}_f\right)}\right)\right]. \end{aligned} \tag{3.115}$$

The values of condensates σ_u, σ_d and σ_s are determined by minimizing the grand canonical potential (see Appendix C.4.2):

$$\frac{\partial \Omega_{\text{MFA}}}{\partial \sigma_u} = \frac{\partial \Omega_{\text{MFA}}}{\partial \sigma_d} = \frac{\partial \Omega_{\text{MFA}}}{\partial \sigma_s} = 0. \tag{3.116}$$

The *gap* equations for three flavours are (see Figure 3.3):

$$M_i = m_i - 4G_S \sigma_i + 2G_D \sigma_j \sigma_k \quad i \neq j \neq k \in \{u, d, s\}. \tag{3.117}$$

here, the quark condensate is given by Equation (3.62).

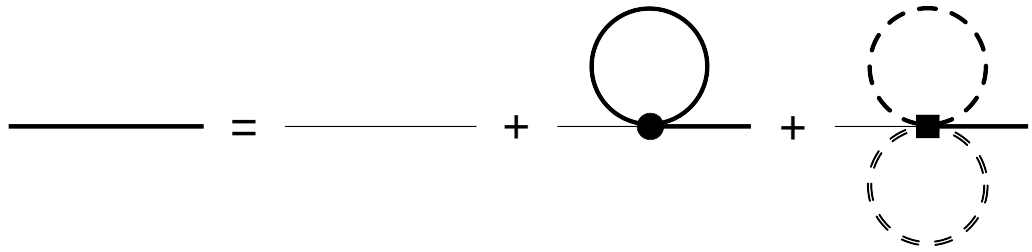

FIGURE 3.3: Diagrammatic representation of the effective mass for flavour i. The dot vertex represents the G_S coupling while the square vertex the G_D coupling. Each type of line (full, dashed, double dashed) corresponds to a contribution of the condensate of each quark flavour.

The quark density is given by Equation (3.63) while, using the thermodynamic relations, we can extract the pressure, energy density and entropy:

$$\begin{aligned} P_{\mathrm{MFA}} = &-\Omega_0 - 2G_S\left(\sigma_u^2+\sigma_d^2+\sigma_s^2\right) + 4G_D\sigma_u\sigma_d\sigma_s \\ &+ \frac{2}{3}G_\omega\left(\rho_u+\rho_d+\rho_s\right)^2 + G_\rho\left(\rho_u-\rho_d\right)^2 + \frac{1}{3}G_\rho\left(\rho_u+\rho_d-2\rho_s\right)^2 \\ &+ 2N_c\sum_{f=u,d,s}\int\frac{d^3p}{(2\pi)^3}\left[E_f + T\ln\left(1+e^{-(E_f+\tilde{\mu}_f)/T}\right) + T\ln\left(1+e^{-(E_f-\tilde{\mu}_f)/T}\right)\right], \end{aligned} \tag{3.118}$$

$$\begin{aligned} \epsilon_{\mathrm{MFA}} = &\Omega_0 + 2G_S\left(\sigma_u^2+\sigma_d^2+\sigma_s^2\right) - 4G_D\sigma_u\sigma_d\sigma_s \\ &- \frac{2}{3}G_\omega\left(\rho_u+\rho_d+\rho_s\right)^2 - G_\rho\left(\rho_u-\rho_d\right)^2 - \frac{1}{3}G_\rho\left(\rho_u+\rho_d-2\rho_s\right)^2 \\ &- 2N_c\sum_{f=u,d,s}\int\frac{d^3p}{(2\pi)^3}\left[E_f\left(1-n_f-\overline{n}_f\right) + n_f\left(\tilde{\mu}_f-\mu_f\right) + \overline{n}_f\left(\mu_f-\tilde{\mu}_f\right)\right]. \end{aligned} \tag{3.119}$$

The entropy is the same as in the two flavour case (3.65), except the sum is extended to the *strange* quark.

3.3.2 $T = 0$ Limit (three flavours)

Following Section 2.4.1 and Appendix D.1.1, in the $T = 0$ limit, the Fermi momentum of the quark of flavour f is:

$$\lambda_{F_f} = \sqrt{\tilde{\mu}_f^2 - M_f^2}. \tag{3.120}$$

Every thermodynamic quantity of interest follows (using Appendix D.1.1):

$$\begin{aligned} P_{\mathrm{MFA}} = &-\Omega_0 - 2G_S\left(\sigma_u^2+\sigma_d^2+\sigma_s^2\right) + 4G_D\sigma_u\sigma_d\sigma_s \\ &+ \frac{2}{3}G_\omega\left(\rho_u+\rho_d+\rho_s\right)^2 + G_\rho\left(\rho_u-\rho_d\right)^2 + \frac{1}{3}G_\rho\left(\rho_u+\rho_d-2\rho_s\right)^2 \\ &+ \frac{N_c}{\pi^2}\sum_{f=u,d,s}\int_{\lambda_{F_f}}^{\Lambda} dpp^2E_f + \frac{N_c}{\pi^2}\sum_{f=u,d,s}\tilde{\mu}_f\frac{\lambda_{F_f}^3}{3}, \end{aligned} \tag{3.121}$$

quark density of flavour f,

$$\rho_f = \frac{N_c}{\pi^2}\frac{\lambda_{F_f}^3}{3}, \tag{3.122}$$

and energy density,

$$\begin{aligned}\epsilon_{\text{MFA}} = \Omega_0 &+ 2G_S\left(\sigma_u^2+\sigma_d^2+\sigma_s^2\right) - 4G_D\sigma_u\sigma_d\sigma_s \\ &- \frac{2}{3}G_\omega\left(\rho_u+\rho_d+\rho_s\right)^2 - G_\rho\left(\rho_u-\rho_d\right)^2 - \frac{1}{3}G_\rho\left(\rho_u+\rho_d-2\rho_s\right)^2 \\ &- \frac{N_c}{\pi^2}\sum_{f=u,d,s}\int_{\lambda_{F_f}}^{\Lambda} dpp^2E_f + \frac{N_c}{\pi^2}\sum_{f=u,d,s}\left(\mu_f-\tilde{\mu}_f\right)\frac{\lambda_{F_f}^3}{3}.\end{aligned} \tag{3.123}$$

The quark condensate in this limit is:

$$\sigma_i = -\frac{N_c}{\pi^2}\int_{\lambda_{F_i}}^{\Lambda} dpp^2\frac{M_i}{E_i}. \tag{3.124}$$

The irrelevant constant Ω_0 is defined as:

$$\Omega_0 = -2G_S\left(\sigma_{u0}^2+\sigma_{d0}^2+\sigma_{s0}^2\right) + 4G_D\sigma_{u0}\sigma_{d0}\sigma_{s0} + \frac{N_c}{\pi^2}\sum_{f=u,d,s}\int_0^{\Lambda} dpp^2E_{f0}, \tag{3.125}$$

where σ_{f0} and E_{f0} are the quark condensate and energy in the vacuum,

$$\sigma_{i0} = -\frac{N_c}{\pi^2}\int_0^{\Lambda} dpp^2\frac{M_{i0}}{E_{i0}}, \tag{3.126}$$

$$E_{i0} = \sqrt{p^2+M_{i0}}. \tag{3.127}$$

Chapter 4

Neutron Stars

4.1 General aspects

Discovered in 1967, neutron stars are one of the most extreme and interesting objects in the Universe. They are one of the three main endpoints of stellar evolution and are currently being used as "laboratories" to study the origins of the Universe and the nature of matter itself. Ultimately, there is a lot of knowledge to acquire about the laws of nature in extreme conditions that do not exist anywhere else.

During the life of a star two forces are in balance, the star's own gravity and the radiation pressure from nuclear fusion. In the later process, lighter elements are fused into heavier ones that accumulate in the core of the star. However, when the fusion process reaches iron, no more elements can be produced within the star and nuclear fusion stops. The core must be supported by electron degeneracy pressure alone (due to Pauli exclusion principle). When the star has a mass superior to 1.4 solar masses (Chandrasekhar limit), electron degeneracy pressure is overcome and electrons and protons fuse into neutrons via electron capture, releasing neutrinos. At this point, neutron degeneracy pressure halts the contraction of the star and the left remnant of the gravitational collapse is a neutron star. If this remnant has more than $1.5 - 3$ solar masses (Tolman–Oppenheimer–Volkoff limit, not exactly known), it collapses further to form a black hole.

Neutron stars have a thin atmosphere of hot plasma at the surface. In the interior they are mostly composed of neutrons however, other particles may exist in its interior (see Figure 4.1). The crust is composed of iron atoms in a sea of electrons. Closer to the core, extreme densities make possible the existence of exotic types of particles and matter like: hyperons, Bose-Einstein condensates and even some kind of ultra-dense quark matter.

The core composition is not currently known and several efforts are being made to determine possible observational signatures that would give some insight about it. The present work tries to infer about the possibility of a quark matter core through a two model approach to the **EoS** of neutron star matter.

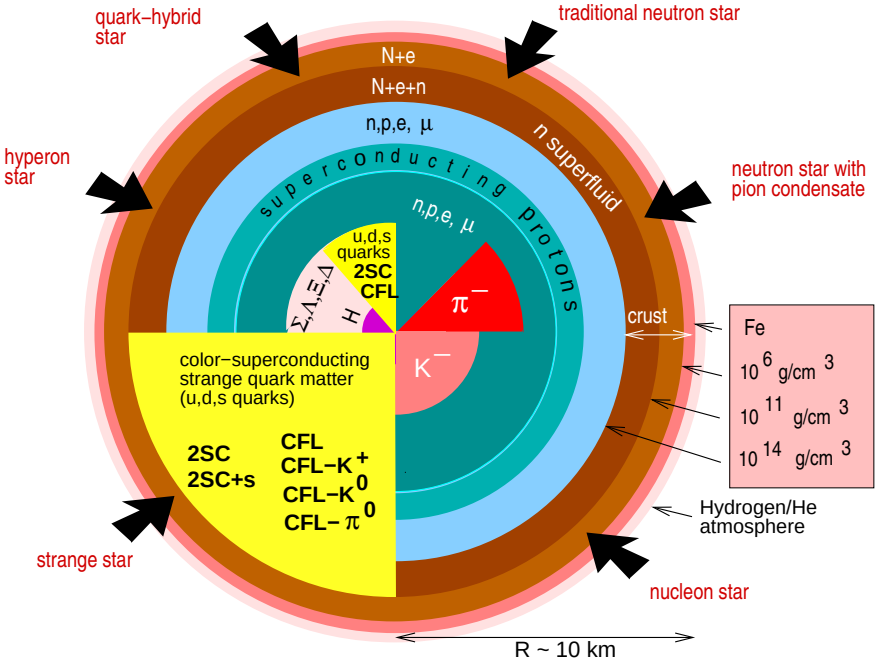

FIGURE 4.1: Different theoretical predictions for the composition of a neutron star. In the present work we study the possiblitiy of a hybrid star with core composed of quarks (Image taken from [57]).

Due to its incredible compact nature and strong gravitational field, neutron stars must be treated with Einstein's general theory of relativity for a more legitimate description.

4.2 Quantum hadrodynamics

Theoretical nuclear physics deals with mathematical models that provide an accurate description of the properties, structures and mechanisms of nuclear matter. An exact theoretical description of the nuclear force (potential) that derives from **QCD** is unknown. These theoretical models must rely on experimental evidences, that provide several empirical properties of nuclear matter:

- The nuclear force between two protons is the same as the force between two neutrons and their masses are almost the same;
- The nuclear force has a very short range;
- Nuclear matter is a saturated system (the addition of a nucleon to the bulk only increases the volume, not the binding energy per nucleon), which implies intermediate attraction;
- The nuclear medium is homogeneous, isotropic and the free path of nucleons is much larger than the nucleon size (independent particles);

These properties led to the creation of the "liquid-drop model", which treats the nucleus as a drop of incompressible nuclear fluid. Within this model, the Bethe–Weizsäcker mass formula (4.1) gives the binding energy E_B, of a nucleus based only on it's mass and atomic

number, A and Z. It has several contributions like volume energy, surface tension, Coulomb repulsion and proton-neutron asymmetry.

$$\begin{aligned} E_B &= E_{Volume} + E_{Surface} + E_{Coulomb} + E_{Asymmetry} = \\ &= a_V A - a_S A^{2/3} - a_C \frac{Z^2}{A^{1/3}} - a_A \frac{(A-2Z)^2}{A}. \end{aligned} \tag{4.1}$$

The constants a_V, a_S, a_C and a_A can be calculated by fitting experimental data and be related to the coupling constants of relativistic nuclear field models.

4.2.1 Relativistic nuclear field theory

Quantum hadrodynamics (**QHD**) is the name given to effective relativistic nuclear field models, whose degrees of freedom are hadrons. To introduce the formalism, we consider the simple $(\sigma - \omega)$ model, originally proposed by Johnson and Teller, Duer and Walecka [58–60] . The $(\sigma - \omega)$ model reproduces some properties of nuclear matter near saturation density and describes the relativistic effects at higher densities. It is based on the fields of four particles: the nucleons, a scalar meson (σ) and a vector meson (ω_μ). In the static limit, one boson exchange of these mesons reproduces the intermediate-range attraction (σ meson),

$$\left(-\nabla^2 + m_\sigma^2\right) \sigma\left(\boldsymbol{x}\right) = -g_\sigma \delta^{(3)}\left(\boldsymbol{x}\right) \Rightarrow \sigma(\boldsymbol{x}) = -\frac{g_\sigma}{4\pi} \frac{e^{-m_{\sigma|\boldsymbol{x}|}}}{|\boldsymbol{x}|}, \tag{4.2}$$

and the short-range repulsion (ω meson),

$$\left(-\nabla^2 + m_\omega^2\right) \gamma^\mu \omega_\mu\left(\boldsymbol{x}\right) = g_\omega \delta^{(3)}\left(\boldsymbol{x}\right) \Rightarrow \gamma^\mu \omega_\mu(\boldsymbol{x}) = \frac{g_\omega}{4\pi} \frac{e^{-m_{\omega|\boldsymbol{x}|}}}{|\boldsymbol{x}|}, \tag{4.3}$$

of the nucleon-nucleon Yukawa potential:

$$\begin{aligned} V_{NN}^{\sigma,\omega}(|\boldsymbol{x}|) &= g_\omega \gamma^\mu \omega_\mu\left(\boldsymbol{x}\right) + g_\sigma \sigma\left(\boldsymbol{x}\right) = \\ &= \left(\frac{g_\omega^2}{4\pi} \frac{e^{-m_\omega|\boldsymbol{x}|}}{|\boldsymbol{x}|}\right) + \left(-\frac{g_\sigma^2}{4\pi} \frac{e^{-m_\sigma|\boldsymbol{x}|}}{|\boldsymbol{x}|}\right). \end{aligned} \tag{4.4}$$

The sign of the coupling constants g_σ and g_ω are chosen to make the σ meson potential attractive and the ω meson repulsive.

The Lagrangian density for the $(\sigma - \omega)$ model is given by the sum of the free Lagrangians of each field (nucleons and meson fields),

$$\mathscr{L}_N^{free} = \overline{\psi}_N \left[i\partial\!\!\!/ - m\right] \psi_N \tag{4.5}$$

$$\mathscr{L}_\sigma^{free} = \frac{1}{2} \left(\partial_\mu \sigma\right) \left(\partial^\mu \sigma\right) - \frac{1}{2} m_\sigma^2 \sigma^2 \tag{4.6}$$

$$\mathscr{L}_\omega^{free} = -\frac{1}{4} \omega_{\mu\nu} \omega^{\mu\nu} + \frac{1}{2} m_\omega^2 \omega_\mu \omega^\mu, \tag{4.7}$$

and an interaction Lagrangian where the scalar meson (σ) is coupled to the scalar density $\overline{\psi}_N\psi_N$ and the vector meson (ω_μ) is coupled to the baryon four current $\overline{\psi}_N\gamma^\mu\psi_N$:

$$\mathscr{L}^{int} = g_\sigma\sigma\overline{\psi}\psi - g_\omega\omega_\mu\overline{\psi}\gamma^\mu\psi. \tag{4.8}$$

Putting all together yields:

$$\begin{aligned}\mathscr{L}^{\sigma-\omega} = &\overline{\psi}_N\left[i\gamma^\mu\left(\partial_\mu + ig_\omega\omega_\mu\right) - \left(m - g_\sigma\sigma\right)\right]\psi_N \\ &+ \frac{1}{2}\left(\partial_\mu\sigma\right)\left(\partial^\mu\sigma\right) - \frac{1}{2}m_\sigma^2\sigma^2 - \frac{1}{4}\omega_{\mu\nu}\omega^{\mu\nu} + \frac{1}{2}m_\omega^2\omega_\mu\omega^\mu.\end{aligned} \tag{4.9}$$

Here, the nucleon field is represented by a Dirac-spinor $\psi = (p,\ n)^T$ as an isospin doublet state of proton and neutron, which have the same mass m. The term $\omega_{\mu\nu} = \partial_\mu\omega_\nu - \partial_\nu\omega_\mu$, is the strength tensor of the vector meson.

The theory parameters $m^* \equiv m - g_\sigma\sigma$, m_σ, m_ω, g_σ and g_ω can be algebraically connected to five important properties of nuclear matter [56]:

- The binding energy per nucleon and nucleon number density at saturation, normalize the **EoS** at one point in the energy-density plane;
- The compression modulus (K) and effective nuclear mass (m^*) at saturation assures that extrapolation to higher density is correct, in the vicinity of saturation (controlling the "stiffness" or softness of the **EoS**);
- The isospin symmetry coefficient (a_A) assures that small extrapolations, to isospin asymmetric systems, are correct.

However, the simple ($\sigma - \omega$) model fails at an accurate description of the compression modulus at saturation ($K \approx 550MeV$, a factor of two times larger than it should be), of the effective nuclear mass ($m^* \approx 0.5$, in poor agreement with empirical range) and the symmetry coefficient ($a_A \sim 15$ MeV, a factor of two times smaller than present experimental data). Both of these properties affect the high-density behaviour of the **EoS**, generating an extremely stiff **EoS**. Due to this flaws, the model is not expected to extrapolate very well to high densities, in neither symmetric or asymmetric matter. As we are interested in describing neutron star matter, extrapolation to high density is of ultimate importance.

4.2.2 The nonlinear Walecka model

Following Boguta and Bodmer [61], to solve the shortcomings of the simple ($\sigma - \omega$) model, we add self-interactions of the scalar field:

$$U\left(\sigma\right) = \frac{1}{3}bm\left(g_\sigma\sigma\right)^3 + \frac{1}{4}c\left(g_\sigma\sigma\right)^4, \tag{4.10}$$

where the additional coupling constants b and c are dimensionless due to the introduction of the mass m. This term allows the model to better reproduce the values of the compression

modulus K and effective mass m^* at saturation, properties of great importance for the high-density behaviour of the **EoS**.

A quartic term in ω,

$$\mathscr{L}_{\omega\omega}^{int} = \frac{1}{4!}\xi g_\omega^4 \left(\omega_\mu \omega^\mu\right)^2, \tag{4.11}$$

was proposed in [62] to be able to fit the ground-state properties of several nuclei and Dirac-Bruecker-Hartree-Fock calculations at large densities.

As we are interested in describing neutron star matter (asymmetric systems) we can add to the theory an isospin restoring interaction, mimicking the Bethe–Weizsäcker mass formula and the valley of beta stability in nuclear physics. Such interaction is given by the $\boldsymbol{\rho}_\mu$ meson, an isospin triplet which couple to the isospin current of the nucleon in the following way:

$$\mathscr{L}_{\rho N}^{int} = -\frac{1}{2}\overline{\psi}_N \gamma^\mu g_\rho \boldsymbol{\tau}\cdot\boldsymbol{\rho}_\mu \psi_N. \tag{4.12}$$

This interactions leads to a quadratic contribution in the deviation from isospin symmetry in the energy density of the theory. The free Lagrangian for this new field is:

$$\mathscr{L}_\rho^{free} = -\frac{1}{4}\boldsymbol{\rho}_{\mu\nu}\cdot\boldsymbol{\rho}^{\mu\nu} + \frac{1}{2}m_\rho^2\,\boldsymbol{\rho}_\mu\cdot\boldsymbol{\rho}^\mu, \tag{4.13}$$

here $\boldsymbol{\rho}_{\mu\nu} = \partial_\mu\boldsymbol{\rho}_\nu - \partial_\nu\boldsymbol{\rho}_\mu$ is the field-strength tensor, an m_ρ is its mass.

We also allow for an interaction between the mesons, ω and $\boldsymbol{\rho}$, through a non-linear interaction term of the type:

$$\mathscr{L}_{\omega\rho}^{int} = \Lambda_\omega \left(g_\omega^2 \omega_\mu \omega^\mu\right)\left(g_\rho^2\,\boldsymbol{\rho}_\mu\cdot\boldsymbol{\rho}^\mu\right). \tag{4.14}$$

This term is needed to get a good slope of the symmetry energy L at saturation density, as suggested in [63].

The NL3$\omega\rho$ model is given by the Lagrangian density with all of these contributions. It can be written as:

$$\begin{aligned}
\mathscr{L}^{\mathrm{NL3}\omega\rho} = {} & \overline{\psi}_N\left[\gamma^\mu\left(i\partial_\mu - g_\omega\omega_\mu - \frac{1}{2}g_\rho\boldsymbol{\tau}\cdot\boldsymbol{\rho_\mu}\right) - (m - g_\sigma\sigma)\right]\psi_N \\
& + \frac{1}{2}\partial^\mu\sigma\partial_\mu\sigma - \frac{1}{2}m_\sigma^2\sigma^2 - \frac{1}{3}bm(g_\sigma\sigma)^3 - \frac{1}{4}c(g_\sigma\sigma)^4 \\
& + \frac{1}{2}m_\omega^2\omega^\mu\omega_\mu - \frac{1}{4}\omega_{\mu\nu}\omega^{\mu\nu} + \frac{1}{4!}\xi g_\omega^4\left(\omega_\mu\omega^\mu\right)^2 \\
& - \frac{1}{4}\boldsymbol{\rho}^{\mu\nu}\cdot\boldsymbol{\rho}_{\mu\nu} + \frac{1}{2}\,m_\rho^2\,\boldsymbol{\rho}^\mu\cdot\boldsymbol{\rho}_\mu \\
& + \Lambda_\omega\left(g_\omega^2\omega_\mu\omega^\mu\right)\left(g_\rho^2\,\boldsymbol{\rho}_\mu\cdot\boldsymbol{\rho}^\mu\right).
\end{aligned} \tag{4.15}$$

Hyperons are expected to appear inside a neutron star, when densities reach two to three times the saturation density. However, we will not consider hyperons in the present work.

Instead, we investigate the onset of *strangeness* in the quark phase inside the star. The onset of this degree of freedom softens the **EoS** leading to smaller neutron star masses [14].

4.2.3 The nonlinear Walecka in the MFA

As implemented in the previous section for the **NJL** model, we are going to work in the **MFA** approximation. As stated previously (Section 3.2.1), only fields whose **VEV** is non-zero should contribute. The ground state is assumed to be a degenerate fermion state with eigenvalues modified by the presence of the (mean) meson fields, implying that the ground state as a definite charge, spin and parity. This means that any meson state which may change these properties must have a vanishing **VEV** (case of the first and second components of the ρ meson). As we are in equilibrium, any Lorentz vector current must vanish as well. Resuming, we will consider (we replace the fields by their respective **VEV**):

$$\langle\sigma\rangle = \sigma, \tag{4.16}$$

$$\langle\omega_0\rangle = \omega_0, \tag{4.17}$$

$$\langle\rho_0^3\rangle = \rho_0^3, \tag{4.18}$$

$$\langle\omega_i\rangle = \langle\boldsymbol{\rho}_i\rangle = \langle\rho_0^1\rangle = \langle\rho_0^2\rangle = 0. \tag{4.19}$$

Adding a chemical potential due to the conserved charge (2.46), the Lagrangian density in the **MFA** takes the form:

$$\begin{aligned}\mathscr{L}_{\text{MFA}} = \overline{\psi}_N &\left[i\gamma^\mu\left(\partial_\mu + ig_\omega\omega_0\delta_\mu^0 + \frac{i}{2}g_\rho\tau^3\rho_0^3\delta_\mu^0\right) - (m - g_\sigma\sigma) + \hat{\mu}\gamma^0\right]\psi_N \\ &- \frac{1}{2}m_\sigma^2\sigma^2 - \frac{1}{3}bm(g_\sigma\sigma)^3 - \frac{1}{4}c(g_\sigma\sigma)^4 + \frac{1}{2}m_\omega^2\left(\omega_0\right)^2 + \frac{1}{4!}\xi g_\omega^4\left(\omega_0\right)^4 \\ &+ \frac{1}{2}\,m_\rho^2\left(\rho_0^3\right)^2 + \Lambda_\omega g_\omega^2 g_\rho^2\left(\omega_0\right)^2\left(\rho_0^3\right)^2.\end{aligned} \tag{4.20}$$

The chemical potential is a diagonal matrix in isospin space, where the entries corresponds to the chemical potential of the proton and neutron, respectively, i.e. $\hat{\mu} = diag\left(\mu_p, \mu_n\right)$. Writing this Lagrangian density in the form given in Equation (2.44) yields:

$$\mathscr{L}_{\text{MFA}} = \overline{\psi}_N\left[i\gamma^\mu\left(\partial_\mu + iV_0\delta_\mu^0\right) - (m + S)\right]\psi_N + U\left(V_0, S\right), \tag{4.21}$$

where:

$$V_0 = g_\omega\omega_0 + \frac{1}{2}g_\rho\tau^3\rho_0^3, \tag{4.22}$$

$$S = -g_\sigma\sigma, \tag{4.23}$$

$$\begin{aligned}U = &-\frac{1}{2}m_\sigma^2\sigma^2 - \frac{1}{3}bm(g_\sigma\sigma)^3 - \frac{1}{4}c(g_\sigma\sigma)^4 + \frac{1}{2}m_\omega^2\left(\omega_0\right)^2 + \frac{1}{4!}\xi g_\omega^4\left(\omega_0\right)^4 \\ &+ \frac{1}{2}\,m_\rho^2\left(\rho_0^3\right)^2 + \Lambda_\omega g_\omega^2 g_\rho^2\left(\omega_0\right)^2\left(\rho_0^3\right)^2.\end{aligned} \tag{4.24}$$

The effective mass M and chemical potential $\hat{\mu}$ are:

$$M = m - g_\sigma \sigma, \tag{4.25}$$

$$\tilde{\mu} = \hat{\mu} - g_\omega \omega_0 - \frac{1}{2} g_\rho \tau^3 \rho_0^3. \tag{4.26}$$

Following Section 2.3, the grand canonical potential for this Lagrangian is calculated. The fermion field ψ is an isospin doublet state of proton and neutron. This means that the set of extra indices I contains only isospin indices, $I = \{i\}$. The grand canonical (2.71) is:

$$\begin{aligned}\Omega_{\mathrm{MFA}} - \Omega_0 = &-\frac{1}{2} m_\sigma^2 \sigma^2 - \frac{1}{3} bm (g_\sigma \sigma)^3 - \frac{1}{4} c (g_\sigma \sigma)^4 + \frac{1}{2} m_\omega^2 (\omega_0)^2 + \frac{1}{4!} \xi g_\omega^4 (\omega_0)^4 \\ &+ \frac{1}{2} m_\rho^2 \left(\rho_0^3\right)^2 + \Lambda_\omega g_\omega^2 g_\rho^2 (\omega_0)^2 \left(\rho_0^3\right)^2 \\ &- 2T \operatorname*{tr}_i \int \frac{d^3p}{(2\pi)^3} \left[\beta E + \ln\left(1 + e^{-\beta(E+\tilde{\mu})}\right) + \ln\left(1 + e^{-\beta(E-\tilde{\mu})}\right)\right].\end{aligned} \tag{4.27}$$

Writing the effective chemical potential in the isospin space yields:

$$\begin{aligned}\tilde{\mu} &= \hat{\mu} - g_\omega \omega_0 - \frac{1}{2} g_\rho \tau^3 \rho_0^3 = \\ &= \begin{pmatrix} \mu_p & 0 \\ 0 & \mu_n \end{pmatrix} - g_\omega \omega_0 \begin{pmatrix} 1 & 0 \\ 0 & 1 \end{pmatrix} - \frac{1}{2} g_\rho \rho_0^3 \begin{pmatrix} 1 & 0 \\ 0 & -1 \end{pmatrix} = \\ &= \begin{pmatrix} \tilde{\mu}_p & 0 \\ 0 & \tilde{\mu}_n \end{pmatrix}.\end{aligned} \tag{4.28}$$

The effective chemical potential for the proton (μ_p) and the neutron (μ_n) have been defined as:

$$\tilde{\mu}_p = \mu_p - g_\omega \omega_0 - \frac{1}{2} g_\rho \rho_0^3, \tag{4.29}$$

$$\tilde{\mu}_n = \mu_n - g_\omega \omega_0 + \frac{1}{2} g_\rho \rho_0^3. \tag{4.30}$$

Following previous sections, the trace operation is simply given by a sum over different isospin states i.e., over the proton and neutron:

$$\begin{aligned}\Omega_{\mathrm{MFA}} - \Omega_0 = &-\frac{1}{2} m_\sigma^2 \sigma^2 - \frac{1}{3} bm (g_\sigma \sigma)^3 - \frac{1}{4} c (g_\sigma \sigma)^4 + \frac{1}{2} m_\omega^2 (\omega_0)^2 + \frac{1}{4!} \xi g_\omega^4 (\omega_0)^4 \\ &+ \frac{1}{2} m_\rho^2 \left(\rho_0^3\right)^2 + \Lambda_\omega g_\omega^2 g_\rho^2 (\omega_0)^2 \left(\rho_0^3\right)^2 \\ &- 2T \sum_{i=p,n} \int \frac{d^3p}{(2\pi)^3} \left[\beta E + \ln\left(1 + e^{-\beta(E+\tilde{\mu}_i)}\right) + \ln\left(1 + e^{-\beta(E-\tilde{\mu}_i)}\right)\right].\end{aligned} \tag{4.31}$$

Once more, Ω_0 is chosen in such a way that the pressure and energy density vanish in the vacuum.

We can now apply the no sea approximation i.e., we do not take the term βE in Equation

(4.31) in consideration. With this approximation, we suppose that the parameters of the theory take into account several effects, including this approximation. One can always use the term βE however, the coupling parameters will be different.

Following Section 2.3, the **VEV** of the fields σ, ω_0 and ρ_0^3, are determined by minimizing the grand canonical potential in relation to them:

$$\frac{\partial \Omega_{\text{MFA}}}{\partial \sigma} = \frac{\partial \Omega_{\text{MFA}}}{\partial \omega_0} = \frac{\partial \Omega_{\text{MFA}}}{\partial \rho_0^3} = 0. \tag{4.32}$$

This yields:

$$m_\sigma^2 \sigma + b m g_\sigma^3 \sigma^2 + c g_\sigma^4 \sigma^3 = -2 g_\sigma \sum_{i=p,n} \int \frac{d^3p}{(2\pi)^3} \frac{M}{E} \left[n_i + \overline{n}_i \right], \tag{4.33}$$

$$m_\omega^2 \omega_0 + \frac{1}{3!} \xi g_\omega^4 \left(\omega_0\right)^3 + 2 \Lambda_\omega g_\omega^2 g_\rho^2 \omega_0 \left(\rho_0^3\right)^2 = -2 g_\omega \sum_{i=p,n} \int \frac{d^3p}{(2\pi)^3} \left[n_i - \overline{n}_i \right], \tag{4.34}$$

$$m_\rho^2 \rho_0^3 + 2 \Lambda_\omega g_\omega^2 g_\rho^2 \left(\omega_0\right)^2 \rho_0^3 = -2 g_\rho \int \frac{d^3p}{(2\pi)^3} \left[n_p - \overline{n}_p \right] + 2 g_\rho \int \frac{d^3p}{(2\pi)^3} \left[n_n - \overline{n}_n \right]. \tag{4.35}$$

Where, n_i and $\overline{n}_i$ are the particle and anti-particle occupation number defined in Equations (2.82) and (2.83). Following previous sections one derives from Equation (4.31) the pressure, energy density, particle density and entropy. The $T = 0$ limit can be obtained by following Section 2.4.1 and Appendix D.1.1.

4.3 The Bag constant and Gibbs construction

As pointed out in [12] the pressure within the **NJL**-type models is defined up to a constant B, similarly to the MIT Bag constant. This constant is usually fixed by requiring that the corrected pressure $P - B$ goes to zero at vanishing baryonic chemical potential. However, the procedure used to fix the effective Bag constant within **NJL** models is crucial for the stability of the star when the phase transition to quark matter is considered. In the same work [12], to fix the Bag constant B^* it is proposed that the deconfinement occurs at the same baryonic chemical potential, μ_B^{crit}, as the chiral phase transition (when chiral symmetry is partially restored).

Here, deconfinement means the change of degrees of freedom, not a phase transition described by an order parameter like the Polyakov loop. In Chapter 6, the Polyakov loop will be included in the study of hybrid stars, through the Polyakov−Nambu–Jona-Lasinio model (**PNJL**).

Indeed, by introducing a low density **EoS** having hadronic degrees of freedom, like the **EoS** of the nonlinear Walecka calculated in Section 4.2.2, and then computing the transition to quark matter (using for example the Gibbs construction), the deconfinement transition can coincide with the chiral transition by adding to the quark **EoS** in $SU_f(2)$ and in $SU_f(3)$ the suitable value of the Bag constant, B^*.

Throughout this work the value of B^* is fixed in such a way that the deconfinement phase transition and the transition to the phase where chiral symmetry is partially restored coincide (same μ_B^{crit}). We investigate the $B^* = 0$ case as well for comparison purposes. The **EoS** for the quark models is changed by the Bag constant in the following way:

$$P_{eff} = P^{\text{ quarks}} + B^*, \tag{4.36}$$

$$\epsilon_{eff} = \epsilon^{\text{ quarks}} - B^*. \tag{4.37}$$

To build the hybrid **EoS** we used the Gibbs condition. The Gibbs condition implies that both phases, must be in chemical, thermal and mechanical equilibrium, i.e.:

$$\mu_B^H = \mu_B^Q, \tag{4.38}$$

$$p_B^H = p_B^Q, \tag{4.39}$$

$$T_B^H = T_B^Q, \tag{4.40}$$

where the H and Q indices represent, respectively, the confined (hadronic) and deconfined (quark) phase.

4.4 Neutron star matter

The temperature in neutron stars older than several minutes is below 1 MeV, negligible when compared to chemical potentials and masses. Thus, the $T = 0$ limit of the **EoS** can be considered, meaning that matter is extremely degenerate.

We will further consider matter in $\beta-$equilibrium, with zero electrical net charge, i.e.,

$$\rho_Q = 0. \tag{4.41}$$

If we consider *strange* matter, this relation imposes (see Table 3.1):

$$\frac{2}{3}\rho_u - \frac{1}{3}\left(\rho_d + \rho_s + 3\rho_e\right) = 0. \tag{4.42}$$

In $\beta-$equilibrium, the neutron decay and electron capture happens at the same rate, i.e.:

$$n \rightleftarrows p + e^- + \overline{\nu}_e \Leftrightarrow d \rightleftarrows u + e^- + \overline{\nu}_e. \tag{4.43}$$

If *strangeness* is considered, we have another equilibrium condition:

$$d \rightleftarrows s. \tag{4.44}$$

These relations act as constrains on the chemical potentials:

$$\mu_d = \mu_u + \mu_{e^-} + \mu_{\overline{\nu}_e} = \mu_s. \tag{4.45}$$

Considering that the neutrinos escape because they interact very poorly with the rest of matter, their chemical potential can be ignored, yielding:

$$\mu_d = \mu_u + \mu_{e^-} = \mu_s. \tag{4.46}$$

4.4.1 Leptonic contribution

To analyse matter in $\beta-$equilibrium, we must consider a leptonic contribution to the **EoS** of the system. This contribution is taken into account by considering the pressure and energy density of a free gas of electrons. Following Section 2.4, the pressure, density, entropy and energy density for a gas of free electrons are given by Equations (2.78), (2.79), (2.80), (2.81), with $N_I = 1$. The $T = 0$ limit of these expressions are calculated in the same section, are explicitly given by:

$$P_e = \frac{1}{\pi^2}\left[\int_{\lambda_{F_e}}^{+\infty} dp\; p^2 E_e + \mu_e \frac{\lambda_{F_e}^3}{3}\right] - \Omega_{0e}, \tag{4.47}$$

$$\rho_e = \frac{\lambda_{F_e}^3}{3\pi^2}, \tag{4.48}$$

and,

$$\epsilon_e = \Omega_{0e} - \frac{1}{\pi^2}\int_{\lambda_{F_e}}^{+\infty} dp p^2 E_e. \tag{4.49}$$

4.5 General relativity

Proposed by Albert Einstein in 1915, general relativity is the geometric description of gravity. The main goal of this theory is to find the metric elements $g_{\mu\nu}$ which can be used to define the line element ds^2:

$$ds^2 = g_{\mu\nu} dx^\mu dx^\nu. \tag{4.50}$$

Once one knows completely the metric function, everything there is to know about a given space-time can be extracted from it. General relativity is usually mentioned as the most beautiful of all physical theories [64] after all, not only does it give an elegant interpretation of gravitational phenomena, but it is also encoded in a single, simple, covariant field equation:

$$G_{\mu\nu} = 8\pi G T_{\mu\nu}, \tag{4.51}$$

where G is Newton's gravitational constant, $T_{\mu\nu}$ is the totally symmetric energy-momentum tensor:

$$T_{\mu\nu} = -Pg_{\mu\nu} + (P + \epsilon)\, u_\mu u_\nu \quad \text{with} \quad u^\mu = \frac{dx^\mu}{d\tau}, \tag{4.52}$$

P is the pressure and ϵ is the energy density. $G_{\mu\nu}$ is the divergenceless Einstein tensor:

$$G_{\mu\nu} = R_{\mu\nu} - \frac{1}{2} R g_{\mu\nu}, \tag{4.53}$$

$R_{\mu\nu}$ is the Ricci tensor and $R = R_{\mu\nu} g^{\mu\nu}$ is the Ricci scalar. The Ricci tensor is obtained by contracting the Riemann(-Christoffel) tensor, defined as:

$$R^\lambda_{\mu\gamma\nu} = \partial_\gamma \Gamma^\lambda_{\mu\nu} - \partial_\nu \Gamma^\lambda_{\mu\lambda} + \Gamma^\alpha_{\mu\nu} \Gamma^\lambda_{\alpha\gamma} - \Gamma^\alpha_{\mu\gamma} \Gamma^\lambda_{\alpha\nu}. \tag{4.54}$$

This tensor is defined in terms of the Christoffel symbols and its first derivatives. The Christoffel symbols are not tensors, but can be defined in the covariant derivative to make the differentiation of a tensor, always a tensor. The covariant derivative of a first order tensor is

$$\nabla_\mu V_\nu = \partial_\mu V_\nu - \Gamma^\lambda_{\mu\nu} V_\lambda. \tag{4.55}$$

Writing the covariant derivative of the metric tensor and re-arranging terms, it is possible to calculate the Christoffel symbols directly from the metric tensor and its first derivatives:

$$\Gamma^\lambda_{\mu\nu} = \frac{1}{2} g^{\lambda\rho} \left(\partial_\mu g_{\nu\rho} + \partial_\nu g_{\rho\mu} - \partial_\rho g_{\mu\nu} \right). \tag{4.56}$$

Plugging (4.56) into the definition of Riemann tensor (4.54), one can extract the following properties:

$$R_{\lambda\mu\gamma\nu} = -R_{\mu\lambda\gamma\nu} = -R_{\lambda\mu\nu\gamma} = R_{\gamma\nu\lambda\mu}, \tag{4.57}$$

$$R_{\lambda\mu\gamma\nu} + R_{\mu\nu\lambda\gamma} + R_{\lambda\nu\mu\gamma} = 0, \tag{4.58}$$

$$\nabla_\alpha R_{\lambda\mu\gamma\nu} + \nabla_\nu R_{\mu\lambda\alpha\gamma} + \nabla_\gamma R_{\lambda\mu\nu\alpha} = 0. \tag{4.59}$$

The set of Equations (4.59) are called the Bianchi identities. If a space-time is flat, all elements of the Riemann tensor must vanish in every point.

Einstein's field equation relates the local geometry of a space-time with its local distribution of energy. Contrary to Newton's point of view, space-time is not just the stage for physical phenomena but plays a role in it: the distribution of matter and energy tells space-time how to curve, and the curvature of space-time tells matter and energy how to move, giving the theory non-linear effects.

4.5.1 Partial decoupling of matter from gravity

Noether's theorem (Appendix A.1) states that, from the invariance of a field theory under space-time translations, a conserved quantity can be defined, the energy-momentum tensor. Under those conditions, the energy-momentum tensor of a field theory, in Minkowski space, is given by:

$$T_{\mu\nu} = \frac{\partial \mathscr{L}}{\partial\left(\partial_\alpha \phi\right)} \eta_{\alpha\mu} \partial_\nu \phi - \eta_{\mu\nu} \mathscr{L}, \tag{4.60}$$

where ϕ is the field (or fields) present in the Lagrangian density. The energy-momentum-tensor defined this way is not guaranteed to be totally symmetric. However, one can always add some irrelevant term (whose divergence is zero) to make the energy-momentum tensor totally symmetric (like the one on the right side of Equation (4.51))[36]. From the principle of general covariance[1] one could write the energy-momentum tensor for a field theory in general relativity just by replacing the Minkowski metric $\eta_{\mu\nu}$ with a general metric $g_{\mu\nu}$ and promoting normal derivatives to covariant ones. This, however, would completely couple the field theory to Einstein's field equations. On the other hand, we are interested in solving Einstein's field equations for a neutron star. In the limit of stellar collapse, the change in the radial component of the metric element ($g_{11} = g_{rr}$ in spherical coordinates) over the spacing of a nucleus of radius $r_0 = 1.2$ fm is of the order of 10^{-19} [56], i.e., the metric change along the radius of a nucleus is negligible. This, together with the fact that, in 1965 Wheeler and collaborators proved the validity of an **EoS** in the description of the interior of a star [65], allows one to describe each small volume in the star by the laws of special relativity. We then solve the field equations for matter in Minkowski space-time and solve Einstein's field equations with a energy-momentum tensor that is diagonal in a comoving Lorentz frame i.e. the energy-momentum tensor of a perfect fluid:

$$T_{\mu\nu} = \begin{pmatrix} \epsilon & 0 & 0 & 0 \\ 0 & P & 0 & 0 \\ 0 & 0 & P & 0 \\ 0 & 0 & 0 & P \end{pmatrix}. \tag{4.61}$$

For a fluid described by this energy-momentum tensor, an observer with velocity $\boldsymbol{v}$ will observe a fluid point with the same velocity (comoving), with energy density ϵ and pressure P.

4.5.2 Tolman–Oppenheimer–Volkoff equations

Due to its compact nature, the description of the structure of a neutron star must come as a solution from general relativity. This means one finds the metric elements around a neutron star, by solving Einstein field Equation (4.51). A good approximation follows

[1] The principle of general covariance states that a law of physics holds in a general gravitational field if it holds in the absence of gravity and it is covariant.

from considering neutron stars as being static and spherically symmetric (also known as a Schwarzschild star). The *ansatz* used for the line element of a static, isotropic and spherically symmetric metric is [56]:

$$ds^2 = e^{2\nu(r)}dt^2 - e^{2\lambda(r)}dr^2 - r^2 d\theta^2 - r^2 \sin^2\theta \, d\phi^2. \tag{4.62}$$

The exponential functions are imposed to guarantee that the metric signature does not change.

For the region outside the star ($r > R$), the energy-momentum tensor is zero. Under these conditions, the Einstein Equation (4.51) becomes[2]: $R_{\mu\nu} = 0$. In a "*tour de force*", it is possible to calculate the Christoffel symbols for the ansatz (4.62) and, from these, calculate the Ricci tensor. For the region outside the star, one finds the famous Schwarzschild solution:

$$ds^2 = \left(1 - \frac{2GM}{r}\right) dt^2 - \left(1 - \frac{2GM}{r}\right)^{-1} dr^2 - r^2 d\theta^2 - r^2 \sin^2\theta \, d\phi^2. \tag{4.63}$$

Here, M is the gravitational mass of the star.

For the region inside the star ($r \leq R$) one has to solve the full Einstein Equation (4.51). Following Section 4.5.1, we can use the energy-momentum tensor for a perfect fluid defined in Equation (4.5.1). Again, calculating every Christoffel symbol, Ricci tensor, Ricci scalar and Einstein tensor, one arrives at the Tolman–Oppenheimer–Volkoff equations (**TOV**) which describe static and spherically symmetric stars [56]:

$$\frac{dP(r)}{dr} = -\frac{G}{r^2}\left[\rho(r) + \frac{P(r)}{c^2}\right]\left[M(r) + 4\pi r^3 \frac{P(r)}{c^2}\right]\left[1 - \frac{2GM(r)}{c^2 r}\right]^{-1}, \tag{4.64}$$

$$M(r) = 4\pi \int_0^r dr \; r^2 \epsilon\,(r)\,. \tag{4.65}$$

The **TOV** equations are integrated from the origin, with $M(0) = 0$ and some central energy density $\epsilon\,(0)$, to a radius R when the pressure is zero, defining the radius of the star R and its gravitational mass $M\,(R)$. The difference between gravitational mass and baryon mass (which corresponds to the mass of all nucleons in the star if they were dispersed to infinity), is the gravitational binding of the star.

[2] In the vacuum, $T_{\mu\nu} = 0$, which means that the Einstein tensor is zero as well, and one can write: $R_{\mu\nu} = \frac{1}{2} R g_{\mu\nu}$, multiplying both sides by the metric tensor yields: $R_{\mu\nu} g^{\mu\nu} = \frac{1}{2} R g_{\mu\nu} g^{\mu\nu} \Leftrightarrow R = 2R \Leftrightarrow R = 0 \Rightarrow R_{\mu\nu} = 0$.

Chapter 5

Results

5.1 The hybrid approach

To describe the hadronic (confined) phase of the system in $\beta-$equilibrium we use the relativistic mean-field model NL3$\omega\rho$ [66, 67], derived in Section 4.2.2. The NL3$\omega\rho$ model has the following properties (see [66, 67]): saturation density $\rho_0 = 0.148$ fm^{-3}, binding energy $E/A = -16.30$ MeV, incompressibility $K = 271.76$ MeV, symmetry energy $J = 31.7$ MeV, symmetry energy slope $L = 55.5$ MeV and effective mass $M^*/M = 0.60$. In [67] it was shown that this model satisfies a reasonable amount of constraints: experimental, astrophysical and from microscopic neutron matter calculations. In particular, the maximum possible neutron star mass is 2.75 $M_\odot$, well above the $2M_\odot$ constraint imposed by the pulsars J0348+043 and J1614-2230 ($M = 2.01\pm0.04$ $M_\odot$ [6] and 1.928 ± 0.017 $M_\odot$ [7, 8], respectively).

We have considered the Baym-Pethick-Sutherland **EoS** [68] for the outer crust and for the inner crust the NL3$\omega\rho$ **EoS** that describes the pasta phases within a Thomas-Fermi approach [69] and links smoothly to the core NL3$\omega\rho$ **EoS**.

To describe the quark (deconfined) phase we will use the **NJL** model in its two and three flavour versions with different vector interactions, derived in Sections 3.2 and 3.3.

The hybrid equations of state will be obtained using the Gibbs construction (see Section 4.3) for zero and nonzero values of the phenomenological Bag constant B^* (which will be such that the chiral symmetry restoration and deconfinement coincide [12]). The Tolmann-Oppenheimer-Volkov Equations (4.64) and (4.65), will be integrated, giving mass-radius and mass-central density diagrams.

5.1.1 Applicability of the quark models

In the $T = 0$ limit, we define the applicability of the quark models through the ratio between the Fermi's moment for each flavour of quark (λ_{F_f}), and the cut-off of the model (Λ): the model is valid for densities and/or baryonic chemical potentials that verify $\lambda_{F_f}/\Lambda \leq 1$. In

$SU_f(2)$, the studied models could be applied to $\rho_B \approx 1.8$ fm$^{-3} \approx 11\rho_0$ (where ρ_0 is the saturation density), a far larger density then the one found inside neutron stars. In $SU_f(3)$, the models are valid until at least 2.4 fm$^{-3} \approx 15\rho_0$, densities far above those found inside neutron stars.

5.2 Results in $SU_f(2)$

In the $SU_f(2)$ **NJL** model, there are three free parameters: the current mass $m_u = m_d$, the model cut-off Λ and the coupling constant G_S. These parameters are usually fixed by reproducing the experimental values of the mass and decay constant for the pion and the value of the quark condensate in the vacuum ($m_\pi = 135.0$ MeV and $f_\pi = 92.4$ MeV [49]).

We are going to study two different parametrizations of the two flavour **NJL** model (presented in Table 5.1). One of them, $SU_f(2)$−I, is usually used in the literature [70]. The other parameter set, $SU_f(2)$−II, is proposed in this work because we want a model which reproduces (in the vacuum), besides m_π and f_π, the same mass for the nucleon as the hadronic model, that is, a parametrization that gives $M_u = M_d \approx 313$ MeV ($3 \times 313 \approx m_{nucleon}$).

We fix the mixing parameter α defined in Equations (3.20) and (3.21) to $\alpha = 1/2$. The addition of a $U_A(1)$ breaking parameter in $SU_f(2)$ can be absorbed by the usual four-quark interaction in the bosonization process, and the actual difference between results is negligible. Therefore, it was not considered in the study with the $SU_f(2)$ **NJL** model[1].

Parameter set	Λ [MeV]	$m_{u,d}$ [MeV]	$G_S\Lambda^2$	$-\langle\overline{u}u\rangle^{1/3}$ [MeV]	$M_{u,d}$ [MeV]
$SU_f(2)$−I [70]	590.0	6.0	2.435	241.5	400
$SU_f(2)$−II	648.0	5.1	2.110	248.2	313

TABLE 5.1: Sets of parameters used throughout the work and reproduced observables in the vacuum, for each parametrization. Λ is the model cut-off, $m_{u,d}$ is the quark current masses, and G_S is the coupling constant. The results for the u-quark condensate, $\langle\overline{u}u\rangle$, and for the constituent masses, $M_{u,d}$, are also presented.

In the present section we discuss the possible existence of hybrid stars within the $SU_f(2)$ **NJL** model, taking as a free parameter the coupling of the vector-isoscalar and/or vector-isovector terms in the Lagrangian density, G_V. These vector interactions, at the Lagrangian level, are given by (see Equations (3.23), (3.24) and (3.25)):

$$\text{NJL(V+P+VI+PI)} : G_V\left[(\overline{\psi}\gamma^\mu\tau^0\psi)^2 + (\overline{\psi}\gamma^\mu\gamma_5\tau^0\psi)^2\right] + G_V\sum_{a=1}^{3}\left[(\overline{\psi}\gamma^\mu\tau^a\psi)^2 + (\overline{\psi}\gamma^\mu\gamma_5\tau^a\psi)^2\right],$$

$$\text{NJL(V+P)} : G_V\left[(\overline{\psi}\gamma^\mu\tau^0\psi)^2 + (\overline{\psi}\gamma^\mu\gamma_5\tau^0\psi)^2\right],$$

$$\text{NJL(VI+PI)} : G_V\sum_{a=1}^{3}\left[(\overline{\psi}\gamma^\mu\tau^a\psi)^2 + (\overline{\psi}\gamma^\mu\gamma_5\tau^a\psi)^2\right].$$

[1] When non-vanishing isospin chemical potential is taken into account this term becomes relevant [70].

The NJL(V+P) model have only the vector-isoscalar contribution and the NJL(VI+PI) model, only the vector-isovector contribution. The NJL(V+P+VI+PI) model have both contributions.

Table 5.2 shows the order of the chiral restoration symmetry for different values of the coupling G_V. For each case we consider $G_V/G_S = 0,\ 0.25,\ 0.5,\ 0.75$. While for the $SU_f(2)$−I parametrization only a sufficiently large value of G_V with the vector-isoscalar interaction term originates a *crossover* instead of a first-order phase transition, the $SU_f(2)$−II parametrization only predicts a first order phase transition if the vector terms are not considered in the Lagrangian density. We may also conclude that for the $SU_f(2)$−II parametrization the phase transition occurs for smaller chemical potentials, generally more than 150 MeV smaller for $G_V \neq 0$.

Model	G_V/G_S	$SU_f(2)$−I		$SU_f(2)$−II	
		Type	μ_B^{crit} [MeV]	Type	μ_B^{crit} [MeV]
NJL	0.00	1st	1171	1st	1119
NJL(V+P+VI+PI)	0.25	1st	1229	co	1055
	0.50	co	1283	co	1099
	0.75	co	1358	co	1149
NJL(V+P)	0.25	1st	1224	co	1051
	0.50	1st	1272	co	1089
	0.75	co	1334	co	1134
NJL(VI+PI)	0.25	1st	1177	co	1022
	0.50	1st	1183	co	1025
	0.75	1st	1189	co	1029

TABLE 5.2: Type of the chiral symmetry phase transition (1st: first-order, co: *crossover*) and respective baryonic chemical potential (μ_B^{crit}), for each value of G_V, model and parameter set.

The several **EoS** with nonzero Bag constant B^* of β−equilibrium matter taking into account the hadron-quark phase transition are shown in Figure 5.1, left panels, for the parametrization $SU_f(2)$−I and different vector contributions. We only present the **EoS** for nonzero B^* because when one considers $B^* = 0$, no star with a pure quark core is predicted, yielding a complete hadronic **EoS** ($\rho^c < \rho^Q$, as one can see in Table 5.3).

For the $SU_f(2)$−II parameter set and different vector contributions, the **EoS** of β−equilibrium matter taking into account the hadron-quark phase transition are shown in Figure 5.2, left panels. We have calculated the mass and radius of hybrid stars integrating the Tolmann-Oppenheimer-Volkov equations [56]. In Figure 5.1 (parametrization $SU_f(2)$−I with $B^* \neq 0$) and in Figure 5.2 (parametrization $SU_f(2)$−II), the mass versus radius and mass versus central density curves of the families of stars described by the **EoS** discussed above are plotted, in the right panels.

In these plots the large coloured circles indicate the central density of the maximum mass configuration. We do not show the **EoS** above these densities. The light-grey bar represents the mass constraint of the J0348+043 pulsar ($M = 2.01 \pm 0.04\ M_\odot$) while the dark-grey

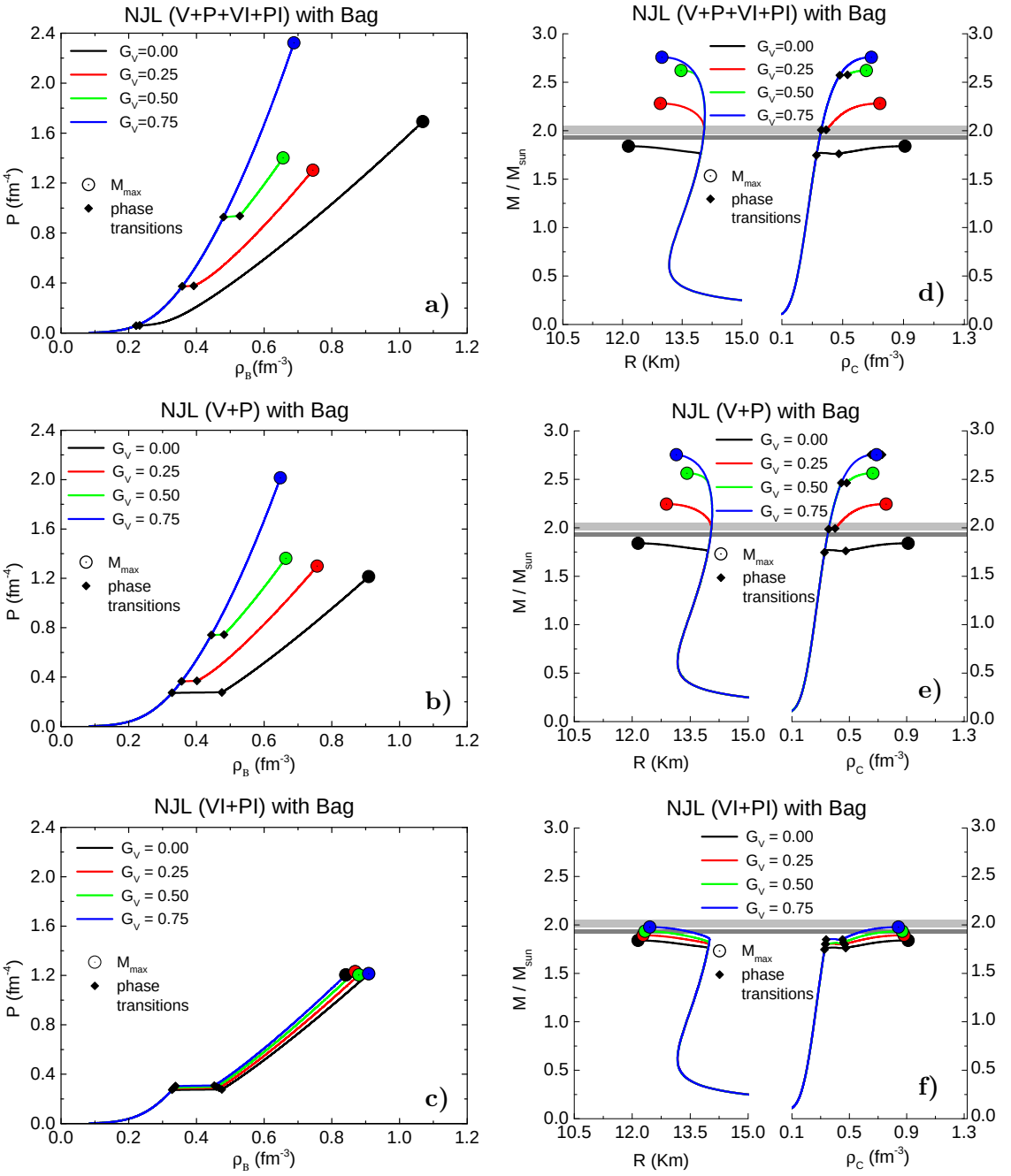

FIGURE 5.1: *Left panels*: equations of state with $B^* \neq 0$, for several values of G_V [G_S], for the $SU_f(2)$−I parameter set of NJL(V+P+VI+PI) (panel a)), NJL(V+P) (panel b)) and NJL(VI+PI) (panel c)) models. The star maximum mass, central density and confinement-deconfinement phase transitions are highlighted. *Right panels*: mass-radius and mass-central density diagrams with $B^* \neq 0$ for several values of G_V [G_S] for the $SU_f(2)$−I parameter set of NJL(V+P+VI+PI) (panel d)), NJL(V+P) (panel e)) and NJL(VI+PI) (panel f)) models. The star maximum mass, central density and confinement-deconfinement phase transitions are highlighted. The light-grey bar represents the mass constraint of the J0348+043 pulsar ($M = 2.01 \pm 0.04$ $M_\odot$) while the dark-grey bar the J1614-2230 pulsar ($M = 1.928 \pm 0.017$ $M_\odot$).

bar the mass constraint of the J1614-2230 pulsar ($M = 1.928 \pm 0.017$ $M_\odot$). Small black diamonds indicate the hadron-quark phase transition. For the $SU_f(2)$−I parameter set only results for $B^* \neq 0$ are presented (Figure 5.1) while for the $SU_f(2)$−II parameter set, full (dashed) lines have been used for the $B^* \neq 0$ ($B^* = 0$) results (Figure 5.2). From

Model	G_V/G_S	B^* [MeV fm^{-3}]	μ_B^t [MeV]	ρ^H [fm^{-3}]	ρ^Q [fm^{-3}]	ρ^c [fm^{-3}]	M_m [M$_\odot$]	M_{bm} [M$_\odot$]	R_m [km]
NJL	0.00	0	1388	0.434	0.808	0.808	2.43	2.89	13.99
NJL	0.25		1662	0.556	0.878	0.557	2.70	3.30	13.55
(V+P	0.50	0	2050	0.728	1.027	0.689	2.76	3.39	13.00
VI+PI)	0.75		2634	0.984	1.283	0.689	2.76	3.39	13.00
NJL	0.25		1632	0.544	0.869	0.868	2.69	3.28	13.60
(V+P)	0.50	0	1965	0.690	0.992	0.879	2.76	3.39	12.99
	0.75		2450	0.904	1.197	0.689	2.76	3.39	12.99
NJL	0.25		1411	0.440	0.811	0.690	2.47	2.94	13.96
(VI+PI)	0.50	0	1433	0.454	0.818	0.698	2.50	2.99	13.94
	0.75		1454	0.464	0.824	0.703	2.53	3.04	13.90
NJL	0.00	54.32	1171	0.328	0.475	0.910	1.84	2.09	12.15
NJL	0.25	74.31	1229	0.358	0.392	0.745	2.28	2.68	12.95
(V+P	0.50	91.44	1490	0.480	0.528	0.656	2.62	3.17	13.47
VI+PI)	0.75	111.32	2049	0.726	0.822	0.689	2.76	3.39	12.99
NJL	0.25	72.53	1224	0.356	0.402	0.757	2.24	2.63	12.89
(V+P)	0.50	88.27	1409	0.444	0.482	0.665	2.56	3.09	13.42
	0.75	104.82	1870	0.648	0.730	0.690	2.75	3.38	13.14
NJL	0.25	56.43	1177	0.332	0.467	0.881	1.89	2.16	12.28
(VI+PI)	0.50	58.39	1183	0.334	0.459	0.869	1.93	2.21	12.33
	0.75	60.27	1189	0.338	0.453	0.843	1.98	2.27	12.46

TABLE 5.3: Baryonic chemical potential (μ_B^t), confinement baryonic density (ρ^H), deconfinement baryonic density (ρ^Q) and respective value of the parameter B^*. Values of central baryonic density (ρ^c), maximum gravitational mass (M_m), maximum baryonic mass (M_{bm}) and radius (R_m) of the respective neutron star, for each model and G_V [G_S] value, for the $SU_f(2)$−I parameter set.

the analysis of these figures some conclusions may be drawn: **a)** the inclusion of $B^* \neq 0$ shifts the deconfinement phase transition to smaller densities, allows the appearance of a quark phase even for a large value of G_V and gives rise to larger central densities; **b)** increasing the coupling G_V in models with vector-isoscalar terms makes the **EoS** harder and central densities of maximum mass configurations are smaller; **c)** the vector-isovector term (NJL(VI+PI)) have a much smaller effect than the vector-isoscalar term (NJL(V+P)), although qualitatively similar; **d)** the model labelled NJL(V+P+VI+PI) incorporates the effects of models NJL(V+P) and NJL(VI+PI) and, therefore, may give rise to larger central pressures; **e)** the $SU_f(2)$−I parameter set only allows the existence of a quark core if a nonzero value for B^* is used for any tested value of G_V/G_S in the NJL(VI+PI) and for G_V/G_S below 0.75 in the NJL(V+P+VI+PI) and NJL(V+P) models.

Other properties of the hybrid stars, in particular of the maximum mass configurations, calculated using the $SU_f(2)$−I and $SU_f(2)$−II parametrizations for the quark phase are also summarized in Tables 5.3 and 5.4. These properties include: the renormalization Bag parameter B^*, the baryonic chemical potential at the transition μ_B^t, the central baryonic density ρ^c, the gravitational M_m and baryonic mass M_{bm} of the maximum mass configuration, and respective radius R_m.

Taking $B^* = 0$ gives rise to unstable stars ($\rho^c < \rho^Q$) as soon as the quark matter sets in when the $SU_f(2)$−I parametrization is considered. The central star density lies always at

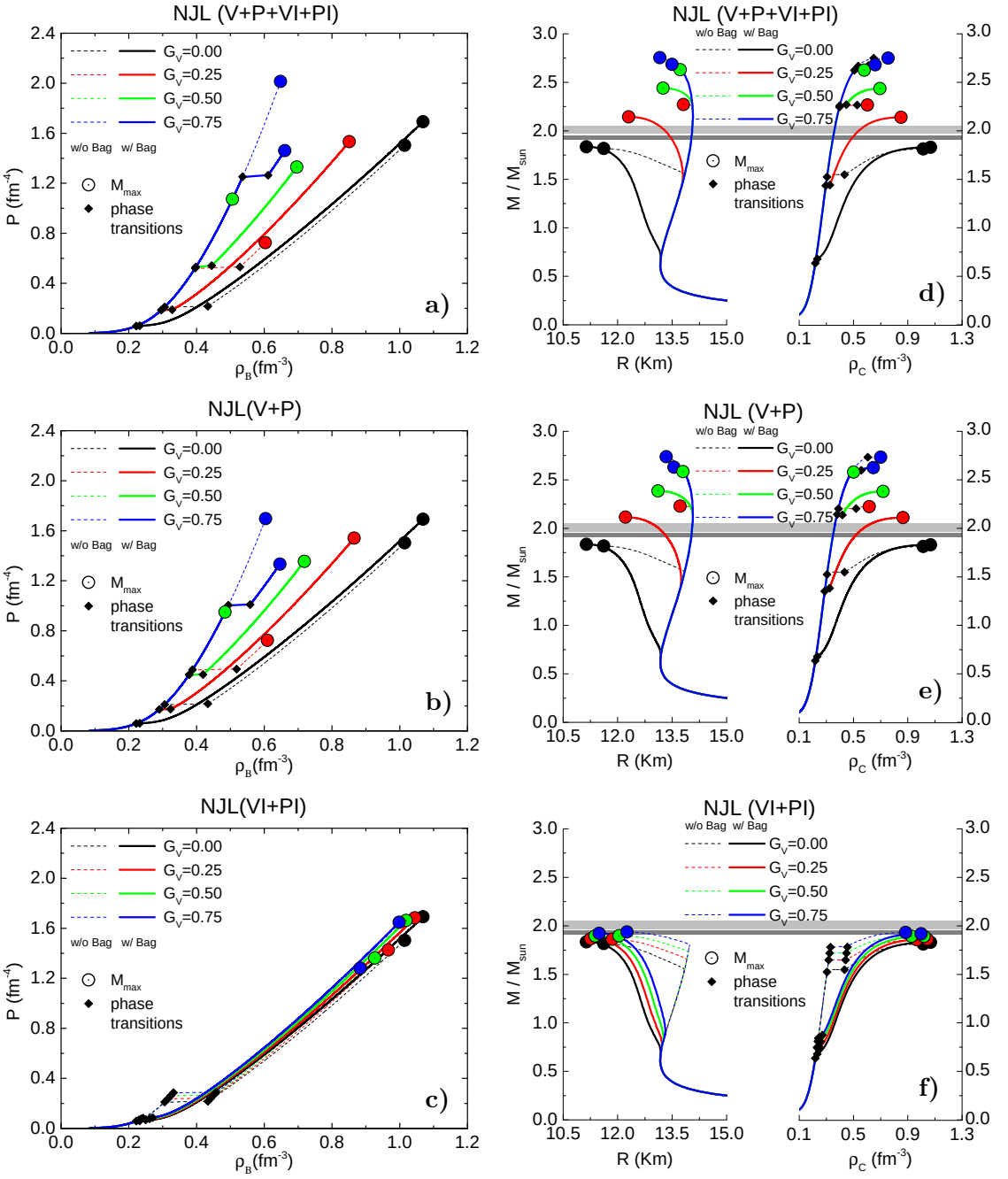

FIGURE 5.2: *Left panels*: equations of state with $B^* \neq 0$ and $B^* = 0$, for several values of G_V [G_S], for the $SU_f(2)$−II parametrization of NJL(V+P+VI+PI) (panel a)), NJL(V+P) (panel b)) and NJL(VI+PI) (panel c)) models. The star maximum mass, central density and confinement-deconfinement phase transitions are highlighted. *Right panels*: mass-radius and mass-central density diagrams with $B^* \neq 0$ and $B^* = 0$ for several values of G_V [G_S] for the $SU_f(2)$−II parametrization of NJL(V+P+VI+PI) (panel d)), NJL(V+P) (panel e)) and NJL(VI+PI) (panel f)) models. The star maximum mass, central density and confinement-deconfinement phase transitions are highlighted. The light-grey bar represents the mass constraint of the J0348+043 pulsar ($M = 2.01 \pm 0.04\ M_\odot$) while the dark-grey bar the J1614-2230 pulsar ($M = 1.928 \pm 0.017\ M_\odot$).

the pure quark phase onset or below. We have considered local electric charge neutrality. If we would have imposed Gibbs conditions with global electric charge neutrality [56], it would probably be possible to find a mixed hadron-quark phase at the star core but not a pure quark phase.

Model	G_V/G_S	B^* [MeV fm^{-3}]	μ_B^t [MeV]	ρ^H [fm^{-3}]	ρ^Q [fm^{-3}]	ρ^c [fm^{-3}]	M_m [M$_\odot$]	M_{bm} [M$_\odot$]	R_m [km]
NJL	0.00	0	1134	0.306	0.434	1.015	1.82	2.07	11.62
NJL (V+P VI+PI)	0.25	0	1308	0.396	0.528	0.603	2.27	2.67	13.81
	0.50		1548	0.506	0.658	0.580	2.63	3.19	13.72
	0.75		1869	0.648	0.824	0.756	2.75	3.38	13.16
NJL (V+P)	0.25	0	1289	0.388	0.518	0.616	2.23	2.61	13.72
	0.50		1497	0.484	0.630	0.501	2.58	3.12	13.80
	0.75		1769	0.604	0.771	0.700	2.74	3.36	13.34
NJL (VI+PI)	0.25	0	1148	0.316	0.442	0.967	1.86	2.12	11.85
	0.50		1163	0.324	0.450	0.928	1.90	2.17	12.04
	0.75		1177	0.332	0.458	0.884	1.94	2.22	12.26
NJL	0.00	9.84	1020	0.222	0.232	1.068	1.84	2.11	11.14
NJL (V+P VI+PI)	0.25	15.16	1116	0.296	0.328	0.851	2.14	2.50	12.30
	0.50	22.09	1313	0.398	0.445	0.695	2.44	2.91	13.25
	0.75	30.84	1616	0.536	0.611	0.660	2.69	3.27	13.50
NJL (V+P)	0.25	14.50	1105	0.290	0.323	0.866	2.12	2.46	12.22
	0.50	20.54	1268	0.378	0.419	0.718	2.39	2.83	13.11
	0.75	28.10	1519	0.494	0.558	0.647	2.63	3.19	13.55
NJL (VI+PI)	0.25	10.29	1027	0.230	0.250	1.045	1.87	2.15	11.26
	0.50	10.75	1034	0.236	0.261	1.020	1.90	2.19	11.38
	0.75	11.22	1041	0.242	0.270	0.999	1.92	2.22	11.49

TABLE 5.4: Baryonic chemical potential (μ_B^t), hadron (ρ^H) and quark (ρ^Q) baryonic density at deconfinement and respective value of the parameter B^*. Values of central baryonic density (ρ^c), maximum gravitational mass (M_m), maximum baryonic mass (M_{bm}) and radius (R_m) of the respective neutron star, for each model and G_V [G_S] value, for the $SU_f(2)$−II parameter set.

A different result is obtained with the $SU_f(2)$−II parametrization: even taking $B^* = 0$, we have found stable hybrid stars with a pure quark core at the center if G_V is not too large for the vector-isoscalar interaction (see Table 5.4).

As a consequence of the **EoS** properties discussed above, we verify that the vector-isoscalar has a much stronger effect on the star structure originating more massive stars for a large G_V, while the effect of the vector-isovector term on the maximum mass is very small, and it is hard to get masses above $\sim 1.92\,M_\odot$, which is within the mass for the PSR J1614-2230 but a bit below the mass of the PSR J0348+0432. Stars with a mass above 2 solar masses are only possible within the vector-isoscalar interaction, taking $G_V/G_S \geq 0.25$ and a non zero B^*.

An important difference between the $SU_f(2)$−I and $SU_f(2)$−II parametrizations is the overall quark content, a larger content occurring inside the stars described with $SU_f(2)$−II mainly because the deconfinement sets in at smaller baryonic densities and larger central densities are attained. One direct consequence of the larger quark content is the smaller maximum masses which are obtained with the $SU_f(2)$−II parametrizations.

Let us still comment on the star radii and the densities attained inside the stars. In general the $SU_f(2)$−II parametrizations predicts smaller radii for hybrid stars, and larger baryonic densities, with the larger densities/smaller radii obtained with the vector-isovector

interaction.

In the right panels of Figure 5.2, we also verify that several models predict $1.4 M_\odot$ stars, or even smaller masses, with a quark core, and radii ~ 12.5 km. However, these models are not able to describe stars with masses above $\sim 2.0\, M_\odot$ (see Figure 5.2 and Table 5.4).

5.3 Results in $SU_f(3)$

In the previous section, the *strange* degree of freedom was not considered, however it is expected that at large densities *strangeness* will set in. In this section we extend the results discussed with the $SU_f(2)$ **NJL** model to the $SU_f(3)$ **NJL** and, as we will see, some of the features discussed in the previous section remain. As before, we will consider a parametrization that predicts a vacuum constituent u and d-quark mass equal to ≈ 313 MeV (see Table 5.5).

There are five free parameters in the three flavour version of the **NJL** model (see Table 5.5), the light quarks current mass $m_u = m_d$, the *strange* mass m_s, the model cut-off Λ, the coupling constant G_S and the coupling constant G_D (which is important to give the right degeneracy between the η and η' mesons). In the present work we will use the $SU_f(3)$−I parameter set, a modified version of the HK parameter set[2] proposed in [15]. This modification is made in such a way that the quark constituent mass in the vacuum, is approximately one third of the baryonic mass of the nucleon (see Table 5.5). In Table 5.6 the pion, kaon and eta masses predicted by the $SU_f(3)$−I parameter set are presented, as well as their respective experimental values. Besides reproducing the vacuum nucleon mass, this parametrization also describes reasonably well the vacuum properties of these mesons.

Parameter set	Λ [MeV]	$m_{u,d}$ [MeV]	m_s [MeV]	$G_S\Lambda^2$	$G_D\Lambda^5$	$M_{u,d}$ [MeV]	M_s [MeV]
$SU_f(3)$−I	630.0	5.5	135.7	1.781	9.29	312	508

TABLE 5.5: Λ is the model cut-off, $m_{u,d}$ and m_s are the quark current masses, G_S and G_D are coupling constants. $M_{u,d}$ and M_s are the resulting constituent quark masses.

Observables	$SU_f(3)$−I	Experimental [28]
m_π [MeV]	138.5	139.6
f_π [MeV]	90.7	92.2
m_K [MeV]	493.5	493.7
f_K [MeV]	96.3	110.4
m_η [MeV]	478.2	547.9
$m_{\eta'}$ [MeV]	953.7	957.8

TABLE 5.6: Masses and decay constants of several mesons within the theory, for the $SU_f(3)$−I parameter set and their respective experimental values.

[2]The HK parameter set is given by: $\Lambda = 631.4$ MeV, $m_{u,d} = 5.5$ MeV, $m_s = 135.7$ MeV, $G_S\Lambda^2 = 4.603$ and $G_D\Lambda^5 = 9.26$.

The vector interactions, in three flavour case, are given by (see Equations (3.77), (3.78) and (3.79)):

$$\text{NJL(V+P+VI+PI)} : G_V \left[(\overline{\psi}\gamma^\mu\lambda^0\psi)^2 + (\overline{\psi}\gamma^\mu\gamma_5\lambda^0\psi)^2\right] + G_V \sum_{a=1}^{8} \left[(\overline{\psi}\gamma^\mu\lambda^a\psi)^2 + (\overline{\psi}\gamma^\mu\gamma_5\lambda^a\psi)^2\right],$$

$$\text{NJL(V+P)} : G_V \left[(\overline{\psi}\gamma^\mu\lambda^0\psi)^2 + (\overline{\psi}\gamma^\mu\gamma_5\lambda^0\psi)^2\right],$$

$$\text{NJL(VI+PI)} : G_V \sum_{a=1}^{8} \left[(\overline{\psi}\gamma^\mu\lambda^a\psi)^2 + (\overline{\psi}\gamma^\mu\gamma_5\lambda^a\psi)^2\right].$$

Again, the NJL(V+P) model have only the vector-isoscalar contribution and the NJL(VI+PI) model, only the vector-isovector contribution. The NJL(V+P+VI+PI) model have both contributions.

In Table 5.7 the type of transition that each model undergoes, at $\beta-$equilibrium, when the vector coupling constant increases is shown: only if G_V is zero or takes a negative value, corresponding to an attractive interaction, do the models present a first-order phase transition, otherwise the inclusion of a repulsive vector interaction turns the transition into a *crossover*. As before, the parameter B^* will be introduced and fixed so that the deconfinement density in the hadron-quark model coincides with the chiral symmetry restoration density of the **NJL** model.

Model	G_V/G_S	Type	μ_B^{crit} [MeV]
NJL	0.00	1st	999
NJL(V+P+VI+PI)	-0.25	1st	975
	0.25	co	1023
	0.50	co	1052
	0.75	co	1087
NJL(V+P)	-0.25	1st	985
	0.25	co	1013
	0.50	co	1028
	0.75	co	1045
NJL(VI+PI)	-0.25	1st	990
	0.25	co	1008
	0.50	co	1018
	0.75	co	1028

TABLE 5.7: Type of the chiral symmetry phase transition (1st: first-order, co: *crossover*) and respective baryonic chemical potential (μ_B^{crit}), for each value of G_V [G_S].

In Figure 5.3 the **EoS**, pressure versus density (left panels), and the mass/radius and mass/density plots (right panels) are presented. The light-grey and dark-grey bars represent, once more, the mass constraint of the J0348+043 and J1614-2230 pulsars. The black diamonds identify again the hadronic and quark transition densities while the coloured circles correspond to the maximum mass configurations. Full (dashed) lines have been used for the $B^* \neq 0$ ($B^* = 0$) results. Properties of hybrid stars, including maximum mass configurations, obtained with the parametrization $SU_f(3)$ are presented in Table 5.8 with

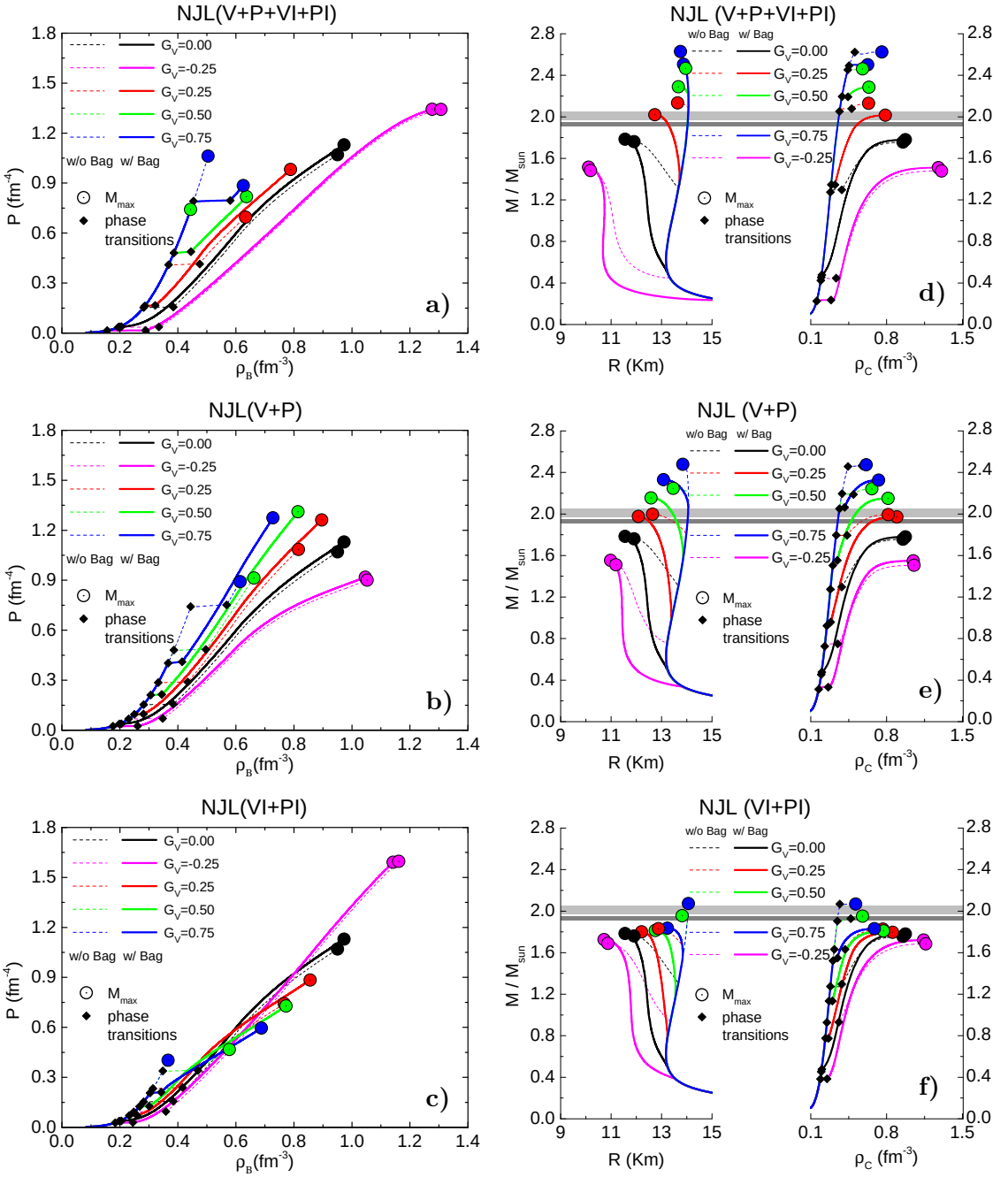

FIGURE 5.3: *Left panels*: equations of state with $B^* \neq 0$ and $B^* = 0$, for each value of G_V [G_S], for the NJL(V+P+VI+PI) (panel a)), NJL(V+P) (panel b)) and NJL(VI+PI) (panel c)) models. The star maximum mass, central density and confinement-deconfinement phase transitions are highlighted. *Right panels*: mass-radius and mass-central density diagrams with $B^* \neq 0$ and $B^* = 0$ for each value of G_V [G_S] for the NJL(V+P+VI+PI) (panel d)), NJL(V+P) (panel e)) and NJL(VI+PI) (panel f)) models. The star maximum mass, central density and confinement-deconfinement phase transitions are highlighted. The light-grey bar represents the mass constraint of the J0348+043 pulsar ($M = 2.01 \pm 0.04\ M_\odot$) while the dark-grey bar the J1614-2230 pulsar ($M = 1.928 \pm 0.017\ M_\odot$).

$B^* = 0$ and a non zero B^*. As before, the following properties are presented: the baryonic chemical potential at the deconfinement phase transition μ_B^t, and respective hadronic and quark densities ρ^H and ρ^Q, the central baryonic density, the maximum gravitational mass M_m, and respective baryonic mass M_{bm} and radius R_m. As expected, the smaller G_V

Model	G_V/G_S	B^* [MeV fm^{-3}]	μ_B^t [MeV]	ρ^H [fm^{-3}]	ρ^Q [fm^{-3}]	ρ^c [fm^{-3}]	M_m [M$_\odot$]	M_{bm} [M$_\odot$]	R_m [km]	ρ_s/ρ_B [%]
NJL	0.00	0	1093	0.282	0.384	0.951	1.76	2.00	11.91	1.32
NJL (V+P VI+PI)	-0.25	0	996	0.194	0.334	1.308	1.48	1.68	10.19	0.35
	0.25		1247	0.368	0.475	0.635	2.13	2.48	13.64	0.53
	0.50		1410	0.444	0.640	0.578	2.47	2.94	13.96	0.04
	0.75		1541	0.504	0.755	0.757	2.63	3.18	13.76	0.01
NJL (V+P)	-0.25	0	1028	0.230	0.347	1.053	1.51	1.69	11.20	1.63
	0.25		1179	0.332	0.434	0.816	2.00	2.30	12.64	0.50
	0.50		1285	0.386	0.496	0.663	2.25	2.63	13.46	0.02
	0.75		1412	0.444	0.568	0.612	2.48	2.96	13.85	~ 0
NJL (VI+PI)	-0.25	0	1047	0.248	0.358	1.162	1.69	1.92	10.88	0.19
	0.25		1147	0.314	0.416	0.766	1.83	2.08	12.88	1.80
	0.50		1208	0.348	0.469	0.578	1.96	2.24	13.82	0.85
	0.75		1243	0.366	0.558	0.515	2.07	2.39	14.07	0.01
NJL	0.00	6.60	999	0.198	0.205	0.974	1.78	2.05	11.55	1.43
NJL (V+P VI+PI)	-0.25	2.89	975	0.156	0.288	1.278	1.51	1.73	10.11	0.31
	0.25	10.09	1100	0.286	0.322	0.789	2.02	2.33	12.73	2.14
	0.50	14.62	1287	0.386	0.445	0.637	2.29	2.69	13.67	1.85
	0.75	20.57	1431	0.454	0.581	0.626	2.51	3.00	13.88	0.46
NJL (V+P)	-0.25	4.40	985	0.176	0.261	1.046	1.55	1.76	10.98	1.51
	0.25	8.61	1049	0.250	0.282	0.896	1.98	2.28	12.08	0.98
	0.50	10.92	1132	0.306	0.344	0.814	2.15	2.51	12.58	0.48
	0.75	13.63	1246	0.366	0.414	0.727	2.33	2.75	13.08	0.12
NJL (VI+PI)	-0.25	5.15	990	0.184	0.245	1.142	1.73	1.99	10.72	0.15
	0.25	7.92	1029	0.232	0.259	0.856	1.80	2.05	12.21	2.83
	0.50	9.33	1072	0.268	0.301	0.772	1.81	2.06	12.75	4.12
	0.75	10.90	1129	0.304	0.342	0.688	1.84	2.08	13.24	4.77

TABLE 5.8: Baryonic chemical potential (μ_B^t), confinement baryonic density (ρ^H), deconfinement baryonic density (ρ^Q) and respective value of the Bag constant (B^*). Values of central baryonic density (ρ^c), maximum gravitational mass (M_m), maximum baryonic mass (M_{bm}), radius (R_m) and percentage of *strangeness* (ρ_s/ρ_B) of the respective neutron star, for each model and value of G_V [G_S], for the $SU_f(3)$−I parameter set.

the earlier the deconfinement phase transition occurs. Also a finite B^* produces a phase transition at lower densities and with a smaller baryonic density discontinuity. As in the $SU_f(2)$ model, the vector-isoscalar term is having the strongest effects on the **EOS** (see Figure 5.3).

We have also considered a possible negative value of G_V (magenta lines in Figure 5.3). In this case we would have very low mass stars with a quark core. These stars are characterized by the smallest radii, ~ 11 km or below. However, this model predicts a maximum mass configuration of the order of $1.5 - 1.7\,M_\odot$ well below $2M_\odot$ (see Table 5.8). Again, similarly to the $SU_f(2)$ model, some parametrizations predict $1.4M_\odot$ stars with a quark content, specially the NJL(VI+PI) model. For those cases, if $G_V \leq 0$, these parametrizations do not describe $2M_\odot$ stars (see Figure 5.3, right panels).

The $SU_f(3)$ **NJL** model includes *strangeness* and it is interesting to study the onset of this new degree of freedom. In Figure 5.4 the s, d and u quark fractions are plotted. As soon as the s-quark sets in the fraction of d-quarks suffers a strong reduction, the fractions of d and s-quarks approach $\sim 1/3$, asymptotically, the first from above a the second from

below. If a large G_V parameter is considered the amount of *strangeness* in the star is residual, except for the NJL(VI+PI) model in this case the *strangeness* fraction increases with larger values of G_V (see Table 5.8).

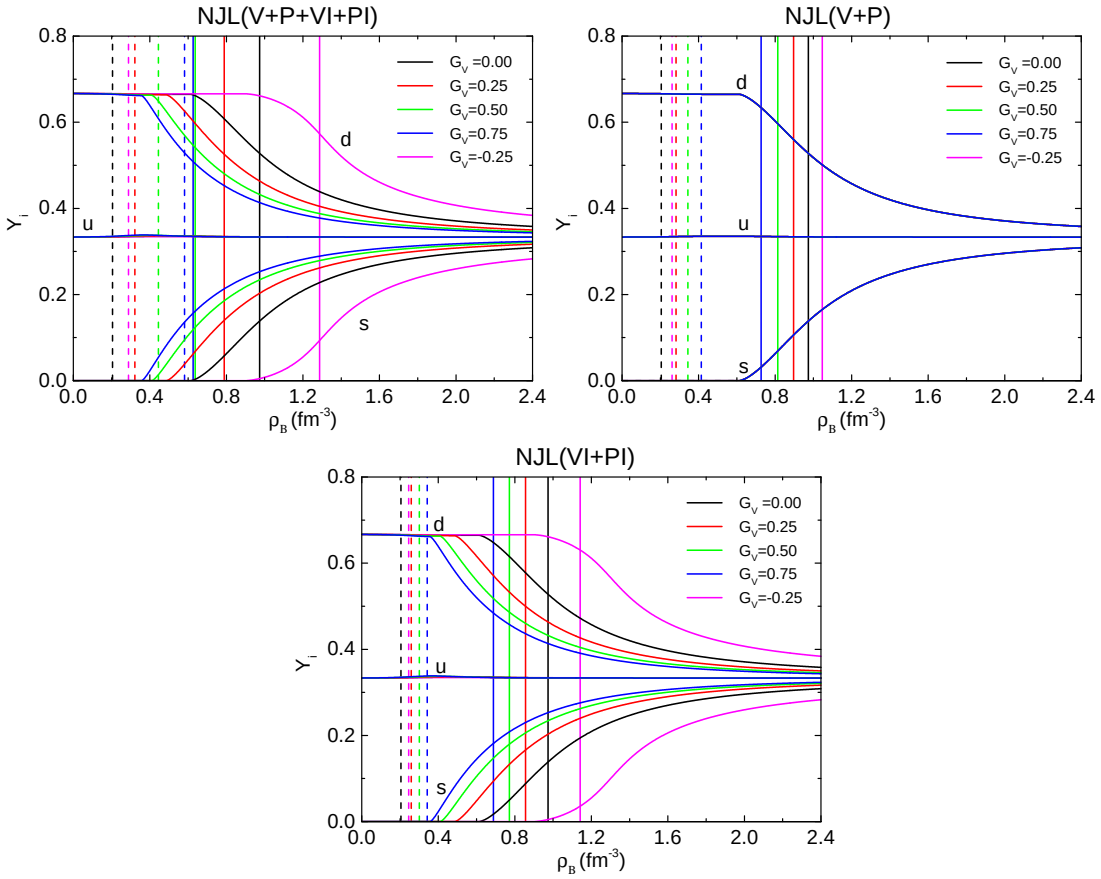

FIGURE 5.4: Fractions of each flavour of quark (Y_i) in function of the baryonic density (ρ_B). The central density (ρ^c) and initial quark phase density (ρ^Q) are shown (full and dashed vertical lines, respectively). The threshold for the emergence of *strange* quarks in the NJL(V+P) model does not depend on G_V (black line).

Taking the vector-isoscalar interaction alone the *strange* fraction does not change with G_V, which is simply explained because the interaction energy does not depend separately on each flavour (see Equations (3.112), (3.113) and (3.114) for $G_\rho = 0$). The vector-isovector interaction distinguishes the flavours (see Equations (3.112), (3.113) and (3.114) for $G_\rho = G_\omega = G_V$ or $G_\omega = 0$) and the larger G_V the earlier occurs the s-quark onset. The u quark fraction is practically independent of density, with a value close to 1/3, except for a deviation that can be as high as 0.005 if $G_V/G_S = 0.75$. This deviation from 1/3 is compensated by the presence of electrons in order to turn matter electrically neutral.

The onset of *strangeness* at quite high densities, generally above 0.5 fm$^{-3} \approx 3\rho_0$, is due to the high constituent mass of the s-quark since the partial restoration of chiral symmetry for the s-quark occurs at high densities [49].

In all cases considered, with $B^* \neq 0$, there exists a pure quark matter in the center of the star. All results obtained with a vector-isoscalar interaction generate maximum masses above $2M_\odot$ and radii above 12 km for $G_V/G_S \geq 0.25$ (see Table 5.8). Smaller radii,

below 12 km or even below 11 km are obtained if $G_V \leq 0$. In this case stars with a mass of the order of $1.4M_\odot$ or even below will have a reasonable amount of quark matter. Taking $G_V/G_S = -0.25$ all stars with $M > 1.4M_\odot$ have a radius just above 10 km. For $G_V/G_S \geq 0.5$ the standard $M = 1.4M_\odot$ star will be a pure nucleonic star with the radius determined by the hadronic **EoS**.

Recently, a mass as low as $1.18^{+0.10}_{-0.11}M_\odot$ of the pulsar PSR J1918-0642 has been measured with quite large precision. The measurement of the corresponding radius would set important constraints. In the present approach, taking a negative G_V, a $1M_\odot$ star is an hybrid star with a radius ~ 2.5 km smaller than an nucleonic star with the same mass.

Since the total *strangeness* contribution is not very large we may ask how much do the predictions of the $SU_f(2)$−II and $SU_f(3)$ **NJL** models differ. In fact, the parametrizations that do not include vector contributions, or the one that include the vector-isoscalar and vector-isovector terms with equal weight (NJL(V+P+VI+PI)) give similar maximum mass star properties, however for the other combinations this is not true. This results from the factor that affects the vector terms: the models NJL(V+P+VI+PI) have the same factor in the definition of the chemical potential,

$$\begin{aligned} SU_f(2):\ \tilde{\mu}_i &= \mu_i - 4G_V\rho_i\ , \quad i \in \{u,d\}, \\ SU_f(3):\ \tilde{\mu}_i &= \mu_i - 4G_V\rho_i\ , \quad i \in \{u,d,s\}, \end{aligned}$$

however for the models, NJL(V+P),

$$\begin{aligned} SU_f(2):\ \tilde{\mu}_i &= \mu_i - 2G_V\left(\rho_i + \rho_j\right), \quad i,j \in \{u,d\} \quad \wedge \quad i \neq j, \\ SU_f(3):\ \tilde{\mu}_i &= \mu_i - \frac{4}{3}G_V\left(\rho_i + \rho_j + \rho_k\right)\ , \quad i,j,k \in \{u,d,s\} \quad \wedge \quad i \neq j \neq k \end{aligned}$$

and NJL(VI+PI),

$$\begin{aligned} SU_f(2):\ \tilde{\mu}_i &= \mu_i - 2G_V\left(\rho_i - \rho_j\right)\ , \quad i,j \in \{u,d\} \quad \wedge \quad i \neq j, \\ SU_f(3):\ \tilde{\mu}_i &= \mu_i - \frac{4}{3}G_V\left(2\rho_i - \rho_j - \rho_k\right)\ , \quad i,j,k \in \{u,d,s\} \quad \wedge \quad i \neq j \neq k, \end{aligned}$$

the factor multiplying the coupling G_V is different. Since the vector terms have a smaller contribution in the $SU_f(3)$ NJL(V+P) and NJL(VI+PI) models, the transition to quark matter occurs for a smaller chemical potential and density and smaller maximum masses are generally obtained.

Chapter 6

Polyakov–Nambu–Jona-Lasinio Model at Zero Temperature

6.1 $Z(N_c)$ symmetry and deconfinement

The **QCD** Lagrangian (1.1), as stated in Section 1.2, is invariant under transformations U, of the gauge group $SU_c(N_c)$. As an element of $SU_c(N_c)$, U satisfies [71]:

$$U^\dagger U = \mathbb{1}_{N_c \times N_c} \quad \wedge \quad \det U = 1. \tag{6.1}$$

Since U is a local gauge transformation, it is a function of space-time. There is a special gauge transformation U_c, constant in space-time that belongs to the group, a constant phase times the unit matrix:

$$U_c = e^{i\alpha} \mathbb{1}_{N_c \times N_c}. \tag{6.2}$$

Being an element of $SU_c(N_c)$, its determinant must be one,

$$\begin{aligned} \det U_c = 1 \Leftrightarrow \det \left[e^{i\alpha} \mathbb{1}_{N_c \times N_c} \right] = 1 \Leftrightarrow \\ \Leftrightarrow \underbrace{e^{i\alpha} \times e^{i\alpha} \times ... \times e^{i\alpha}}_{N_c} = e^{i\alpha N_c} = 1. \end{aligned} \tag{6.3}$$

Using Euler's identity, the above condition requires,

$$\alpha = \frac{2\pi n}{N_c} \quad n = 0, 1, ... (N_c - 1). \tag{6.4}$$

Since the integer n, cannot change continuously from point to point, this defines a global $Z(N_c)$ symmetry. This symmetry requires that the fields are rotated by the same element of $Z(N_c)$ at every space-time, maintaining the **QCD** Lagrangian invariant.

6.1.1 $Z(N_c)$ symmetry at finite temperature

The Matsubara formalism introduced in Section 2.2.1 requires that gluons (bosons, $\mathcal{A}_\mu$) must be periodic in imaginary time, while quarks (fermions, ψ_q) must be antiperiodic (2.39) i.e.:

$$\mathcal{A}_\mu(\beta, \boldsymbol{x}) = \mathcal{A}_\mu(0, \boldsymbol{x}), \tag{6.5}$$

$$\psi_q(\beta, \boldsymbol{x}) = -\psi_q(0, \boldsymbol{x}). \tag{6.6}$$

Once the Lagrangian is invariant under transformations of the $SU_c(N_c)$, the fields transformations at the boundaries have the following expressions:

$$\psi_q(0, \boldsymbol{x}) \to U(0, \boldsymbol{x})\,\psi_q(0, \boldsymbol{x}), \tag{6.7}$$

$$\psi_q(\beta, \boldsymbol{x}) \to U(\beta, \boldsymbol{x})\,\psi_q(\beta, \boldsymbol{x}), \tag{6.8}$$

$$\mathcal{A}_\mu(0, \boldsymbol{x}) \to U^\dagger(0, \boldsymbol{x})\,\mathcal{A}_\mu(0, \boldsymbol{x})\,U(0, \boldsymbol{x}), \tag{6.9}$$

$$\mathcal{A}_\mu(\beta, \boldsymbol{x}) \to U^\dagger(\beta, \boldsymbol{x})\,\mathcal{A}_\mu(\beta, \boldsymbol{x})\,U(\beta, \boldsymbol{x}). \tag{6.10}$$

As already stated in Section 1.2, gluons are adjoint fields and their transformation, Equations (6.9) and (6.10), also involves the inverse transformation matrix. Considering the periodic relation for the gluon field given in Equation (6.5) and using the transformation properties (6.9) and (6.10), we have,

$$U^\dagger(0, \boldsymbol{x})\,\mathcal{A}_\mu(0, \boldsymbol{x})\,U(0, \boldsymbol{x}) = U^\dagger(\beta, \boldsymbol{x})\,\mathcal{A}_\mu(\beta, \boldsymbol{x})\,U(\beta, \boldsymbol{x}). \tag{6.11}$$

If we relate the transformation matrices $U(0, \boldsymbol{x})$ and $U(\beta, \boldsymbol{x})$ through a matrix that commutes with the gluon field, the periodic relation is respected. By definition, the $SU_c(N_c)$ matrices that commute with all gluon fields constitute the $Z(N_c)$ group. As a result, gauge transformations for the boundary conditions of the gluon fields must be periodic up to an element of the $Z(N_c)$ group, i.e.,

$$U(0, \boldsymbol{x}) = zU(\beta, \boldsymbol{x}) \quad z \in Z(N_c). \tag{6.12}$$

Using this in Equation (6.11), we may write:

$$U^\dagger(\beta, \boldsymbol{x})\,z^\dagger\mathcal{A}_\mu(0, \boldsymbol{x})\,zU(\beta, \boldsymbol{x}) = U^\dagger(\beta, \boldsymbol{x})\,\mathcal{A}_\mu(\beta, \boldsymbol{x})\,U(\beta, \boldsymbol{x}), \tag{6.13}$$

Due to the fact that the gluon field is invariant under global $Z(N_c)$ transformations, we can write:

$$z^\dagger\mathcal{A}_\mu(0, \boldsymbol{x})\,z = \mathcal{A}_\mu(0, \boldsymbol{x}) \quad z \in Z(N_c). \tag{6.14}$$

Substituting this in Equation (6.13), yields:

$$\mathcal{A}_\mu(0, \boldsymbol{x}) = \mathcal{A}_\mu(\beta, \boldsymbol{x}). \tag{6.15}$$

However, quarks does not behave in the same manner. Quarks are in the fundamental representation of the gauge group $SU_c(N_c)$, which means their transformation properties involve only one transformation matrix. Considering the antiperiodic relation for the quark field given in Equation (6.6) and using the transformation properties (6.7) and (6.8), one has,

$$U(0,\boldsymbol{x})\,\psi_q(0,\boldsymbol{x}) = -U(\beta,\boldsymbol{x})\,\psi_q(\beta,\boldsymbol{x})\,. \tag{6.16}$$

This relation seems to imply that, to respect the antiperiodicity of the fermionic fields, $U(0,\boldsymbol{x})$ must be exactly equal to $U(\beta,\boldsymbol{x})$ i.e.,

$$U(0,\boldsymbol{x}) = U(\beta,\boldsymbol{x})\,. \tag{6.17}$$

Comparing Equations (6.12) and (6.17), only a particular choice of z (an element of $Z(N_c)$), will respect the antiperiodicity of the quark field. The $Z(N_c)$ symmetry of the boundary conditions[1] is respected by the gluon fields, but is explicitly broken when dynamical quarks are included in the theory.

6.1.2 The Polyakov loop

If we consider the pure glue theory (quarks with infinite mass), the boundary conditions are respected by the $Z(N_c)$ symmetry. However, as already stated in Section 2.1, a symmetry of the Lagrangian density may not be a symmetry of the vacuum, and a spontaneous symmetry breaking may occur. An order parameter for the possible $Z(N_c)$ symmetry breaking can be defined using the thermal Wilson line $L(\boldsymbol{x})$,

$$L(\boldsymbol{x}) = \mathcal{P}\exp\left[i\int_0^\beta d\tau\; A_4(\tau,\boldsymbol{x})\right]. \tag{6.18}$$

$\mathcal{P}$ is the path ordering operator[2] and A_4 is the gluon field in the time direction,

$$A_4 = ig_s\mathcal{A}_\mu^a\frac{\lambda_a}{2}\delta_0^\mu, \quad a = 1,...,N_c^2-1. \tag{6.19}$$

Here, $\mathcal{A}_\mu^a$ is the gluon field of colour index a.

Under gauge transformations the Wilson line transforms as the gluon field. This means we can write:

$$L(\boldsymbol{x}) \to U^\dagger(\beta,\boldsymbol{x})\,L(\boldsymbol{x})\,U(0,\boldsymbol{x})\,. \tag{6.20}$$

[1] Not to be mistaken with the global $Z(N_c)$ symmetry of the Lagrangian which corresponds to rotating the fields by the same element of $Z(N_c)$ at every space-time event. The $Z(N_c)$ symmetry of the boundary conditions is a symmetry of the gluon fields at $\tau = \beta$.

[2] The fields in the power series expansion of the exponential are in the order they appear in the taken path.

The Polyakov loop Φ can be defined as the trace over colour of the thermal Wilson line:

$$\Phi = \frac{1}{N_c} \operatorname*{tr}_c L(\boldsymbol{x}). \tag{6.21}$$

Under a global $Z(N_c)$ symmetry, the Polyakov loop transform as the quarks, i.e., only a particular choice of element of $Z(N_c)$ maintains the symmetry:

$$\Phi \to z\Phi \quad z \in Z(N_c). \tag{6.22}$$

This means that, to respect the $Z(N_c)$ symmetry, the **VEV** of the Polyakov loop must be zero. However, due to asymptotic freedom, at high energies (temperatures and/or densities), the strong coupling constant of **QCD** in Equation (6.19) and consequently in Equation (6.18) is expected to vanish. In these conditions, the thermal Wilson line and Polyakov loop tend to one [71]. At this point, any element of $Z(N_c)$ is equally good in Equation (6.22), but only one very specific element (identity), will respect the $Z(N_c)$ symmetry of the theory, signalling the spontaneous breakdown of the symmetry. Summarizing, the Polyakov loop work as an order parameter in the following way:

$$\langle \Phi \rangle = z\Phi_0 \quad z \in Z(N_c), \tag{6.23}$$

$$\Phi_0 = \begin{cases} 0, & \text{if the symmetry is respected,} \\ > 0, & \text{if the symmetry is spontaneously broken.} \end{cases} \tag{6.24}$$

6.1.3 Polyakov loop and deconfinement

Studying the connection between the Polyakov loop and the (Helmholtz) free energy of a system of quarks in a static gluonic background, leads to interpreting the phase where the Polyakov loop is zero ($Z(N_c)$ symmetry is respected) as a confined phase, and when the Polyakov loop is bigger then zero ($Z(N_c)$ symmetry is spontaneously broken) as a deconfined phase.

In order to see this feature, we start with the static Dirac equation (in imaginary time), coupled to a static gluonic background field [72]:

$$\left[i\gamma^0 \partial_\tau - \gamma^0 A_4 + m \right] \psi(\tau, \boldsymbol{x}) = 0, \tag{6.25}$$

whose positive energy solution is:

$$\psi(\tau, \boldsymbol{x}) = e^{-m\tau} \mathcal{T} \exp\left[i \int_0^\tau d\tau' A_4(\tau', \boldsymbol{x}) \right] \psi(0, \boldsymbol{x}), \tag{6.26}$$

where $\mathcal{T}$ is the time ordering operator which, in this case, is equivalent to the path ordering operator $\mathcal{P}$. The Helmholtz free energy of the quark can be written as,

$$e^{-\beta F_q} = \frac{1}{N_c} \sum_{i,n} \langle n | \psi_i(0, \boldsymbol{x}) e^{-\beta \hat{\mathcal{H}}} \psi_i^\dagger(0, \boldsymbol{x}) | n \rangle, \tag{6.27}$$

where the sum is made over gluonic states $|n\rangle$ and colour states i. $\psi_i(0,\boldsymbol{x})$ ($\psi_i^\dagger(0,\boldsymbol{x})$) creates (detroys) a quark of colour i at the point $\boldsymbol{x}$. Relation (2.37) allows us to write,

$$e^{\beta\hat{\mathcal{H}}}\psi_i(0,\boldsymbol{x})\,e^{-\beta\hat{\mathcal{H}}} = \psi_i(\beta,\boldsymbol{x})\,. \tag{6.28}$$

By using this relation in Equation (6.27) we have,

$$e^{-\beta F_q} = \frac{1}{N_c}\sum_{i,n}\langle n|e^{-\beta\hat{\mathcal{H}}}e^{\beta\hat{\mathcal{H}}}\psi_i(0,\boldsymbol{x})\,e^{-\beta\hat{\mathcal{H}}}\psi_i^\dagger(0,\boldsymbol{x})\,|n\rangle = \tag{6.29}$$

$$= \frac{1}{N_c}\sum_{i,n}\langle n|e^{-\beta\hat{\mathcal{H}}}\psi_i(\beta,\boldsymbol{x})\,\psi_i^\dagger(0,\boldsymbol{x})\,|n\rangle\,. \tag{6.30}$$

We use Equation (6.26) in $\psi_i(\beta,\boldsymbol{x})$, to write:

$$\begin{aligned} e^{-\beta F_q} &= e^{-m\beta}\sum_{i,n}\langle n|e^{-\beta\hat{\mathcal{H}}}\left(\frac{1}{N_c}\mathcal{T}\exp\left[i\int_0^\beta d\tau A_4(\tau,\boldsymbol{x})\right]\right)_{ij}\underbrace{\psi_j(0,\boldsymbol{x})\,\psi_i^\dagger(0,\boldsymbol{x})}_{=\delta_{ij}}|n\rangle = \\ &= e^{-m\beta}\sum_{i,n}\langle n|e^{-\beta\hat{\mathcal{H}}}|n\rangle\langle n|\left(\frac{1}{N_c}\mathcal{T}\exp\left[i\int_0^\beta d\tau A_4(\tau,\boldsymbol{x})\right]\right)|n\rangle = \\ &= e^{-m\beta}\sum_n e^{-\beta E_n}\langle n|\underset{i}{\mathrm{tr}}\left(\frac{1}{N_c}\mathcal{T}\exp\left[i\int_0^\beta d\tau A_4(\tau,\boldsymbol{x})\right]\right)|n\rangle\,. \end{aligned} \tag{6.31}$$

Using the definition of the Polyakov loop (6.21):

$$e^{-\beta F_q} = e^{-m\beta}\sum_n e^{-\beta E_n}\langle n|\Phi|n\rangle = \tag{6.32}$$

$$= e^{-m\beta}\sum_n\langle n|e^{-\beta\hat{\mathcal{H}}}\Phi|n\rangle \tag{6.33}$$

$$= e^{-m\beta}\,\mathrm{tr}\left[e^{-\beta\hat{\mathcal{H}}}\Phi\right]. \tag{6.34}$$

Comparing the Equation above with Equation (2.25), the trace operation is the thermal average of the Polyakov loop at zero chemical potential times the partition function for free gluons, i.e.,

$$e^{-\beta F_q} = e^{-m\beta}\mathcal{Z}_g\langle\Phi\rangle_{\mu=0}\,. \tag{6.35}$$

The free energy for a single quark is (subtracting F_0, the free energy of gluons):

$$F_q = F_0 + m - \frac{1}{\beta}\ln\left[\langle\Phi\rangle_{\mu=0}\right]. \tag{6.36}$$

Analysing Equation (6.36), two distinct scenarios emerge: $\langle\Phi\rangle_{\mu=0}\to 0$ or $\langle\Phi\rangle_{\mu=0} > 0$. If $\langle\Phi\rangle_{\mu=0}$ is zero, it is necessary an infinite amount of energy to create a quark in a gluonic background i.e, states with a single quark are not possible. However, if $\langle\Phi\rangle_{\mu=0}$ is bigger than zero, it is necessary a finite amount of energy to create a quark in a gluonic background i.e, states with a single quark are possible. The Polyakov loop at zero chemical potential is associated with the free energy necessary to create a single quark in a gluonic

background field. Thus the Polyakov loop function as an order parameter for the confined and deconfined phase of nuclear matter. Summarizing:

- $\langle\Phi\rangle_{\mu=0} \to 0 \Rightarrow F_q \to +\infty$: confined phase;
- $\langle\Phi\rangle_{\mu=0} > 0 \Rightarrow F_q$ is finite: deconfined phase;

This suggests that the confinement-deconfinement phase transition is deeply related to the spontaneous breaking of the $Z(N_c)$ symmetry. At finite chemical potential the free energy is not totally real, and the argument given above is not totally correct, but the Polyakov loop continues being a good order parameter. In [71], it is proposed that the Polyakov loop should be interpreted as the propagator of the quark, and confinement is equivalent with the vanishing of this propagator.

6.2 The PNJL model

In Chapter 3, we used the **NJL** model as an effective model of **QCD** due to its similar characteristics to **QCD**, like continuous symmetries and spontaneous chiral symmetry breaking. However, the **NJL** model is not gauge invariant, indeed, the gluonic degrees of freedom are frozen and in a certain way, contained in the G_s coupling constant (Figure (3.1)). This means that the $Z(N_c)$ spontaneous symmetry breaking of finite temperature **QCD** and the confinement-deconfinement phase transition (they are connected as laid out in previous sections) are features that cannot be studied within the formalism of the **NJL** model. The Polyakov–Nambu–Jona-Lasinio model (**PNJL**), was introduced to include the confinement-deconfinement phase transition in the **NJL** model.

In such model it is necessary to include an effective potential which contains the spontaneous symmetry breaking of the $Z(N_c)$ symmetry. The Polyakov loop effective potential can be constructed using the Ginzburg-Landau theory of phase transitions. Within this approach, the effective potential has to respect the $Z(N_c)$ symmetry and to reproduce its spontaneous breaking at some high temperature. There are several effective potentials who fulfill these properties, in this work we will consider the commonly used logarithmic form [3, 73, 74]:

$$\frac{\mathcal{U}\left(\Phi,\overline{\Phi};T\right)}{T^4} = -\frac{1}{2}a\left(T\right)\overline{\Phi}\Phi + b\left(T\right)\ln\left[1 - 6\overline{\Phi}\Phi + 4\left(\overline{\Phi}^3 + \Phi^3\right) - 3\left(\overline{\Phi}\Phi\right)^2\right], \tag{6.37}$$

with the T-dependent parameters [3, 74]:

$$a\left(T\right) = a_0 + a_1\left(\frac{T_0}{T}\right) + a_2\left(\frac{T_0}{T}\right)^2, \tag{6.38}$$

$$b\left(T\right) = b_3\left(\frac{T_0}{T}\right)^3. \tag{6.39}$$

For simplicity, we can write the argument in the logarithm as:

$$X(\Phi,\overline{\Phi}) = 1 - 6\Phi\overline{\Phi} + 4(\Phi^3 + \overline{\Phi}^3) - 3(\Phi\overline{\Phi})^2. \tag{6.40}$$

The parameters T_0, a_0, a_1, a_2 and a_3 are fixed by reproducing *lattice* **QCD** results at $\mu = 0$ [75–77]. A commonly used set is:

$$T_0 = 270 \quad \text{in the pure gauge sector,} \tag{6.41}$$

$$a_0 = 3.51, \quad a_1 = -2.47, \tag{6.42}$$

$$a_2 = 15.2, \quad a_3 = -1.75. \tag{6.43}$$

However, in the presence of quarks, T_0 may depend on the number of flavours, and even on the chemical potential of each quark [78–82]. In the later sections, we will consider a T_0 which depends explicitly on the chemical potential, allowing for calculations at zero temperature[3].

The Lagrangian density of the **PNJL** model for a three flavour quark system, considering vector interactions is:

$$\begin{aligned}\mathscr{L}^{\mathrm{PNJL}} = \overline{\psi}\left(i\gamma^\mu D_\mu - \hat{m} + \hat{\mu}\gamma^0\right)\psi + G_S\sum_{a=0}^{8}\left[\left(\overline{\psi}\lambda^a\psi\right)^2 + \left(\overline{\psi}i\gamma_5\lambda^a\psi\right)^2\right] \\ - \mathscr{L}^{det} - \mathscr{L}^{vec} - \mathcal{U}\left(\Phi,\overline{\Phi};T\right).\end{aligned} \tag{6.44}$$

The terms $\mathscr{L}^{det}$ and $\mathscr{L}^{vec}$ are given by Equations (3.4) and (3.77), respectively. This Lagrangian density is analogous to the three flavour **NJL** Lagrangian in Equation (3.75) however, in this case, we have a contribution from the gluonic sector of **QCD**. The effective Polyakov loop potential $\mathcal{U}\left(\Phi,\overline{\Phi};T\right)$ brings the spontaneous breaking of $Z(N_c)$ symmetry while a static gluonic background field interacts with the quark field ψ through the covariant derivative:

$$D_\mu = \partial_\mu - A_4\delta^0_\mu. \tag{6.45}$$

Here A_4 is the gluonic background field given in Equation (6.19). This covariant derivative is the zero component of the covariant derivative in **QCD**, defined in Equation (1.4).

[3] In the $T = 0$ limit, the **PNJL** model yields the **NJL** model. By adding a μ dependence on the effective Polyakov loop, this is not the case, as we will see.

6.2.1 PNJL model in the MFA

Following the same steps as in Section 3.3.1, the **PNJL** Lagrangian can be linearised to yield:

$$\begin{aligned}
\mathscr{L}_{\mathrm{MFA}} = & \overline{\psi}\left[i\gamma^{\mu}\left(\partial_{\mu} - A_4\delta^0_{\mu}\right) - \hat{m} + \hat{\mu}\gamma^0\right]\psi - \mathcal{U}\left(\Phi,\overline{\Phi};T\right) \\
& + 2G_S\left(\overline{\psi}\lambda^0\psi\right)\sqrt{\frac{2}{3}}\left(\sigma_u+\sigma_d+\sigma_s\right) - \frac{2}{3}G_S\left(\sigma_u+\sigma_d+\sigma_s\right)^2 \\
& + 2G_S\left(\overline{\psi}\lambda^3\psi\right)\left(\sigma_u-\sigma_d\right) - G_S\left(\sigma_u-\sigma_d\right)^2 \\
& + 2G_S\left(\overline{\psi}\lambda^8\psi\right)\frac{1}{\sqrt{3}}\left(\sigma_u+\sigma_d-2\sigma_s\right) - \frac{1}{3}G_S\left(\sigma_u+\sigma_d-2\sigma_s\right)^2 \\
& - 2G_D\overline{\psi}\Delta\psi + 4G_D\sigma_u\sigma_d\sigma_s \\
& - 2G_{\omega}\left(\overline{\psi}\gamma^0\lambda^0\psi\right)\sqrt{\frac{2}{3}}\left(\rho_u+\rho_d+\rho_s\right) + \frac{2}{3}G_{\omega}\left(\rho_u+\rho_d+\rho_s\right)^2 \\
& - 2G_{\rho}\left(\overline{\psi}\gamma^0\lambda^3\psi\right)\left(\rho_u-\rho_d\right) + G_{\rho}\left(\rho_u-\rho_d\right)^2 \\
& - 2G_{\rho}\left(\overline{\psi}\gamma^0\lambda^8\psi\right)\frac{1}{\sqrt{3}}\left(\rho_u+\rho_d-2\rho_s\right) + \frac{1}{3}G_{\rho}\left(\rho_u+\rho_d-2\rho_s\right)^2. \qquad (6.46)
\end{aligned}$$

Expressing the Lagrangian in the form given by Equation (2.44) yields:

$$\mathscr{L}_{\mathrm{MFA}} = \overline{\psi}\left[i\gamma^{\mu}\left(\partial_{\mu} + iV_0\delta^0_{\mu}\right) - (\hat{m}+S)\right]\psi + U. \qquad (6.47)$$

The auxiliary field S is given by Equation (3.102) while V_0 and U are written:

$$V_0 = V_0^{\mathrm{NJL}} + iA_4, \qquad (6.48)$$

$$U = U^{\mathrm{NJL}} - \mathcal{U}\left(\Phi,\overline{\Phi};T\right). \qquad (6.49)$$

V_0^{NJL} and U^{NJL} are the auxiliary V_0 field and the mean field potential U in the three flavour **NJL** model give in Equations (3.101) and (3.103), respectively.

The effective mass is the same as in the **NJL** model, i.e., given by Equation (3.104). In a similar way to the auxiliary field V_0 and mean field potential U, we can write the effective chemical potential of the **PNJL** using the one obtained in the usual **NJL** ($\tilde{\mu}^{\mathrm{NJL}}$ is defined in Equation (3.105)):

$$\tilde{\mu} = \tilde{\mu}^{\mathrm{NJL}} - iA_4, \qquad (6.50)$$

The grand canonical potential is:

$$\begin{aligned}
\Omega_{\mathrm{MFA}} - \Omega_0 = & \mathcal{U}\left(\Phi,\overline{\Phi};T\right) - U^{\mathrm{NJL}} \\
& - 2T\operatorname*{tr}_{f,c}\int\frac{d^3p}{(2\pi)^3}\left[\beta E + \ln\left(1+e^{-\beta(E+\tilde{\mu})}\right) + \ln\left(1+e^{-\beta(E-\tilde{\mu})}\right)\right]. \qquad (6.51)
\end{aligned}$$

The effective mass for each flavour of quark is given in Equations (3.108), (3.109) and (3.110). The effective chemical potential in flavour space is:

$$\tilde{\mu} = \begin{pmatrix} \tilde{\mu}_u^{\mathrm{NJL}} & 0 & 0 \\ 0 & \tilde{\mu}_d^{\mathrm{NJL}} & 0 \\ 0 & 0 & \tilde{\mu}_s^{\mathrm{NJL}} \end{pmatrix} - \begin{pmatrix} iA_4 & 0 & 0 \\ 0 & iA_4 & 0 \\ 0 & 0 & iA_4 \end{pmatrix} = \begin{pmatrix} \tilde{\mu}_u & 0 & 0 \\ 0 & \tilde{\mu}_d & 0 \\ 0 & 0 & \tilde{\mu}_s \end{pmatrix}, \tag{6.52}$$

$$\tilde{\mu}_u = \tilde{\mu}_u^{\mathrm{NJL}} - iA_4, \tag{6.53}$$

$$\tilde{\mu}_d = \tilde{\mu}_d^{\mathrm{NJL}} - iA_4, \tag{6.54}$$

$$\tilde{\mu}_s = \tilde{\mu}_d^{\mathrm{NJL}} - iA_4. \tag{6.55}$$

The effective chemical potentials for each flavour $\tilde{\mu}_u^{\mathrm{NJL}}$, $\tilde{\mu}_d^{\mathrm{NJL}}$ and $\tilde{\mu}_s^{\mathrm{NJL}}$ are defined in Equations (3.112), (3.113) and (3.114) respectively.

Like for the **NJL** model, the trace over flavour space yields a sum over flavours. However, now the trace over colour is not simply a N_c factor. Due to the contribution of the gluonic background field, the effective chemical potential has internal structure in colour space. Explicitly, the grand canonical potential is (using the identity $\mathrm{tr}\ln A = \ln\det A$):

$$\begin{aligned} \Omega_{\mathrm{MFA}} - \Omega_0 = {} & \mathcal{U}\left(\Phi, \overline{\Phi}; T\right) - U^{\mathrm{NJL}} \\ & - 2T \sum_{f=u,d,s} \int \frac{d^3p}{(2\pi)^3} \left\{ N_c \beta E_f + \ln \det_c \left[1 + e^{-\beta\left(E_f + \tilde{\mu}_f\right)}\right] \right. \\ & \qquad \left. + \ln \det_c \left[1 + e^{-\beta\left(E_f - \tilde{\mu}_f\right)}\right] \right\} = \\ = {} & \mathcal{U}\left(\Phi, \overline{\Phi}; T\right) - U^{\mathrm{NJL}} \\ & - 2T \sum_{f=u,d,s} \int \frac{d^3p}{(2\pi)^3} \left\{ N_c \beta E_f + \ln \det_c \left[1 + e^{-\beta\left(E_f + \tilde{\mu}_f^{\mathrm{NJL}} - iA_4\right)}\right] \right. \\ & \qquad \left. + \ln \det_c \left[1 + e^{-\beta\left(E_f - \tilde{\mu}_f^{\mathrm{NJL}} + iA_4\right)}\right] \right\}. \end{aligned} \tag{6.56}$$

Using the definition of the thermal Wilson line (Equation (6.18)) for a static gluonic background field we may write:

$$L = e^{i\beta A_4}, \tag{6.57}$$

$$L^\dagger = e^{-i\beta A_4}. \tag{6.58}$$

The terms with colour structure can then be rearranged to yield:

$$\det_c \left[1 + e^{-\beta\left(E_f - \tilde{\mu}_f^{\mathrm{NJL}} + iA_4\right)}\right] = \det_c \left[1 + L^\dagger\, e^{-\beta\left(E_f - \tilde{\mu}_f^{\mathrm{NJL}}\right)}\right], \tag{6.59}$$

$$\det_c \left[1 + e^{-\beta\left(E_f + \tilde{\mu}_f^{\mathrm{NJL}} - iA_4\right)}\right] = \det_c \left[1 + L\, e^{-\beta\left(E_f + \tilde{\mu}_f^{\mathrm{NJL}}\right)}\right]. \tag{6.60}$$

To calculate the determinant over colour space, without loss of generality we can work

on the Polyakov gauge proposed in [83]. In this gauge A_4 is diagonal with components $A_4 = diag\,(A_{11}, A_{22}, A_{33})$. Besides, because L belongs to the $SU_c(N_c)$ group, it is a traceless matrix. This means,

$$A_{11} + A_{22} + A_{33} = 0. \tag{6.61}$$

Writing (6.59) in matrix form in colour space, and performing the determinant yields (the case for (6.60) is analogous),

$$\det_c \left[1 + L^\dagger\, e^{-\beta\left(E_f - \tilde{\mu}_f^{\rm NJL}\right)}\right] = \det_c \left[\mathbb{1}_{3\times 3} + e^{-\beta\left(E_f - \tilde{\mu}_f^{\rm NJL}\right)} \exp \begin{pmatrix} -i\beta A_{11} & 0 & 0 \\ 0 & -i\beta A_{22} & 0 \\ 0 & 0 & -i\beta A_{33} \end{pmatrix}\right]. \tag{6.62}$$

Using (6.61) we can write the determinant in (6.59) as:

$$\begin{aligned} \det_c \left[1 + L^\dagger\, e^{-\beta\left(E_f - \tilde{\mu}_f^{\rm NJL}\right)}\right] = 1 &+ e^{-\beta\left(E_f - \tilde{\mu}_f^{\rm NJL}\right)} \left[e^{-i\beta A_{11}} + e^{-i\beta A_{22}} + e^{-i\beta A_{33}}\right] \\ &+ e^{-2\beta\left(E_f - \tilde{\mu}_f^{\rm NJL}\right)} \left[e^{i\beta A_{11}} + e^{i\beta A_{22}} + e^{i\beta A_{33}}\right] \\ &+ e^{-3\beta\left(E_f - \tilde{\mu}_f^{\rm NJL}\right)}. \end{aligned} \tag{6.63}$$

Besides, from the definition of Polyakov loop we may write:

$$\Phi = \frac{1}{N_c} \operatorname*{tr}_c L = \frac{1}{N_c} \left[e^{i\beta A_{11}} + e^{i\beta A_{22}} + e^{i\beta A_{33}}\right], \tag{6.64}$$

$$\overline{\Phi} = \frac{1}{N_c} \operatorname*{tr}_c L^\dagger = \frac{1}{N_c} \left[e^{-i\beta A_{11}} + e^{-i\beta A_{22}} + e^{-i\beta A_{33}}\right]. \tag{6.65}$$

Using (6.64) and (6.65), the determinant yields:

$$\det_c \left[1 + L^\dagger\, e^{-\beta\left(E_f - \tilde{\mu}_f^{\rm NJL}\right)}\right] = 1 + N_c \overline{\Phi} e^{-\beta\left(E_f - \tilde{\mu}_f^{\rm NJL}\right)} + N_c \Phi e^{-2\beta\left(E_f - \tilde{\mu}_f^{\rm NJL}\right)} + e^{-3\beta\left(E_f - \tilde{\mu}_f^{\rm NJL}\right)}. \tag{6.66}$$

Repeating the calculations to calculate the determinant in (6.60) yields:

$$\det_c \left[1 + L\, e^{-\beta\left(E_f + \tilde{\mu}_f^{\rm NJL}\right)}\right] = 1 + N_c \Phi e^{-\beta\left(E_f + \tilde{\mu}_f^{\rm NJL}\right)} + N_c \overline{\Phi} e^{-2\beta\left(E_f + \tilde{\mu}_f^{\rm NJL}\right)} + e^{-3\beta\left(E_f + \tilde{\mu}_f^{\rm NJL}\right)}. \tag{6.67}$$

Putting all together, the grand canonical potential for the **PNJL** model is now:

$$\Omega_{\rm MFA}-\Omega_0=\mathcal{U}\left(\Phi,\overline{\Phi};T\right)-U^{\rm NJL}-2\sum_{f=u,d,s}\left\{\int\frac{d^3p}{(2\pi)^3}N_cE_f\right.$$
$$+T\int\frac{d^3p}{(2\pi)^3}\ln\left[1+N_c\Phi e^{-\beta\left(E_f+\tilde{\mu}_f^{\rm NJL}\right)}+N_c\overline{\Phi}e^{-2\beta\left(E_f+\tilde{\mu}_f^{\rm NJL}\right)}+e^{-3\beta\left(E_f+\tilde{\mu}_f^{\rm NJL}\right)}\right]$$
$$\left.+T\int\frac{d^3p}{(2\pi)^3}\ln\left[1+N_c\overline{\Phi}e^{-\beta\left(E_f-\tilde{\mu}_f^{\rm NJL}\right)}+N_c\Phi e^{-2\beta\left(E_f-\tilde{\mu}_f^{\rm NJL}\right)}+e^{-3\beta\left(E_f-\tilde{\mu}_f^{\rm NJL}\right)}\right]\right\}. \quad (6.68)$$

Defining the thermal functions $\mathcal{F}$ and $\mathcal{F}^*$,

$$\mathcal{F}\left(\boldsymbol{p},T,\tilde{\mu}_f^{\rm NJL}\right)=T\ln\left[1+e^{-3\left(E_f-\tilde{\mu}_f^{\rm NJL}\right)/T}+N_c\overline{\Phi}e^{-\left(E_f-\tilde{\mu}_f^{\rm NJL}\right)/T}+N_c\Phi e^{-2\left(E_f-\tilde{\mu}_f^{\rm NJL}\right)/T}\right], \quad (6.69)$$

$$\mathcal{F}^*\left(\boldsymbol{p},T,\tilde{\mu}_f^{\rm NJL}\right)=T\ln\left[1+e^{-3\left(E_f+\tilde{\mu}_f^{\rm NJL}\right)/T}+N_c\Phi e^{-\left(E_f+\tilde{\mu}_f^{\rm NJL}\right)/T}+N_c\overline{\Phi}e^{-2\left(E_f+\tilde{\mu}_f^{\rm NJL}\right)/T}\right], \quad (6.70)$$

we can write the grand canonical potential in a simpler form:

$$\Omega_{\rm MFA}-\Omega_0=\mathcal{U}\left(\Phi,\overline{\Phi};T\right)-U^{\rm NJL}-2N_c\sum_f\int\frac{d^3p}{(2\pi)^3}E_f$$
$$-2\sum_f\int\frac{d^3p}{(2\pi)^3}\left[\mathcal{F}\left(\boldsymbol{p},T,\tilde{\mu}_f^{\rm NJL}\right)+\mathcal{F}^*\left(\boldsymbol{p},T,\tilde{\mu}_f^{\rm NJL}\right)\right]. \quad (6.71)$$

To evaluate the thermodynamics we apply the thermodynamic consistency relations (Section 2.3):

$$\frac{\partial\Omega_{\rm MFA}}{\partial\sigma_f}=\frac{\partial\Omega_{\rm MFA}}{\partial\Phi}=\frac{\partial\Omega_{\rm MFA}}{\partial\overline{\Phi}}=0,\quad f=u,d,s. \quad (6.72)$$

These relations define the value of the quark condensate (see Appendix C.4.3):

$$\sigma_u=-2\,N_c\int\frac{d^3p}{(2\pi)^3}\frac{M_u}{E_u}\left(1-\nu_u-\overline{\nu}_u\right), \quad (6.73)$$

$$\sigma_d=-2\,N_c\int\frac{d^3p}{(2\pi)^3}\frac{M_d}{E_d}\left(1-\nu_d-\overline{\nu}_d\right), \quad (6.74)$$

$$\sigma_s=-2\,N_c\int\frac{d^3p}{(2\pi)^3}\frac{M_s}{E_s}\left(1-\nu_s-\overline{\nu}_s\right). \quad (6.75)$$

Here ν_f and $\overline{\nu}_f$ are the particle and antiparticle occupation numbers in the **PNJL** model, defined as:

$$\nu_f = \frac{\frac{3}{N_c}e^{-3\left(E_f-\tilde{\mu}_f^{\mathrm{NJL}}\right)/T} + \overline{\Phi}e^{-\left(E_f-\tilde{\mu}_f^{\mathrm{NJL}}\right)/T} + 2\Phi e^{-2\left(E_f-\tilde{\mu}_f^{\mathrm{NJL}}\right)/T}}{1 + e^{-3\left(E_f-\tilde{\mu}_f^{\mathrm{NJL}}\right)/T} + N_c\overline{\Phi}e^{-\left(E_f-\tilde{\mu}_f^{\mathrm{NJL}}\right)/T} + N_c\Phi e^{-2\left(E_f-\tilde{\mu}_f^{\mathrm{NJL}}\right)/T}}, \tag{6.76}$$

$$\overline{\nu}_f = \frac{\frac{3}{N_c}e^{-3\left(E_f+\tilde{\mu}_f^{\mathrm{NJL}}\right)/T} + \Phi e^{-\left(E_f+\tilde{\mu}_f^{\mathrm{NJL}}\right)/T} + 2\overline{\Phi}e^{-2\left(E_f+\tilde{\mu}_f^{\mathrm{NJL}}\right)/T}}{1 + e^{-3\left(E_f+\tilde{\mu}_f^{\mathrm{NJL}}\right)/T} + N_c\Phi e^{-\left(E_f+\tilde{\mu}_f^{\mathrm{NJL}}\right)/T} + N_c\overline{\Phi}e^{-2\left(E_f+\tilde{\mu}_f^{\mathrm{NJL}}\right)/T}}. \tag{6.77}$$

The *gap* equations for the Polyakov loop fields Φ and $\overline{\Phi}$ are (see Appendix C.4.3):

$$T^4\left[-\frac{1}{2}a\left(T\right)\overline{\Phi} - \frac{6b\left(T\right)\left(\overline{\Phi} - 2\Phi^2 + \overline{\Phi}^2\Phi\right)}{1 - 6\overline{\Phi}\Phi + 4\left(\overline{\Phi}^3 + \Phi^3\right) - 3\left(\overline{\Phi}\Phi\right)^2}\right] = 2N_cT\sum_f\int\frac{d^3p}{(2\pi)^3}\left[\frac{e^{-\left(E_f+\tilde{\mu}_f^{\mathrm{NJL}}\right)/T}}{e^{\mathcal{F}^*\left(\boldsymbol{p},T,\tilde{\mu}_f^{\mathrm{NJL}}\right)/T}} + \frac{e^{-2\left(E_f-\tilde{\mu}_f^{\mathrm{NJL}}\right)/T}}{e^{\mathcal{F}\left(\boldsymbol{p},T,\tilde{\mu}_f^{\mathrm{NJL}}\right)/T}}\right], \tag{6.78}$$

$$T^4\left[-\frac{1}{2}a\left(T\right)\Phi - \frac{6b\left(T\right)\left(\Phi - 2\overline{\Phi}^2 + \overline{\Phi}\Phi^2\right)}{1 - 6\overline{\Phi}\Phi + 4\left(\overline{\Phi}^3 + \Phi^3\right) - 3\left(\overline{\Phi}\Phi\right)^2}\right] = 2N_cT\sum_f\int\frac{d^3p}{(2\pi)^3}\left[\frac{e^{-\left(E_f-\tilde{\mu}_f^{\mathrm{NJL}}\right)/T}}{e^{\mathcal{F}\left(\boldsymbol{p},T,\tilde{\mu}_f^{\mathrm{NJL}}\right)/T}} + \frac{e^{-2\left(E_f+\tilde{\mu}_f^{\mathrm{NJL}}\right)/T}}{e^{\mathcal{F}^*\left(\boldsymbol{p},T,\tilde{\mu}_f^{\mathrm{NJL}}\right)/T}}\right]. \tag{6.79}$$

Equations (6.73), (6.74), (6.75), (6.78) and (6.79) alongside the effective mass for each flavour of quark (Equations (3.108), (3.109) and (3.110)), define the *gap* equations of the **PNJL** model.

6.3 The modified Polyakov loop potential

From the definition of the Polyakov loop effective potential and from the *gap* equations of the Polyakov loop field (Equations (6.78) and (6.79)) it is clear that when the limit $T = 0$ is taken, the **PNJL** model becomes the **NJL** model of Section 3.3. If we want to treat neutron stars with a model that have built in an order parameter for the confinement-deconfinement phase transition, we should adopt a different scheme, modify the **PNJL** in such a way that the Polyakov loop effective potential does not vanish in such a regime ($T = 0$, for extremely degenerate matter).

It has been proposed by many authors [78–81], that an explicit dependence on the chemical potential and number of flavours of quarks could be added to the T_0 parameter of the effective potential.

6.3.1 Stefan-Boltzmann pressure

Following [84], to modify the effective Polyakov loop potential we modify both sides of the definition of the Polyakov loop potential (Equation (6.37)). To modify the left side of Equation (6.37), we use the pressure for the **QCD** plasma, which to first-order in the coupling constant, is the Stefan-Boltzmann pressure for an ideal gas of quarks and gluons.

The pressure for a gas of massless quarks P_q can be extracted from Equation (2.94), putting $N_I = N_c$, the number of colours, and making a sum over the flavours of quarks:

$$P_q = \sum_f P_f = N_c N_f \frac{7\pi^2 T^4}{180} + N_c \sum_f \left(\frac{T^2 \mu_f^2}{6} + \frac{\mu_f^4}{12\pi^2} \right). \tag{6.80}$$

The pressure for a gas of massless gluons P_G can be obtained from Equation (2.122), by setting $N_I = 2\left(N_c^2 - 1\right)$, where these represent the degrees of freedom of the gluons, there are $N_c^2 - 1$ gluon fields, each with two transverse propagating modes (number of polarizations a spin-1 particle can have):

$$P_G = 2\left(N_c^2 - 1\right) \frac{\pi^2 T^4}{90}. \tag{6.81}$$

In $SU_c(3) \otimes SU_f(3)$ we have $N_c = 3$ and $N_f = 3$. The Stefan-Boltzmann pressure P_{SB} is the sum of the quark and gluon contributions:

$$\begin{aligned} P_{SB} &= P_q + P_G = \\ &= \frac{19\pi^2 T^4}{36} + \sum_f \left(\frac{T^2 \mu_f^2}{2} + \frac{\mu_f^4}{4\pi^2} \right) = \frac{19\pi^2}{36} \left[T^4 + \sum_f \left(\frac{18}{19\pi^2} T^2 \mu_f^2 + \frac{9}{19\pi^4} \mu_f^4 \right) \right]. \end{aligned} \tag{6.82}$$

The first modification to the effective Polyakov loop potential is the substitution of the global T^4 dependence on the left side of Equation (6.37) by the dependence in the Stefan-Boltzmann pressure [84]:

$$T^4 \to T^4 + \sum_f \left(\frac{18}{19\pi^2} T^2 \mu_f^2 + \frac{9}{19\pi^4} \mu_f^4 \right). \tag{6.83}$$

Note that when $\mu_f = 0$, we recover the usual effective Polyakov loop. This idea is inspired by the Dyson–Schwinger calculation in [78].

The μ dependence on the right side of Equation (6.37) will be given by μ dependent T_0. Perturbative calculations (hard thermal loop and hard dense loop calculations of perturbative **QCD**) allows the following substitution [79]:

$$\frac{T_0}{T} \to \frac{T_0(\mu)}{T} = \frac{T_\tau e^{-\frac{1}{C_1 - C_2 \mu^2}}}{T}. \tag{6.84}$$

The constants C_1 and C_2 are:

$$C_1 = \frac{\alpha_0}{6\pi}\left(11N_c - 2N_f\right), \tag{6.85}$$

$$C_2 = \frac{16\alpha_0}{\pi}\frac{N_f}{T_\tau^2}. \tag{6.86}$$

The parameters T_τ and α_0 are free. In [85], T_τ is chosen to be the temperature scale, $T_\tau = 1.77$ GeV. This constitutes a reasonable UV scale for the **MFA**. The parameter α_0 is fixed by requiring $T_0 = 270$ MeV, when pure Yang-Mills theory ($N_f = 0$) is considered, in that case $\alpha_0 = 0.304$.

In the present work this parametrization will be different. We will consider a fixed value for $\alpha_0 = 0.304$ and choose a certain value for T_0. This will then lead to some temperature scale, T_τ. This approach allows the study of the relation between the deconfinement and chiral transitions at $T = 0$, for different T_0 when quarks are considered. Fixing T_0 and then calculating the energy scale, is a valid approximation if the chemical potentials for a given flavour of quark are not higher then the calculated scale.

The $T_0(\mu_f)/T$ in Equation (6.84), have a divergence at $T = 0$, exactly the limit we are interested in. Following [5], in order to study the $T \to 0$ limit of the modified Polyakov loop potential, a phenomenological function is adopted,

$$\frac{T_0}{T} \to \frac{T_0}{\sqrt{T^2 + g(\mu_f)}}, \tag{6.87}$$

where the function $g(\mu_f)$ is expanded as a power series in μ_f. With this approach we are fitting Equation (6.84) as

$$g(\mu_f) = \sum_{n=1}^{\infty} \eta_n \mu_f^n. \tag{6.88}$$

By Taylor expanding (6.84) around the *lattice* **QCD** deconfinement temperature at vanishing chemical potential, $(T, \mu_f) = (T_{lat}^{\mathrm{dec}}, 0)$, one can match the coefficients η_i in the Taylor expansion of Equation (6.87) around the same point, $(T_{lat}^{\mathrm{dec}}, 0)$. The sum starts in $n = 1$ in order to recover the usual T_0/T when $\mu_f = 0$. Making the expansion to sixth order in μ_f we can write:

$$g(\mu_f) = \eta_2\mu_f^2 + \eta_4\mu_f^4 + \eta_6\mu_f^6. \tag{6.89}$$

Taylor expanding Equations (6.84) and (6.87), and using Equation (6.89), to sixth order in μ_f, one can match the coefficients of equal power in μ_f and write:

$$g(\mu_f = 0) \quad : \quad T_0 = T_\tau e^{-\frac{1}{C_1}}, \tag{6.90}$$

$$\mu_f^2 \quad : \quad \eta_2 = 2\left(T_{lat}^{\rm dec}\right)^2 \frac{C_2}{C_1^2}, \tag{6.91}$$

$$\mu_f^4 \quad : \quad \eta_4 = \frac{\eta_2^2(1+C_1)}{2\left(T_{lat}^{\rm dec}\right)^2}, \tag{6.92}$$

$$\mu_f^6 \quad : \quad \eta_6 = \frac{\left(T_{lat}^{\rm dec}\right)^2}{3C_1^6}\left[\left(6C_1^2 - 6C_1 + 1\right)C_2^3\right] - \frac{5\eta_2^3}{8\left(T_{lat}^{\rm dec}\right)^4} + \frac{3\eta_2\eta_4}{2\left(T_{lat}^{\rm dec}\right)^2}. \tag{6.93}$$

The parameters $a(T)$ and $b(T)$ will have an explicit dependence on the chemical potential, $a(T, \mu_f)$ and $b(T, \mu_f)$. Each flavour of quark can have different contributions to these parameters (in the case where the chemical potentials are different). Thus, it is necessary to make an explicit sum of these parameters over the flavour space:

$$a(T) \to \frac{1}{N_f}\sum_f a(T, \mu_f), \tag{6.94}$$

$$b(T) \to \frac{1}{N_f}\sum_f b(T, \mu_f). \tag{6.95}$$

The factor $1/N_f$ is a normalization constant that allows us to retrieve the usual Polyakov loop effective potential (6.37), in the limit $\mu_f \to 0$. The modified Polyakov loop potential can finally be written as:

$$\frac{\mathcal{U}(\Phi, \overline{\Phi}; T, \mu_f)}{T^4 + \sum_f\left(\frac{18}{19\pi^2}T^2\mu_f^2 + \frac{9}{19\pi^4}\mu_f^4\right)} = -\frac{\Phi\overline{\Phi}}{2N_f}\sum_f a(T, \mu_f) + \frac{1}{N_f}\sum_f b(T, \mu_f)\ln\left[X(\Phi, \overline{\Phi})\right]. \tag{6.96}$$

Where $a(T, \mu_f)$ and $b(T, \mu_f)$ are now parameters that depend on temperature and quark chemical potential in the following way:

$$a(T, \mu_f) = a_0 + a_1\frac{T_0}{\left[T^2 + g(\mu_f)\right]^{1/2}} + a_2\frac{T_0^2}{\left[T^2 + g(\mu_f)\right]}, \tag{6.97}$$

$$b(T, \mu_f) = b_3\frac{T_0^3}{\left[T^2 + g(\mu_f)\right]^{3/2}}. \tag{6.98}$$

6.4 The modified PNJL model

The modified PNJL (**mPNJL**) Lagrangian is exactly the same as the one for the **PNJL** model (6.44), except that we introduce the modified Polyakov potential of Equation (6.96):

$$\mathscr{L}^{\mathrm{mPNJL}} = \overline{\psi}\left(i\gamma^{\mu}D_{\mu} - \hat{m} + \hat{\mu}\gamma^{0}\right)\psi + G_S\sum_{a=0}^{8}\left[\left(\overline{\psi}\lambda^{a}\psi\right)^{2} + \left(\overline{\psi}i\gamma_5\lambda^{a}\psi\right)^{2}\right] - \mathscr{L}^{det} - \mathscr{L}^{vec} - \mathcal{U}(\Phi,\overline{\Phi};T,\mu_f). \tag{6.99}$$

The grand canonical potential for this theory, in the mean field approximation, is (the sum over flavour is to be made over $f = u, d, s$):

$$\Omega_{\mathrm{MFA}} - \Omega_0 = \mathcal{U}\left(\Phi,\overline{\Phi};T,\mu_f\right) - U^{\mathrm{NJL}} - 2N_c\sum_f\int\frac{d^3p}{(2\pi)^3}E_f - 2\sum_f\int\frac{d^3p}{(2\pi)^3}\left[\mathcal{F}\left(\boldsymbol{p},T,\tilde{\mu}_f^{\mathrm{NJL}}\right) + \mathcal{F}^{*}\left(\boldsymbol{p},T,\tilde{\mu}_f^{\mathrm{NJL}}\right)\right], \tag{6.100}$$

Here, U^{NJL} is given by Equation (3.103).

6.4.1 $T = 0$ Limit

We are interested in the $T \to 0$ limit of the **mPNJL** model. We may write:

$$\begin{aligned}\Omega_{\mathrm{MFA}}(\mu_f) &= \lim_{T\to 0}\Omega_{\mathrm{MFA}}(\mu_f,T) = \\ &= \Omega_0 + \lim_{T\to 0}\mathcal{U}\left(\Phi,\overline{\Phi};T,\mu_f\right) - U^{\mathrm{NJL}} - 2N_c\sum_f\int\frac{d^3p}{(2\pi)^3}E_f \\ &\quad - 2\sum_f\int\frac{d^3p}{(2\pi)^3}\left[\lim_{T\to 0}\mathcal{F}\left(\boldsymbol{p},T,\tilde{\mu}_f^{\mathrm{NJL}}\right) + \lim_{T\to 0}\mathcal{F}^{*}\left(\boldsymbol{p},T,\tilde{\mu}_f^{\mathrm{NJL}}\right)\right].\end{aligned} \tag{6.101}$$

The thermal functions (6.69) and (6.70) have the following limits (presented in the Appendix D.1.2):

$$\lim_{T\to 0}\mathcal{F}\left(\boldsymbol{p},T,\tilde{\mu}_f^{\mathrm{NJL}}\right) = 3\left(\tilde{\mu}_f^{\mathrm{NJL}} - E_f\right)\theta\left(E_f - \tilde{\mu}_f^{\mathrm{NJL}}\right), \tag{6.102}$$

$$\lim_{T\to 0}\mathcal{F}^{*}\left(\boldsymbol{p},T,\tilde{\mu}_f^{\mathrm{NJL}}\right) = 0. \tag{6.103}$$

Where $\theta(E_f - \tilde{\mu}_f^{\rm NJL})$ is the heaviside step function. The modified Polyakov loop potential in the $T \to 0$ limit is,

$$\frac{\mathcal{U}\left(\Phi,\overline{\Phi};\mu_f\right)}{\frac{9}{19\pi^4}\sum_f \mu_f^4} = -\frac{\Phi\overline{\Phi}}{2N_f}\sum_f a(\mu_f) + \frac{1}{N_f}\sum_f b(\mu_f)\ln\left[1 - 6\Phi\overline{\Phi} + 4\left(\Phi^3 + \overline{\Phi}^3\right) - 3\left(\Phi\overline{\Phi}\right)^2\right], \tag{6.104}$$

$$a(\mu_f) = a_0 + a_1\frac{T_0}{[g(\mu_f)]^{1/2}} + a_2\frac{T_0^2}{[g(\mu_f)]}, \tag{6.105}$$

$$b(\mu_f) = b_3\frac{T_0^3}{[g(\mu_f)]^{3/2}}. \tag{6.106}$$

The grand canonical potential in the $T = 0$ limit is,

$$\Omega_{\rm MFA} - \Omega_0 = \mathcal{U}\left(\Phi,\overline{\Phi};\mu_f\right) - U^{\rm NJL} - 6\sum_f \int \frac{d^3p}{(2\pi)^3}\left[E_f + \left(\tilde{\mu}_f^{\rm NJL} - E_f\right)\theta\left(E_f - \tilde{\mu}_f^{\rm NJL}\right)\right]. \tag{6.107}$$

Where Ω_0 is the vacuum contribution defined in Equation (3.125). We are now able to derive the thermodynamics of the system in this limit, by applying Equations (6.72) to the grand canonical potential. This yields the following *gap* equations:

$$\frac{\partial\Omega}{\partial\sigma_i} = 0 \quad \Rightarrow \quad M_i = m_i - 4g_S\sigma_i + 2g_D\sigma_j\sigma_k \quad i \neq j \neq k, \tag{6.108}$$

$$\frac{\partial\Omega}{\partial\Phi} = 0 \quad \Rightarrow \quad -\frac{\overline{\Phi}}{2N_f}\sum_f a(\mu_f) = \frac{6}{N_f}\sum_f b(\mu_f)\frac{\overline{\Phi} - 2\Phi^2 + \overline{\Phi}^2\Phi}{X(\Phi,\overline{\Phi})}, \tag{6.109}$$

$$\frac{\partial\Omega}{\partial\overline{\Phi}} = 0 \quad \Rightarrow \quad -\frac{\Phi}{2N_f}\sum_f a(\mu_f) = \frac{6}{N_f}\sum_f b(\mu_f)\frac{\Phi - 2\overline{\Phi}^2 + \overline{\Phi}\Phi^2}{X(\Phi,\overline{\Phi})}. \tag{6.110}$$

The pressure, and energy density will be the same as in the **NJL** model (Equations (3.121) and (3.123)). The additional chemical dependence in the Polyakov loop potential will modify the quark densities:

$$\rho_f = -\frac{\partial\Omega}{\partial\mu_f} = 6\int\frac{d^3p}{(2\pi)^3}\theta\left(E_f - \mu_f\right) - \frac{\partial\mathcal{U}\left(\Phi,\overline{\Phi};\mu_f\right)}{\partial\mu_f} = \frac{\lambda_{F_f}^3}{\pi^2} - \frac{\partial\mathcal{U}\left(\Phi,\overline{\Phi};\mu_f\right)}{\partial\mu_f}. \tag{6.111}$$

Where λ_{F_f} is the Fermi momentum of the quark of flavour f and:

$$\begin{aligned}\frac{\partial \mathcal{U}\left(\Phi,\overline{\Phi};\mu_f\right)}{\partial\mu_f} &= \left[\frac{9}{19\pi^4}\frac{\partial}{\partial\mu_f}\sum_f \mu_f^4\right]\left[-\frac{\Phi\overline{\Phi}}{2N_f}\sum_f a(\mu_f)+\frac{1}{N_f}\sum_f b(\mu_f)\ln\left[X(\Phi,\overline{\Phi})\right]\right]\\ &\quad+\left[\frac{9}{19\pi^4}\sum_f \mu_f^4\right]\frac{\partial}{\partial\mu_f}\left[-\frac{\Phi\overline{\Phi}}{2N_f}\sum_f a(\mu_f)+\frac{1}{N_f}\sum_f b(\mu_f)\ln\left[X(\Phi,\overline{\Phi})\right]\right]\\ &= -\frac{9}{19\pi^4}\frac{\Phi\overline{\Phi}}{2N_f}\left[4\mu_f^3\sum_f a(\mu_f)+\frac{da(\mu_f)}{d\mu_f}\sum_f\mu_f^4\right]\\ &\quad+\frac{9}{19\pi^4}\frac{1}{N_f}\ln\left[X(\Phi,\overline{\Phi})\right]\left[4\mu_f^3\sum_f b(\mu_f)+\frac{db(\mu_f)}{d\mu_f}\sum_f\mu_f^4\right], \end{aligned} \tag{6.112}$$

$$\frac{da(\mu_f)}{d\mu_f} = -\left(\frac{a_1}{2}\frac{T_0}{[g(\mu_f)]^{3/2}}+a_2\frac{T_0^2}{[g(\mu_f)]^2}\right)\frac{dg(\mu_f)}{d\mu_f}, \tag{6.113}$$

$$\frac{db(\mu_f)}{d\mu_f} = -\left(\frac{3b_3}{2}\frac{T_0^3}{[g(\mu_f)]^{5/2}}\right)\frac{dg(\mu_f)}{d\mu_f}, \tag{6.114}$$

$$\frac{dg(\mu_f)}{d\mu_f} = \frac{d}{d\mu_f}\sum_{n=1}^{\infty}\eta_n\mu_f^n = \sum_{n=1}^{\infty} n\eta_n\mu_f^{n-1}. \tag{6.115}$$

To sixth order in μ_f we can write Equation (6.115) as,

$$\frac{dg(\mu_f)}{d\mu_f} = 2\eta_2\mu_f+4\eta_4\mu_f^3+6\eta_6\mu_f^5. \tag{6.116}$$

The quark density is finally given by:

$$\begin{aligned}\rho_f &= \frac{\lambda_{F_f}^3}{\pi^2}+\frac{9}{19\pi^4}\frac{\Phi\overline{\Phi}}{2N_f}\left[4\mu_f^3\sum_f a(\mu_f)+\frac{da(\mu_f)}{d\mu_f}\sum_f\mu_f^4\right]\\ &\quad-\frac{9}{19\pi^4}\frac{1}{N_f}\ln\left[X(\Phi,\overline{\Phi})\right]\left[4\mu_f^3\sum_f b(\mu_f)+\frac{db(\mu_f)}{d\mu_f}\sum_f\mu_f^4\right]. \end{aligned} \tag{6.117}$$

Where the derivatives are given by Equations (6.113), (6.114) and (6.115). Note that in the limit $\Phi\to 0$, the quark density reduces to the one of the **NJL** model (see Equation (3.122)).

In this limit, the pressure and energy density are the ones calculated for the $SU_f(3)$ **NJL** model (Equations (3.121) and (3.123)), with a contribution from the modified Polyakov loop effective potential:

$$P_{\mathrm{MFA}} = -\Omega_0-\mathcal{U}\left(\Phi,\overline{\Phi};\mu_f\right)+U^{\mathrm{NJL}}+\frac{3}{\pi^2}\sum_f\int_{\lambda_{F_f}}^{\Lambda}dpp^2E_f+\sum_f\tilde{\mu}_f^{\mathrm{NJL}}\frac{\lambda_{F_f}^3}{\pi^2}, \tag{6.118}$$

$$\epsilon_{\rm MFA} = \Omega_0 + \mathcal{U}\left(\Phi, \overline{\Phi}; \mu_f\right) - U^{\rm NJL} - \frac{3}{\pi^2}\sum_f \int_{\lambda_{F_f}}^{\Lambda} dp p^2 E_f + \sum_f \left(\mu_f - \tilde{\mu}_f^{\rm NJL}\right)\frac{\lambda_{F_f}^3}{\pi^2}. \quad (6.119)$$

The major changes between the **NJL** in $SU_f(3)$ and the modified Polyakov loop at zero temperature is the additional terms in the particle density (Equation (6.117)) and the contribution of the modified Polyakov loop potential to the pressure (Equation (6.118)) and to the energy density (Equation (6.119)). This extra contribution may be compared to the phenomenological Bag constant introduced in Section 4.3. However, this Bag is not simply a constant, but it depends on the chemical potential of the quarks and it is related to gluonic degrees of freedom through the Polyakov loop field.

6.5 The deconfinement phase transition at T=0

Focusing on the *gap* equations for the Polyakov loop field Φ, Equation (6.109) and $\overline{\Phi}$, Equation (6.110), one can realize that these equations are independent from the quark condensates (6.108) and respective constituent masses. This means that they can be solved separately from the other *gap* equations. Isolating $X(\Phi, \overline{\Phi})$ on both equations, yields:

$$X(\Phi, \overline{\Phi})\sum_f a(\mu_f) = -12\sum_f b(\mu_f)\frac{\overline{\Phi} - 2\Phi^2 + \overline{\Phi}^2\Phi}{\overline{\Phi}}, \quad (6.120)$$

$$X(\Phi, \overline{\Phi})\sum_f a(\mu_f) = -12\sum_f b(\mu_f)\frac{\Phi - 2\overline{\Phi}^2 + \overline{\Phi}\Phi^2}{\Phi}. \quad (6.121)$$

Equating the right sides of the above equations gives:

$$\begin{aligned} \frac{\overline{\Phi} - 2\Phi^2 + \overline{\Phi}^2\Phi}{\overline{\Phi}} &= \frac{\Phi - 2\overline{\Phi}^2 + \overline{\Phi}\Phi^2}{\Phi} \Leftrightarrow \\ \Leftrightarrow \Phi\overline{\Phi} - 2\Phi^3 + \overline{\Phi}^2\Phi^2 &= \Phi\overline{\Phi} - 2\overline{\Phi}^3 + \overline{\Phi}^2\Phi^2 \Leftrightarrow \\ \Leftrightarrow \Phi^3 &= \overline{\Phi}^3 \Leftrightarrow \\ \Leftrightarrow \Phi &= \overline{\Phi}. \end{aligned} \quad (6.122)$$

This means we only have one independent Polyakov loop field. Substituting this in Equations (6.120) and (6.121), yields,

$$\Phi\sum_f a(\mu_f) = -12\sum_f b(\mu_f)\frac{\Phi - 2\Phi^2 + \Phi^3}{1 - 6\Phi^2 + 8\Phi^3 - 3\Phi^4}. \quad (6.123)$$

We define the sums over flavour of the chemical potential dependent parameters as:

$$\sum_f a(\mu_f) = A, \quad (6.124)$$

$$\sum_f b(\mu_f) = B, \quad (6.125)$$

and write (6.123) as:

$$\Phi A\left(1-6\Phi^2+8\Phi^3-3\Phi^4\right)+12B\left(\Phi-2\Phi^2+\Phi^3\right)=0. \tag{6.126}$$

This equation is simply the calculation of the five zeros of some fifth order polynomial function, which depends on the parameters A and B (defined in (6.124) and (6.125)). If we factorize the above equation, we can re-write it as:

$$(\Phi-1)^2\ \Phi\left(A+12B+2A\Phi-3A\Phi^2\right)=0. \tag{6.127}$$

The five solutions of (6.127) are:

$$\Phi=0, \tag{6.128}$$

$$\Phi=1 \quad \text{(double solution)}, \tag{6.129}$$

$$\Phi=\frac{1}{3}\mp\frac{2}{3}\sqrt{1+9\frac{B}{A}}. \tag{6.130}$$

The first solution (6.128) implies that the Polyakov loop will be always zero, meaning we always have a confined phase i.e., a spontaneous symmetry breaking of the $Z(3)$ symmetry does not occur. The second solution Equation (6.129), represents the opposite, the symmetry is explicitly broken because the Polyakov loop will always be bigger than zero. The third solution (6.130) depends on the parameters A and B, i.e., depend on the chemical potential of the quarks. Substituting the definition of these parameters the third solution is:

$$\Phi^{\mp}=\frac{1}{3}\mp\frac{2}{3}\sqrt{1+9\frac{\sum_f b(\mu_f)}{\sum_f a(\mu_f)}}. \tag{6.131}$$

To evaluate how the Polyakov loop field Φ behaves, we have to provide some relation between the chemical potentials so we have some $\Phi(\mu)$. In order to do this, we consider equal chemical potentials for each flavour of quark[4]:

$$\mu_u=\mu_d=\mu_s=\frac{\mu_B}{3}. \tag{6.132}$$

Next, we fix $G_V=0$ and following [86], fix $T_{lat}^{\text{dec}}=170$ MeV. We then search for the value of the T_0 parameter which, in the usual **PNJL**, yields this deconfinement temperature. We obtained the parametrization given in Table 6.1.

In Figure 6.1 we can see the plot of the Polyakov loop versus the chemical potential. From this figure we can extract some information: the chemical potential and Polyakov loop are positive, implying that some solutions are unphysical; The Polyakov loop becomes larger

[4]Later, when applying the modified **PNJL** to neutron star matter, the relation between the chemical potential will be given by the $\beta-$equilibrium. This represent a more complicated case than considering all chemical potentials to be equal, due to the influence of the electrons.

T_0[MeV]	T_τ[GeV]	η_2	$\eta_4 \times 10^{-6}$	$\eta_6 \times 10^{-11}$
214.00	2.127	0.313	2.432	1.585

TABLE 6.1: T_0 parameter which reproduces $T_{lat}^{\text{dec}} = 170$ MeV in the **PNJL** model. Calculated T_τ (energy scale) and parameters η_2, η_4, η_6.

than zero when it changes from the trivial solution $\Phi = 0$ (red line) to Φ^- (green dashed line), which in turn becomes Φ^+ (blue line).

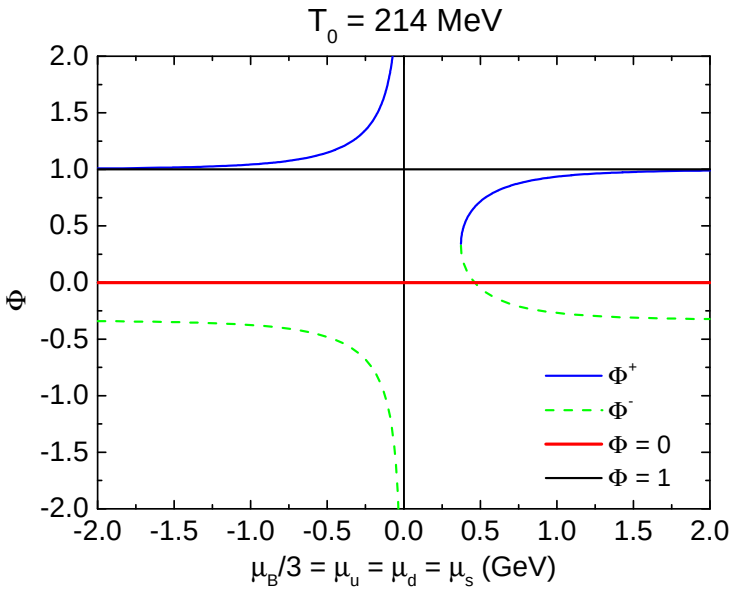

FIGURE 6.1: All the five solutions of the Polyakov loop field, considering equal chemical potential for every flavour of quark ($T_0 = 214$MeV).

In Figure 6.2, the chemical potential and Polyakov loop are restricted to positive values. We can define *conditions* that must be satisfied for the Polyakov loop to change from solution $\Phi = 0$ to Φ^- (*condition 1*) and Φ^- to Φ^+ (*condition 2*). The points in which these *conditions* are met are drawn in Figure 6.2.

Condition 1, as already stated, is satisfied when Φ changes from solution $\Phi = 0$ to Φ^-. This means we can find some constraint on the parameters A and B (defined in Equations (6.124) and (6.125)) by imposing:

$$\begin{aligned}
\Phi^- = 0 \Leftrightarrow \frac{1}{3} &= \frac{2}{3}\sqrt{1+9\frac{B}{A}} \Leftrightarrow \\
&\Leftrightarrow 1 = 4\left(1+9\frac{B}{A}\right) \Leftrightarrow \\
&\Leftrightarrow A + 12B = 0 \Leftrightarrow \\
&\Leftrightarrow \sum_f a(\mu_f) + 12\sum_f b(\mu_f) = 0.
\end{aligned} \tag{6.133}$$

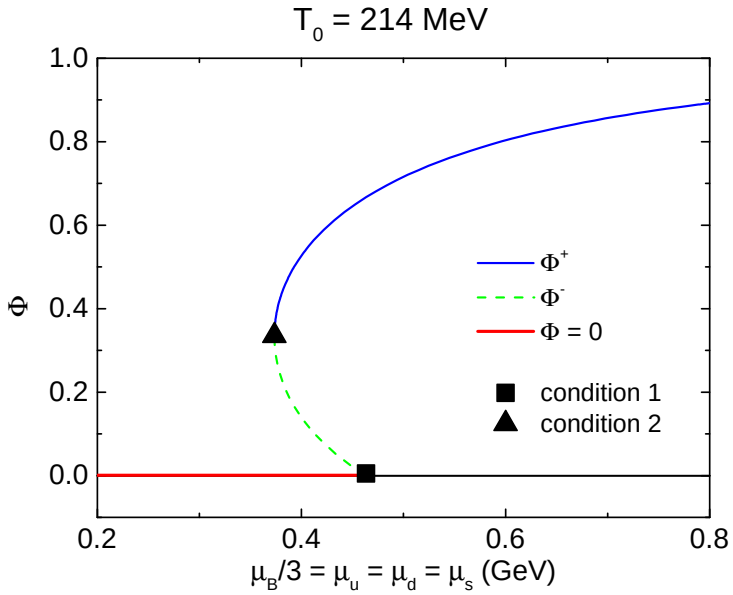

FIGURE 6.2: Physical solutions of the Polyakov loop field, considering equal chemical potential for every flavour of quark ($T_0 = 214$MeV). The points in which *conditions 1* and *2* are verified are drawn (square and triangle, respectively).

Condition 2 is satisfied when Φ changes from solution Φ^- to Φ^+. Following the previous steps, we can find the constraint on the parameters A and B, by writing:

$$\begin{aligned} \Phi^+ = \Phi^- \Leftrightarrow \\ \Leftrightarrow \frac{1}{3} + \frac{2}{3}\sqrt{1+9\frac{B}{A}} = \frac{1}{3} - \frac{2}{3}\sqrt{1+9\frac{B}{A}} \Leftrightarrow \\ \Leftrightarrow \sqrt{1+9\frac{B}{A}} = -\sqrt{1+9\frac{B}{A}}. \end{aligned} \tag{6.134}$$

The quantities under the square roots must be positive (they are sums of chemical potentials). This means that the above equality is only true if both sides are equal to zero,

$$\begin{aligned} \sqrt{1+9\frac{B}{A}} = 0 \Rightarrow A + 9B = 0 \Leftrightarrow \\ \Leftrightarrow \sum_f a(\mu_f) + 9\sum_f b(\mu_f) = 0. \end{aligned} \tag{6.135}$$

Condition 2 is verified when the above equation is verified. Although we have derived these *conditions* by observing the behaviour of the Polyakov loop field when the chemical potentials are all equal, Equations (6.133) and (6.135) hold for other relations between the chemical potentials. This is true because these relations have been derived using the solutions of the Polyakov loop field written in terms of sums of the chemical potential dependent parameters A and B.

The change of the value of the Polyakov loop field from zero to some positive value, can be used as an order parameter for the spontaneous breaking of the $Z(3)$ symmetry which is

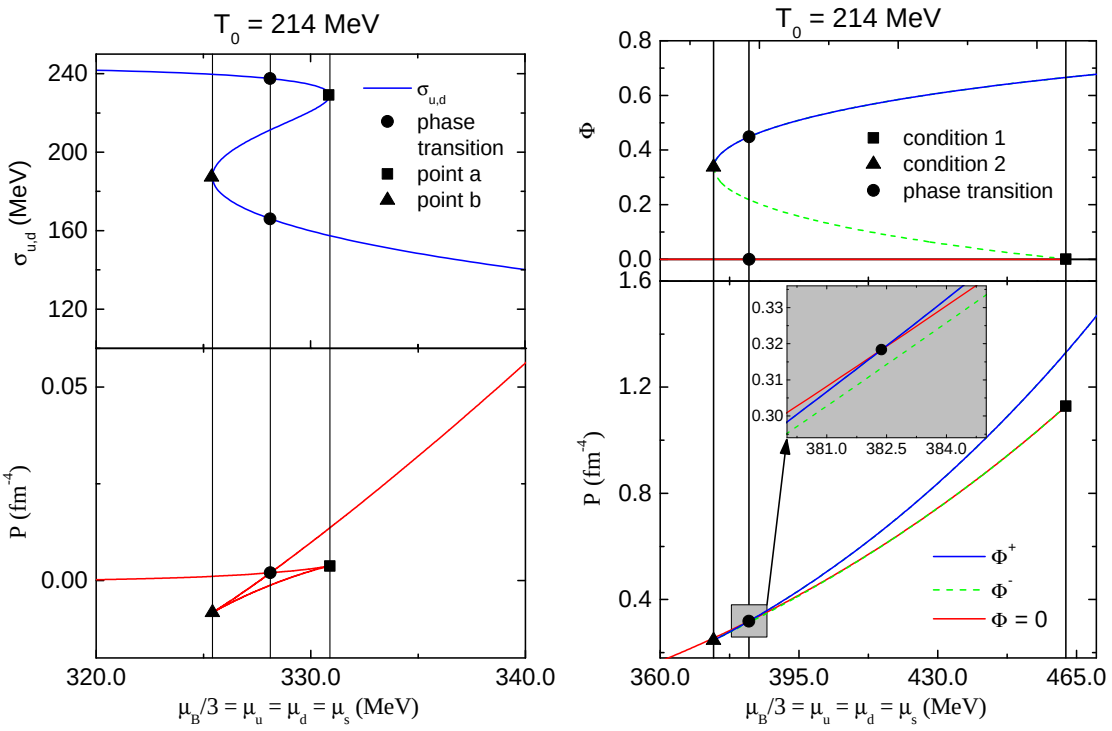

FIGURE 6.3: *Left panel*: Quark condensate (up) and pressure (down) versus the baryonic chemical potential for the $SU_f(3)$ **mPNJL** model with $T_0 = 214$ MeV and $G_V = 0$. The chiral phase transition is highlighted (black dot). *Right panel*: Polyakov loop field (up) and pressure (down) versus the baryonic chemical potential for the $SU_f(3)$ **mPNJL** model with $T_0 = 214$ MeV and $G_V = 0$. The confinement-deconfinement phase transition is highlighted (black dot).

related to the transition from a confined phase, to a deconfined phase (see Section 6.1). This phase transition can be defined like the chiral symmetry restoration (see Section 3.1.5).

The pressure and light quark condensates plotted as a function of the baryonic chemical potential (Figure 6.3, left panel), shows the presence of branches with stable, metastable and unstable solutions, for baryonic chemical potentials in the domain $\mu_B^a < \mu_B < \mu_B^b$, which corresponds to three solutions of the *gap* equations (see Figure 6.3, top left panel). The stable solutions are realized by the minimum of the thermodynamic potential or, equivalently, maximum of the pressure. When stable and metastable solutions give the same value for the thermodynamic potential at the same μ_B, the phase transition occurs as illustrated in Figure 6.3 (left panel). This results in a first-order phase transition (black dot), defined as the μ_B^χ at which there is a discontinuity in the quark condensate (see bottom left panel of Figure 6.3). The phase of broken symmetry is realized for $\mu_B < \mu_B^\chi$ and the "symmetric" phase is realized for $\mu_B > \mu_B^\chi$. At this crossing point of the curve, the two phases are in thermal and chemical equilibrium (obeying the Gibbs criteria, see Figure 6.4 and Section 4.3). All first-order phase transitions found throughout this work, have this type of behaviour. For a more detailed discussion see [3].

The confinement-deconfinement phase transition (Figure 6.3, right), is completely analogous to the chiral transition, a first-order phase transition, characterized by a discontinuity on

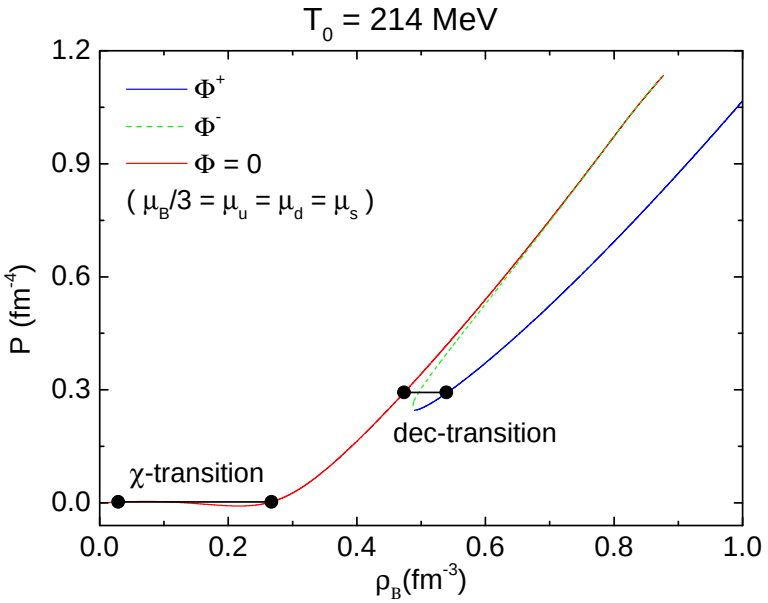

FIGURE 6.4: Pressure versus the baryonic chemical potential and Gibbs construction for the chiral (χ-transition) and deconfinement (dec-transition) transitions in the **mPNJL** model. Each flavour of quark has the same chemical potential and $T_0 = 214$ MeV. The different colors (red, green and blue) correspond to different solutions of the Polyakov loop field.

the first derivative of the pressure. The deconfinement point ($\mu_B^{\rm dec}$) is defined as the μ_B at which there is a discontinuity in the Polyakov loop field, the order parameter (see right panel of Figure 6.3).

6.6 Results

In the present Section we follow Chapter 5 and investigate the existence of hybrid stars described by the modified **PNJL** model derived in this chapter and the possibility of describing the gluonic degrees of freedom by the modified Polyakov loop potential at $T = 0$. Therefore, we do not use the phenomenological parameter B^* in this Section. The effect of the T_0 parameter in the position of the deconfinement point ($\mu_B^{\rm dec}$) and the position of the chiral symmetry restoration point (μ_B^{χ}) is studied, and a value for T_0 is found in such a way that the transition from the hadronic **EoS** to the quark **EoS**, coincides with the confinement-deconfinement phase transition. We will use the hadronic **EoS** from the previous Sections.

We remark on the difference between the definition of deconfinement in the present Section from the definition used in the previous Chapters. Previously, deconfinement was defined as the change of degrees of freedom i.e., the change from a hadronic **EoS** to a quark **EoS**. In the present Section we still have this kind of phase transition but it will be called explicitly as the change from the hadronic **EoS** to a quark **EoS**. Deconfinement will be related to the spontaneous symmetry breaking of the $Z(3)$ symmetry, measured by the respective order parameter, the Polyakov loop.

We will impose $\beta-$equilibrium to describe neutron star matter and use the $SU_f(3)-$I parameter set (given in Table 5.5) alongside the usual parametrization of the Polyakov loop given in Equations (6.42) and (6.43). The parameter T_0 however, will be left free and its effect on the **EoS** will be studied. As we are only interested in understanding the effect of the modified Polyakov loop potential, we will not take into account vector interactions i.e., $G_\omega = G_\rho = G_V = 0$. The effect of the vector interactions in the **mPNJL** model is left for future work. The applicability of the **mPNJL** model is defined in the same way as the previous quark models (see Section 5.1.1).

We fix the *lattice* deconfinement temperature to $T_{lat}^{\rm dec} = 170$ MeV [86] and consider the $T_0 = 214, 210, 206, 202, 198$ MeV. From these values we extract the temperature scale T_τ and the fitting parameters η_2, η_4 and η_6. Results are presented in Table 6.2.

T_0[MeV]	T_τ[GeV]	η_2	$\eta_4 \times 10^6$	$\eta_6 \times 10^{11}$
214.00	2.127	0.313	2.43	1.58
210.00	2.087	0.325	2.62	1.77
206.00	2.045	0.338	2.83	1.99
202.00	2.008	0.351	3.06	2.24
198.00	1.968	0.366	3.32	2.53

TABLE 6.2: Different T_0 parameters and respective temperature scale T_τ and the fitting parameters η_2, η_4 and η_6 obatined by fixing $T_{lat}^{\rm dec} = 170$ MeV.

In Table 6.3 the type of chiral transition and confinement-deconfinement phase transition that the model undergoes at $\beta-$equilibrium, when the T_0 parameter decreases, is shown. From this Table, some remarks may be done: **a)** All transitions are first-order phase

T_0 [MeV]	Type$_\chi$	μ_B^χ [MeV]	Type$_{\rm dec}$	$\mu_B^{\rm dec}$ [MeV]
214	1^{st}- order	999	1^{st}- order	1201
210	1^{st}- order	999	1^{st}- order	1155
206	1^{st}- order	999	1^{st}- order	1109
202	1^{st}- order	999	1^{st}- order	1060
198	1^{st}- order	1003	1^{st}- order	983

TABLE 6.3: Type of the chiral symmetry phase transition and confinement-deconfinement phase transition and respective baryonic chemical potentials of phase transition (μ_B^χ and $\mu_B^{\rm dec}$, respectively).

transitions; **b)** The T_0 parameter does not influence the type of phase transition; **c)** Decreasing the value of T_0 makes the confinement-deconfinement closer to the chiral transition; **d)** The confinement-deconfinement phase transition always happens after the chiral symmetry restoration of the model, except when $T_0 = 198$ MeV. In this case the deconfinement phase transition occurs first.

The fact that the chiral symmetry restoration occurs before the confinement-deconfinement phase transition implies the existence of a quarkyonic phase which is confined, yet chirally symmetric [87] i.e., a phase of quark matter where chiral symmetry is restored but quarks

are still confined. With the decrease of the T_0 parameter, the range of existence of this phase shrinks but it does not disappear (at least until the deconfinement phase transition occurs before the chiral transition, e.g. $T_0 = 198$ MeV). In fact, it is not possible to find a T_0 parameter for which this phase does not exist, i.e., where the chiral symmetry restoration coincide exactly with the confinement-deconfinement phase transition ($\mu_B^{\chi} = \mu_B^{\rm dec}$). When the confinement-deconfinement phase transition approaches the chiral transition, a complicated behaviour takes place: instead of appearing only two stable phases of quark matter, one which is confined and chirally broken and one which is deconfined and chirally symmetric, other two intermediate phases appear. In the first of these intermediate phases, matter is deconfined and chirally broken and in the second, matter is chirally symmetric but confined. This non-trivial behaviour owes its existence to the unstable and metastable solutions of the Polyakov loop field, not being possible to make the chiral transition and confinement-deconfinement transition perfectly coincide in the present model. However, if the chiral transition were a *crossover*, coinciding the transitions might be possible. As we saw from Chapter 5, in the $SU_f(3)$ **NJL** model, the chiral transition is a *crossover* if we consider a positive G_V parameter. This is left for further work.

In Figure 6.5 we can see the behaviour of the Polyakov loop field versus the baryonic chemical potential in $\beta-$equilibrium. Comparing with Figure 6.2, where equal chemical potentials for each flavour of quark were considered, we see that the Polyakov loop in $\beta-$equilibrium has the same qualitative behaviour. The only exception, is when $T_0 = 198$ MeV, the case where the chiral transition occurs after the deconfinement and there is no quarkyonic (confined-chirally symmetric) phase.

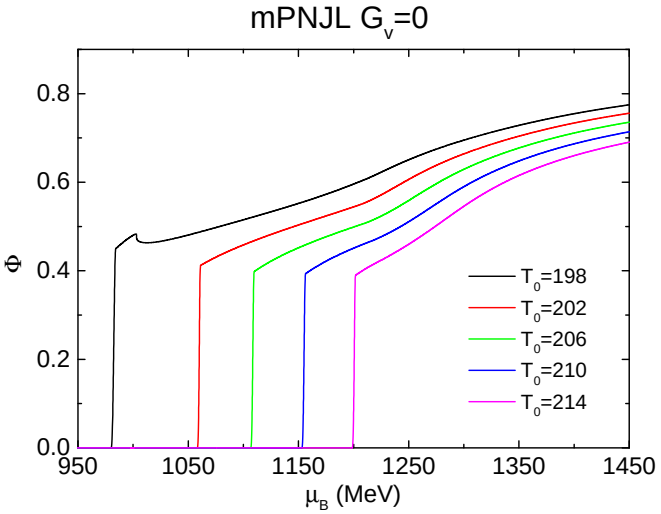

FIGURE 6.5: Polyakov loop field in $\beta-$equilibrium for several values of the T_0[MeV] parameter.

In Figure 6.6 the **EoS**, pressure versus density (left panel), and the mass/radius and mass/density plots (right panel) are presented. The light-grey and dark-grey bars represent again the mass constraint of the J0348+043 and J1614-2230 pulsars. The big dots correspond to the maximum mass configurations.

From the analysis of these figures some comments may be drawn: **a)** The T_0 parameter does not have a major influence in the central density of the star, but decreasing this parameter translates into increasing maximum star masses (see also Table 6.4); **b)** Decreasing the parameter T_0 makes the **EoS** a little harder; **c)** For $T_0 = 202$ MeV and $T_0 = 198$ MeV, the transition of the hadronic model to the quark model, occurs to a deconfined quark phase, i.e., we change from a hadronic **EoS** to a deconfined quark **EoS**.

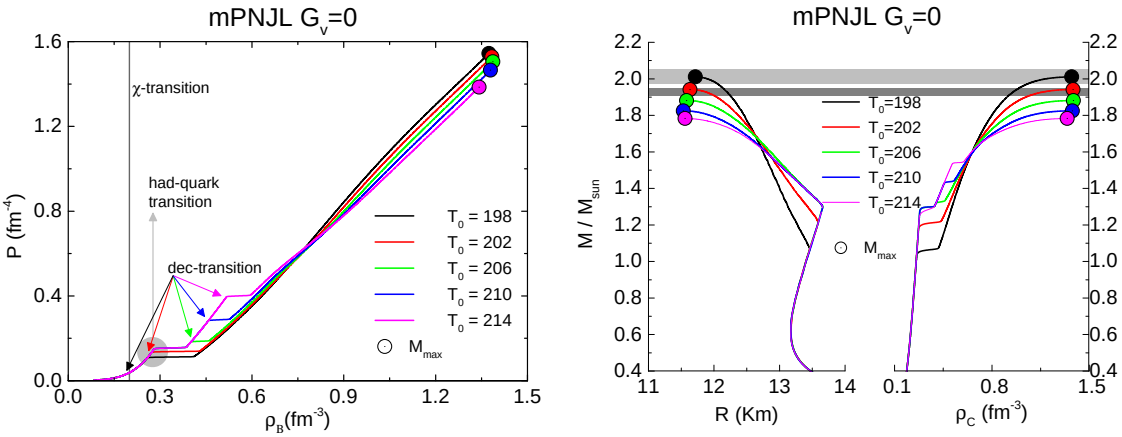

FIGURE 6.6: *Left panel*: equations of state, for each value of T_0[MeV], for the **mPNJL** model. The star maximum mass, central density, the chiral transition ($\chi-$transition), the hadronic-quark model transition (had-quark transition) and confinement-deconfinement phase transitions (dec-transition) are highlighted. *Right panel*: mass-radius and mass-central density diagrams for each value of T_0[MeV] for the **mPNJL** model. The star maximum mass, central density, hadronic-quark model transition and confinement-deconfinement transition are highlighted. The light-grey bar represents the mass constraint of the J0348+043 pulsar ($M = 2.01\pm0.04\ M_\odot$) while the dark-grey bar the J1614-2230 pulsar ($M = 1.928 \pm 0.017\ M_\odot$).

In Figure 6.7 the s, d and u quark fractions are plotted. Decreasing T_0 makes the onset of *strangeness* occur earlier, giving rise to stars with a larger *strangeness* content. This effect is due to the additional term in the quark densities, as a result of the modified Polyakov loop effective potential, as one can see in Equation (6.117). When $\Phi = 0$, the quark fractions are the same as the one in the **NJL** model. However, when $\Phi > 0$, the quark densities are changed due to a new term in Equation (6.117).

In Table 6.4 we present, for several values of T_0, the baryonic chemical potential (μ_B^t) of the transition between the hadronic **EoS** and quark **EoS**, baryonic density of the end of the hadronic phase (ρ^H), baryonic density of the beginning of the quark phase (ρ^Q), baryonic density of the end of the confined (ρ^{conf}) and beginning of the deconfined ρ^{dec}) phases. The respective values of central baryonic density (ρ^c), maximum gravitational mass (M_m), maximum baryonic mass (M_{bm}), radius (R_m) and fraction of *strangeness* (ρ_s/ρ_B).

From Table 6.4, several conclusions may be drawn: **a)** The baryonic chemical potential (μ_B^t) of the transition between the hadronic and quark model and the respective baryonic densities of transition (ρ^H and ρ^Q) are the same for $T_0 = 214, 210, 206$ MeV because the system changes from the hadronic **EoS** to the confined quark **EoS**, which is T_0 independent; **b)** The central density (ρ^c) and maximum radius (R_m) are almost T_0 independent; **c)** The

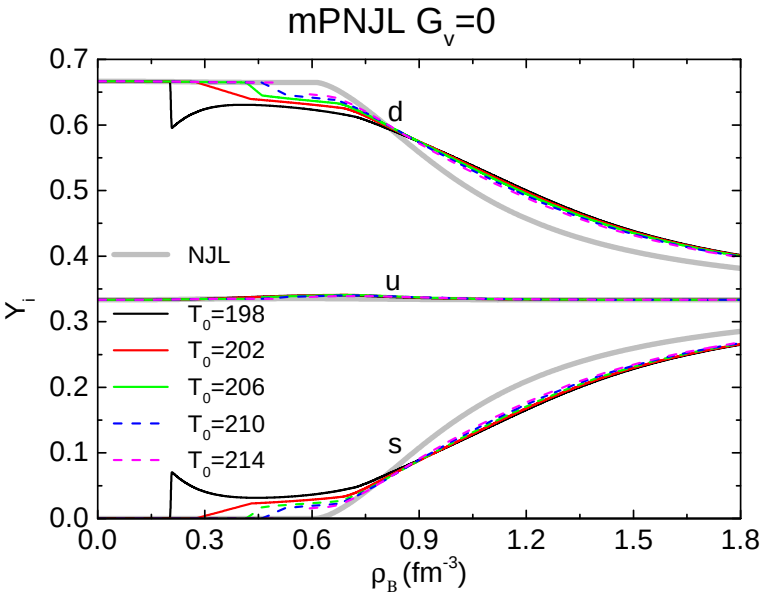

FIGURE 6.7: Fractions of each flavour of quark (Y_i) in function of the baryonic density (ρ_B) for several values of the T_0[MeV] parameter. The quark fraction for the usual $SU_f(3)$ **NJL** model is represented for comparisons purposes.

T_0 [MeV]	μ_B^t [MeV]	ρ^H [fm^{-3}]	ρ^Q [fm^{-3}]	ρ^{conf} [fm^{-3}]	ρ^{dec} [fm^{-3}]	ρ^c [fm^{-3}]	M_m [M$_\odot$]	M_{bm} [M$_\odot$]	R_m [km]	ρ_s/ρ_B [%]
214	1093	0.282	0.384	0.518	0.594	1.342	1.78	2.19	11.56	9.29
210	1093	0.282	0.384	0.459	0.526	1.379	1.82	2.33	11.53	10.90
206	1093	0.282	0.384	0.402	0.459	1.387	1.88	2.51	11.58	12.09
202	1081	0.274	0.429	0.274	0.429	1.384	1.94	2.70	11.64	13.19
198	1062	0.260	0.410	0.260	0.410	1.374	2.01	2.92	11.71	14.63

TABLE 6.4: T_0 parameter, baryonic chemical potential (μ_B^t) of the transition between the hadronic and quark model, baryonic density of the end of the hadronic phase (ρ^H), baryonic density of the beginning of the quark phase (ρ^Q), baryonic density of the end of the confined phase (ρ^{conf}) and baryonic density of the beginning of the deconfined phase (ρ^{dec}). Values of central baryonic density (ρ^c), maximum gravitational mass (M_m), maximum baryonic mass (M_{bm}), radius (R_m) and percentage of *strangeness* (ρ_s/ρ_B) of the respective neutron star for the **mPNJL** model.

maximum gravitational and baryonic masses and *strangeness* percentage, increases with decreasing T_0 since the onset of *strangeness* occurs earlier.

We look for the T_0 parameter for which the transition from the hadronic **EoS** to the quark **EoS** coincides exactly with the confinement-deconfinement phase transition i.e., $\mu_B^t = \mu_B^{\text{dec}}$, the transition from the hadronic **EoS** to the quark **EoS**[5] exactly coincides with the confinement-deconfinement phase transition related to the Polyakov loop and spontaneous breaking of the $Z(3)$ symmetry in the **mPNJL** model. In Table 6.5, this T_0 and respective temperature scale T_τ and fitting parameters (η_2, η_4 and η_6) are presented.

As previously stated, the type of chiral transition is T_0 independent, resulting in a first-order

[5]This phase transition corresponds to a change of degrees of freedom and respective Lagrangian (called deconfinement in Chapter 5).

$\mu_B^t = \mu_B^{\rm dec}$	T_0[MeV]	T_τ[GeV]	η_2	$\eta_4 \times 10^6$	$\eta_6 \times 10^{11}$
1093	204.65	2.034	0.342	2.91	2.07

TABLE 6.5: T_0 in which $\mu_B^t = \mu_B^{\rm dec}$ and respective temperature scale T_τ and the fitting parameters η_2, η_4 and η_6 obatined by fixing $T_{lat}^{\rm dec} = 170$ MeV.

phase transition. The confinement-deconfinement phase transition is also a first-order phase transition. The baryonic chemical potentials of each phase transition are presented in Table 6.6.

T_0 [MeV]	Type$_\chi$	μ_B^χ [MeV]	Type$_{\rm dec}$	$\mu_B^{\rm dec}$ [MeV]
204.65	1^{st}- order	999.24	1^{st}- order	1093

TABLE 6.6: T_0 in which $\mu_B^t = \mu_B^{\rm dec}$, type of chiral and confinement-deconfinement phase transitions and respective baryonic chemical potentials (μ_B^χ and $\mu_B^{\rm dec}$) in the **mPNJL** model.

As we can see from Table 6.6, the chiral transition has already occurred when the system changes from the hadronic **EoS** to the deconfined quark **EoS**. This means we have a transition from a hadronic **EoS** to a deconfined, chirally symmetric quark **EoS**.

In Table 6.7, we present the results from integrating the **TOV** equations for this choice of T_0. We stress the high fraction of *strangeness* in a star described by this **EoS**, as well as a gravitational mass, which is within the mass constraints given by the J0348+043 ($M = 2.01 \pm 0.04\ M_\odot$) and the J1614-2230 ($M = 1.928 \pm 0.017\ M_\odot$) pulsars.

T_0 [MeV]	μ_B^t [MeV]	ρ^H [fm^{-3}]	ρ^Q [fm^{-3}]	$\rho^{\rm conf}$ [fm^{-3}]	$\rho^{\rm dec}$ [fm^{-3}]	ρ^c [fm^{-3}]	M_m [M$_\odot$]	M_{bm} [M$_\odot$]	R_m [km]	ρ_s/ρ_B [%]
204.65	1093	0.282	0.437	0.282	0.437	1.383	1.90	2.58	11.62	12.43

TABLE 6.7: T_0 parameter in which $\mu_B^t = \mu_B^{\rm dec}$, baryonic chemical potential (μ_B^t) of the transition between the hadronic and quark model, baryonic density of the end of the hadronic phase (ρ^H), baryonic density of the beginning of the quark phase (ρ^Q), baryonic density of the end of the confined phase ($\rho^{\rm conf}$) and baryonic density of the beginning of the deconfined phase ($\rho^{\rm dec}$). Values of central baryonic density (ρ^c), maximum gravitational mass (M_m), maximum baryonic mass (M_{bm}), radius (R_m) and percentage of *strangeness* (ρ_s/ρ_B) of the respective neutron star for the **mPNJL** model.

Comparing the results for the usual $SU_f(3)$ **NJL** model with $G_V = 0$, without Bag constant presented in Table 6.8, with the results for the $SU_f(3)$ **mPNJL** (see Table 6.7), we can take some conclusions: **a)** By introducing gluonic degrees of freedom, the **mPNJL** predicts stable hybrid stars with larger masses (both gravitational and baryonic) and central densities; **b)** The fraction of *strangeness* is much larger for the **mPNJL** model than for the usual **NJL** model without Bag constant. This can be justified with the additional term in the quark density (see Equation (6.117)).

Model	G_V/G_S	B^* [MeV fm^{-3}]	μ_B^t [MeV]	ρ^H [fm^{-3}]	ρ^Q [fm^{-3}]	ρ^c [fm^{-3}]	M_m [M$_\odot$]	M_{bm} [M$_\odot$]	R_m [km]	ρ_s/ρ_B [%]
$SU_f(3)$ **NJL**	0.00	0	1093	0.282	0.384	0.951	1.76	2.00	11.91	1.32

TABLE 6.8: Baryonic chemical potential (μ_B^t), confinement baryonic density (ρ^H), deconfinement baryonic density (ρ^Q) and respective value of the added Bag constant (B^*). Values of central baryonic density (ρ^c), maximum gravitational mass (M_m), maximum baryonic mass (M_{bm}), radius (R_m) and percentage of *strangeness* (ρ_s/ρ_B) of the respective neutron star, for $G_V = 0$, for the $SU_f(3)$−I parameter set. Results taken from Table 5.8.

Chapter 7

Conclusions and Outlook

7.1 Conclusions

We have analyzed the possibility of obtaining hybrid stars with a quark core described within the $SU_f(2)$ and $SU_f(3)$ **NJL** and $SU_f(3)$ **mPNJL** models. Previous works showed that it was not possible to predict a pure quark matter core [9] but, in some conditions, it could be possible that non-homogeneous hadron-quark matter would exist in the center of the star. However, in [12, 13] a pure quark matter core was predicted if the **NJL** model **EoS** is determined in such a way that the hadron-quark deconfinement transition coincides with the **NJL** chiral symmetry restoration. This result shows that the use of a non-unified **EoS** to describe the hadron and quark matter should be considered with care and it is important to conciliate the properties of the hadron and the quark phase. In the present work besides considering the coincidence between the deconfinement phase transition and the chiral symmetry restoration, two new parametrizations of the $SU_f(2)$ and $SU_f(3)$ **NJL** models are proposed that satisfy the condition that the vacuum mass of three quarks equals the vacuum mass of a nucleon, as well as reproducing approximately the usual vacuum properties.

We have considered together with the usual scalar and pseudoscalar terms in the **NJL** model also vector-isoscalar and vector-isovector terms. The first ones have an important effect on the order of the chiral phase transition and turns the **EoS** harder: if $G_V/G_S \geq 0.25$ the chiral phase transition in $\beta-$equilibrium matter becomes a *crossover*. This, in fact, is also true for the vector-isovector model, although the **EoS** does not become so hard and smaller maximum mass configurations are obtained. A larger coupling G_V shifts the deconfinement to larger densities and gives rise to a smaller quark contribution to the hybrid star properties. If the $2M_\odot$ constraint is considered as defining acceptable hadronic models, **NJL** models should include vector-isoscalar terms. We also have considered the possibility of including both vector- isoscalar and isovector terms, having equal strength. This choice gives only indicative results and the relative strength in the vacuum could

be defined by experimental results, such as predicting correctly the mass of the ω and ρ mesons.

In the present work we have fixed the bag term B^* imposing that the deconfinement and chiral phase transitions coincide. Presently, it is still not clear if both phase transitions coincide, and other scenarios are possible, such as a chiral symmetry restoration occurs before the deconfinement is attained, giving rise to a quarkyonic phase like the one observed in the **mPNJL** model (see Section 6.6). Imposing different constraints on the B^* will have essentially quantitative effects, shifting the onset of quark matter and giving rise to a smaller or larger density jump at the first-order phase transition, but the qualitative features are similar to the ones discussed imposing the coincidence of the chiral and deconfinement transitions. The inclusion of gluonic degrees of freedom in the **mPNJL** model showed a similar behaviour to the **NJL** model with a Bag pressure B^* (with $G_V = 0$) and stable stars with quark cores were also obtained. This seems to indicate that the addition of a Bag constant is a phenomenological way of introducing the pressure of gluonic degrees of freedom when deconfinement occurs. However, introducing these degrees of freedom through the Polyakov loop potential hardens the **EoS** and gives rise to $2M_\odot$ stars even without vector terms.

The main conclusion of the present work is the importance of choosing conveniently the quark model and respective parameters when building a hadron-quark **EoS**. We have shown that fixing the vacuum quark constituent mass with a value that is one third of the vacuum nucleon mass allows the appearance of a pure quark core in the center of a neutron star. Choosing a strong enough coupling G_V will result in maximum mass configurations with masses above $2M_\odot$, if vector-isoscalar terms are considered. However, as in previous studies that have included the *strangeness* degree of freedom, the *strangeness* content of these stars is generally very small. However, using the **mPNJL** model, due to the additional term, the onset of *strangeness* happens at smaller densities which gives rise to larger fractions of *strange* quarks in stars.

7.2 Further work

Throughout the work several possible ideas for future investigations emerged.

A different approach to the calculation of the effective action instead of the **MFA**, like the 1-loop approximation or Functional Renormalization Group would give some insight on the importance on going beyond mean field theory.

Neutrons star have intense magnetic fields and their inclusion in the **PNJL** model is known to affect the chiral transition and pressure [88]. This way, it would be interesting to see the effect of magnetic fields on the hadronic-quark transition, as well as on the confinement-deconfinement phase transition in the **mPNJL** model.

Another way to improve the models would be to include pion condensation and color-superconductivity. Pion condensation is known to appear if the isospin chemical potential exceeds the mass of the pion [49].

One might try another regularization approach to the models. Avoiding the 3-momentum cut-off, allows the **NJL** model to bound baryons as chiral solitons or as quark-diquark structures [40]. One may calculate the nucleon mass and compare it with a the hadronic model and propose a parametrization which makes the nucleon mass from the **NJL** model equal to the hadronic model.

Regarding more technical aspects, as stated in Section 6.6, if the chiral transition in the **mPNJL** is a *crossover*, it may be possible to make this transition coincide with the confinement-deconfinement transition. As we saw from Chapter 5, in the $SU_f(3)$ **NJL** model, the chiral transition is a *crossover* if we consider a positive G_V parameter.

One should also test a different modified Polyakov loop effective potential based on the Stefan-Boltzmann pressure only, i.e. using Equation (6.83) alongside a different substitution of Equation (6.87),

$$\frac{T_0}{T} \to \frac{T_0}{\sqrt[4]{T^4 + \sum_f \left(\frac{18}{19\pi^2} T^2 \mu_f^2 + \frac{9}{19\pi^4} \mu_f^4\right)}}, \tag{7.1}$$

and compare with the results from this work.

The **mPNJL** model may improve some constraints on the hadronic model in the two-model approach used in this work. When making the transition between some hadronic model and the **mPNJL** coincide with the confinement-deconfinement transition of the **mPNJL**, the hadronic model may be constrained to make the hadron-quark transition happen for a T_0 parameter which, at zero chemical potential and finite temperature reproduces the *lattice* **QCD** results for the deconfinement temperature and chiral symmetry restoration.

Appendix A

Theorems

A.1 Noether's theorem

Noether's theorem states that every continuous global symmetries of the Lagrangian density gives rise to a conserved current $j^\mu(x)$ i.e.,

$$\partial_\mu j^\mu(x) = 0. \tag{A.1}$$

To prove this theorem we work infinitesimally (following the derivation made in [36]). First we derive the Euler-Lagrange equations of motion.

The equations of motion can be derived through the principle of least action:

$$\delta\mathcal{S}[\phi_a] = 0 \Rightarrow \delta\mathcal{S}[\phi_a] = \int d^4x \left[\frac{\partial\mathscr{L}}{\partial\phi_a}\delta\phi_a + \frac{\partial\mathscr{L}}{\partial\left(\partial_\mu\phi_a\right)}\partial_\mu\left(\delta\phi_a\right)\right] = \tag{A.2}$$

$$= \int d^4x \left\{\left[\frac{\partial\mathscr{L}}{\partial\phi_a} - \partial_\mu\frac{\partial\mathscr{L}}{\partial\left(\partial_\mu\phi_a\right)}\right]\delta\phi_a + \partial_\mu\left(\frac{\partial\mathscr{L}}{\partial\left(\partial_\mu\phi_a\right)}\delta\phi_a\right)\right\} = 0. \tag{A.3}$$

The last term is a total derivative and vanishes for any $\delta\phi_a(t,\boldsymbol{x})$ that goes to zero at spatial infinity and obeys $\delta\phi_a(t_1,\boldsymbol{x}) = \delta\phi_a(t_2,\boldsymbol{x}) = 0$. Requiring that $\delta\mathcal{S}[\phi_a] = 0$, yields the equations of motion for the fields ϕ_a,

$$\frac{\partial\mathscr{L}}{\partial\phi_a} - \partial_\mu\frac{\partial\mathscr{L}}{\partial\left(\partial_\mu\phi_a\right)} = 0. \tag{A.4}$$

Finally, to prove the theorem, we say that the transformation:

$$\delta\phi_a(x) = X_a\left(\phi\right), \tag{A.5}$$

is a symmetry if the Lagrangian density changes by a total derivative,

$$\delta\mathscr{L} = \partial_\mu F^\mu, \tag{A.6}$$

for some functions $F^\mu(\phi)$. We make an arbitrary transformation of the fields ϕ_a. Then:

$$\begin{aligned}\delta\mathscr{L} &= \frac{\partial\mathscr{L}}{\partial\phi_a}\delta\phi_a + \frac{\partial\mathscr{L}}{\partial\left(\partial_\mu\phi_a\right)}\partial_\mu\left(\delta\phi_a\right) = \\ &= \left[\frac{\partial\mathscr{L}}{\partial\phi_a} - \partial_\mu\frac{\partial\mathscr{L}}{\partial\left(\partial_\mu\phi_a\right)}\right]\delta\phi_a + \partial_\mu\left(\frac{\partial\mathscr{L}}{\partial\left(\partial_\mu\phi_a\right)}\delta\phi_a\right).\end{aligned} \tag{A.7}$$

When the Equations of motion (A.4) are satisfied, the first term vanishes. We are left with:

$$\delta\mathscr{L} = \partial_\mu\left(\frac{\partial\mathscr{L}}{\partial\left(\partial_\mu\phi_a\right)}\delta\phi_a\right). \tag{A.8}$$

For the symmetry transformation $\delta\phi_a = X_a\left(\phi\right)$, we have by definition $\delta\mathscr{L} = \partial_\mu F^\mu$. We can write:

$$\delta\mathscr{L} = \partial_\mu\left(\frac{\partial\mathscr{L}}{\partial\left(\partial_\mu\phi_a\right)}X_a\left(\phi\right)\right) = \partial_\mu F^\mu. \tag{A.9}$$

Which means we can write:

$$\partial_\mu\left(\frac{\partial\mathscr{L}}{\partial\left(\partial_\mu\phi_a\right)}X_a\left(\phi\right) - F^\mu\right) = 0. \tag{A.10}$$

Defining the current j^μ as:

$$j^\mu = \frac{\partial\mathscr{L}}{\partial\left(\partial_\mu\phi_a\right)}X_a\left(\phi\right) - F^\mu. \tag{A.11}$$

The current conservation follows from Equation (A.10):

$$\partial_\mu j^\mu(x) = 0. \tag{A.12}$$

Appendix B

Definitions and conventions

B.1 Dirac matrices

The Dirac matrices are defined as $\gamma^\mu = (\gamma^0, \boldsymbol{\gamma})$. They obey the anticommutation relations:

$$\{\gamma^\mu, \gamma^\nu\} = \gamma^\mu\gamma^\nu + \gamma^\nu\gamma^\mu = 2g_{\mu\nu}. \tag{B.1}$$

They have the following properties:

$$\left(\gamma^0\right)^\dagger = \gamma^0, \tag{B.2}$$

$$\left(\gamma^i\right)^\dagger = -\gamma^i, \tag{B.3}$$

$$\left(\gamma^0\right)^2 = \mathbb{1}_{4\times4}, \tag{B.4}$$

$$\left(\gamma^i\right)^2 = -\mathbb{1}_{4\times4}. \tag{B.5}$$

The γ_5 matrix, is defined as the product of the four gamma matrices as follows:

$$\gamma_5 \equiv i\gamma^0\gamma^1\gamma^2\gamma^3. \tag{B.6}$$

This matrix anticommutes with the other Dirac matrices:

$$\{\gamma_5, \gamma^\mu\} = \gamma_5\gamma^\mu + \gamma^\mu\gamma_5 = 0, \tag{B.7}$$

and it has the following properties:

$$(\gamma_5)^\dagger = \gamma_5, \tag{B.8}$$

$$(\gamma_5)^2 = \mathbb{1}_{4\times4}. \tag{B.9}$$

In the Dirac basis this matrices are given by:

$$\gamma^0 = \begin{pmatrix} \mathbb{1}_{2\times2} & 0 \\ 0 & -\mathbb{1}_{2\times2} \end{pmatrix}, \quad \gamma^i = \begin{pmatrix} 0 & \sigma^i \\ -\sigma^i & 0 \end{pmatrix}, \quad \gamma_5 = \begin{pmatrix} 0 & \mathbb{1}_{2\times2} \\ \mathbb{1}_{2\times2} & 0 \end{pmatrix}. \tag{B.10}$$

Here, σ^i are the three Pauli matrices of the $SU(2)$ group (see Appendix B.2).

B.2 $SU(N)$ and $U(N)$ matrices

We denote the matrices that form the algebra of the $SU(N)$ group by Γ^i. The matrices $\frac{1}{2}\Gamma^a$ are the generators of the $U(N)$ group and are normalized by:

$$\operatorname{tr} \Gamma^a \Gamma^b = 2\delta^{ab} \quad (a,b) = 1, 2, ..., N^2 - 1. \tag{B.11}$$

For $N = 2$ we have the three Pauli matrices of $SU(2)$:

$$\tau^1 = \begin{pmatrix} 0 & 1 \\ 1 & 0 \end{pmatrix}, \quad \tau^2 = \begin{pmatrix} 0 & -i \\ i & 0 \end{pmatrix}, \quad \tau^3 = \begin{pmatrix} 1 & 0 \\ 0 & -1 \end{pmatrix}. \tag{B.12}$$

The commutation relations for the $SU(2)$ algebra are

$$[\tau_a, \tau_b] = 2i\varepsilon_{abc}\, \tau_c. \tag{B.13}$$

The anticommutation relations are

$$\{\tau_a, \tau_b\} = 2\delta_{ab}\mathbb{1}. \tag{B.14}$$

For $N = 3$ we have the eight Gell-Mann matrices of $SU(3)$:

$$\lambda^1 = \begin{pmatrix} 0 & 1 & 0 \\ 1 & 0 & 0 \\ 0 & 0 & 0 \end{pmatrix}, \quad \lambda^2 = \begin{pmatrix} 0 & -i & 0 \\ i & 0 & 0 \\ 0 & 0 & 0 \end{pmatrix}, \tag{B.15}$$

$$\lambda^3 = \begin{pmatrix} 1 & 0 & 0 \\ 0 & -1 & 0 \\ 0 & 0 & 0 \end{pmatrix}, \quad \lambda^4 = \begin{pmatrix} 0 & 0 & 1 \\ 0 & 0 & 0 \\ 1 & 0 & 0 \end{pmatrix}, \quad \lambda_5 = \begin{pmatrix} 0 & 0 & -i \\ 0 & 0 & 0 \\ i & 0 & 0 \end{pmatrix}, \tag{B.16}$$

$$\lambda^6 = \begin{pmatrix} 0 & 0 & 0 \\ 0 & 0 & 1 \\ 0 & 1 & 0 \end{pmatrix}, \quad \lambda^7 = \begin{pmatrix} 0 & 0 & 0 \\ 0 & 0 & -i \\ 0 & i & 0 \end{pmatrix}, \quad \lambda^8 = \sqrt{\frac{1}{3}} \begin{pmatrix} 1 & 0 & 0 \\ 0 & 1 & 0 \\ 0 & 0 & -2 \end{pmatrix}. \tag{B.17}$$

The commutation relations for the $SU(3)$ algebra are

$$[\lambda_a, \lambda_b] = 2if_{abc}\lambda_c. \tag{B.18}$$

The anticommutation relations are

$$\{\lambda_a, \lambda_b\} = \frac{4}{3}\delta_{ab} + 2d_{abc}\lambda_c. \tag{B.19}$$

The antisymmetric structure constants f_{abc} are:

$$f_{123} = 1, \tag{B.20}$$

$$f_{147} = -f_{156} = f_{246} = f_{257} = f_{345} = -f_{367} = \frac{1}{2}, \tag{B.21}$$

$$f_{458} = f_{678} = \frac{\sqrt{3}}{2}. \tag{B.22}$$

while all other not related to these by permutation are zero. The symmetric structure constants d_{abc} are:

$$d_{118} = d_{228} = d_{338} = -d_{888} = \frac{1}{\sqrt{3}}, \tag{B.23}$$

$$d_{448} = d_{558} = d_{668} = d_{778} = -\frac{1}{2\sqrt{3}}, \tag{B.24}$$

$$d_{146} = d_{157} = -d_{247} = d_{256} = d_{344} = d_{355} = -d_{366} = -d_{377} = \frac{1}{2}. \tag{B.25}$$

Adding the identity to the $SU(N)$ algebra, $\Gamma^0 = \sqrt{2/N}\mathbb{1}$, we obtain the $U(N)$ algebra. In this case the commutators and anticommutators are:

$$[\Gamma_a, \Gamma_b] = 2if_{abc}\Gamma_c, \tag{B.26}$$

$$\{\Gamma_a, \Gamma_b\} = 2d_{abc}T_c. \tag{B.27}$$

Where the additional totally symmetric and totally antisymmetric structure constants are:

$$d_{0ab} = \sqrt{\frac{2}{N}}\delta_{ab} \quad \wedge \quad f_{0ab} = 0. \tag{B.28}$$

For $N = 2$, the additional τ^0 matrix is:

$$\tau^0 = \begin{pmatrix} 1 & 0 \\ 0 & 1 \end{pmatrix}, \tag{B.29}$$

while for $N = 3$ it is:

$$\lambda^0 = \sqrt{\frac{2}{3}} \begin{pmatrix} 1 & 0 & 0 \\ 0 & 1 & 0 \\ 0 & 0 & 1 \end{pmatrix}. \tag{B.30}$$

B.3 Polylogarithm function

The polylogarithm $\mathrm{Li}_n(z)$, is a function defined as:

$$\mathrm{Li}_n(z) = \sum_{k=1}^{\infty} \frac{z^k}{k^n}. \tag{B.31}$$

In the special case when $z = 1$, this function (B.31) reduces to the Riemann zeta function. These functions may arise in the closed form of the integrals of the Fermi-Dirac and Bose-Einstein distributions. Their integral representation can be written as:

$$\int_0^{+\infty} dx \frac{x^j}{e^{x-\mu} + 1} = -\Gamma(j+1)\,\mathrm{Li}_{(j+1)}\left(-e^{\mu}\right), \tag{B.32}$$

for the Fermi-Dirac case, and:

$$\int_0^{+\infty} dx \frac{x^j}{e^{x-\mu} - 1} = \Gamma(j+1)\,\mathrm{Li}_{(j+1)}\left(e^{\mu}\right), \tag{B.33}$$

for the Bose-Einstein case. Here, $\Gamma(n)$ is the gamma function, an extension of the factorial function, with its argument shifted by one, to real and complex numbers.

Appendix C

Auxiliary calculations

C.1 Product between two and three operators in the MFA

First we write an operator $\hat{\mathcal{O}}_i$ as its own expectation value, plus a small perturbation $\delta\hat{\mathcal{O}}_i$ around it:

$$\hat{\mathcal{O}}_i = \langle\hat{\mathcal{O}}_i\rangle + \left(\hat{\mathcal{O}}_i - \langle\hat{\mathcal{O}}_i\rangle\right) = \langle\hat{\mathcal{O}}_i\rangle + \delta\hat{\mathcal{O}}_i, \tag{C.1}$$

here, the perturbation is defined as:

$$\delta\mathcal{O}_i = \hat{\mathcal{O}}_i - \langle\hat{\mathcal{O}}_i\rangle\,. \tag{C.2}$$

The product between two operators in this approximation is:

$$\begin{aligned}\hat{\mathcal{O}}_i\hat{\mathcal{O}}_j &= \left(\langle\hat{\mathcal{O}}_i\rangle + \delta\hat{\mathcal{O}}_i\right)\left(\langle\hat{\mathcal{O}}_j\rangle + \delta\hat{\mathcal{O}}_j\right) = \\ &= \langle\hat{\mathcal{O}}_i\rangle\langle\hat{\mathcal{O}}_j\rangle + \langle\hat{\mathcal{O}}_i\rangle\delta\hat{\mathcal{O}}_j + \delta\hat{\mathcal{O}}_i\langle\hat{\mathcal{O}}_j\rangle + \delta\hat{\mathcal{O}}_i\delta\hat{\mathcal{O}}_j,\end{aligned} \tag{C.3}$$

we keep only linear terms on the perturbations, i.e., $\delta\hat{\mathcal{O}}_i\delta\hat{\mathcal{O}}_j \approx 0$. Writing the perturbation as in Equation (C.2), yields:

$$\begin{aligned}\hat{\mathcal{O}}_i\hat{\mathcal{O}}_j &\approx \langle\hat{\mathcal{O}}_i\rangle\langle\hat{\mathcal{O}}_j\rangle + \langle\hat{\mathcal{O}}_i\rangle\left(\hat{\mathcal{O}}_j - \langle\hat{\mathcal{O}}_j\rangle\right) + \left(\hat{\mathcal{O}}_i - \langle\hat{\mathcal{O}}_i\rangle\right)\langle\hat{\mathcal{O}}_j\rangle = \\ &= \langle\hat{\mathcal{O}}_i\rangle\langle\hat{\mathcal{O}}_j\rangle + \langle\hat{\mathcal{O}}_i\rangle\hat{\mathcal{O}}_j - \langle\hat{\mathcal{O}}_i\rangle\langle\hat{\mathcal{O}}_j\rangle + \hat{\mathcal{O}}_i\langle\hat{\mathcal{O}}_j\rangle - \langle\hat{\mathcal{O}}_i\rangle\langle\hat{\mathcal{O}}_j\rangle\,.\end{aligned} \tag{C.4}$$

This yields the **MFA** of the product between two operators:

$$\hat{\mathcal{O}}_i\hat{\mathcal{O}}_j \approx \langle\hat{\mathcal{O}}_i\rangle\hat{\mathcal{O}}_j + \hat{\mathcal{O}}_i\langle\hat{\mathcal{O}}_j\rangle - \langle\hat{\mathcal{O}}_i\rangle\langle\hat{\mathcal{O}}_j\rangle\,. \tag{C.5}$$

Within this approach, the product between three operators is:

$$\begin{aligned}\hat{\mathcal{O}}_i\hat{\mathcal{O}}_j\hat{\mathcal{O}}_k &= \left(\langle\hat{\mathcal{O}}_i\rangle + \delta\hat{\mathcal{O}}_i\right)\left(\langle\hat{\mathcal{O}}_j\rangle + \delta\hat{\mathcal{O}}_j\right)\left(\langle\hat{\mathcal{O}}_k\rangle + \delta\hat{\mathcal{O}}_k\right) = \\ &= \left(\langle\hat{\mathcal{O}}_i\rangle\langle\hat{\mathcal{O}}_j\rangle + \langle\hat{\mathcal{O}}_i\rangle\delta\hat{\mathcal{O}}_j + \delta\hat{\mathcal{O}}_i\langle\hat{\mathcal{O}}_j\rangle + \delta\hat{\mathcal{O}}_i\delta\hat{\mathcal{O}}_j\right)\left(\langle\hat{\mathcal{O}}_k\rangle + \delta\hat{\mathcal{O}}_k\right) = \\ &= \langle\hat{\mathcal{O}}_i\rangle\langle\hat{\mathcal{O}}_j\rangle\langle\hat{\mathcal{O}}_k\rangle + \langle\hat{\mathcal{O}}_i\rangle\delta\hat{\mathcal{O}}_j\langle\hat{\mathcal{O}}_k\rangle + \delta\hat{\mathcal{O}}_i\langle\hat{\mathcal{O}}_j\rangle\langle\hat{\mathcal{O}}_k\rangle + \langle\hat{\mathcal{O}}_i\rangle\langle\hat{\mathcal{O}}_j\rangle\delta\hat{\mathcal{O}}_k \\ &\quad + \delta\hat{\mathcal{O}}_i\delta\hat{\mathcal{O}}_j\langle\hat{\mathcal{O}}_k\rangle + \langle\hat{\mathcal{O}}\rangle_i\delta\hat{\mathcal{O}}_j\delta\hat{\mathcal{O}}_k + \delta\hat{\mathcal{O}}_i\langle\hat{\mathcal{O}}\rangle_j\delta\hat{\mathcal{O}}_k + \delta\hat{\mathcal{O}}_i\delta\hat{\mathcal{O}}_j\delta\hat{\mathcal{O}}_k. \end{aligned} \tag{C.6}$$

Once again, keeping only terms linear in perturbation, and using Equation (C.2) yields:

$$\begin{aligned}\hat{\mathcal{O}}_i\hat{\mathcal{O}}_j\hat{\mathcal{O}}_k &\approx \langle\hat{\mathcal{O}}_i\rangle\langle\hat{\mathcal{O}}_j\rangle\langle\hat{\mathcal{O}}_k\rangle + \langle\hat{\mathcal{O}}_i\rangle\delta\hat{\mathcal{O}}_j\langle\hat{\mathcal{O}}_k\rangle + \delta\hat{\mathcal{O}}_i\langle\hat{\mathcal{O}}_j\rangle\langle\hat{\mathcal{O}}_k\rangle + \langle\hat{\mathcal{O}}_i\rangle\langle\hat{\mathcal{O}}_j\rangle\delta\hat{\mathcal{O}}_k \\ &= \langle\hat{\mathcal{O}}_i\rangle\langle\hat{\mathcal{O}}_j\rangle\langle\hat{\mathcal{O}}_k\rangle + \langle\hat{\mathcal{O}}_i\rangle\langle\hat{\mathcal{O}}_j\rangle\hat{\mathcal{O}}_k - \langle\hat{\mathcal{O}}_i\rangle\langle\hat{\mathcal{O}}_j\rangle\langle\hat{\mathcal{O}}_k\rangle + \langle\hat{\mathcal{O}}_i\rangle\hat{\mathcal{O}}_j\langle\hat{\mathcal{O}}_k\rangle \\ &\quad - \langle\hat{\mathcal{O}}_i\rangle\langle\hat{\mathcal{O}}_j\rangle\langle\hat{\mathcal{O}}_k\rangle + \hat{\mathcal{O}}_i\langle\hat{\mathcal{O}}_j\rangle\langle\hat{\mathcal{O}}_k\rangle - \langle\hat{\mathcal{O}}_i\rangle\langle\hat{\mathcal{O}}_j\rangle\langle\hat{\mathcal{O}}_k\rangle. \end{aligned} \tag{C.7}$$

The product between three operators in the **MFA** approximation is finally given by:

$$\hat{\mathcal{O}}_i\hat{\mathcal{O}}_j\hat{\mathcal{O}}_k \approx \hat{\mathcal{O}}_i\langle\hat{\mathcal{O}}_j\rangle\langle\hat{\mathcal{O}}_k\rangle + \langle\hat{\mathcal{O}}_i\rangle\hat{\mathcal{O}}_j\langle\hat{\mathcal{O}}_k\rangle + \langle\hat{\mathcal{O}}_i\rangle\langle\hat{\mathcal{O}}_j\rangle\hat{\mathcal{O}}_k - 2\langle\hat{\mathcal{O}}_i\rangle\langle\hat{\mathcal{O}}_j\rangle\langle\hat{\mathcal{O}}_k\rangle. \tag{C.8}$$

C.2 't Hooft determinant in $SU_f(2)$

The 't Hooft determinant for two flavours of quarks can be written as:

$$\mathscr{L}^{det} = G_D\left(\det_f\left[\overline{\psi}\left(1+\gamma_5\right)\psi\right] + \det_f\left[\overline{\psi}\left(1-\gamma_5\right)\psi\right]\right), \tag{C.9}$$

where $\psi^T = (\psi_u \;\; \psi_d)$:

$$\begin{aligned}\det_f \overline{\psi}\mathcal{O}\psi &\equiv \sum_{i,j}\varepsilon_{ij}\left(\overline{\psi}_u\mathcal{O}\psi_i\right)\left(\overline{\psi}_d\mathcal{O}\psi_j\right) \\ &= \varepsilon_{11}\left(\overline{\psi}_1\mathcal{O}\psi_1\right)\left(\overline{\psi}_2\mathcal{O}\psi_1\right) + \varepsilon_{21}\left(\overline{\psi}_1\mathcal{O}\psi_2\right)\left(\overline{\psi}_2\mathcal{O}\psi_1\right) \\ &\quad + \varepsilon_{12}\left(\overline{\psi}_1\mathcal{O}\psi_1\right)\left(\overline{\psi}_2\mathcal{O}\psi_2\right) + \varepsilon_{22}\left(\overline{\psi}_1\mathcal{O}\psi_2\right)\left(\overline{\psi}_2\mathcal{O}\psi_2\right). \end{aligned} \tag{C.10}$$

Here we made the following correspondence $u = 1$ and $d = 2$. Using the definition of the two-dimensional Levi-Civita symbol:

$$\varepsilon_{ij} = \begin{cases} +1 & \text{if } (i,j) \text{ is } (1,2), \\ -1 & \text{if } (i,j) \text{ is } (2,1), \\ \;\;0 & \text{if } i = j \end{cases} \tag{C.11}$$

we can write Equation (C.10) as:

$$\det_f \overline{\psi}\mathcal{O}\psi = \left(\overline{\psi}_u\mathcal{O}\psi_u\right)\left(\overline{\psi}_d\mathcal{O}\psi_d\right) - \left(\overline{\psi}_u\mathcal{O}\psi_d\right)\left(\overline{\psi}_d\mathcal{O}\psi_u\right). \tag{C.12}$$

Substituting $\mathcal{O} = (1 \pm \gamma_5)$, we can write the 't Hooft determinant as:

$$\begin{aligned}\mathscr{L}^{det} =& 2G_D \left[\left(\overline{\psi}_u \psi_u\right) \left(\overline{\psi}_d \psi_d\right) + \left(\overline{\psi}_u \gamma_5 \psi_u\right) \left(\overline{\psi}_d \gamma_5 \psi_d\right) \right. && \text{(C.13)} \\ & \left. - \left(\overline{\psi}_u \psi_d\right) \left(\overline{\psi}_d \psi_u\right) - \left(\overline{\psi}_u \gamma_5 \psi_d\right) \left(\overline{\psi}_d \gamma_5 \psi_u\right) \right]. && \text{(C.14)}\end{aligned}$$

Using the three Pauli matrices of $SU(2)$ and the identity matrix (Appendix B.2), we can write [89]:

$$\begin{aligned}\overline{\psi}\tau^0 \mathcal{O}\psi &= \overline{\psi}_u \mathcal{O}\psi_u + \overline{\psi}_d \mathcal{O}\psi_d, && \text{(C.15)} \\ \overline{\psi}\tau^1 \mathcal{O}\psi &= \overline{\psi}_u \mathcal{O}\psi_d + \overline{\psi}_d \mathcal{O}\psi_u, && \text{(C.16)} \\ \overline{\psi}\tau^2 \mathcal{O}\psi &= -i \left(\overline{\psi}_u \mathcal{O}\psi_d - \overline{\psi}_d \mathcal{O}\psi_u\right), && \text{(C.17)} \\ \overline{\psi}\tau^3 \mathcal{O}\psi &= \overline{\psi}_u \mathcal{O}\psi_u - \overline{\psi}_d \mathcal{O}\psi_d. && \text{(C.18)}\end{aligned}$$

Squaring the equations above gives:

$$\begin{aligned}\left(\overline{\psi}\tau^0 \mathcal{O}\psi\right)^2 &= \left(\overline{\psi}_u \mathcal{O}\psi_u\right)^2 + 2\left(\overline{\psi}_u \mathcal{O}\psi_u\right)\left(\overline{\psi}_d \mathcal{O}\psi_d\right) + \left(\overline{\psi}_d \mathcal{O}\psi_d\right)^2, && \text{(C.19)} \\ \left(\overline{\psi}\tau^1 \mathcal{O}\psi\right)^2 &= \left(\overline{\psi}_u \mathcal{O}\psi_d\right)^2 + 2\left(\overline{\psi}_u \mathcal{O}\psi_d\right)\left(\overline{\psi}_d \mathcal{O}\psi_u\right) + \left(\overline{\psi}_d \mathcal{O}\psi_u\right)^2, && \text{(C.20)} \\ \left(\overline{\psi}\tau^2 \mathcal{O}\psi\right)^2 &= -\left(\overline{\psi}_u \mathcal{O}\psi_d\right)^2 + 2\left(\overline{\psi}_u \mathcal{O}\psi_d\right)\left(\overline{\psi}_d \mathcal{O}\psi_u\right) - \left(\overline{\psi}_d \mathcal{O}\psi_u\right)^2, && \text{(C.21)} \\ \left(\overline{\psi}\tau^3 \mathcal{O}\psi\right)^2 &= \left(\overline{\psi}_u \mathcal{O}\psi_u\right)^2 - 2\left(\overline{\psi}_u \mathcal{O}\psi_u\right)\left(\overline{\psi}_d \mathcal{O}\psi_d\right) + \left(\overline{\psi}_d \mathcal{O}\psi_d\right)^2. && \text{(C.22)}\end{aligned}$$

Writing $\mathcal{O} = \mathbb{1}$ and $\mathcal{O} = i\gamma_5$, we can write the following equality:

$$\begin{aligned}&\frac{G_D}{2}\left\{\left(\overline{\psi}\tau^0\psi\right)^2 - \left(\overline{\psi}i\gamma_5\tau^0\psi\right)^2 - \sum_{i=1}^{3}\left[\left(\overline{\psi}\tau^i\psi\right)^2 - \left(\overline{\psi}i\gamma_5\tau^i\psi\right)^2\right]\right\} = \\ &\qquad = 2G_D\left[\left(\overline{\psi}_u\psi_u\right)\left(\overline{\psi}_d\psi_d\right) + \left(\overline{\psi}_u\gamma_5\psi_u\right)\left(\overline{\psi}_d\gamma_5\psi_d\right)\right. \\ &\qquad\quad \left. - \left(\overline{\psi}_u\psi_d\right)\left(\overline{\psi}_d\psi_u\right) - \left(\overline{\psi}_u\gamma_5\psi_d\right)\left(\overline{\psi}_d\gamma_5\psi_u\right)\right] = \mathscr{L}^{det}. \qquad \text{(C.23)}\end{aligned}$$

This means we can write the 't Hooft determinant in $SU_f(2)$ given by Equation (C.9), as:

$$\mathscr{L}^{det} = \frac{G_D}{2}\left\{\left(\overline{\psi}\tau^0\psi\right)^2 - \left(\overline{\psi}i\gamma_5\tau^0\psi\right)^2 - \sum_{i=1}^{3}\left[\left(\overline{\psi}\tau^i\psi\right)^2 - \left(\overline{\psi}i\gamma_5\tau^i\psi\right)^2\right]\right\}. \qquad \text{(C.24)}$$

C.3 't Hooft determinant in the MFA (two and three flavours)

In this section, we calculate the 't Hooft determinant in the **MFA**, for two and three flavours of quarks.

C.3.1 Two flavours

The 't Hooft determinant for two flavours can be calculated through:

$$\det_f \overline{\psi}\mathcal{O}\psi \equiv \sum_{i,j} \varepsilon_{ij} \left(\overline{\psi}_u \mathcal{O}\psi_i\right)\left(\overline{\psi}_d \mathcal{O}\psi_j\right). \tag{C.25}$$

Using the **MFA** of the product between two operators (C.5), one can write:

$$\begin{aligned}\det_f \overline{\psi}\mathcal{O}\psi \approx \sum_{i,j} \varepsilon_{ij} \Big[&\left(\overline{\psi}_u \mathcal{O}\psi_i\right)\langle\overline{\psi}_d \mathcal{O}\psi_j\rangle + \langle\overline{\psi}_u \mathcal{O}\psi_i\rangle\left(\overline{\psi}_d \mathcal{O}\psi_j\right) - \langle\overline{\psi}_u \mathcal{O}\psi_i\rangle\langle\overline{\psi}_d \mathcal{O}\psi_j\rangle\Big] = \\ = &\left(\overline{\psi}_u \mathcal{O}\psi_u\right)\langle\overline{\psi}_d \mathcal{O}\psi_d\rangle - \left(\overline{\psi}_u \mathcal{O}\psi_d\right)\langle\overline{\psi}_d \mathcal{O}\psi_u\rangle \\ &+ \langle\overline{\psi}_u \mathcal{O}\psi_u\rangle\left(\overline{\psi}_d \mathcal{O}\psi_d\right) - \langle\overline{\psi}_u \mathcal{O}\psi_d\rangle\left(\overline{\psi}_d \mathcal{O}\psi_u\right) \\ &- \langle\overline{\psi}_u \mathcal{O}\psi_u\rangle\langle\overline{\psi}_d \mathcal{O}\psi_d\rangle + \langle\overline{\psi}_u \mathcal{O}\psi_d\rangle\langle\overline{\psi}_d \mathcal{O}\psi_u\rangle.\end{aligned} \tag{C.26}$$

Only condensates who will have a non-vanishing **VEV** (in our approximation) will contribute, i.e., we consider:

$$\langle\overline{\psi}_i \psi_j\rangle = \langle\overline{\psi}_i \psi_i\rangle \delta_{ij}, \tag{C.27}$$

$$\langle\overline{\psi}_i \gamma_5 \psi_j\rangle = 0. \tag{C.28}$$

Inserting the operator $\mathcal{O} = 1 \pm \gamma_5$ and taking only non-vanishing condensates, the 't Hooft determinant for two flavours is:

$$\begin{aligned}\mathscr{L}^{det} &= G_D\left(\det_f\left[\overline{\psi}\left(1+\gamma_5\right)\psi\right] + \det_f\left[\overline{\psi}\left(1-\gamma_5\right)\psi\right]\right) \approx \\ &\approx 2G_D\left[\left(\overline{\psi}_u\psi_u\right)\langle\overline{\psi}_d\psi_d\rangle + \langle\overline{\psi}_u\psi_u\rangle\left(\overline{\psi}_d\psi_d\right) - \langle\overline{\psi}_u\psi_u\rangle\langle\overline{\psi}_d\psi_d\rangle\right].\end{aligned} \tag{C.29}$$

C.3.2 Three flavours

The 't Hooft determinant for two flavours can be calculated through:

$$\det_f \overline{\psi}\mathcal{O}\psi \equiv \sum_{i,j,k} \varepsilon_{ijk} \left(\overline{\psi}_u \mathcal{O}\psi_i\right)\left(\overline{\psi}_d \mathcal{O}\psi_j\right)\left(\overline{\psi}_s \mathcal{O}\psi_k\right). \tag{C.30}$$

Using the **MFA** of the product between two operators (C.5), one can write:

$$\begin{aligned}\det_f \overline{\psi}\mathcal{O}\psi \approx \sum_{i,j,k} \varepsilon_{ijk} \Big[&\left(\overline{\psi}_u \mathcal{O}\psi_i\right)\langle\overline{\psi}_d \mathcal{O}\psi_j\rangle\langle\overline{\psi}_s \mathcal{O}\psi_k\rangle + \langle\overline{\psi}_u \mathcal{O}\psi_i\rangle\left(\overline{\psi}_d \mathcal{O}\psi_j\right)\langle\overline{\psi}_s \mathcal{O}\psi_k\rangle \\ &+ \langle\overline{\psi}_u \mathcal{O}\psi_i\rangle\langle\overline{\psi}_d \mathcal{O}\psi_j\rangle\left(\overline{\psi}_s \mathcal{O}\psi_k\right) - 2\langle\overline{\psi}_u \mathcal{O}\psi_i\rangle\langle\overline{\psi}_d \mathcal{O}\psi_j\rangle\langle\overline{\psi}_s \mathcal{O}\psi_k\rangle\Big].\end{aligned} \tag{C.31}$$

The Levi-Civita symbol in three dimensions is defined as:

$$\varepsilon_{ijk} = \begin{cases} +1 & \text{if } (i,j,k) \text{ is } (1,2,3),(2,3,1) \text{ or } (3,1,2), \\ -1 & \text{if } (i,j,k) \text{ is } (3,2,1),(1,3,2) \text{ or } (2,1,3), \\ 0 & \text{if } i=j \text{ or } j=k \text{ or } k=i. \end{cases} \tag{C.32}$$

Let's calculate every term individually (we make the following correspondence $u=1$, $d=2$, $s=3$):

$$\begin{aligned} \sum_{i,j,k} \varepsilon_{ijk} \left(\overline{\psi}_u \mathcal{O} \psi_i\right) \langle \overline{\psi}_d \mathcal{O} \psi_j \rangle \langle \overline{\psi}_s \mathcal{O} \psi_k \rangle = \\ = \left(\overline{\psi}_u \mathcal{O} \psi_u\right) \left[\langle \overline{\psi}_d \mathcal{O} \psi_d \rangle \langle \overline{\psi}_s \mathcal{O} \psi_s \rangle - \langle \overline{\psi}_d \mathcal{O} \psi_s \rangle \langle \overline{\psi}_s \mathcal{O} \psi_d \rangle\right] \\ + \left(\overline{\psi}_u \mathcal{O} \psi_d\right) \left[\langle \overline{\psi}_d \mathcal{O} \psi_s \rangle \langle \overline{\psi}_s \mathcal{O} \psi_u \rangle - \langle \overline{\psi}_d \mathcal{O} \psi_u \rangle \langle \overline{\psi}_s \mathcal{O} \psi_s \rangle\right] \\ + \left(\overline{\psi}_u \mathcal{O} \psi_s\right) \left[\langle \overline{\psi}_d \mathcal{O} \psi_u \rangle \langle \overline{\psi}_s \mathcal{O} \psi_d \rangle - \langle \overline{\psi}_d \mathcal{O} \psi_d \rangle \langle \overline{\psi}_s \mathcal{O} \psi_u \rangle\right]. \end{aligned} \tag{C.33}$$

$$\begin{aligned} \sum_{i,j,k} \varepsilon_{ijk} \langle \overline{\psi}_u \mathcal{O} \psi_i \rangle \left(\overline{\psi}_d \mathcal{O} \psi_j\right) \langle \overline{\psi}_s \mathcal{O} \psi_k \rangle = \\ = \left(\overline{\psi}_d \mathcal{O} \psi_u\right) \left[\langle \overline{\psi}_u \mathcal{O} \psi_s \rangle \langle \overline{\psi}_s \mathcal{O} \psi_d \rangle - \langle \overline{\psi}_u \mathcal{O} \psi_d \rangle \langle \overline{\psi}_s \mathcal{O} \psi_s \rangle\right] \\ + \left(\overline{\psi}_d \mathcal{O} \psi_d\right) \left[\langle \overline{\psi}_u \mathcal{O} \psi_u \rangle \langle \overline{\psi}_s \mathcal{O} \psi_s \rangle - \langle \overline{\psi}_u \mathcal{O} \psi_s \rangle \langle \overline{\psi}_s \mathcal{O} \psi_u \rangle\right] \\ + \left(\overline{\psi}_d \mathcal{O} \psi_s\right) \left[\langle \overline{\psi}_u \mathcal{O} \psi_d \rangle \langle \overline{\psi}_s \mathcal{O} \psi_u \rangle - \langle \overline{\psi}_u \mathcal{O} \psi_u \rangle \langle \overline{\psi}_s \mathcal{O} \psi_d \rangle\right]. \end{aligned} \tag{C.34}$$

$$\begin{aligned} \sum_{i,j,k} \varepsilon_{ijk} \langle \overline{\psi}_u \mathcal{O} \psi_i \rangle \langle \overline{\psi}_d \mathcal{O} \psi_j \rangle \left(\overline{\psi}_s \mathcal{O} \psi_k\right) = \\ = \left(\overline{\psi}_s \mathcal{O} \psi_u\right) \left[\langle \overline{\psi}_u \mathcal{O} \psi_d \rangle \langle \overline{\psi}_d \mathcal{O} \psi_s \rangle - \langle \overline{\psi}_u \mathcal{O} \psi_s \rangle \langle \overline{\psi}_d \mathcal{O} \psi_d \rangle\right] \\ + \left(\overline{\psi}_s \mathcal{O} \psi_d\right) \left[\langle \overline{\psi}_u \mathcal{O} \psi_s \rangle \langle \overline{\psi}_d \mathcal{O} \psi_u \rangle - \langle \overline{\psi}_u \mathcal{O} \psi_u \rangle \langle \overline{\psi}_d \mathcal{O} \psi_s \rangle\right] \\ + \left(\overline{\psi}_s \mathcal{O} \psi_s\right) \left[\langle \overline{\psi}_u \mathcal{O} \psi_u \rangle \langle \overline{\psi}_d \mathcal{O} \psi_d \rangle - \langle \overline{\psi}_u \mathcal{O} \psi_d \rangle \langle \overline{\psi}_d \mathcal{O} \psi_u \rangle\right]. \end{aligned} \tag{C.35}$$

$$\begin{aligned} \sum_{i,j,k} \varepsilon_{ijk} \langle \overline{\psi}_u \mathcal{O} \psi_i \rangle \langle \overline{\psi}_d \mathcal{O} \psi_j \rangle \langle \overline{\psi}_s \mathcal{O} \psi_k \rangle = \\ = \langle \overline{\psi}_u \mathcal{O} \psi_u \rangle \left[\langle \overline{\psi}_d \mathcal{O} \psi_d \rangle \langle \overline{\psi}_s \mathcal{O} \psi_s \rangle - \langle \overline{\psi}_d \mathcal{O} \psi_s \rangle \langle \overline{\psi}_s \mathcal{O} \psi_d \rangle\right] \\ + \langle \overline{\psi}_u \mathcal{O} \psi_d \rangle \left[\langle \overline{\psi}_d \mathcal{O} \psi_s \rangle \langle \overline{\psi}_s \mathcal{O} \psi_u \rangle - \langle \overline{\psi}_d \mathcal{O} \psi_u \rangle \langle \overline{\psi}_s \mathcal{O} \psi_s \rangle\right] \\ + \langle \overline{\psi}_u \mathcal{O} \psi_s \rangle \left[\langle \overline{\psi}_d \mathcal{O} \psi_u \rangle \langle \overline{\psi}_s \mathcal{O} \psi_d \rangle - \langle \overline{\psi}_d \mathcal{O} \psi_d \rangle \langle \overline{\psi}_s \mathcal{O} \psi_u \rangle\right]. \end{aligned} \tag{C.36}$$

Only condensates who will have a non-vanishing **VEV** (in our approximation) will contribute, i.e., we consider:

$$\langle \overline{\psi}_i \psi_j \rangle = \langle \overline{\psi}_i \psi_i \rangle \, \delta_{ij}, \tag{C.37}$$

$$\langle \overline{\psi}_i \gamma_5 \psi_j \rangle = 0. \tag{C.38}$$

Inserting the operator $\mathcal{O} = 1 \pm \gamma_5$ and taking only non-vanishing condensates, the 't Hooft determinant for two flavours is:

$$\mathscr{L}^{det} \approx -2G_D \left[\left(\overline{\psi}_u\psi_u\right) \langle\overline{\psi}_d\psi_d\rangle \langle\overline{\psi}_s\psi_s\rangle + \langle\overline{\psi}_u\psi_u\rangle \left(\overline{\psi}_d\psi_d\right) \langle\overline{\psi}_s\psi_s\rangle \right.$$
$$\left. - \langle\overline{\psi}_u\psi_u\rangle \langle\overline{\psi}_d\psi_d\rangle \left(\overline{\psi}_s\psi_s\right) - 2 \langle\overline{\psi}_u\psi_u\rangle \langle\overline{\psi}_d\psi_d\rangle \langle\overline{\psi}_s\psi_s\rangle \right]. \tag{C.39}$$

C.4 *Gap* equations

C.4.1 NJL model in $SU_f(2)$

The *gap* equations of the two flavour **NJL** model can be found by using Equation (3.60):

$$\frac{\partial\Omega_{\text{MFA}}}{\partial\sigma_u} = \frac{\partial\Omega_{\text{MFA}}}{\partial\sigma_d} = 0, \tag{C.40}$$

which defines the values of the quark condensates σ_u and σ_d. The grand canonical potential of this model is given by Equation (3.59):

$$\Omega_{\text{MFA}} = \Omega_0 + 2G_S\left(\sigma_u^2 + \sigma_d^2\right) + 2G_D\sigma_u\sigma_d - G_\omega\left(\rho_u + \rho_d\right)^2 - G_\rho\left(\rho_u - \rho_d\right)^2$$
$$- 2T\ N_c \sum_{f=u,d} \int \frac{d^3p}{(2\pi)^3} \left[\beta E_f + \ln\left(1 + e^{-\beta\left(E_f + \tilde{\mu}_f\right)}\right) + \ln\left(1 + e^{-\beta\left(E_f - \tilde{\mu}_f\right)}\right)\right]. \tag{C.41}$$

And, the effective mass is (Equation (3.61)):

$$M_i = m_i - 4G_S\sigma_i - 2G_D\sigma_j, \quad i \neq j \in \{u, d\}. \tag{C.42}$$

Using Equation (C.40) one can write:

$$\frac{\partial\Omega_{\text{MFA}}}{\partial\sigma_u} = \frac{\partial\Omega_{\text{MFA}}}{\partial\sigma_u} + \frac{\partial\Omega_{\text{MFA}}}{\partial M_i}\frac{\partial M_i}{\partial\sigma_u} = \frac{\partial\Omega_{\text{MFA}}}{\partial\sigma_u} + \frac{\partial\Omega_{\text{MFA}}}{\partial M_u}\frac{\partial M_u}{\partial\sigma_u} + \frac{\partial\Omega_{\text{MFA}}}{\partial M_d}\frac{\partial M_d}{\partial\sigma_u} = 0, \tag{C.43}$$
$$\frac{\partial\Omega_{\text{MFA}}}{\partial\sigma_d} = \frac{\partial\Omega_{\text{MFA}}}{\partial\sigma_d} + \frac{\partial\Omega_{\text{MFA}}}{\partial M_i}\frac{\partial M_i}{\partial\sigma_d} = \frac{\partial\Omega_{\text{MFA}}}{\partial\sigma_d} + \frac{\partial\Omega_{\text{MFA}}}{\partial M_u}\frac{\partial M_u}{\partial\sigma_d} + \frac{\partial\Omega_{\text{MFA}}}{\partial M_d}\frac{\partial M_d}{\partial\sigma_d} = 0. \tag{C.44}$$

Using Equations (C.41) and (C.42), for the *up* quark, each term yields:

$$\frac{\partial\Omega_{\text{MFA}}}{\partial\sigma_u} = 4G_S\sigma_u + 2G_D\sigma_d, \tag{C.45}$$
$$\frac{\partial M_u}{\partial\sigma_u} = -4G_S, \tag{C.46}$$
$$\frac{\partial M_d}{\partial\sigma_u} = -2G_D, \tag{C.47}$$
$$\frac{\partial\Omega_{\text{MFA}}}{\partial M_f} = -2T\ N_c \int \frac{d^3p}{(2\pi)^3} \frac{\partial}{\partial M_f} \left[\beta E_f + \ln\left(1 + e^{-\beta\left(E_f + \tilde{\mu}_f\right)}\right) + \ln\left(1 + e^{-\beta\left(E_f - \tilde{\mu}_f\right)}\right)\right] =$$
$$= -2\ N_c \int \frac{d^3p}{(2\pi)^3} \frac{M_f}{E_f} \left(1 - n_f - \overline{n}_f\right) = I_f. \tag{C.48}$$

Here, n_f and $\overline{n}_f$ are the particle and anti-particle occupation numbers defined in Equations (2.82) and (2.83). Putting it all together, Equation (C.43) yields:

$$4G_S\left(\sigma_u - I_u\right) + 2G_D\left(\sigma_d - I_d\right) = 0. \tag{C.49}$$

In a similar way, Equation (C.44) yields:

$$4G_S\left(\sigma_d - I_d\right) + 2G_D\left(\sigma_u - I_u\right) = 0. \tag{C.50}$$

If G_S and G_D are non-zero, the above equalities verify if and only if:

$$\sigma_u = I_u = -2\ N_c \int \frac{d^3p}{(2\pi)^3} \frac{M_u}{E_u}\left(1 - n_u - \overline{n}_u\right), \tag{C.51}$$

$$\sigma_d = I_d = -2\ N_c \int \frac{d^3p}{(2\pi)^3} \frac{M_d}{E_d}\left(1 - n_d - \overline{n}_d\right). \tag{C.52}$$

Defining the quark condensates and the *gap* equations.

C.4.2 NJL model in $SU_f(3)$

The *gap* equations of the three flavour **NJL** model can be found by using Equation (3.116):

$$\frac{\partial\Omega_{\text{MFA}}}{\partial\sigma_u} = \frac{\partial\Omega_{\text{MFA}}}{\partial\sigma_d} = \frac{\partial\Omega_{\text{MFA}}}{\partial\sigma_s} = 0, \tag{C.53}$$

which defines the values of the quark condensates σ_u, σ_d and σ_s. The grand canonical potential of this model is given by Equation (3.115):

$$\begin{aligned}\Omega_{\text{MFA}} = \Omega_0 &+ 2G_S\left(\sigma_u^2 + \sigma_d^2 + \sigma_s^2\right) - 4G_D\sigma_u\sigma_d\sigma_s \\ &- \frac{2}{3}G_\omega\left(\rho_u + \rho_d + \rho_s\right)^2 - G_\rho\left(\rho_u - \rho_d\right)^2 - \frac{1}{3}G_\rho\left(\rho_u + \rho_d - 2\rho_s\right)^2 \\ &- 2T\ N_c \sum_{f=u,d,s} \int \frac{d^3p}{(2\pi)^3}\left[\beta E_f + \ln\left(1 + e^{-\beta\left(E_f + \tilde{\mu}_f\right)}\right) + \ln\left(1 + e^{-\beta\left(E_f - \tilde{\mu}_f\right)}\right)\right].\end{aligned} \tag{C.54}$$

The effective mass is (Equation (3.117)):

$$M_i = m_i - 4G_S\sigma_i + 2G_D\sigma_j\sigma_k \quad i \neq j \neq k \in \{u, d, s\}. \tag{C.55}$$

Like for the two flavour case, using Equation (C.53) one can write:

$$\frac{\partial\Omega_{\text{MFA}}}{\partial\sigma_u} = \frac{\partial\Omega_{\text{MFA}}}{\partial\sigma_u} + \frac{\partial\Omega_{\text{MFA}}}{\partial M_u}\frac{\partial M_u}{\partial\sigma_u} + \frac{\partial\Omega_{\text{MFA}}}{\partial M_d}\frac{\partial M_d}{\partial\sigma_u} + \frac{\partial\Omega_{\text{MFA}}}{\partial M_s}\frac{\partial M_s}{\partial\sigma_u} = 0, \tag{C.56}$$

$$\frac{\partial\Omega_{\text{MFA}}}{\partial\sigma_d} = \frac{\partial\Omega_{\text{MFA}}}{\partial\sigma_d} + \frac{\partial\Omega_{\text{MFA}}}{\partial M_u}\frac{\partial M_u}{\partial\sigma_d} + \frac{\partial\Omega_{\text{MFA}}}{\partial M_d}\frac{\partial M_d}{\partial\sigma_d} + \frac{\partial\Omega_{\text{MFA}}}{\partial M_s}\frac{\partial M_s}{\partial\sigma_d} = 0, \tag{C.57}$$

$$\frac{\partial\Omega_{\text{MFA}}}{\partial\sigma_s} = \frac{\partial\Omega_{\text{MFA}}}{\partial\sigma_s} + \frac{\partial\Omega_{\text{MFA}}}{\partial M_u}\frac{\partial M_u}{\partial\sigma_s} + \frac{\partial\Omega_{\text{MFA}}}{\partial M_d}\frac{\partial M_d}{\partial\sigma_s} + \frac{\partial\Omega_{\text{MFA}}}{\partial M_s}\frac{\partial M_s}{\partial\sigma_s} = 0. \tag{C.58}$$

Using (C.54) and (C.55), for the *up* quark, each term yields:

$$\frac{\partial \Omega_{\text{MFA}}}{\partial \sigma_u} = 4G_S\sigma_u - 4G_D\sigma_d\sigma_s, \tag{C.59}$$

$$\frac{\partial M_u}{\partial \sigma_u} = -4G_S, \tag{C.60}$$

$$\frac{\partial M_d}{\partial \sigma_u} = 2G_D\sigma_s, \tag{C.61}$$

$$\frac{\partial M_s}{\partial \sigma_u} = 2G_D\sigma_d, \tag{C.62}$$

$$\begin{aligned}\frac{\partial \Omega_{\text{MFA}}}{\partial M_f} &= -2T\ N_c \int \frac{d^3p}{(2\pi)^3} \frac{\partial}{\partial M_f} \left[\beta E_f + \ln\left(1 + e^{-\beta\left(E_f + \tilde{\mu}_f\right)}\right) + \ln\left(1 + e^{-\beta\left(E_f - \tilde{\mu}_f\right)}\right)\right] = \\ &= -2\ N_c \int \frac{d^3p}{(2\pi)^3} \frac{M_f}{E_f} \left(1 - n_f - \overline{n}_f\right) = I_f. \end{aligned} \tag{C.63}$$

Once again, n_f and $\overline{n}_f$ are the particle and anti-particle occupation numbers defined in Equations (2.82) and (2.83). Putting it all together, Equation (C.56) yields:

$$4G_S\left(\sigma_u - I_u\right) + 2G_D\left(\sigma_s I_d + \sigma_d I_s - 2\sigma_d\sigma_s\right) = 0. \tag{C.64}$$

In a similar way, Equations (C.57) and (C.58) are given by:

$$4G_S\left(\sigma_d - I_d\right) + 2G_D\left(\sigma_u I_s + \sigma_s I_u - 2\sigma_s\sigma_u\right) = 0, \tag{C.65}$$

$$4G_S\left(\sigma_s - I_s\right) + 2G_D\left(\sigma_d I_u + \sigma_u I_d - 2\sigma_u\sigma_d\right) = 0. \tag{C.66}$$

If G_S and G_D are non-zero, the above equalities verify if and only if:

$$\sigma_u = I_u = -2\ N_c \int \frac{d^3p}{(2\pi)^3} \frac{M_u}{E_u} \left(1 - n_u - \overline{n}_u\right), \tag{C.67}$$

$$\sigma_d = I_d = -2\ N_c \int \frac{d^3p}{(2\pi)^3} \frac{M_d}{E_d} \left(1 - n_d - \overline{n}_d\right), \tag{C.68}$$

$$\sigma_s = I_s = -2\ N_c \int \frac{d^3p}{(2\pi)^3} \frac{M_s}{E_s} \left(1 - n_s - \overline{n}_s\right). \tag{C.69}$$

Defining the quark condensates and the *gap* equations.

C.4.3 PNJL model in $SU_f(3)$

The *gap* equations of the three flavour **PNJL** model can be found just like in the **NJL** case, done in Appendix C.4.2. We use:

$$\frac{\partial \Omega_{\text{MFA}}}{\partial \sigma_u} = \frac{\partial \Omega_{\text{MFA}}}{\partial \sigma_d} = \frac{\partial \Omega_{\text{MFA}}}{\partial \sigma_s} = \frac{\partial \Omega_{\text{MFA}}}{\partial \Phi} = \frac{\partial \Omega_{\text{MFA}}}{\partial \overline{\Phi}} = 0, \tag{C.70}$$

which defines the values of the quark condensates σ_u, σ_d and σ_s and the Polyakov loop fields Φ and $\overline{\Phi}$. The grand canonical potential of the **PNJL** model is given by Equation

(6.71):

$$\Omega_{\rm MFA}-\Omega_0=\mathcal{U}\left(\Phi,\overline{\Phi};T\right)-U^{\rm NJL}-2N_c\sum_f\int\frac{d^3p}{(2\pi)^3}E_f \\ -2\sum_f\int\frac{d^3p}{(2\pi)^3}\left[\mathcal{F}\left(\boldsymbol{p},T,\tilde{\mu}_f^{\rm NJL}\right)+\mathcal{F}^*\left(\boldsymbol{p},T,\tilde{\mu}_f^{\rm NJL}\right)\right]. \quad \text{(C.71)}$$

Where the the thermal functions $\mathcal{F}$ and $\mathcal{F}^*$ are given by Equations (6.69) and (6.70), respectively. The effective mass in the **PNJL** model is given by Equation (3.117), exactly the same effective mass as in the **NJL** model. We use the relations given in Equations (C.56), (C.57) and (C.58) to define the value of the condensates. For the *up* quark, each term yields:

$$\frac{\partial\Omega_{\rm MFA}}{\partial\sigma_u}=4G_S\sigma_u-4G_D\sigma_d\sigma_s, \quad \text{(C.72)}$$

$$\frac{\partial M_u}{\partial\sigma_u}=-4G_S, \quad \text{(C.73)}$$

$$\frac{\partial M_d}{\partial\sigma_u}=2G_D\sigma_s, \quad \text{(C.74)}$$

$$\frac{\partial M_s}{\partial\sigma_u}=2G_D\sigma_d, \quad \text{(C.75)}$$

$$\frac{\partial\Omega_{\rm MFA}}{\partial M_f}=-2\int\frac{d^3p}{(2\pi)^3}\left[N_c\frac{\partial E_f}{\partial M_f}+\frac{\partial}{\partial M_f}\mathcal{F}^*\left(\boldsymbol{p},T,\tilde{\mu}_f^{\rm NJL}\right)+\frac{\partial}{\partial M_f}\mathcal{F}\left(\boldsymbol{p},T,\tilde{\mu}_f^{\rm NJL}\right)\right]. \quad \text{(C.76)}$$

The major difference between the **NJL** and **PNJL** model comes from Equation (C.76). The thermal functions $\mathcal{F}$ and $\mathcal{F}^*$ are defined in Equations (6.69) and (6.70),

$$\mathcal{F}\left(\boldsymbol{p},T,\tilde{\mu}_f^{\rm NJL}\right)=T\ln\left[1+e^{-3\left(E_f-\tilde{\mu}_f^{\rm NJL}\right)/T}+N_c\overline{\Phi}e^{-\left(E_f-\tilde{\mu}_f^{\rm NJL}\right)/T}+N_c\Phi e^{-2\left(E_f-\tilde{\mu}_f^{\rm NJL}\right)/T}\right], \quad \text{(C.77)}$$

$$\mathcal{F}^*\left(\boldsymbol{p},T,\tilde{\mu}_f^{\rm NJL}\right)=T\ln\left[1+e^{-3\left(E_f+\tilde{\mu}_f^{\rm NJL}\right)/T}+N_c\Phi e^{-\left(E_f+\tilde{\mu}_f^{\rm NJL}\right)/T}+N_c\overline{\Phi}e^{-2\left(E_f+\tilde{\mu}_f^{\rm NJL}\right)/T}\right]. \quad \text{(C.78)}$$

The derivatives in Equation (C.76) are given by:

$$\frac{\partial E_f}{\partial M_f}=\frac{M_f}{E_f}, \quad \text{(C.79)}$$

$$\frac{\partial}{\partial M_f}\mathcal{F}\left(\boldsymbol{p},T,\tilde{\mu}_f^{\rm NJL}\right)=-N_c\frac{M_f}{E_f}\nu_f, \quad \text{(C.80)}$$

$$\frac{\partial}{\partial M_f}\mathcal{F}^*\left(\boldsymbol{p},T,\tilde{\mu}_f^{\rm NJL}\right)=-N_c\frac{M_f}{E_f}\overline{\nu}_f. \quad \text{(C.81)}$$

Where ν_f and $\overline{\nu}_f$ are the particle and antiparticle occupation numbers in the **PNJL** model (Equations (6.76) and (6.77)), defined as:

$$\nu_f = \frac{\frac{3}{N_c} e^{-3\left(E_f - \tilde{\mu}_f^{\mathrm{NJL}}\right)/T} + \overline{\Phi} e^{-\left(E_f - \tilde{\mu}_f^{\mathrm{NJL}}\right)/T} + 2\Phi e^{-2\left(E_f - \tilde{\mu}_f^{\mathrm{NJL}}\right)/T}}{1 + e^{-3\left(E_f - \tilde{\mu}_f^{\mathrm{NJL}}\right)/T} + N_c \overline{\Phi} e^{-\left(E_f - \tilde{\mu}_f^{\mathrm{NJL}}\right)/T} + N_c \Phi e^{-2\left(E_f - \tilde{\mu}_f^{\mathrm{NJL}}\right)/T}}, \tag{C.82}$$

$$\overline{\nu}_f = \frac{\frac{3}{N_c} e^{-3\left(E_f + \tilde{\mu}_f^{\mathrm{NJL}}\right)/T} + \Phi e^{-\left(E_f + \tilde{\mu}_f^{\mathrm{NJL}}\right)/T} + 2\overline{\Phi} e^{-2\left(E_f + \tilde{\mu}_f^{\mathrm{NJL}}\right)/T}}{1 + e^{-3\left(E_f + \tilde{\mu}_f^{\mathrm{NJL}}\right)/T} + N_c \Phi e^{-\left(E_f + \tilde{\mu}_f^{\mathrm{NJL}}\right)/T} + N_c \overline{\Phi} e^{-2\left(E_f + \tilde{\mu}_f^{\mathrm{NJL}}\right)/T}}. \tag{C.83}$$

Substituting Equations (C.79), (C.80) and (C.81) in Equation (C.76), it yields:

$$\frac{\partial \Omega_{\mathrm{MFA}}}{\partial M_f} = -2\, N_c \int \frac{d^3p}{(2\pi)^3} \frac{M_f}{E_f} \left(1 - \nu_f - \overline{\nu}_f\right) = I_f. \tag{C.84}$$

Replicating the above calculations for the other flavours of quarks and using the same arguments as in Appendix C.4.2, the condensates for each flavour of quark in the **PNJL** model are defined as:

$$\sigma_u = I_u = -2\, N_c \int \frac{d^3p}{(2\pi)^3} \frac{M_u}{E_u} \left(1 - \nu_u - \overline{\nu}_u\right), \tag{C.85}$$

$$\sigma_d = I_d = -2\, N_c \int \frac{d^3p}{(2\pi)^3} \frac{M_d}{E_d} \left(1 - \nu_d - \overline{\nu}_d\right), \tag{C.86}$$

$$\sigma_s = I_s = -2\, N_c \int \frac{d^3p}{(2\pi)^3} \frac{M_s}{E_s} \left(1 - \nu_s - \overline{\nu}_s\right). \tag{C.87}$$

To complete the calculations we have to define the value of the Polyakov loop field Φ and its complex conjugate $\overline{\Phi}$ using Equation (C.70). We treat Φ and $\overline{\Phi}$ as being independent real variables, even though they are by definition complex. This is made to avoid problems arising from minimizing a complex potential [46, 82]. We write:

$$\frac{\partial \Omega_{\mathrm{MFA}}}{\partial \Phi} = \frac{\partial}{\partial \Phi} \mathcal{U}\left(\Phi, \overline{\Phi}; T\right) - 2 \sum_f \int \frac{d^3p}{(2\pi)^3} \left[\frac{\partial}{\partial \Phi} \mathcal{F}\left(\boldsymbol{p}, T, \tilde{\mu}_f^{\mathrm{NJL}}\right) + \frac{\partial}{\partial \Phi} \mathcal{F}^*\left(\boldsymbol{p}, T, \tilde{\mu}_f^{\mathrm{NJL}}\right)\right] = 0, \tag{C.88}$$

$$\frac{\partial \Omega_{\mathrm{MFA}}}{\partial \overline{\Phi}} = \frac{\partial}{\partial \overline{\Phi}} \mathcal{U}\left(\Phi, \overline{\Phi}; T\right) - 2 \sum_f \int \frac{d^3p}{(2\pi)^3} \left[\frac{\partial}{\partial \overline{\Phi}} \mathcal{F}\left(\boldsymbol{p}, T, \tilde{\mu}_f^{\mathrm{NJL}}\right) + \frac{\partial}{\partial \overline{\Phi}} \mathcal{F}^*\left(\boldsymbol{p}, T, \tilde{\mu}_f^{\mathrm{NJL}}\right)\right] = 0. \tag{C.89}$$

Considering the logarithmic Polyakov loop effective potential defined in Equation (6.37),

$$\frac{\mathcal{U}\left(\Phi, \overline{\Phi}; T\right)}{T^4} = -\frac{1}{2} a\left(T\right) \overline{\Phi}\Phi + b\left(T\right) \ln\left[1 - 6\overline{\Phi}\Phi + 4\left(\overline{\Phi}^3 + \Phi^3\right) - 3\left(\overline{\Phi}\Phi\right)^2\right], \tag{C.90}$$

its derivatives are:

$$\frac{\partial}{\partial\Phi}\mathcal{U}\left(\Phi,\overline{\Phi};T\right)=T^4\left[-\frac{1}{2}a\left(T\right)\overline{\Phi}-\frac{6b\left(T\right)\left(\overline{\Phi}-2\Phi^2+\overline{\Phi}^2\Phi\right)}{1-6\overline{\Phi}\Phi+4\left(\overline{\Phi}^3+\Phi^3\right)-3\left(\overline{\Phi}\Phi\right)^2}\right], \tag{C.91}$$

$$\frac{\partial}{\partial\Phi}\mathcal{U}\left(\Phi,\overline{\Phi};T\right)=T^4\left[-\frac{1}{2}a\left(T\right)\Phi-\frac{6b\left(T\right)\left(\Phi-2\overline{\Phi}^2+\overline{\Phi}\Phi^2\right)}{1-6\overline{\Phi}\Phi+4\left(\overline{\Phi}^3+\Phi^3\right)-3\left(\overline{\Phi}\Phi\right)^2}\right]. \tag{C.92}$$

The derivatives of the thermal functions are given by:

$$\frac{\partial}{\partial\Phi}\mathcal{F}\left(\boldsymbol{p},T,\tilde{\mu}_f^{\mathrm{NJL}}\right)=T\frac{N_c\,e^{-2\left(E_f-\tilde{\mu}_f^{\mathrm{NJL}}\right)/T}}{e^{\mathcal{F}\left(\boldsymbol{p},T,\tilde{\mu}_f^{\mathrm{NJL}}\right)/T}}, \tag{C.93}$$

$$\frac{\partial}{\partial\overline{\Phi}}\mathcal{F}\left(\boldsymbol{p},T,\tilde{\mu}_f^{\mathrm{NJL}}\right)=T\frac{N_c\,e^{-\left(E_f-\tilde{\mu}_f^{\mathrm{NJL}}\right)/T}}{e^{\mathcal{F}\left(\boldsymbol{p},T,\tilde{\mu}_f^{\mathrm{NJL}}\right)/T}}, \tag{C.94}$$

$$\frac{\partial}{\partial\Phi}\mathcal{F}^*\left(\boldsymbol{p},T,\tilde{\mu}_f^{\mathrm{NJL}}\right)=T\frac{N_c\,e^{-\left(E_f+\tilde{\mu}_f^{\mathrm{NJL}}\right)/T}}{e^{\mathcal{F}^*\left(\boldsymbol{p},T,\tilde{\mu}_f^{\mathrm{NJL}}\right)/T}}, \tag{C.95}$$

$$\frac{\partial}{\partial\overline{\Phi}}\mathcal{F}^*\left(\boldsymbol{p},T,\tilde{\mu}_f^{\mathrm{NJL}}\right)=T\frac{N_c\,e^{-2\left(E_f+\tilde{\mu}_f^{\mathrm{NJL}}\right)/T}}{e^{\mathcal{F}^*\left(\boldsymbol{p},T,\tilde{\mu}_f^{\mathrm{NJL}}\right)/T}}. \tag{C.96}$$

Gathering all the results yields the *gap* equations for the Polyakov loop:

$$T^4\left[-\frac{1}{2}a\left(T\right)\overline{\Phi}-\frac{6b\left(T\right)\left(\overline{\Phi}-2\Phi^2+\overline{\Phi}^2\Phi\right)}{1-6\overline{\Phi}\Phi+4\left(\overline{\Phi}^3+\Phi^3\right)-3\left(\overline{\Phi}\Phi\right)^2}\right]=$$
$$2N_cT\sum_f\int\frac{d^3p}{(2\pi)^3}\left[\frac{e^{-\left(E_f+\tilde{\mu}_f^{\mathrm{NJL}}\right)/T}}{e^{\mathcal{F}^*\left(\boldsymbol{p},T,\tilde{\mu}_f^{\mathrm{NJL}}\right)/T}}+\frac{e^{-2\left(E_f-\tilde{\mu}_f^{\mathrm{NJL}}\right)/T}}{e^{\mathcal{F}\left(\boldsymbol{p},T,\tilde{\mu}_f^{\mathrm{NJL}}\right)/T}}\right], \tag{C.97}$$

$$T^4\left[-\frac{1}{2}a\left(T\right)\Phi-\frac{6b\left(T\right)\left(\Phi-2\overline{\Phi}^2+\overline{\Phi}\Phi^2\right)}{1-6\overline{\Phi}\Phi+4\left(\overline{\Phi}^3+\Phi^3\right)-3\left(\overline{\Phi}\Phi\right)^2}\right]=$$
$$2N_cT\sum_f\int\frac{d^3p}{(2\pi)^3}\left[\frac{e^{-\left(E_f-\tilde{\mu}_f^{\mathrm{NJL}}\right)/T}}{e^{\mathcal{F}\left(\boldsymbol{p},T,\tilde{\mu}_f^{\mathrm{NJL}}\right)/T}}+\frac{e^{-2\left(E_f+\tilde{\mu}_f^{\mathrm{NJL}}\right)/T}}{e^{\mathcal{F}^*\left(\boldsymbol{p},T,\tilde{\mu}_f^{\mathrm{NJL}}\right)/T}}\right]. \tag{C.98}$$

Appendix D

Thermal limits

D.1 T=0 limit of thermal functions

D.1.1 General thermal functions

Consider the $T = 0$ limit of the following thermal functions (we suppose that $\tilde{\mu}_f \geqslant 0$):

$$n_f\left(\tilde{\mu}_f, T\right) = \frac{1}{e^{\left(E_f - \tilde{\mu}_f\right)/T} + 1}, \tag{D.1}$$

$$\overline{n}_f\left(\tilde{\mu}_f, T\right) = \frac{1}{e^{\left(E_f + \tilde{\mu}_f\right)/T} + 1}, \tag{D.2}$$

$$f_f^+\left(\tilde{\mu}_f, T\right) = T \ln\left(1 + e^{-\left(E_f + \tilde{\mu}_f\right)/T}\right), \tag{D.3}$$

$$f_f^-\left(\tilde{\mu}_f, T\right) = T \ln\left(1 + e^{-\left(E_f - \tilde{\mu}_f\right)/T}\right). \tag{D.4}$$

Equations (D.1) and (D.2) define the particle and anti-particle $\overline{n}_f$ occupation numbers, respectively. The thermal functions (D.3) and (D.3) are defined in the grand canonical potential of several studied models. The $T = 0$ limit of Equations (D.1) and (D.2) are given by:

$$\lim_{T \to 0} n_f\left(\tilde{\mu}_f, T\right) = \begin{cases} 1 & \text{if} \quad E_f < \tilde{\mu}_f \\ 0 & \text{if} \quad E_f > \tilde{\mu}_f \end{cases} = \theta\left(E_f - \tilde{\mu}_f\right), \tag{D.5}$$

$$\lim_{T \to 0} \overline{n}_f\left(\tilde{\mu}_f, T\right) = 0 \quad , \text{ because } \tilde{\mu}_f \geqslant 0. \tag{D.6}$$

The $T = 0$ limit of the thermal functions (D.3) and (D.3) are:

$$\lim_{T \to 0} f_f^+\left(\tilde{\mu}_f, T\right) = 0 \quad , \text{ because } \tilde{\mu}_f \geqslant 0, \tag{D.7}$$

$$\lim_{T\to 0} f_f^- \left(\tilde{\mu}_f, T\right) = \lim_{T\to 0} T \ln\left(1 + e^{-\left(E_f - \tilde{\mu}_f\right)/T}\right) \quad \wedge \quad k = \left(E_f - \tilde{\mu}_f\right) \ , \ k/T = x$$

$$= \begin{cases} \lim\limits_{x\to+\infty} k \frac{\ln\left(1+e^{-x}\right)}{x} & \text{if} \quad k > 0 \\ \lim\limits_{x\to-\infty} k \frac{\ln\left(1+e^{-x}\right)}{x} & \text{if} \quad k < 0 \end{cases} =$$

$$= \begin{cases} k \lim\limits_{x\to+\infty} \frac{\frac{d}{dx}\ln\left(1+e^{-x}\right)}{\frac{d}{dx}x} & \text{if} \quad k > 0 \\ k \lim\limits_{x\to-\infty} \frac{\frac{d}{dx}\ln\left(1+e^{-x}\right)}{\frac{d}{dx}x} & \text{if} \quad k < 0 \end{cases} =$$

$$= \begin{cases} -k \lim\limits_{x\to+\infty} \frac{1}{e^x+1} & \text{if} \quad k > 0 \\ -k \lim\limits_{x\to-\infty} \frac{1}{e^x+1} & \text{if} \quad k < 0 \end{cases} =$$

$$= \begin{cases} 0 & \text{if} \quad k > 0 \\ -k & \text{if} \quad k < 0 \end{cases} = -\left(E_f - \tilde{\mu}_f\right)\theta\left(E_f - \tilde{\mu}_f\right) =$$

$$= \left(\tilde{\mu}_f - E_f\right)\theta\left(E_f - \tilde{\mu}_f\right). \tag{D.8}$$

D.1.2 Thermal functions in the PNJL model

To simplify the Equations (6.69) and (6.70), one can write:

$$x_f = \left(E_f - \tilde{\mu}_f\right)/T, \tag{D.9}$$

$$x_f^* = \left(E_f + \tilde{\mu}_f\right)/T. \tag{D.10}$$

The thermal functions are then given by:

$$\mathcal{F}\left(\boldsymbol{p}, T, \tilde{\mu}_f\right) = T \ln\left(1 + e^{-3x_f} + N_c\overline{\Phi}e^{-x_f} + N_c\Phi e^{-2x_f}\right), \tag{D.11}$$

$$\mathcal{F}^*\left(\boldsymbol{p}, T, \tilde{\mu}_f\right) = T \ln\left(1 + e^{-3x_f^*} + N_c\Phi e^{-x_f^*} + N_c\overline{\Phi}e^{-2x_f^*}\right). \tag{D.12}$$

The $T = 0$ limit is (for $N_c = 3$):

$$\lim_{T\to 0} \mathcal{F}\left(\boldsymbol{p}, T, \tilde{\mu}_f\right) = \lim_{T\to 0} T \ln\left(1 + e^{-3x_f} + 3\overline{\Phi}e^{-x_f} + 3\Phi e^{-2x_f}\right), \tag{D.13}$$

$$\lim_{T\to 0} \mathcal{F}^*\left(\boldsymbol{p}, T, \tilde{\mu}_f\right) = \lim_{T\to 0} T \ln\left(1 + e^{-3x_f^*} + 3\Phi e^{-x_f^*} + 3\overline{\Phi}e^{-2x_f^*}\right). \tag{D.14}$$

We assume that $\mu_f \geq 0$. For Equation (D.13) we have:

$$\lim_{T\to 0} \mathcal{F}\left(\boldsymbol{p}, T, \tilde{\mu}_f\right) = \begin{cases} \lim\limits_{x_f\to+\infty} \frac{E_f - \tilde{\mu}_f}{x_f} \ln\left(1 + e^{-3x_f} + 3\overline{\Phi}e^{-x_f} + 3\Phi e^{-2x_f}\right) & \text{if } E_f > \tilde{\mu}_f, \\ \lim\limits_{x_f\to-\infty} \frac{E_f - \tilde{\mu}_f}{x_f} \ln\left(1 + e^{-3x_f} + 3\overline{\Phi}e^{-x_f} + 3\Phi e^{-2x_f}\right) & \text{if } E_f < \tilde{\mu}_f. \end{cases} \tag{D.15}$$

If $E_f > \tilde{\mu}_f$ one can use L'Hôpital's rule to help evaluate the limit:

$$\begin{aligned}
&\lim_{x_f\to+\infty} \frac{E_f-\tilde{\mu}_f}{x_f} \ln\left(1+e^{-3x_f}+3\overline{\Phi}e^{-x_f}+3\Phi e^{-2x_f}\right) = \\
&= (E_f-\tilde{\mu}_f) \lim_{x_f\to+\infty} \frac{\frac{d}{dx_f}\ln\left(1+e^{-3x_f}+3\overline{\Phi}e^{-x_f}+3\Phi e^{-2x_f}\right)}{\frac{d}{dx_f}x_f} = \\
&= (\tilde{\mu}_f-E_f) \lim_{x_f\to+\infty} \frac{3e^{-3x_f}+3\overline{\Phi}e^{-x_f}+6\Phi e^{-2x_f}}{1+e^{-3x_f}+3\overline{\Phi}e^{-x_f}+3\Phi e^{-2x_f}}.
\end{aligned} \tag{D.16}$$

Term by term:

$$\begin{aligned}
&(\tilde{\mu}_f-E_f) \lim_{x_f\to+\infty} \frac{3e^{-3x_f}}{1+e^{-3x_f}+3\overline{\Phi}e^{-x_f}+3\Phi e^{-2x_f}} = \\
&= 3\,(\tilde{\mu}_f-E_f) \lim_{x_f\to+\infty} \frac{1}{1+e^{3x_f}+3\overline{\Phi}e^{2x_f}+3\Phi e^{x_f}} = 0,
\end{aligned}$$

$$\begin{aligned}
&(\tilde{\mu}_f-E_f) \lim_{x_f\to+\infty} \frac{3\overline{\Phi}e^{-x_f}}{1+e^{-3x_f}+3\overline{\Phi}e^{-x_f}+3\Phi e^{-2x_f}} \\
&= 3\overline{\Phi}\,(\tilde{\mu}_f-E_f) \lim_{x_f\to+\infty} \frac{1}{e^{x_f}+e^{-2x_f}+3\overline{\Phi}+3\Phi e^{-x_f}} = 0,
\end{aligned}$$

$$\begin{aligned}
&(\tilde{\mu}_f-E_f) \lim_{x_f\to+\infty} \frac{6\Phi e^{-2x_f}}{1+e^{-3x_f}+3\overline{\Phi}e^{-x_f}+3\Phi e^{-2x_f}} = \\
&= 6\Phi\,(\tilde{\mu}_f-E_f) \lim_{x_f\to+\infty} \frac{1}{e^{2x_f}+e^{-x_f}+3\overline{\Phi}e^{x_f}+3\Phi} = 0.
\end{aligned}$$

This implies that, for $E_f > \tilde{\mu}_f$:

$$\lim_{T\to 0} \mathcal{F}\left(\boldsymbol{p}, T, \tilde{\mu}_f\right) = 0. \tag{D.17}$$

If $E_f < \tilde{\mu}_f$:

$$\begin{aligned}
&\lim_{x_f\to-\infty} \frac{E_f-\tilde{\mu}_f}{x_f} \ln\left(1+e^{-3x_f}+3\overline{\Phi}e^{-x_f}+3\Phi e^{-2x_f}\right) = \\
&= (\tilde{\mu}_f-E_f) \lim_{x_f\to-\infty} \frac{3e^{-3x_f}+3\overline{\Phi}e^{-x_f}+6\Phi e^{-2x_f}}{1+e^{-3x_f}+3\overline{\Phi}e^{-x_f}+3\Phi e^{-2x_f}}.
\end{aligned} \tag{D.18}$$

Term by term:

$$\begin{aligned}
&(\tilde{\mu}_f-E_f) \lim_{x_f\to-\infty} \frac{3e^{-3x_f}}{1+e^{-3x_f}+3\overline{\Phi}e^{-x_f}+3\Phi e^{-2x_f}} = \\
&= 3\,(\tilde{\mu}_f-E_f) \lim_{x_f\to-\infty} \frac{1}{1+e^{3x_f}+3\overline{\Phi}e^{2x_f}+3\Phi e^{x_f}} = 3\,(\tilde{\mu}_f-E_f)\,,
\end{aligned}$$

$$(\tilde{\mu}_f - E_f) \lim_{x_f \to -\infty} \frac{3\overline{\Phi} e^{-x_f}}{1 + e^{-3x_f} + 3\overline{\Phi} e^{-x_f} + 3\Phi e^{-2x_f}} =$$
$$= 3\overline{\Phi} (\tilde{\mu}_f - E_f) \lim_{x_f \to -\infty} \frac{1}{e^{x_f} + e^{-2x_f} + 3\overline{\Phi} + 3\Phi e^{-x_f}} = 0,$$

$$(\tilde{\mu}_f - E_f) \lim_{x_f \to -\infty} \frac{6\Phi e^{-2x_f}}{1 + e^{-3x_f} + 3\overline{\Phi} e^{-x_f} + 3\Phi e^{-2x_f}} =$$
$$= 6\Phi (\tilde{\mu}_f - E_f) \lim_{x_f \to -\infty} \frac{1}{e^{2x_f} + e^{-x_f} + 3\overline{\Phi} e^{x_f} + 3\Phi} = 0.$$

This implies that, for $E_f < \tilde{\mu}_f$:

$$\lim_{T \to 0} \mathcal{F}(\boldsymbol{p}, T, \tilde{\mu}_f) = 3 (\tilde{\mu}_f - E_f).$$

Assuming again that $\mu_f \geq 0$, Equation (D.14) gives:

$$\lim_{T \to 0} \mathcal{F}^*(\boldsymbol{p}, T, \tilde{\mu}_f) = \lim_{T \to 0} T \ln \left(1 + e^{-3x_f^*} + 3\Phi e^{-x_f^*} + 3\overline{\Phi} e^{-2x_f^*}\right)$$
$$= (\tilde{\mu}_f - E_f) \lim_{x_f^* \to +\infty} \frac{3e^{-3x_f^*} + 3\Phi e^{-x_f^*} + 6\overline{\Phi} e^{-2x_f^*}}{1 + e^{-3x_f^*} + 3\Phi e^{-x_f^*} + 3\overline{\Phi} e^{-2x_f^*}} = 0,$$

after all, this expression is similar to the previous calculated limits. Summarizing:

$$\lim_{T \to 0} \mathcal{F}(\boldsymbol{p}, T, \tilde{\mu}_f) = 3 (\tilde{\mu}_f - E_f) \theta (E_f - \tilde{\mu}_f), \tag{D.19}$$

$$\lim_{T \to 0} \mathcal{F}^*(\boldsymbol{p}, T, \tilde{\mu}_f) = 0). \tag{D.20}$$

$\theta (E_f - \tilde{\mu}_f)$ is the Heaviside step function.

Bibliography

[1] H. Hansen et al. “Mesonic correlation functions at finite temperature and density in the Nambu-Jona-Lasinio model with a Polyakov loop”. In: *Phys. Rev.* D75 (2007), p. 065004. DOI: 10.1103/PhysRevD.75.065004. arXiv: hep-ph/0609116 [hep-ph].

[2] M. Cheng et al. “Equation of State for physical quark masses”. In: *Phys. Rev.* D81 (2010), p. 054504. DOI: 10.1103/PhysRevD.81.054504. arXiv: 0911.2215 [hep-lat].

[3] Pedro Costa et al. “Phase diagram and critical properties within an effective model of QCD: the Nambu-Jona-Lasinio model coupled to the Polyakov loop”. In: *Symmetry* 2 (2010), pp. 1338–1374. DOI: 10.3390/sym2031338. arXiv: 1007.1380 [hep-ph].

[4] T. Klähn, R. Łastowiecki, and D. B. Blaschke. “Implications of the measurement of pulsars with two solar masses for quark matter in compact stars and heavy-ion collisions: A Nambu–Jona-Lasinio model case study”. In: *Phys. Rev.* D88.8 (2013), p. 085001. DOI: 10.1103/PhysRevD.88.085001. arXiv: 1307.6996.

[5] Xian-yin Xin, Si-xue Qin, and Yu-xin Liu. “Improvement on the Polyakov–Nambu–Jona-Lasinio model and the QCD phase transitions”. In: *Phys. Rev.* D89.9 (2014), p. 094012. DOI: 10.1103/PhysRevD.89.094012.

[6] John Antoniadis et al. “A Massive Pulsar in a Compact Relativistic Binary”. In: *Science* 340 (2013), p. 6131. DOI: 10.1126/science.1233232. arXiv: 1304.6875 [astro-ph.HE].

[7] Paul Demorest et al. “Shapiro Delay Measurement of A Two Solar Mass Neutron Star”. In: *Nature* 467 (2010), pp. 1081–1083. DOI: 10.1038/nature09466. arXiv: 1010.5788 [astro-ph.HE].

[8] Emmanuel Fonseca et al. “The NANOGrav Nine-year Data Set: Mass and Geometric Measurements of Binary Millisecond Pulsars”. In: (2016). arXiv: 1603.00545 [astro-ph.HE].

[9] Klaus Schertler, Stefan Leupold, and Jurgen Schaffner-Bielich. “Neutron stars and quark phases in the NJL model”. In: *Phys. Rev.* C60 (1999), p. 025801. DOI: 10.1103/PhysRevC.60.025801. arXiv: astro-ph/9901152 [astro-ph].

[10] M. Baldo et al. “Neutron stars and the transition to color superconducting quark matter”. In: *Phys. Lett.* B562 (2003), pp. 153–160. DOI: 10.1016/S0370-2693(03)00556-2. arXiv: nucl-th/0212096 [nucl-th].

[11] D. P. Menezes and C. Providencia. "Warm stellar matter with deconfinement: Application to compact stars". In: *Phys. Rev.* C68 (2003), p. 035804. DOI: 10.1103/PhysRevC.68.035804. arXiv: nucl-th/0308041 [nucl-th].

[12] G. Pagliara and J. Schaffner-Bielich. "Stability of CFL cores in Hybrid Stars". In: *Phys. Rev.* D77 (2008), p. 063004. DOI: 10.1103/PhysRevD.77.063004. arXiv: 0711.1119 [astro-ph].

[13] Luca Bonanno and Armen Sedrakian. "Composition and stability of hybrid stars with hyperons and quark color-superconductivity". In: *Astron. Astrophys.* 539 (2012), A16. DOI: 10.1051/0004-6361/201117832. arXiv: 1108.0559 [astro-ph.SR].

[14] Domenico Logoteta, Constança Providência, and Isaac Vidaña. "Formation of hybrid stars from metastable hadronic stars". In: *Phys. Rev.* C88.5 (2013), p. 055802. DOI: 10.1103/PhysRevC.88.055802. arXiv: 1311.0618 [nucl-th].

[15] Tetsuo Hatsuda and Teiji Kunihiro. "QCD phenomenology based on a chiral effective Lagrangian". In: *Phys. Rept.* 247 (1994), pp. 221–367. DOI: 10.1016/0370-1573(94)90022-1. arXiv: hep-ph/9401310 [hep-ph].

[16] P. Rehberg, S. P. Klevansky, and J. Hufner. "Hadronization in the SU(3) Nambu-Jona-Lasinio model". In: *Phys. Rev.* C53 (1996), pp. 410–429. DOI: 10.1103/PhysRevC.53.410. arXiv: hep-ph/9506436 [hep-ph].

[17] M. Hanauske et al. "Strange quark stars within the Nambu-Jona-Lasinio model". In: *Phys. Rev.* D64 (2001), p. 043005. DOI: 10.1103/PhysRevD.64.043005. arXiv: astro-ph/0101267 [astro-ph].

[18] C. H. Lenzi and G. Lugones. "Hybrid stars in the light of the massive pulsar PSR J1614-2230". In: *Astrophys. J.* 759 (2012), p. 57. DOI: 10.1088/0004-637X/759/1/57. arXiv: 1206.4108 [astro-ph.SR].

[19] Kota Masuda, Tetsuo Hatsuda, and Tatsuyuki Takatsuka. "Hadron–quark crossover and massive hybrid stars". In: *PTEP* 2013.7 (2013), p. 073D01. DOI: 10.1093/ptep/ptt045. arXiv: 1212.6803 [nucl-th].

[20] Helena Pais, Débora P. Menezes, and Constança Providência. "Neutron stars: from the inner crust to the core with the (Extended) Nambu-Jona-Lasinio model". In: (2016). arXiv: 1603.01239 [nucl-th].

[21] Débora P. Menezes et al. "Repulsive Vector Interaction in Three Flavor Magnetized Quark and Stellar Matter". In: *Phys. Rev.* C89.5 (2014), p. 055207. DOI: 10.1103/PhysRevC.89.055207. arXiv: 1403.2502 [nucl-th].

[22] Thomas Klahn and Tobias Fischer. "Vector interaction enhanced bag model for astrophysical applications". In: *Astrophys. J.* 810.2 (2015), p. 134. DOI: 10.1088/0004-637X/810/2/134. arXiv: 1503.07442 [nucl-th].

[23] E. J. Ferrer, V. de la Incera, and L. Paulucci. "Gluon effects on the equation of state of color superconducting strange stars". In: *Phys. Rev.* D92.4 (2015), p. 043010. DOI: 10.1103/PhysRevD.92.043010. arXiv: 1501.06597 [hep-ph].

[24] Matthias F. M. Lutz, S. Klimt, and W. Weise. "Meson properties at finite temperature and baryon density". In: *Nucl. Phys.* A542 (1992), pp. 521–558. DOI: 10.1016/0375-9474(92)90256-J.

[25] Kenji Fukushima. "Phase diagrams in the three-flavor Nambu-Jona-Lasinio model with the Polyakov loop". In: *Phys. Rev.* D77 (2008), p. 114028. DOI: 10.1103/PhysRevD.77.114028,10.1103/PhysRevD.78.039902. arXiv: 0803.3318 [hep-ph].

[26] David J. Gross. "Twenty five years of asymptotic freedom". In: *Nucl. Phys. Proc. Suppl.* 74 (1999), pp. 426–446. DOI: 10.1016/S0920-5632(99)00208-X. arXiv: hep-th/9809060 [hep-th].

[27] Peter Skands. "Introduction to QCD". In: *Proceedings, Theoretical Advanced Study Institute in Elementary Particle Physics: Searching for New Physics at Small and Large Scales (TASI 2012)*. 2013, pp. 341–420. DOI: 10.1142/9789814525220_0008. arXiv: 1207.2389 [hep-ph]. URL: https://inspirehep.net/record/1121892/files/arXiv:1207.2389.pdf.

[28] K. A. Olive et al. "Review of Particle Physics". In: *Chin. Phys.* C38 (2014), p. 090001. DOI: 10.1088/1674-1137/38/9/090001.

[29] P. G. Harris et al. "New Experimental Limit on the Electric Dipole Moment of the Neutron". In: *Phys. Rev. Lett.* 82 (5 1999), pp. 904–907. DOI: 10.1103/PhysRevLett.82.904. URL: http://link.aps.org/doi/10.1103/PhysRevLett.82.904.

[30] H. Suganuma et al. "Quark confinement physics from lattice QCD". In: *Quantum chromodynamics and color confinement. Proceedings, International Symposium, Confinement 2000, Osaka, Japan, March 7-10, 2000.* 2004, pp. 103–119. arXiv: hep-lat/0407020 [hep-lat].

[31] Mikhail Shifman. "Understanding Confinement in QCD: Elements of a Big Picture". In: *Int. J. Mod. Phys.* A25 (2010). [,57(2010)], pp. 4015–4031. DOI: 10.1142/9789814335614_0007,10.1142/S0217751X10050548. arXiv: 1007.0531 [hep-th].

[32] Gerard 't Hooft. "How Instantons Solve the U(1) Problem". In: *Phys. Rept.* 142 (1986), pp. 357–387. DOI: 10.1016/0370-1573(86)90117-1.

[33] Gerard 't Hooft. "Computation of the Quantum Effects Due to a Four-Dimensional Pseudoparticle". In: *Phys. Rev.* D14 (1976). [Erratum: Phys. Rev.D18,2199(1978)], pp. 3432–3450. DOI: 10.1103/PhysRevD.18.2199.3,10.1103/PhysRevD.14.3432.

[34] Julia Danzer et al. "A Study of the sign problem for lattice QCD with chemical potential". In: *Phys. Lett.* B682 (2009), pp. 240–245. DOI: 10.1016/j.physletb.2009.11.004. arXiv: 0907.3084 [hep-lat].

[35] Frank Wilczek. "Quantum field theory". In: *Rev. Mod. Phys.* 71 (1999), S85–S95. DOI: 10.1103/RevModPhys.71.S85. arXiv: hep-th/9803075 [hep-th].

[36] David Tong. *Quantum Field Theory - University of Cambridge Part III Mathematical Tripos.*

[37] R. P. Feynman. "Space-Time Approach to Non-Relativistic Quantum Mechanics". In: *Rev. Mod. Phys.* 20 (2 1948), pp. 367–387. DOI: 10.1103/RevModPhys.20.367. URL: http://link.aps.org/doi/10.1103/RevModPhys.20.367.

[38] A. Das. *Field Theory: A Path Integral Approach.* World Scientific Lecture Notes in Physics. 1993. ISBN: 9789814504195. URL: https://books.google.pt/books?id=UbzsCgAAQBAJ.

[39] M.E. Peskin and D.V. Schroeder. *An Introduction To Quantum Field Theory*. Frontiers in physics. Westview Press, 1995. ISBN: 9780813345437. URL: https://books.google.pt/books?id=EVeNNcslvX0C.

[40] G. Ripka. *Quarks Bound by Chiral Fields: The Quark Structure of the Vacuum and of Light Mesons and Baryons*. Oxford science publications. Clarendon Press, 1997. ISBN: 9780198517849. URL: https://books.google.pt/books?id=ntrPDA6zE1wC.

[41] J.P. Casquilho and P.I.C. Teixeira. *Introduction to Statistical Physics*. Cambridge University Press, 2014. ISBN: 9781316213995. URL: https://books.google.pt/books?id=eRv1BQAAQBAJ.

[42] J.I. Kapusta and C. Gale. *Finite-Temperature Field Theory: Principles and Applications*. Cambridge Monographs on Mathematical Physics. Cambridge University Press, 2006. ISBN: 9781139457620. URL: https://books.google.pt/books?id=rll8dJ2iTpsC.

[43] David Tong. *Statistical Physics - University of Cambridge Part II Mathematical Tripos*.

[44] A. Das. *Finite Temperature Field Theory*. 1997. ISBN: 9789814498234. URL: https://books.google.pt/books?id=kQPtCgAAQBAJ.

[45] Inga Strumke. "Field Theory at finite Temperature and Density-Applications to Quark Stars". MA thesis. Norwegian University of Science and Technology.

[46] Topi Kähärä. "THERMODYNAMICS OF TWO–FLAVOR QCD FROM CHIRAL MODELS WITH POLYAKOV LOOP". PhD thesis. University of Jyväskylä.

[47] M.L. Bellac. *Thermal Field Theory*. Cambridge Monographs on Mathematical Physics. Cambridge University Press, 2000. ISBN: 9780521654777. URL: https://books.google.pt/books?id=00_x6GR8GXoC.

[48] Yoichiro Nambu and G. Jona-Lasinio. "DYNAMICAL MODEL OF ELEMENTARY PARTICLES BASED ON AN ANALOGY WITH SUPERCONDUCTIVITY. II". In: *Phys. Rev.* 124 (1961), pp. 246–254. DOI: 10.1103/PhysRev.124.246.

[49] Michael Buballa. "NJL model analysis of quark matter at large density". In: *Phys. Rept.* 407 (2005), pp. 205–376. DOI: 10.1016/j.physrep.2004.11.004. arXiv: hep-ph/0402234 [hep-ph].

[50] U. Vogl and W. Weise. "The Nambu and Jona Lasinio model: Its implications for hadrons and nuclei". In: *Prog. Part. Nucl. Phys.* 27 (1991), pp. 195–272. DOI: 10.1016/0146-6410(91)90005-9.

[51] S. P. Klevansky. "The Nambu—Jona-Lasinio model of quantum chromodynamics". In: *Rev. Mod. Phys.* 64 (3 1992), pp. 649–708. DOI: 10.1103/RevModPhys.64.649. URL: http://link.aps.org/doi/10.1103/RevModPhys.64.649.

[52] M. Kobayashi and T. Maskawa. "CHIRAL SYMMETRY AND eta–X MIXING." In: *Progr. Theor. Phys. (Kyoto) 44: 1422-4(Nov 1970).* (1970). DOI: 10.1143/PTP.44.1422.

[53] Veronique Bernard and Ulf G. Meissner. "Properties of Vector and Axial Vector Mesons from a Generalized Nambu-Jona-Lasinio Model". In: *Nucl. Phys.* A489 (1988), p. 647. DOI: 10.1016/0375-9474(88)90114-5.

[54] Nino M. Bratovic, Tetsuo Hatsuda, and Wolfram Weise. "Role of Vector Interaction and Axial Anomaly in the PNJL Modeling of the QCD Phase Diagram". In: *Phys. Lett.* B719 (2013), pp. 131–135. DOI: 10.1016/j.physletb.2013.01.003. arXiv: 1204.3788 [hep-ph].

[55] M. Asakawa and K. Yazaki. "Chiral Restoration at Finite Density and Temperature". In: *Nucl. Phys.* A504 (1989), pp. 668–684. DOI: 10.1016/0375-9474(89)90002-X.

[56] Norman K. Glendenning. *Compact Stars*. New York: Springer-Verlag, 2000.

[57] Fridolin Weber et al. "Strangeness in Neutron Stars". In: *Int. J. Mod. Phys.* D16 (2007), pp. 231–245. DOI: 10.1142/S0218271807009966. arXiv: astro-ph/0604422 [astro-ph].

[58] M. H. Johnson and E. Teller. "Classical Field Theory of Nuclear Forces". In: *Phys. Rev.* 98 (3 1955), pp. 783–787. DOI: 10.1103/PhysRev.98.783. URL: http://link.aps.org/doi/10.1103/PhysRev.98.783.

[59] Hans-Peter Duerr. "Relativistic Effects in Nuclear Forces". In: *Phys. Rev.* 103 (2 1956), pp. 469–480. DOI: 10.1103/PhysRev.103.469. URL: http://link.aps.org/doi/10.1103/PhysRev.103.469.

[60] J.D Walecka. "A theory of highly condensed matter". In: *Annals of Physics* 83.2 (1974), pp. 491 –529. ISSN: 0003-4916. DOI: http://dx.doi.org/10.1016/0003-4916(74)90208-5. URL: http://www.sciencedirect.com/science/article/pii/0003491674902085.

[61] J. Boguta and A.R. Bodmer. "Relativistic calculation of nuclear matter and the nuclear surface". In: *Nuclear Physics A* 292.3 (1977), pp. 413 –428. ISSN: 0375-9474. DOI: http://dx.doi.org/10.1016/0375-9474(77)90626-1. URL: http://www.sciencedirect.com/science/article/pii/0375947477906261.

[62] Y. Sugahara and H. Toki. "Relativistic mean field theory for unstable nuclei with nonlinear sigma and omega terms". In: *Nucl. Phys.* A579 (1994), pp. 557–572. DOI: 10.1016/0375-9474(94)90923-7.

[63] C. J. Horowitz and J. Piekarewicz. "Neutron radii of ^{208}Pb and neutron stars". In: *Phys. Rev. C* 64 (6 2001), p. 062802. DOI: 10.1103/PhysRevC.64.062802. URL: http://link.aps.org/doi/10.1103/PhysRevC.64.062802.

[64] S.M. Carroll. *Spacetime and Geometry: An Introduction to General Relativity*. Addison Wesley, 2004. ISBN: 9780805387322. URL: https://books.google.pt/books?id=1SKFQgAACAAJ.

[65] B.K. HARRISON et al. *Gravitation Theory and Gravitational Collapse. [By] B. Kent Harrison ... Kip S. Thorne ... Masami Wakano ... John Archibald Wheeler*. Chicago & London, 1965. URL: https://books.google.pt/books?id=8S0dMwEACAAJ.

[66] C. J. Horowitz and J. Piekarewicz. "Neutron star structure and the neutron radius of Pb-208". In: *Phys. Rev. Lett.* 86 (2001), p. 5647. DOI: 10.1103/PhysRevLett.86.5647. arXiv: astro-ph/0010227 [astro-ph].

[67] M. Fortin et al. "Neutron star radii and crusts: uncertainties and unified equations of state". In: (2016). arXiv: 1604.01944 [astro-ph.SR].

[68] Gordon Baym, Christopher Pethick, and Peter Sutherland. "The Ground state of matter at high densities: Equation of state and stellar models". In: *Astrophys. J.* 170 (1971), pp. 299–317. DOI: 10.1086/151216.

[69] Fabrizio Grill et al. "Equation of state and thickness of the inner crust of neutron stars". In: *Phys. Rev.* C90.4 (2014), p. 045803. DOI: 10.1103/PhysRevC.90.045803. arXiv: 1404.2753 [nucl-th].

[70] M. Frank, M. Buballa, and M. Oertel. "Flavor mixing effects on the QCD phase diagram at nonvanishing isospin chemical potential: One or two phase transitions?" In: *Phys. Lett.* B562 (2003), pp. 221–226. DOI: 10.1016/S0370-2693(03)00607-5. arXiv: hep-ph/0303109 [hep-ph].

[71] Robert D. Pisarski. "Notes on the deconfining phase transition". In: *QCD perspectives on hot and dense matter. Proceedings, NATO Advanced Study Institute, Summer School, Cargese, France, August 6-18, 2001.* 2002, pp. 353–384. arXiv: hep-ph/0203271 [hep-ph]. URL: http://alice.cern.ch/format/showfull?sysnb=2302511.

[72] Claudia Ratti. "Thermodynamics of the Quark-Gluon Plasma". In: *International School on Quark-Gluon Plasma and Heavy Ion Collisions : past, present, future.*

[73] Kenji Fukushima. "Chiral effective model with the Polyakov loop". In: *Phys. Lett.* B591 (2004), pp. 277–284. DOI: 10.1016/j.physletb.2004.04.027. arXiv: hep-ph/0310121 [hep-ph].

[74] Simon Roessner, Claudia Ratti, and W. Weise. "Polyakov loop, diquarks and the two-flavour phase diagram". In: *Phys. Rev.* D75 (2007), p. 034007. DOI: 10.1103/PhysRevD.75.034007. arXiv: hep-ph/0609281 [hep-ph].

[75] S. Ejiri, Y. Iwasaki, and K. Kanaya. "Nonperturbative determination of anisotropy coefficients in lattice gauge theories". In: *Phys. Rev.* D58 (1998), p. 094505. DOI: 10.1103/PhysRevD.58.094505. arXiv: hep-lat/9806007 [hep-lat].

[76] G. Boyd et al. "Thermodynamics of SU(3) lattice gauge theory". In: *Nucl. Phys.* B469 (1996), pp. 419–444. DOI: 10.1016/0550-3213(96)00170-8. arXiv: hep-lat/9602007 [hep-lat].

[77] O. Kaczmarek et al. "Heavy quark anti-quark free energy and the renormalized Polyakov loop". In: *Phys. Lett.* B543 (2002), pp. 41–47. DOI: 10.1016/S0370-2693(02)02415-2. arXiv: hep-lat/0207002 [hep-lat].

[78] Christian S. Fischer et al. "Polyakov loop potential at finite density". In: *Phys. Lett.* B732 (2014), pp. 273–277. DOI: 10.1016/j.physletb.2014.03.057. arXiv: 1306.6022 [hep-ph].

[79] Bernd-Jochen Schaefer, Jan M. Pawlowski, and Jochen Wambach. "The Phase Structure of the Polyakov–Quark-Meson Model". In: *Phys. Rev.* D76 (2007), p. 074023. DOI: 10.1103/PhysRevD.76.074023. arXiv: 0704.3234 [hep-ph].

[80] H. Abuki et al. "Chiral crossover, deconfinement and quarkyonic matter within a Nambu-Jona Lasinio model with the Polyakov loop". In: *Phys. Rev.* D78 (2008), p. 034034. DOI: 10.1103/PhysRevD.78.034034. arXiv: 0805.1509 [hep-ph].

[81] Guo-yun Shao et al. "Phase transition of strongly interacting matter with a chemical potential dependent Polyakov loop potential". In: (2016). arXiv: 1603.09033 [nucl-th].

[82] Eric Blanquier. "Color superconductivity in the Nambu Jona-Lasinio model complemented by a Polyakov loop". In: (2016). arXiv: 1606.02672 [hep-ph].

[83] Gerard 't Hooft. "Topology of the Gauge Condition and New Confinement Phases in Nonabelian Gauge Theories". In: *Nucl. Phys.* B190 (1981), pp. 455–478. DOI: 10.1016/0550-3213(81)90442-9.

[84] Xian-yin Xin, Si-xue Qin, and Yu-xin Liu. "Improvement on the Polyakov–Nambu–Jona-Lasinio model and the QCD phase transitions". In: *Phys. Rev. D* 89 (9 2014), p. 094012. DOI: 10.1103/PhysRevD.89.094012. URL: http://link.aps.org/doi/10.1103/PhysRevD.89.094012.

[85] Tina Katharina Herbst, Jan M. Pawlowski, and Bernd-Jochen Schaefer. "The phase structure of the Polyakov–quark–meson model beyond mean field". In: *Phys. Lett.* B696 (2011), pp. 58–67. DOI: 10.1016/j.physletb.2010.12.003. arXiv: 1008.0081 [hep-ph].

[86] Sourendu Gupta et al. "Scale for the Phase Diagram of Quantum Chromodynamics". In: *Science* 332 (2011), pp. 1525–1528. DOI: 10.1126/science.1204621. arXiv: 1105.3934 [hep-ph].

[87] Larry McLerran and Robert D. Pisarski. "Phases of cold, dense quarks at large N(c)". In: *Nucl. Phys.* A796 (2007), pp. 83–100. DOI: 10.1016/j.nuclphysa.2007.08.013. arXiv: 0706.2191 [hep-ph].

[88] Márcio Ferreira, Pedro Costa, and Constança Providência. "Strange quark chiral phase transition in hot 2+1-flavor magnetized quark matter". In: *Phys. Rev.* D90.1 (2014), p. 016012. DOI: 10.1103/PhysRevD.90.016012. arXiv: 1406.3608 [hep-ph].

[89] Mário Jorge César dos Santos. "Restauração das Simetrias Quiral e Axial a Temperatura Finita no Modelo de Nambu Jona-Lasinio com dois Sabores". MA thesis. Universidade de Coimbra.